2010

Toward A Real-time Celestial Body Information System

Brian Mitchell Guise
University of Central Florida

TOWARD A REAL-TIME CELESTIAL BODY INFORMATION SYSTEM

By

BRIAN MITCHELL GUISE
B.S.E.E. University of Central Florida, 1988
M.S. University of Central Florida, 1997

A dissertation submitted in partial fulfillment of the requirements
for the degree of Doctor of Philosophy
in the Department of Industrial Engineering and Management Systems
in the College of Engineering and Computer Science
at the University of Central Florida
Orlando, Florida

Summer Term
2010

Major Professor: Michael D. Proctor

ABSTRACT

The National Aeronautics and Space Administration maintains a challenging schedule of planned and on-going space exploration missions that extend to the outer reaches of our galaxy. New missions represent a huge investment, in terms of actual costs for equipment and support infrastructure, and personnel training. The success of a mission is critical considering both the monetary investment, and for manned missions, the lives which are put at risk. Tragedies involving Challenger, Columbia, Apollo 7, and the near tragedy of Apollo 13 exemplify that space exploration is a dangerous endeavor, posing extreme environmental conditions on both equipment and personnel. NASA, the National Science Foundation' and numerous independent researchers indicate that predictive simulations have the potential to decrease risk and increase efficiency and effectiveness in space exploration activity. Simulations provide the capability to conduct planning and rehearsal of missions, allowing risk reducing designs and techniques to be discovered and tested. Real-time simulations may improve the quality of the response in a real-time crisis situation.

The US Army developed Layered Terrain Format (LTF) database is a uniquely architected database approach that provides high fidelity representation of terrain and specialized terrain query functions that are optimized to support real-time simulations. This dissertation investigates the question; can the unique LTF database architecture be applied to the general problem of celestial body representation? And if so, what benefits might it bring for mission planners and personnel executing the mission? Due to data limitations, this research investigates these questions through a lunar analog setting

involving S band and Earth-bound communication signals as might be needed to conduct manned and/or robotic mission on the moon.

The target terrain data set includes portions of the Black Point Lava Flow in Arizona which will be used for NASA's 2010 Desert RATS analog studies. Applied Research Associates Inc, the developer of the LTF product, generated Black Point databases and made limited modifications to the LTF Viewer tool, RAVEN, which is used for visualization of the database. Through the results attained during this research it is concluded that LTF product does provide a useful simulation capability which could be used by mission personnel both in pre-mission planning and during mission execution. Additionally, LTF is shown to have application an information system, allowing geo-specific data of interest to the mission to be implemented within its layers.

The Florida Space Research & Education Grant Program sponsored by FSGC, Space Florida and UCF provided a grant of $31,500 to perform this research.

TABLE OF CONTENTS

LIST OF FIGURES

LIST OF TABLES

LIST OF ACRONYMS

API - Application programming interface

ARA - Applied Research Associates, Inc

ATHLETE - All-terrain, hex-limbed, extra-terrestrial explorer

A-TESS - Army tactical engagement simulation system

BP - Black Point, Arizona

BVH - Bounding volume hierarchy

COLLADA - Collaborative Design Activity (an XML schema for graphical design)

COTS - Commercial off the shelf

db - decibel

DB - Database

DEM - Digital elevation map

DSES - Distributed Space Exploration Simulation

DSNet - Distributed simulation network

DTED - Digital terrain elevation data

EVA - Extravehicular activity

FOM - Federation Object Model

FOV - Field of view

FSGC - Florida Space Grant Consortium

GIS - Geographic information system

GOTS - Government off the shelf

GP - Geometric pairing

GPS - Global positioning system

HLA - High level architecture

KML - Keyhole markup language

KSC - Kennedy Space Center

LCT - Lunar communications terminal

LIDAR - Light detection and ranging

LMMP - Lunar Mapping and Modeling Project

LOLA - Lunar Orbiter Laser Altimeter

LOS - Line of site

LRO - Lunar Reconnaissance Observer

LROC - LRO Camera

LSOS - Lunar surface operations simulator

LSS - Lunar surface systems

LTF - Layered Terrain Format

MILES - Multiple Integrated Laser Engagement System

NASA - National Aeronautics and Space Administration

PC - Personal computer

PEO STRICOM –Program Executive Office Simulation Training and Instrument Command

RATS - Research and technology studies

RDECOM - Research Development and Engineering Command

RF - Radio frequency

RUGUD - Rapid Unified Generation of Urban Databases

SBES - Simulation-based engineering science

SBIR - Small business innovative research

SNE - Synthetic natural environment

SRTM - Shuttle radar topography mission

STTR - Small business technology transfer

1 GENERAL LITERATURE ON CELESTIAL BODY MODELING AND SIMULATION

Chapter 1 reviews the need for simulations supporting heliophysic, celestial body science and exploration, and space exploration mission rehearsal. A description of current and planned simulations systems developed by the National Aeronautics and Space Administration (NASA) in support of on-going and future exploration missions is provided. The US Army's Layered Terrain Format (LTF) database is introduced and a general overview of its capabilities and use in military training is included. The motivation for the proposed layered celestial body database research will be identified by the gaps in current space mission planning, mission rehearsal, mission support, and mission mirroring capabilities that could potentially be satisfied by the LTF database product.

1.1 Simulation Needs for Space Exploration

The Bush administration's 2004 Vision for Space Exploration launched NASA on a challenging new mission to resume both robotic and manned exploration missions to the celestial bodies within our solar system, including the creation of sustained human habitats on both the Moon and Mars. NASA, in response to the vision, has developed an aggressive exploration program with near term goals of Lunar and Mars robotic missions and longer term goals of exploring celestial bodies within and outside of our solar system. Early robotic Mars and Lunar missions are expected to provide proof of mission architectures which will support longer range missions (Connolly, 2006). NASA has since been engaged in numerous architecture studies and analog field trials aimed at developing systems which support these new exploration endeavors. The development of simulations systems to support the new exploration missions is currently ongoing.

NASA's recognition of the importance of simulation to space exploration is evident through its history of development of mission specific simulators. Throughout the early space programs (Mercury, Gemini, and Apollo), astronauts would spend one third or more of total training time in simulators. NASA simulators range from full-motion full function mission simulators to task targeted part task trainers. The Apollo program alone used 15 simulators which logged a total of nearly 30,000 training hours during the multi-year program (Tomayko, 1988). Since the end of the Apollo program, NASA has expanded the use of simulation beyond just crew training, leveraging simulation tools for planning, risk assessments, design analysis, and mission rehearsal.

As the tragedies involving the Challenger, the Columbia, Apollo 7, and the near tragedy of Apollo 13 exemplify, space exploration is a dangerous endeavor, posing extreme environmental conditions on both equipment and personnel. NASA's future planned missions will require long term exposure to both dynamic heliophysic and planetary effects. NASA's Bioastronautics roadmap was generated to document the expected risk to humans of such extended exposure and to provide guidance for risk assessment and reduction activities. Table 1 provides a small sampling of the health risks identified in this report (NASA/SP-2004-6113, 2005).

Table 1 Sample of Human Health Risks of Space Exploration

Risk No.	Risk Title	Risk Description
22	Medical Informatics, Technologies and Support Systems	Limited communication capability during space flight results in the compromised ability to provide medical care and may have adverse consequences for crew health.
26	Mismatch between Crew Cognitive Capabilities and Task Demands	Human performance failure may occur due to inadequate design of tools, interfaces, tasks and information support systems. Task saturation may also occur due to compromises in crew health, human factors and cognitive capabilities.
28	Carcinogenesis	Increased cancer morbidity or mortality risk in astronauts may be caused by occupational radiation exposure.
31	Acute Radiation Risks	Acute radiation syndromes may occur due to occupational radiation exposure.
44	Mismatch between Crew Physical Capabilities and Task Demands	Human performance failure may occur due to human factors inadequacies in the physical work environments (e.g., workplaces, equipment, protective clothing, tools and tasks).
45	Poorly Integrated Ground, Crew, and Automation Functions	Mission performance failure may occur without adequate operational concepts, design requirements and design tools for integration of multiple factors that affect mission performance, such as ground-crew interaction, communication time, and level of automation.

Additionally NASA's 2009 SBIR/STTR Program Solicitation (Topic X6: Lunar Operations) states " Reducing risk and ensuring mission success depends on the coordinated interaction of many functional surface systems including life support, power, communications infrastructure, and transportation."   Simulation is a key tool in the modeling, development, and integration of interacting complex systems, as well as the prediction of risk, minimization of risk through design, and determining action in the face of unavoidable occurrences of risk. NASA will have simulations running throughout the lunar missions to aid in mission planning and execution, and handling of unexpected events.

The National Science Foundation's Simulation-Based Engineering Science Final Report states that predictive simulations provide the ability to optimize human activity and infrastructure in respect to adverse events or trends and real-time simulation the ability to identify rational responses to crisis. The report highlights the September 11 World Trade Center tragedy as an example, "…if real time simulation had been available, the emergency response team would have realized the importance of the immediate evacuation of the building complex." (SBES Final Report)

1.2 NASA Exploration Programs and DSES

NASA's Vision for Space Exploration initiative defines the requirement for a Distributed Space Exploration Simulation (DSES) project. The purpose of DSES is to develop and implement a Simulation Based Acquisition process where simulation will play a role throughout an exploration mission's life cycle. DSES outlines an Integrated Modeling and Simulation strategy that includes key policies of reuse of simulation from other organizations/projects and implementation of distributed simulations. (Crues, 2006). Future NASA programs will be supported by a suite of simulation systems that model everything from launch of the space vehicles to the task operations planned for execution on the celestial body surface. And according to Monell (2007), modeling and simulation will be integral to every aspect of a space exploration mission including planning, architecture analysis, technology evaluation, requirements definition, risk assessment, supportability, operability & affordability analyses, performance analysis, test and verification, training and operations.

A primary DSES component of interest to this dissertation is the Lunar Surface Operations Simulator (LSOS). LSOS is a physics-based simulator providing realistic visual simulation of lunar surface operations. The LSOS requirements are summarized in the following bullets:

- To provide a virtual environment that represents the best knowledge of the lunar surface in which to simulate operations including surface topography, lighting, radiation environmental features
- To incorporate surface elements (rovers, habitats, crew) at their currently-known level of detail (geometry, structure, function and behavior) into that environment
- To accurately portray exploration and science operations performed by those elements in that environment, assessing how well the elements can perform the operations (e.g., rover driving, towing, digging/hauling, assembly/disassembly)
- To enable analysts to expose limitations imposed by element functionality and/or environment on the success of the operations at an early time in the design cycle so that the analysts/designers can address them
- To gain experience in simulation of mock lunar operations at terrestrial sites (validates simulations, systems and scenarios). (Wall, 2007)

The LSOS simulation interfaces with other DSES components via the NASA Distributed Simulation Network (DSNet) using IEEE 1516 High Level Architecture (HLA). The

DSES Federation Object Model defines the interoperable data types which DSES components use to exchange data. The models currently available within DSES include simulation programs developed by 5 NASA centers which provide a current capability to simulate the launch of space vehicles and simulation of surface activities provided through LSOS. Future evolution of DSES capabilities will include addition/reuse of Government and Commercial off the shelf (GOTS, COTS) simulations which contribute to the DSES mission (Crues, Chung, Blum, Bowman, 2007).

1.3 NASA Desert Research And Technology Studies

NASA's Desert Research and Technology Studies (RATS) are an annual series of analog tests performed by NASA at sites having terrain and terrain features geographically similar to the lunar surface. The 2009 Desert RATS field test ran from August 28th through September 18th. The purpose of these field tests is to assess preliminary exploration operational concepts and prototype systems including rovers, extravehicular activity (EVA) timelines, and ground support by providing hands-on experience with simulated planetary surface exploration EVA hardware and procedures (NASA web).

1.4 NASA's Reuse of Existing Technology

In addition to the DSES charter to reuse GOTS and COTS software, several NASA sources have encouraged the reuse of existing technology to reduce cost and development times for NASA projects. "NASA plans to work with other government agencies and the private sector to develop space systems that can address national and commercial needs" and " .. focus on innovations that reduce the cost of sustained space operations" (NASA, The Vision For Space Exploration, 2004).

1.5 Army Simulation Terrain Databases

Army training devices are categorized in three domains: Live, Virtual, and Constructive. Live domain is a representation of military operations using Live forces and instrumented weapons and exercise ranges to simulate actual operational conditions. Virtual simulations include training devices that provide force on force engagements in a visible artificial world. Constructive simulations include training simulations that provide force on force engagements in a non-visible artificial world (PEO STRICOM). Terrain databases developed for training system within each group are specialized to fulfill specific domain needs.

Virtual training device typically allow the operator to view a virtual world via computer generated images and display systems. The terrain databases developed for virtual simulators are typically very large and contain detailed data required to render realistic looking scenes including terrain, vehicles, human models, buildings, trees, etc. Resolution and feature attributes of virtual terrain databases must often support target recognition and engagements at modern weapon ranges. Constructive training devices usually lack the out-the-window viewing features and typically do not have the high fidelity scene rendering capabilities of a virtual system. However the modeled agents and entities within a constructive environment often require the same level of detail from the terrain database to allow path planning, movement, engagement and similar autonomous decision tasks. Terrain attributes such as soil type, water depths, and road networks must be included to support both virtual and constructive systems (Campos, Borkman, Peele, Cambell, 2008). In live training, human participants do most of the planning and decision making that is agent based in constructive and virtual systems. Less attribute data is required for the terrain database because trainees infer the same information via their own senses. Live training has specific database requirements that differ from other training systems (Borkman, Peele, Cambell, 2007).

A tactical engagement simulation system is a live training device that allows soldiers and combat vehicles to simulate weapon firing, target hits and misses. The Army's Multiple Integrated Laser Engagement System (MILES) is a laser based tactical engagement system, which is similar to a commercial laser tag game. Weapons are fitted with lasers, and potential targets (dismounted infantry and vehicles) have laser detectors. Data encoded within a single laser shot identifies the shooter and munitions type allowing determination of damage/kill status of the target. Although the MILES system was successful, smoke and weather effects severely hindered operations. Additionally, non-line of site weapons, and weapons such as grenades could not be simulated. The Army's newest engagement simulator, Army-Tactical Engagement Simulation System (A-TESS), was designed to provide the MILES functionality without using lasers. Weapons are fitted with high fidelity gyros and inertial devices and players have personnel location systems that allow determination of weapon and target orientation and location. A weapon's trigger pull launches a line of site calculation against the terrain database to determine the intermediate and terminal impact points of the simulated projectile and register target/shooter pairings when successful hits are calculated. The database and executing code reside on a wearable PC carried by the shooter (Borkman et al., 2007).

The LTF database was developed to support the A-TESS program. Specific LTF design constraints included:

- Layered data scheme to provide query optimization for different data types.
- High resolution feature and terrain representation
- Scalable – supports additional data layers, expansion of terrain area.
- 10 Km x 10Km minimum terrain coverage
- Terrain attributes tagging to allow munitions to pass through various surfaces

1.5.1 LTF Terrain Database Generation

Due to the high resolution requirements of LTF, databases compiled for Live training events are typically generated from high resolution light detection and ranging (LIDAR) environment data. The RUGUD Toolkit is a suite of tools which generate the LTF database. The input source data, can also include digital elevation data, photo maps, or LIDAR source data. The RUGUD is also capable of generating various other common terrain database formats such as openFlight, COLLADA, etc.

1.6 Application of LTF in NASA Simulations

Because the LTF is optimized to provide the rapid LOS calculations, as required by A-TESS, applications of LTF within NASA space exploration simulations should be considered to leverage these capabilities. Recent discussions with NASA KSC Lunar Surface Systems (LSS) group has identified the capability to quickly generate and represent lunar surface communications mapping as a gap in current NASA capabilities which is a likely application of LTF. NASA currently uses LSOS and other products, such as Radio Mobile, to generate coverage maps, but these tools lack the real-time LOS execution capabilities provided by LTF. NASA desires the capability to provide fast updates to coverage predictions given the likely dynamic nature of celestial body exploration mission execution and re-planning. A further benefit LTF may provide is the representation of other types of geo-specific data. The communications use case for example will provide an LTF layer to represent radio hardware assets and their parameters. A mining mission may benefit from the addition of an LTF materials layer containing geo-specific mineralogy data from previous missions or satellite sensors. Layers contain details of surface type and slope could be added to support route planning and navigation tasks.

That leads to the general research question for this dissertation: Can the unique LTF database architecture be applied to the general problem of celestial body representation? Due to research limitations, this database architecture will be investigated for general celestial body representation not through a clinical study but rather through literature research and a case study in an analog setting. The case study will investigate one layer both in terms of modeling and representational characteristics. The communications mapping is intended to provide astronauts and/or robotic controllers with a visual indication of areas in which they can explore or traverse while still staying with LOS and transmission range of moon base, earth, or satellite communications antennas. The potential application of LTF for this use case allows us to further define the question: *(RQ1) As analogs to Planetary and Heliophysiscs effects, what factors must the LTF database represent and at what resolution must the LTF database model these factors in* *order to represent attenuation of various communications signals due to geospatial and atmospheric effect to the extent that they influence planning and execution of analog lunar surface operations ?*

NASA’s current lunar communications architecture specifies the use of S and Ka band RF signals for voice and data transmissions and for use in lunar surface navigation systems. GPS-based navigation will likely not be available on exploration missions, due to the prohibitive cost of the constellation of satellites that would be required. Instead NASA will employ a hybrid navigation system relying on both terrain references and radio transmissions. This system will be highly dependent on the LOS-based communications network. (Schier, 2007) Section 2 provides more detailed discussions of NASA's communications architecture.

If LTF can be successfully leveraged for communications predictions, then usability leads to a second general research question:

(RQ2) What are the human systems integration/interface components and what should their characteristics be so that astronauts or mission controllers receive spatial representations of various communications signal attenuations to affect timely and effective planning and execution of analog lunar surface operations?

There are no tested research hypotheses derived from this general question, in part due to a lack of research funds required to implement specific LTF features desired by NASA, and also due to a schedule slip in the NASA Desert RATS trials which will prevent review of the product by relevant astronaut analogs. Recent meetings with NASA

Kennedy Space Center scientists have yielded discussions of visual display concepts such as coverage maps, routes, and exploration points that are rendered within the LTF tool as semi-transparent overlays as a proof of concept for overlay files which could be exported to other viewing systems. NASA has also indicated that dynamic communications maps, which update due to relay antenna deployment or transmitter repositioning, are desired. The current plan is to provide a proof of concept demonstration of these capabilities and collect any personal anecdotal feedback to be included in the results section of this dissertation to aid future researchers that wish to pursue such study.

1.6.1 Lunar Reconnaissance Orbiter (LRO) Terrain Data

NASA's LRO is tasked with finding safe landing sites, potential resources (such as frozen water) and characterizing the radiation environment of the Lunar polar regions. The LRO was launched in July 2009 and is currently in a low polar orbit for a planned 1 year mission. Data from the LRO's instrument package began arriving on September 17, 2009.

One of the primary instrument packages aboard the LRO is the Lunar Orbiter Laser Altimeter (LOLA). LOLA will gather lunar topography data providing lunar digital elevation maps (DEM) that will support landing events and mobility during surface activities. Additional LRO instruments include the Lunar Reconnaissance Orbiter Camera (LROC) which will collect images of the lunar surface. LROC incorporates 2 narrow and 1 wide field of view cameras. Images from the narrow FOV cameras will provide meter-scale mapping of select lunar polar regions that are of exploration interest to NASA (NASA Press Kit, 2009). The accuracy of digital elevation data gathered by the laser altimeter data will be ± 10 centimeters, with a grid resolution of 25 meters between posts (NASA LOLA Fact Sheet, 2009).

For the proposed research, it will not be possible to collect actual lunar RF transmission data against which to test the LTF performance. Instead RF measurements data collected at the planned 2010 Desert RATS site will be used. LTF will model that site (Black Point, Arizona) using two sources of topographical data to produce two different resolution LTF databases. One Black Point (BP) database will be generated from (Shuttle Radar Topography Mission) SRTM datasets. The other database will be generated from high fidelity LIDAR data recently collected by NASA.

1.7 Motivation For Research

Fulfilling requirements for planning and rehearsal of space exploration missions has historically involved creation of mission specific simulations that incur both a major cost element and a potential schedule impact to the program. The DSES program is a forward thinking initiative by NASA, providing a reusable set of simulation capabilities which will benefit future space exploration endeavors. However, because space exploration poses extreme risks to both equipment and humans, it is imperative that developed simulations realistically model both the systems and environmental conditions under which they will operate. NASA recognition of this need is identified in internal briefings which require developers to develop and implement processes for verification, validation and accreditation of software models and simulations (Monell, 2007).

The motivation for our research is to investigate the re-use of a mature Army developed high fidelity terrain database capability to satisfy existing requirements or improve upon current capabilities of current or planned NASA simulations. The layered architecture of the LTF database may provide a good fit for the identified communications layer task. LTF is optimized to provide rapid line of sight calculation, provides LOS attenuation capabilities based on terrain and feature attributes, and allows addition of layers which can accommodate terrain specific attributes that affect RF transmission. The US Army version of LTF lacks models for RF signal propagation and attenuation. The US Army is currently funding additional research and development tasks to improve and expand the capabilities of LTF which may further benefit NASA requirements. The research approach will verify, through the scientific method, the validity of implementing LTF terrain databases to model attenuation for lunar surface communications. Additionally this research will:

- Support reuse strategies outlined in NASA's DESD program objectives
- Implement a scope limited celestial body information system within LTF - providing proof of concept for additional mission specific data layers
- Support Florida Space Grant Consortium objectives to supporting research opportunities, and academic-NASA-industry partnerships.

1.8 Research Summary

The goal of this case study is to determine the feasibility of re-purposing a matured Army simulation product, the LTF database, for use by NASA to fulfill gaps within their current mission simulation capabilities.

Our specific objectives are:

- Creation of LTF databases from existing lunar analog surface topology data:
  - 2010 Desert RATS exercise area digital elevation data to be provided by NASA
  - SRTM DTED level 2 elevation data for the same site.
- Identification of an S-band communications model that can be embedded in LTF
- Creation of a corresponding communications data layer within the LTF database
- Create of LOS communications overlays and queries on the selected analog database for both local and analog earth bound signals
- Conduct actual communications signal power readings samples from the site of NASA's planned 2010 Desert RATS analog tests, using the points of interest and antenna locations provided by NASA.
- Conduct analysis to identify per cell accuracy of prediction to actual field reading. Research will include inferential statistical analysis of correct positives, correct negatives, incorrect positives, and incorrect negatives.
- Publication and dissemination of findings

1.9 Dissertation Overview

Chapter 2 provides further discussion of the LTF product, ongoing Army development activities, and the RUGUD database generation tool which is used to build the LTF database. NASA's lunar communications architecture is examined and the current approaches to Lunar and Earth based communication simulations are reviewed from the literature. The identified general research questions are developed into detailed research questions which address the capability of LTF to fulfill both NASA simulation requirements and to address the gaps identified in the current lunar communications modeling knowledge base.

Chapter 3 defines the research methods used for statistical analysis. Limitations of the research are defined. Hypotheses are developed, and the statistical tests planned for each hypothesis is stated. A discussion of post processing of field collected RF measurement data is also provided.

Chapter 4 provides the statistical test results for tested hypotheses. The raw data collected during the data collection trip is provided. The specific subset of data used for each test is provided in Appendices which are referenced within the chapter 4 body text.

Chapter 5 provides a summary of the overall effort of this research, findings and conclusions. The specific contributions of this research to the body of knowledge is provided as well as generalization of findings to additional domains. Finally a discussion of future research opportunities and potential improvements to the developed LTF capabilities is provided.

2 BACKGROUND AND RELATED CELESTIAL BODY MODELING AND SIMULATION WORK

Chapter 2 starts with a review of literature for recent research related to layered terrain databases, then the current requirements and capabilities of the Army's Layered Terrain Format (LTF) database are discussed. A preliminary assessment of where and how LTF capabilities could enhance NASA simulations will be discussed. NASA's lunar communications architecture is examined and the current approaches to Lunar and Earth based communication simulations are reviewed from the literature. The literature review will identify key requirements and gaps within current and planned NASA developed celestial body terrain databases. The general research questions identified in chapter 1 are developed into detailed research questions which address the capability of LTF to fulfill both NASA simulation requirements and to address the gaps identified in the current lunar communications modeling knowledge base.

2.1 Layered Databases

References to layered terrain databases within the literature are primarily focused on Geographic Information Systems GIS, specifically, virtual globes such as Google Earth, Microsoft Virtual Earth, and NASA World Wind. The capability of integrating satellite imagery, aerial photography, and digital map data with user specific geospatial information has popularized the use of virtual globes across many domains. For the research community, these systems have enabled easier collaboration on and sharing of research projects and research findings (Chen, Leptoukhm, Kempler, Di, 2008). Kamadjeu (2009), states that "Google Earth is becoming an important mapping structure for public health". His case study involved tracking of a polio outbreak and eradication program response within the Democratic Republic of Congo. Addition examples of Google Earth use within the healthcare ranges from the geographic tracking of infectious diseases, such as Avian Flu, to studies of molecular epidemiology enabled through mapping of genetic differences across geographic areas. The capability to extract data from independent sources (or layers) and provide 2D or 3D overlays integrated with the topographic layer is referred to as "mashups" and is one key to the popularity and success of the virtual globe systems (Boulos, Scotch, Cheung, Burden, 2008).

In addition to the virtual globe applications, there are numerous examples of customized GIS samples which overlay user specific data on custom topographic databases. These systems often require greater geographic accuracy or additional interface capabilities not available via Google Earth or Microsoft Virtual Earth. Hydroseek, for example, is a geo-spatial search engine developed to links hydrological data from three repositories, the National Water Information System, Chesapeake Bay Information Management System, and National Atmospheric Deposition Program to a satellite image based user query interface (Beran, Piaseki, 2009). Microsoft is developing a system called Sensor Map which is designed to interact with real-time sensors and web based information sources to provide geo-spatial mapping of user specified data. (Nath, 2007).

2.2 Requirements and Development of the Army's Layered Terrain Format Database

The majority of Synthetic Natural Environment (SNE) terrain databases developed by the US Army have supported virtual and constructive domain simulation systems. As stated in section 1.3, live training systems have unique database needs because the training is done in a real world environment and the trainee is exposed to both the real environment and the calculations run within the virtual environment. For example if a tree exists (on the real world training field) between a shooter and his intended target then a simulated weapon fire must be blocked, preventing a kill or damage score. This requires accurate positioning and sizing of the tree within the database as well as accurate representation of both participants' locations within the simulation. Thus the live training database must very accurately correlate with the real training environment for elements which could hinder munition flyout such as terrain and features.

The design approach for A-TESS is Terrain Augmented Geometric Pairing (GP). GP systems use GPS positions and pointing sensors in order to determine weapon firing trajectories. Terrain augmented GP adds terrain knowledge to the calculations preventing modeled projectiles from shooting through hills or other represented features (Baer, Campbell, Campos, Powel, 2008). Resolution requirements for LTF result from consideration of the inherent inaccuracies within the GP system. GPS systems have a nominal error of two meters for 2-D position. GPS vertical inaccuracies are much larger so the elevation is retrieved from the LTF database, given the GPS position. The "Foxhole Problem" defines a situation where a player is at a terrain feature where 2 different elevations exist, such as a foxhole. Determining the correct elevation of the player at this point is challenging given the positional inaccuracy of the GPS. The LTF terrain grid resolution of 1 meter was found to provide a 75 percent probability of correctly determining a player's elevation in this situation.

The 10 cm elevation accuracy was derived considering the overshoot and under shoot errors when modeling shallow angle shots for short range weapons such as the M203 and Mark 19 (grenade launchers). Weapon elevation sensor inaccuracies are also considered. The 10 cm elevation accuracy was found to provide a small enough overshoot/undershoot error that the intended target is still within the effective range of the munitions blast area (Baer et al., 2008).

Since the Army's LTF was a ground up development project, it leveraged commercial graphics and computer science domains to implement data storage structures and algorithms which provide rapid LOS calculation. Terrain data is stored in pages that represent 1 square kilometer of terrain. Terrain elevations are provided as a 16 bit integer value at grid post spacing of 1 meter. Culling grids are defined for 10 by 10 post areas and for larger 100 by 100 post areas. The terrain skin is stored in a hierarchical three level tree structure - the lowest level being the 1 meter grid and the highest being the 100x100 post grid.

Line of site calculations use the two-dimensional digital difference analyzer (2DDDA) which is highly optimized to rapidly traverse a regularly spaced grid. This LOS routine checks the ray against height of terrain against culling grids which it crosses, starting with the largest grid and calculating child nodes (smaller grids) only if the ray is lower than the terrain height of the parent grid.

Within LTF features (trees, buildings, etc.) are represented as nodes in a bounding volume hierarchy (BVH) tree. Each node in a BVH tree is a spatial volume that fully contains all of it child nodes. Geometry of individual nodes can be basic or complex geometry types: ellipsoids, columns, triangle meshes, etc. Higher level culling volumes use simple solid geometry types to allow faster intersection checks. The feature intersection algorithm detects root node intersections and if the intersected node is defined as a culling node then its child nodes will be checked for intersection. The BVH tree is optimized for attenuated LOS calculations and will always check closest nodes first. Material attributes can be assigned to features in order to calculate attenuation of the LOS ray (Borkman et al., 2007).

Ongoing efforts funded by the Army continue to improve and expand the LTF capabilities. These efforts include the addition of dynamic terrain capabilities, and extension of compatibility to other Army simulations systems.

2.3 Application of LTF in NASA Products

LTF appears to be uniquely well-suited for modeling an arbitrary planetary body. The terrain database representation and runtime reasoning services operate entirely in Cartesian coordinates, with no assumptions whatsoever about the planetary reference ellipsoid. All calculations are performed in local Cartesian coordinate systems tangent to the reference ellipsoid; a global Cartesian system is used to coordinate between different local systems. Due to the Cartesian representation, LTF has no difficulty handling high-latitude or polar regions. The offline terrain compiler generates both the local and global Cartesian coordinate system and would require some minor modifications to properly create the local Cartesian coordinate systems for non-Earth planetary ellipsoids.

Elongated ellipsoids combined with this Cartesian coordinate approach will also permit the modeling of non-spherical bodies such as near earth objects.

The difference in curvature of a celestial body vs. the Earth surface may require changes in the terrain data storage structure. LTF was originally implemented to support full round-earth coverage, but where each defined flat earth terrain tile (1 km x 1 km) is normal to the systems local Z vector. This introduces a minimal error (within the 10 cm accuracy requirements) at the edges of the tile. One approach being considered to deal with the greater curvature of the lunar surface is requiring terrain tile sizes to be reduced in order to minimize errors at tile edges. The primary challenge is to ensure that the gravity vector in each LTF local Cartesian system does not significantly differ from the system's local Z vector, since the assumption that the two are interchangeable is key to the performance of the line-of-sight and height of terrain services.

Based on the preceding review of NASA simulations and the stated LTF capabilities, there are several functional areas identified below which may benefit from LTF:

Communications Simulation: The 2009 Desert RATS utilized LSOS line of site calculation capabilities to generate communication coverage maps between planned sortie locations and the fixed antenna locations. These maps were not generated in real-time, rather they were generated the night preceding each mission test due to the execution time required. LTF’s optimized LOS capabilities can be utilized to perform this task in or near real-time. This becomes even more critical for the planned 2010 Desert RATS tests where movable LCTs, or rover mounted communication relay devices will be used to extend excursion ranges. LTF also provides the capability to calculate attenuated LOS values – a capability not provided by LSOS. Within LTF, regolith attributes causing RF transmission attenuation could be captured in a newly defined feature layer. Attenuation algorithms can then be executed against line of site queries to provide a more realistic simulation of short wavelength radio transmission across the lunar surface.

Navigation Simulation: Because navigation on the lunar surface is highly dependent on communications for both time and location reference, the same real-time LOS issues are present.

Embedded Navigation Aid: LTF's small memory and processing footprint make it a candidate for embedding into target lunar surface hardware where the LOS capabilities could be used for terrain referenced navigation functions. Within this context, another potential benefit of LTF is the capability to wirelessly stream database updates. The streaming capability would allow pre-mission generated terrain (LRO resolution) databases to be augmented with locally collected terrain data. Although wireless streaming is only currently implemented for features, the on-going RDECOM financed SHADE program is researching additional capabilities for dynamic LTF databases.

Coverage Maps for other Electromagnetic Signals and Interference Sources: LTF layers could be created to identify location specific areas affected by interference from natural or manmade sources, such as a power generation station, or identify areas shielded from radiations sources external to the celestial body.

Routing Plans for Explorations: LTF could provide route planning for either manned or robotic missions. Routing could be optimized to either minimize exposure to heliophysical elements by staying in areas shadowed by mountains or craters, or maximize solar exposure in order to keep power array output at its peak. Path planning could also consider multiple LTF layers - for example providing a route to maximize data transmission to earth while exploring known mineral deposit areas.

Geographic Resource Mapping: Location specific resource data gathered through robotic, manned, or satellite sensor exploration can be embedded within LTF layers to provide future mission or future task reference to celestial body geographic resources.

LMMP User Interface: NASA's Lunar Mapping and Modeling Project LMMP is intended to be a repository of Lunar data acquired from many sources. The data will be available to researchers via public outreach programs. The repository will provide tools to allow viewing of the lunar data, and while no specific tools are mentioned, the geo-registered requirements for the bulk of the data requirements suggest that a GIS or virtual Earth type system such as Google Earth could be used. While the current focus of this research project will involve Earth based terrain modeling as a case-based analog, the end goal of the LTF research is to identify a suitable multi-layer celestial body database where layers can be visualized and easily applied by humans or robots in the conduct of real-time tasks. The source data for any future lunar LTF databases will likely come from LMMP or other sources such as SELENE data. Table 2 below identifies a subset of the draft Level 2 requirements for the LMMP project which are of interest to the proposed research (Cohen, Nall, French, Muery, Lavoie, 2008).

Table 2 LMMP Requirement Subset

Requirement
The LMMP shall provide geo-registered global and local albedo (visible image) base maps of the Moon
The LMMP shall provide geo-registered global and local surface roughness and rock size frequency and distribution maps of the Moon
The LMMP shall provide geo-registered terrain feature maps of the Moon (e.g., mountains, rilles, craters).
The LMMP shall provide tools with the capability to superimpose, based upon user input, human associated activities such as architectural elements, surface modifications, surface debris, chemicals, organics, and logistical information such as route planning to support lunar surface mission planning and operations.
The LMMP shall provide geo-registered global and local surface digital elevation models (DEM) of the Moon.
The LMMP shall provide geo-registered lunar lighting maps and models that provide lunar lighting information for any location at or near the lunar surface for any lunar time reference.
The LMMP shall provide geo-registered lunar temperature maps and models that provide lunar temperature information for any location and for any lunar time reference
The LMMP shall provide geo-registered global resource maps of the Moon.

As these requirements indicate, in addition to basic topography, there are other lunar attributes such as surface elements and resource data which could be embedded into an LTF database within the communications layer or as feature attributes.

As previously mentioned, one of the stated basic goals of the LMMP is to provide a set of tools which allow users to visualize the collected lunar data. The LTF database and viewer tool could be leveraged as both a visualization tool and an experimentation tool for LMMP lunar and other celestial body scientific information.

2.4 Lunar Space Communications Architecture

Apollo missions required complete planning of every mission detail prior to launch plus continuous monitoring by hundreds of experts throughout each flight. Continuous communications were maintained with the flight systems and crew except on the far side in lunar orbit through the use of 12-15 Earth based Communications and Tracking (C&T) stations geographically dispersed to maintain 3-4 stations with continuous coverage. The next lunar generation needs to allow the crew or robotic vehicle much more autonomy and opportunity to do their own planning and to perform exploration and scientific operations with limited oversight from controllers on Earth. Continuous Earth-based coverage for real-time control is not an option for the eventual human missions to Mars (Schier, 2007).

NASA's Evolutionary Space Communications Architecture Model defines components that provide robotic and human exploration elements access to high speed data communications throughout the solar system through an envisioned deployment of communications relay satellite constellations at or between the earth and celestial bodies of exploration interest (Bhasin, Hayden, 2004). The return to the moon by manned or robotic missions will be much more of than just a lunar exploration event. The lunar missions will all be testing grounds for analyzing system architectures and operation concepts that will be used in the future voyages to Mars and other celestial bodies. The communications systems deployed to support the future Lunar missions will serve to validate the overall Space Communications Architecture approach. Table 3 lists the major communications components defined by NASA's current lunar communications architecture.

Table 3 Lunar Communications Architecture Major Components

COMPONENT	FUNCTION	COMMENT
Earth Based Ground System (EBGS)	Fixed position transmitter/receiver	
Lunar Relay Satellite (LRS)	Relay from lunar surface devices to EBGS or other lunar surface device	Placed in Earth Moon LaGrangian Orbits
Lunar Communication Terminal (LCT)	Base station for wireless LAN, Navigation tracking and time services, Communication relay between surface network and LRS or EBGS	
User Radios	Common family of interoperable radios supporting of S and Ka band communication	fixed base radio, mobile user radio, EVA Radio

While the necessity for constant communication links between the Earth and Moon is expected to be less critical, availability of constant communication between lunar surface elements is critical for both coordination of surface exploration sorties, control of robotic elements, and navigation. Surface elements currently under development by NASA include:

- Habitats – modular elements similar to International Space Station nodes that provide living quarter and lab space. Habitats are located at fixed sites.
- Pressurized Rover – Transports crew and equipment on lunar surface.
- Chariot – six wheel drivable platform – used as chassis for Pressurized Rover

- ATHLETE – all terrain cargo handling device capable of unloading, transporting and manipulating cargo. The Athlete is remotely controlled. (NASA Fact Sheet, ATHLETE)

On the lunar surface LCTs and user radios provide communications over an 802.16 mesh network within a line of site range of approximately 6 km on flat terrain. The actual effective range of the surface LAN will be dependent on the local lunar terrain. When LOS to the LCT is unavailable the user radios can link to the LRS to communicate over S/Ka band radios with other surface based users or to the EBGS. However the LRS satellites are only available during 14 hours of the lunar day. Satellite in the loop communications are also less desirable due to higher power consumption. Among the most significant issues listed by Schier for near term research, is the LOS limitation for surface communication due to use of S-band and realistic Lunar terrain (Schier, 2007).

Navigation systems provided for lunar surface elements cannot rely on the GPS technologies employed on Earth. Lunar navigation will be supported by hybrid systems that use radio signals from fixes site antennas, satellite signals when available and will incorporate terrain referenced navigation capabilities. Passive optical navigation will be available to augment radio-based navigation yielding a system that can operate in the event of communications faults. Coronal Mass Ejection (CME) is a credible risk that could cause interference preventing the radio-based navigation system from working. The need for a radio-free navigation system on-board future space exploration elements implies that surface mobile systems need to be able to determine their location relative with sufficient accuracy to return to base safely without mission support (Shier, 2007).

2.5 Lunar and Earth Based Communications Models

Currently, NASA is using the Lunar Surface Operations Simulator (LSOS) to simulate lunar surface operations including LOS communications. LSOS is a visual simulator that enables assessment of lunar surface operations. The functional requirements of the LSOS are:

- To provide a virtual environment that represents the best knowledge of the lunar surface in which to simulate operations (Surface, Lighting, Radiation, Environmental features)
- To incorporate surface elements at their currently-known level of detail into that environment (Rovers, habitats,crew), (Correct geometry, structure, function and behavior)
- To accurately portray exploration and science operations (conops/scenarios) performed by those elements in that environment, assessing how well the elements can perform the operations (rover driving, towing, digging/hauling,assembly/disassembly)
- To enable analysts to expose limitations imposed by element functionality and/or environment on the success of the operations at an early time in the design cycle so that the analysts/designers can address them
- To gain experience in simulation of mock lunar operations at terrestrial sites (Validates simulations, systems and conops) (Wall, 2007)

LSOS was build upon Dshell++, a NASA Jet Propulsion Laboratory simulation framework (Nayar, 2009). Dshell++ is a physics based framework that was developed to support simulation needs across multiple space exploration domains including cruise vehicles, planetary rovers, and orbiting spacecraft. Dshell++ provides realistic visual rendering at 30 frames per second and can support multiple viewports via its OpenGL based rendering engine. Due to the 3-D visualization computation requirements Dshell++ is capable of running in a distributed mode across multiple cores or workstations.

In addition to scene rendering, Dshell++ provides a number of functions which are heavily used by LSOS including Power Analysis, Horizon Detection, Camera Modeling, and Line of Site Computation. The LOS computations are performed by attaching (during simulation setup) specially colored ornamental geometry to a specific LOS query location, such as a communications antenna. At run time during an LOS query, the ornamental geometry object is enabled and the scene is rendered from the point of view at the other coordinate (such as a vehicle sensor). If the ornamental geometry object is detected at the center of the scene then LOS is assumed to be valid. LOS calculations are described as being computationally expensive within the Dshell++ framework (Pomerantz, 2009).

LSOS does not perform RF signal attenuation, only a line of site check between the transmitting and receiving antennas, providing an indication of transmissions that are likely to be blocked by terrain. The current architecture of LTF and the proposed communications layer provide the same line of site check for terrain blockage, and also with the addition of the proposed communications layer, the capability to determine RF signal attenuation for transmissions not blocked by terrain.

The need to define what source data must be input to the LTF layers is the premise of several specific research questions:

(RQ1A) For the Black Point lunar analog database, what Terra Firma elevation model accuracy and resolution levels are significant to the accurate estimation of the actual signal strength attenuation within an LTF Communication Layer?

And looking specifically at replicating the terrain blockage capability currently provided by NASA's LSOS:

(RQ1B) For the Black Point lunar analog database and without regard to terra firma material or atmospheric properties, what Terra Firma elevation model accuracy and resolution levels are significant to the accurate estimation of signal attenuation due to terrain blockage?

These first two question address the accuracy of the source data used to generate the LTF terrain topography (terrain layer). They respond in part to Shier's call for further research into the effects of realistic terrain on Lunar communications architecture (section 1.3). In addition to the selection of applicable levels of resolution and accuracy of topographic source data, selection of RF attenuation models to be embedded within the LTF simulation is critical. Earth-based attenuation models must account for multiple sources of attenuation including (McLarnon, 1997):

- Free space path loss - The loss of power as the RF signal propagates over a distance without any interfering objects or atmospheric effects.

- Reflections - Radio waves that are reflected off of some object, terrain, or atmospheric temperature inversion and eventually arrive at the receiving antenna. Depending on the distance that the reflected wave travels it may be phase shifted from the primary transmission wave. If the reflected and primary waves are in sync, reflections can produce up to a 6 DB gain over a pure free space path transmission. If out of phase the signal loss can be as high as 20 DB.
- Refractions - Earth's atmosphere causes radio wave path to bend slightly downwards toward Earth rather than propagating in a straight line. This property can actually permit line of site RF to transmit beyond the optical LOS. Atmospheric refraction is affected by weather.
- Diffraction - Diffraction effects occur from object near the direct LOS path that disturb the RF wave resulting in uneven power density across the wave front.

The LTF database is capable of representing localized attributes of both terrain and features that would affect attenuation of RF transmissions. These specific attenuation sources thus provide further research questions:

(RQ1C) For the Black Point lunar analog database, what terra firma material properties are significant to the accurate modeling of RF transmission signal attenuation within an LTF Communications layer?

(RQ1D) For the Black Point lunar analog database, what feature and object properties are significant to the accurate modeling of RF transmission communications signal attenuation within an LTF Communications layer?

(RQ1E) For the Black Point lunar analog database, what atmospheric attenuation properties are significant to the accurate modeling of RF transmission communications signal attenuation within an LTF Communications layer?

Beyond specifying the feature and terrain attributes contributing to signal attenuation, the attenuation algorithm(s) must be selected. There are numerous RF attenuation models available which are designed for outdoor transmission in the GHz range. Ray-tracing based radio propagation models have gained popularity for simulation of accurate mobile communications. These models use multiple rays to model the paths of both the LOS signal as well as reflected signals to determine the total propagation gain or loss at the receiver. However execution of these models is processor intensive and would likely require parallel processing capability to meet the near real-time goals for coverage prediction of this experiment (Cavalcante, Jose de Sousa, Costa, Frances, Cavalcante, 2007).

A recent study by Hwu (Hwu, Upanavage, Sham, 2008) of lunar surface attenuation of high frequency RF signals, found that propagation loss was dependant on antenna height, lunar surface material and terrain geometry. Specifically, the path loss is found to be a function of the square of the transmission range (R^2) up to a breakpoint where it becomes a function of $R^{4.}$ The defining breakpoint is dependent on antenna height. For S-band transmission. the breakpoint for two meter antennas is round 50 meters, for ten meter tall antennas the breakpoint moves out to 300 meters (Hwu, 2008).

In order to minimize the execution time impact of attenuation calculation, we will focus on single ray models which incorporate more than just free space loss, among them are the ITU Terrain Model, the Egli Model, and the Longley-Rice Model.

The ITU Terrain Model is expressed mathematically as:

$A = 10 - 20C_N$, where A = Diffraction Loss in DB

$C_N = \frac{h}{F_1}$, where C_N = is the normalized terrain clearance

$h = h_L - h_O$, where h is the difference of the height of LOS link and obstruction height

$F_1 = \sqrt{\frac{d_1 d_2}{fd}}$, F_1 = height of first Fresnel zone.

d_1 = distance of obstruction from one antenna

d_2 = distance of obstruction from the other antenna

d = distance from transmitter to receiver in meters

f = frequency in MHz.

The ITU model uses a normalized terrain clearance and would not be a good candidate for the Black Point 2 area because of the high terrain irregularities (The propagation Model, 2008; Seybold, 2005).

The Elgi model is expressed mathematically as:

$L = G_B G_M \left[\frac{h_B h_M}{d^2}\right]^2 \left[\frac{40}{f}\right]^2$ where,

G_B = Gain of base station antenna, G_M = Gain of mobile antenna (db)

h_B = Height of base station antenna, h_M = height of mobile station antenna (meters)

d = distance from base station antenna to mobile antenna (meters)

f = frequency in MHz.

The Elgi model calculates path loss in one expression rather than summing losses from free space and the other attenuation sources presented above. A listed limitation of this model is its lack of accounting for vegetative obstruction; however this limitation should not impact calculations for either Black Point or the lunar surface (Lavergnat & Sylvain, 2000).

The Longley-Rice Model, also known as the Irregular Terrain Model (ITM), is a complex set of models each accounting for specific propagation loss sources (Seybold, 2005). Foore and Ida used the ITM to determine a set of fade depth values (dependant on frequency and antenna heights) which could be used in conjunction with a simpler path loss model to calculate expected loss for lunar surface radio transmission (Foore and Ida, 2007). Their recommended path loss equation follows:

L = $G_T G_R \left(\frac{h_T h_R}{d^2}\right)^2$, where

L = path loss

GT = Transmitter Gain (db)

GR = Receiver Gain (db)

h_T = height of transmitting antenna (meters)

h_R = height of receiving antenna (meters)

d = distance between transmitter and receiver (meters)

The research will analyze the performance of multiple attenuation algorithms in predicting the actual signal strength values measured at the Black Point test site in order to answer the following research question:

(RQ1F) For the Black Point lunar analog database as represented within an LTF Communications layer and ignoring effects due to terrain elevation variability, signal reflection, signal refraction, and Fresnel effect, what LTF S and Ka signal based generation and attenuation models and representational techniques are significant to the accurate estimation of the actual signal strength attenuation that are related to the distance between the transmitting and receiving stations?

NASA has requested that the communications signal strength indication provided to the user in a 3 level format, in order to reduce the contribution to user information overload. Current discussions with NASA scientists have focused on using (for coverage maps) green shading for good reception areas, yellow for lower transmission capability, and clear (no shading) for locations where signal transmission are predicted to be blocked. Considering this user interface requirement, it is possible that LTF communications prediction may not need to accurately match measured signal strengths in order to provide the correct indication to the user. This is the premise of the next research question:

(RQ1G) For the Black Point lunar analog database as represented within an LTF Communication layer, what LTF S band signal based generation and attenuation models and representational techniques are significant to the display of accurate signal strength prediction information to the user?

The graphical presentation of communications prediction information could be displayed in multiple formats depending on the available user interface. Since Google Earth is a current interface provided to the astronaut analogs, Keyhole Markup Language (KML) overlays are probable. However since EVA suits do not have the Google Earth interface, presentation for EVA analogs will likely be on a heads up type overlay and could consist of various formats. The following questions specifically address the end user display types, and display generation capabilities which are beneficial to both vehicle mounted and dismounted astronauts.

(RQ2A) For the Black Point lunar analog database, what graphical characterization in LTF is significant to the successful usability of the communications attenuation model to an astronaut analog?

(RQ2B) For the Black Point lunar analog database, what algorithmic techniques are significant to the rapid and accurate transfers of the chosen LTF communications attenuation model to active formats and venues with the greatest number of end-user systems such as Google Earth(Moon)?

3 RESEARCH METHOD

Chapter 3 provides details to inferential statistical research methodology used in this dissertation. The scope and limitations of the proposed research are defined in section 3.1. Section 3.2 reviews the general research questions posed in chapter 1 which are the basis for the derived specific research questions. Section 3.3 reviews each of the specific research questions, develops hypotheses for each, and proposes the specific test method for each. A summary of research questions and test methods is presented at the end of this chapter in Table 5.

3.1 Scope and Research Limitations

While the general research questions proposed above address celestial body exploration, the specific research questions address estimation and representation of a communications attenuation model of the BP2 lunar analog database. The scope of the analog research will be limited by available data and access to current NASA activities which support execution of the proposed experiments. Specifically, NASA is conducting lunar analogs at Black Point Lava Flow, Arizona because the terrain characteristics are similar to those encountered on the lunar surface. The ability to have line of sight between two points is thought to be a component to attenuation of a RF signal between the points. Line of Sight calculations executed within the LTF simulation are dependent upon accuracy of the modeled terrain and other factors that may not be available such as atmospheric conditions and material properties of the terra firma between transmitting and receiving stations. A coverage map layer that addresses solely signals blocked by terrain may be produced by showing line-of-sight from a given point to surrounding points.

Additionally, RF signal attenuation is also thought to be related to the type of signal and distance between the transmitting and receiving sites. Distance may contribute to the dissipation of strength signal as may other factors related to distance such as moisture in the air and minerals. A coverage map layer may be produced to show signal strength levels resulting from signal blockage and signal strength level distance attenuation. NASA scientists have requested three color indicators. Less than 78 decibels no coloration. Less than 82 decibels transparent yellow coloration. Above 82 decibels transparent green coloration.

For this research, a number of analysis will be performed as indicated below. In general, the signal strength predictions generate by LTF will be compared to actual signal strength measurements taken at Black Point for particular cells in and around scientific points of interest and along routes to and from those points. Routes to and from points of scientific interest will be pre-determined using LTF. Pre-determination of routes will be based on optimizing continuous communication coverage with analog earth and local base or relay stations.

Additional analysis will involve converting both actual and LTF estimated signal strength into the three categories Green, Yellow, and None for signal coverage maps and Green, Yellow, and Red for route signal coverage.. Analysis will involve categorical inferential analysis of the frequency distribution between correct colorations and incorrect colorations between LTF signal estimates and actual signal strengths converted into colorations.

Measurement of signal attenuation at Black Point will be done as part of operations and not experimentally designed to test the level of each factor influencing attenuation. Confounding of the factors can not be avoided given the fore mentioned limitations. Therefore, a single attenuation algorithm to be embedded within LTF will be focused on free space path loss. The classic path loss equation for energy dissipation is $P_R = P_T \left(\frac{\lambda}{4\pi d}\right)^2$, where λ= frequency, d= distance, P_R = power at receiver, P_T = Transmitter power (McLarnon, 1997). The Friis transmission equation adds transmitting antenna gain (G1) and receiving antenna gain (G2) to the path loss equation to yield: $P_R = G_1 G_2 P_T \left(\frac{\lambda}{4\pi d}\right)^2$.

For high frequency signals (100Mhz and above) with distances greater than a cutoff distance $d_c = \frac{4}{\lambda} h_T h_R$, the equation can be rewritten as the fourth power distance law (Linmartz, 1996):

$P_R = G_1 G_2 P_T \left(\frac{h_T h_R}{d^2}\right)^2$.

For our case the S band wavelength (0.128 meters), transmit antenna height (10 meters) and receiver antenna height (2 meters) provide a d_c = 625 meters. Since NASA has indicated that the range of the surface communications is 7 km, we assume the majority of transmissions will occur beyond the cutoff distance, so the fourth power distance equation is selected for the embedded LTF attenuation model.

It is important to note that this model is also a component of both the Elgi model and the Foore and Ida model discussed in Chapter 3. This will allow us to calculate the loss results of these alternate models using the output data from LTF and addition known variables. The Elgi and Foore and Ida models will be required for one of the tests define later in this chapter. The additional loss factors in these alternate models partially account for confounded losses resulting from reflections, refractions, and diffractions.

3.2 General Research Questions:

The general research question posed in chapter 1 are repeated here for reference. The following section 3.3 will review the specific research question derived from each general question, as well as hypotheses and test approach proposed for each. Table 5, at the end of this chapter, provides a summarized relational view of the research questions, hypotheses, and tests.

(RQ1) As analogs to Planetary and Heliophysic effects, what factors must the LTF database represent and at what resolution must the LTF database model these factors in order to represent attenuation of various communications signals due to geospatial and atmospheric effect to the extent that they influence planning and execution of analog lunar surface operations?

(RQ2) What are the human systems integration/interface components and what should their characteristics be so that astronauts receive spatial representations of various communications signal attenuations to affect timely and effective planning and execution of analog lunar surface operations?

RQ2 is not formally evaluated as part of this research. The research question and related research hypotheses are posed for expository purposes only. Insights on the research question and hypotheses will guide gathering of antidotal observations. It is hoped that the antidotal observations will guide interface improvements and refine the usability research question and hypotheses should this become a priority and resources be made available to investigate them.

3.3 Specific Research Questions

The following sections provide detailed discussion of the specific research questions arrived at in chapter 2. The discussion includes the development of hypotheses for each research question, and provides plans for testing the hypotheses where feasible given the research limitations provided in section 3.1.

3.3.1 Question RQ1A

(RQ1A) For the Black Point lunar analog database, what Terra Firma elevation model accuracy and resolution levels are significant to the accurate estimation of the actual signal strength attenuation within an LTF Communication Layer?

The resolution (post spacing distance) and elevation accuracy of the source topography data used to generate the LTF database is likely significant to the accurate prediction of terrain blockage and terrain based attenuation of RF transmissions. The following hypotheses are generated to express the expected outcome of each source data parameter.

(RQ1AH1) Source data elevation accuracy is correlated to the accurate prediction of signal attenuation; greater elevation accuracy will yield more accurate attenuation predictions within the LTF communications layer.

(RQ1AH2) Source data elevation post spacing is correlated with the accurate prediction of signal attenuation; smaller post spacing will yield more accurate attenuation predictions within the LTF communications layer.

(RQ1AH3) Generated database elevation post spacing is correlated with the accurate prediction of signal attenuation; smaller post spacing in the generated database will yield more accurate predictions within the LTF communications layer.

RQ1AH1, RQ1AH2, RQ1AH3 are not tested due to the confounding of the DB attributes which will not allow us to evaluate the influence of either individual attribute on the predicted signal attenuation. In order to perform these tests a minimum of 4 databases having the following characteristics would be required:

DB1 : A post spacing, X elevation accuracy

DB2 : A post spacing, Y elevation accuracy

DB3: B post spacing, X elevation accuracy

DB4: B post spacing, Y elevation accuracy.

3.3.2 Question RQ1B

(RQ1B) For the Black Point lunar analog database and without regard to effects arising from terra firma material or atmospheric properties, what terra firma elevation model accuracy and resolution levels are significant to the accurate estimation of signal attenuation due to terrain blockage?

Greater accuracy and resolution in the simulated terrain database should provide a more accurate simulation of signals blocked by terrain. The following hypotheses are derived from RQ1B.

(RQ1BH1) For S band signal types and without regard to terra firma material or atmospheric properties, databases generated from lower elevation accuracy and lower resolution (larger post spacing) source data will demonstrate lower accuracy for signal strength attenuation based on the first elevation post height along a line-of-sight azimuth between the signal source and the receiving station that is greater than both the elevation height of the signal source and the receiving station elevation post.

For the purposes of this experiment there are two terrain database sources available for the Black Point exercise area: SRTM DTED Level 2 and the NASA provided DEM derived from LIDAR data. These two source files have different post spacing, and different elevation accuracy. The SRTM source data has both lower resolution and lower elevation accuracy than the NASA provided source. Therefore hypothesis RQ1BH1 can be tested.

Data collection was planned as follows: During the Black Point March 2010 site visit, RF signal strength data would be collected for this hypothesis and hypotheses as applicable below. Signal strength readings would be taken between a fixed location (Base) antenna and a mobile radio moving along a route and/or within exploration interest areas. At each data collection point, GPS location and S band signal strength would be recorded. The RF data collection points were to be in and around specific points of interest identified by NASA based on planned activities for the 2010 Desert RATS analogs. Equipment required for collection of signal strength data included:

- GPS receiver
- RF signal measurement.

NASA had provided a set of Black Point coordinates which identified locations to be explored during the 2010 Desert RATS analogs currently scheduled for late May. At NASA's request, these data points are not published. NASA had also provided the coordinates for a base station transmitter. The data collection plan was to transmit a fixed strength S-band signal from a fixed antenna location. The data collection team would then traverse the Black Point site to each of the identified exploration points. RF signal strength measurements would be recorded along the traverse path, and at multiple location in the immediate vicinity of each exploration point. A NASA communications representative would accompany the data collection team to provide additional guidance on measurement locations.

NASA had also provided location coordinates for a point which represents the Earth low on the lunar horizon (as it would be for a lunar south pole exploration mission).

For this hypothesis, signal strength at each given terrain coordinate would be compared to simulation results in each database. The comparison of simulated results against measured field results would determine which database best predicted transmissions blocked by terrain.

A Chi Square Test with the following parameters would be used: Medium effect size, $\alpha = 0.05$, $\beta = 0.02$, 188 independent samples from each treatment. (Cohen, 1992).

Table 4 Proposed Test Matrix for RQ1BH1

Prediction	LIDAR predicts blockage	SRTM predicts blockage
Measured signal matched prediction		
Measured signal does not match prediction		

Null hypothesis (H_0): Observed = Expected.

Alternative hypothesis (H_a): Observed ≠ expected.

3.3.3 Question RQ1C

(RQ1C) For the Black Point lunar analog database, what terra firma material properties are significant to the accurate modeling of RF transmission signal attenuation within an LTF Communications layer?

(RQ1CH1) Completeness and accuracy of source and generated terrain material properties is correlated with the accuracy of predicted communications attenuation within the LTF communications layer.

Attenuation due to material properties cannot be removed from the collected actual RF signal strength data, or collected separately from other attenuation factors, so this hypotheses is not tested.

3.3.4 Question RQ1D

(RQ1D) For the Black Point lunar analog database, what feature and object properties are significant to the accurate modeling of RF transmission communications signal attenuation within an LTF Communications layer?

(RQ1DH1) Completeness and accuracy of source and generated objects near the communications line of sight is correlated with the accuracy of predicted communications attenuation within the LTF communications layer.

Attenuation due to features and objects cannot be removed from the collected actual RF signal strength data, or collected separately from other attenuation factors, so this hypotheses is not tested.

3.3.5 Question RQ1E

(RQ1E) For the Black Point lunar analog database, what atmospheric attenuation properties are significant to the accurate modeling of RF transmission communications signal attenuation within an LTF Communications layer?

(RQ1EH1) Completeness and accuracy of source and generated atmospheric conditions are correlated with the accuracy of predicted communications attenuation within the LTF communications layer.

Attenuation due to atmospheric conditions cannot be removed from the collected actual RF signal strength data, or collected separately from other attenuation factors, so this hypothesis is not tested.

3.3.6 Question RQ1F

(RQ1F) For the Black Point lunar analog database as represented within an LTF Communications layer and ignoring effects due to terrain elevation variability, what LTF S and Ka signal based generation and attenuation models and representational techniques are significant to the accurate estimation of the actual signal strength attenuation that are related to the distance between the transmitting and receiving stations?

LTF communications attenuation algorithms will include components representing attenuation due to free space path loss, reflection, diffraction, and refraction. The LTF communications layer is capable of storing terrain material parameters which affect the attenuation algorithms. The following hypotheses are derived from RQ1F.

(RQ1FH1) The LTF communication layer signal generation and attenuation algorithm and related models account for all generation and attenuation sources including signal source power, frequency, free space path loss, reflection, diffraction, and refraction with

respect to each earth-based RF communication signal that significantly influences astronaut communications during the Black Point analog exercises.

Terrain material properties which may affect attenuation are not available for the Black Point analog locations, therefore this hypothesis is not tested.

(RQ1FH2) For the Black Point lunar analog database as represented within an LTF Communications layer and ignoring effects due to terrain elevation variability, signal reflection, signal refraction, and Fresnel effect , the LTF S band generation and attenuation model will predict signal strength reception for transmissions which are not blocked by the terrain.

The attenuation model implemented within LTF will be a fourth power distance model of free space path loss:

$L = G_B G_M \left[\frac{h_B h_M}{d^2}\right]^2$ where,

G_B = Gain of base station antenna, G_M = Gain of mobile antenna

h_B = Height of base station antenna, h_M = height of mobile station antenna

d = distance from base station antenna to mobile antenna

The LTF Signal Strength predictions based on the embedded loss model above will be compared to the actual signal strength measurements recorded at Black Point. This test is only run against the higher fidelity LIDAR derived LTF database since it is believed that this database will be more accurate than the SRTM derived database.

Two tailed Independent t Test with $\alpha = 0.01$, and $\beta = 0.01$, requiring a sample size of 64. The degrees of freedom = 128 - 2 = 126. (Faul, Erdfelder, Buchner, Lang, 2009).

μ_{LTFSS} = mean LTF signal strength prediction error

Null hypothesis (H_0): $\mu_{LTFSS} = 0$

The alternative hypothesis (H_a): $\mu_{LTFSS} \neq 0$

(RQ1FH3) For the Black Point lunar analog database as represented within an LTF Communications layer and ignoring effects due to terrain elevation variability, signal reflection, signal refraction, and Fresnel effect , the LTF Ka band generation and attenuation models will predict signal strength reception for transmissions which are not blocked by the terrain. The required assets to transmit and receive Ka band transmissions will not be available during the data collection trip, hence this hypothesis is not tested.

(RQ1FH4) For S band signal types tested and without regard to terra firma material or atmospheric properties, databases generated from lower elevation accuracy and lower resolution (larger post spacing) source data will demonstrate lower accuracy for signal strength attenuation based on greater distance between the signal source and the receiving station for signals not blocked by terrain.

This hypothesis will be tested for S band signal transmissions which are not blocked by the terrain for each terrain model. The LTF predicted signal strength will be based on the embedded attenuation algorithm defined in RQ1F2 above.

Independent T Test with $\alpha = 0.05$, and $\beta = 0.2$, requiring a sample size for each group of 64. The degrees of freedom = 128 - 2 = 126. (Faul et al., 2009).

For each terrain model prediction error will be calculated as:

PE = Prediction error = Predicted signal strength - Actual Signal Strength

μ_{DB1PE} = mean error for predictions from database 1 (LIDAR source)

μ_{DB2PE} = mean error for predictions from database 2 (SRTM source)

Null hypothesis (H_0):$\mu_{DB1PE} = \mu_{DB2PE}$

The alternative hypothesis (H_a): $\mu_{DB1PE} \neq \mu_{DB2PE}$

(RQ1FH5) For Ka band signal types tested and without regard to signal source power, terra firma material or atmospheric properties, databases generated from lower elevation accuracy and lower resolution (larger post spacing) source data will demonstrate lower accuracy for signal strength attenuation based on greater distance between the signal source and the receiving station for signals not blocked by terrain. The required assets to transmit and receive Ka band transmissions will not be available during the data collection trip, therefore this hypothesis is not tested.

3.3.7 Question RQ1G

(RQ1G) For the BP2 lunar analog database as represented within an LTF Communication layer, what LTF S band signal based generation and attenuation models and representational techniques are significant to the display of accurate signal strength prediction information to the user?

(RQ1GH1) Given the 3 level RF signal strength depiction scheme requested by NASA, LTF signal attenuation models may not need to account for all attenuation sources (free space path loss, reflection, refraction, and diffraction) to accurately depict signal strength predictions to the user.

Each measured and predicted signal strength will be assigned a depiction level (0, 1, or 2) to represent the 3 levels of graphical depiction desired by NASA. The DB ranges to be assigned to each depiction level will be determined by NASA. This hypothesis will be tested with the non-parametric Cochran test. The degrees of freedom = 2, and $\alpha = 0.05$. 52 samples will be used for each treatment. The Critical region will be $T > \chi^2_{.950}$ =0.012587. (Mendenhall, 1995). The 3 treatments are - Free space model, Elgi model, and Free Space + Fade Depth values. The free space model will be based on the embedded LTF attenuation model. Since the free space loss is a component of the Elgi loss model, Elgi loss will be calculated as:

Free Space Path Loss * $\left[\frac{40}{f}\right]^2$ where, f = frequency in Mhz

For the Free space + Fade Depth loss, the Fade Depth values developed by Foore and Ida (Foore and Ida, 2007) for 2 meter antenna will be summed with the LTF calculated free space path loss. The value assigned each sample will be 0 if calculated signal strength provides the same color value as the black point measured signal strength, otherwise a 1 will be assigned. Null hypothesis (H_0): the three models do not provide equivalent graphical output. The alternative hypothesis (H_a): the three models do provide equivalent graphical output.

3.3.8 Questions RQ2A and RQ2B

Research questions RQ2A and RQ2B investigate the user needs related to graphical depiction of LTF output data. The initial test approach was to include collection and analysis of user surveys to test the related hypotheses. However rescheduling of the 2010 Black Point field trials has precluded the survey as only two NASA participant were available. These questions/hypotheses are retained here for any future researchers interested in pursuing such study.

(RQ2A) For the Black Point lunar analog database, what graphical characterization in LTF is significant to the successful usability of the communications attenuation model to an astronaut analog?

(RQ2AH1) The LTF communications predictions depicted as coverage maps will provide useful input for the user when antenna repositioning or relay antenna deployment is required to maintain LOS to the base antenna.

(RQ2AH2) The LTF communication predictions depicted as metered scales will provide useful input for determining current self or own vehicle communication capability while minimizing data load on the operator.

(RQ2B) For the Black Point lunar analog database, what algorithmic techniques are significant to the rapid and accurate transfers of the chosen LTF communications attenuation model to active formats and venues with the greatest number of end-user systems such as Google Earth(Moon)?

(RQ2BH1) LTF will need to support generation of KML coverage maps, for Google Earth end users, and will need to support extraction of query of location specific signal strength through the native API to accommodate all requirements of the NASA end users.

3.4 Post Processing of Collected Black Point Data

Post processing of the collected Black Point data was performed to create an LTF format LOS Ray Query configuration file. The LOS Ray Query file is a list of coordinate pairs (in geocentric coordinates) which are used by the LTF Viewer to executions a batch of LOS queries against an LTF terrain database. The list created from Black Point data will use the base antenna location as the first coordinate and the receiver location recorded for each measurement as the second coordinate. Where relay antennas are deployed, two coordinate pairs will be created (base antenna location, relay location) and (relay location, receiver location). When the configuration file queries are executed within the LTF Viewer tool, a signal strength value (at the receiver) will be calculated for each query using the (user input) transmit power value and the signal loss attenuation algorithm embedded in the LTF code. The calculated signal strength output is tested against the measured signal strength as defined earlier in this chapter.

Additional attenuation loss factors, used for the Elgi model, and the Foore and Ida fade depths, will be calculated within an excel spreadsheet and summed with the LTF calculated signal strength for use in the RQ1G hypothesis testing.

A second configuration file will be generated using the provided "Earth" location data in place of the base antenna location to allow generation of visual coverage maps indicating direct Earth communication capability. The generated Direct Earth coverage map will be shown in the usability concept demonstration.

3.5 Discussion of Reliability of LTF

Reliability specifications for LTF were a parameter requested by NASA at one of the research related meetings. Reliability is a numeric attribute which describes the average amount of time a component or system will operate between failures. Typically, the failure rate of hardware component is specified as the quantity of failures per 1 million hours of operation or 1 million cycles of operation dependant on the hardware being tested. Failure rates of individual components are summed up to determine failure rate of a higher level component/system and Mean Time Between Failures (MTBF), which is the mathematical inverse of failure rate, has become a commonly collected or required parameter in Government procurements. When dealing with a non-hardware system such as LTF, failures do not manifest themselves with the same clarity and certainty as with hardware. Software will inherently not fail – it does not age or fatigue with time as hardware does. Failure attributed to software systems more generally are the result of operator errors or errant input data. One approach to address reliability of a non-hardware system is to look at its potential to provide a desired correct output. Specifically, the "functional reliability" of a system can be defined as the percentage of time the system produces the correct output when tasked to perform. For LTF, the task is predicting RF signal reception given two antenna locations; output can be specified as a color (red/yellow/green) indication to the user of the predicted signal strength; and correct output being one that matches measured data. Reliability within the context of LTF performance will be calculated as: (number of correct predictions)/(total number of predictions). While this functional reliability approach, based on our limited data set, may not provide the equivalent confidence level of a 1 million hour test of hardware, it does provide a benchmark by which other systems performing similar functions can be compared, or which could be used to determine reliability improvements to LTF resulting from future ARA product line enhancements or research based modifications.

Table 5 Summary of Research Questions, Hypotheses, and Test Methods

Research Question	Specific Research Question	Hypotheses	Test Method or Not Tested.
(RQ1) As analogs to Planetary and Heliophysic effects, what factors must the LTF database represent and at what resolution must the LTF database model these factors in order to represent attenuation of various communications signals due to geospatial and atmospheric effect to the extent that they influence planning and execution of analog lunar surface operations ?	(RQ1A) For the Black Point lunar analog database, what Terra Firma elevation model accuracy and resolution levels are significant to the accurate estimation of the actual signal strength attenuation within an LTF Communication Layer?	(RQ1AH1) Source data elevation accuracy is correlated to the accurate prediction of signal attenuation; greater elevation accuracy will yield more accurate attenuation predictions within the LTF communications layer.	Not tested.
		(RQ1AH2) Source data elevation post spacing is correlated with the accurate prediction of signal attenuation; smaller post spacing will yield more accurate attenuation predictions within the LTF communications layer.	Not tested.
		(RQ1AH3) Generated database elevation post spacing is correlated with the accurate prediction of signal attenuation; smaller post spacing in the generated database will yield more accurate predictions within the LTF communications layer.	Not tested.
	(RQ1B) For the Black Point lunar analog database and without regard to effects arising from Terra Firma material or atmospheric properties, what Terra Firma elevation model accuracy and resolution levels are significant to the accurate estimation of signal attenuation due to terrain blockage?	(RQ1BH1) For all signal types tested and without regard to terra firma material or atmospheric properties, databases generated from lower elevation accuracy and lower resolution (larger post spacing) source data will demonstrate lower accuracy for signal strength attenuation based on the first elevation post height along a line-of-sight azimuth between the signal source and the receiving station that is greater than both the elevation height of the signal source and the receiving station elevation post.	Chi Square Test with one degree of freedom. $\alpha = 0.05$ Prediction | DB1 | DB2 | Correct | | | Incorrect | | | Null hypothesis (H0): NumberCorrectDB1 >= NumberCorrectDB2 Alternative hypothesis (Ha): NumberCorrectDB1 $<$ NumberCorrectDB2

Research Question	Specific Research Question	Hypotheses	Test Method or Not Tested.
(RQ1) As analogs to Planetary and Heliophysic effects, what factors must the LTF database represent and at what resolution must the LTF database model these factors in order to represent attenuation of various communications signals due to geospatial and atmospheric effect to the extent that they influence planning and execution of analog lunar surface operations ?	(RQ1C) For the Black Point lunar analog database, what terra firma material properties are significant to the accurate modeling of RF transmission signal attenuation within an LTF Communications layer?	(RQ1CH1) Completeness and accuracy of source and generated terrain material properties is correlated with the accuracy of predicted communications attenuation within the LTF communications layer.	Not tested.
	(RQ1D) For the Black Point lunar analog database, what feature and object properties are significant to the accurate modeling of RF transmission communications signal attenuation within an LTF Communications layer?	(RQ1DH1) Completeness and accuracy of source and generated features and objects near the communications line of sight is correlated with the accuracy of predicted communications attenuation within the LTF communications layer.	Not tested.
	(RQ1E) For the Black Point lunar analog, what atmospheric attenuation properties are significant to the accurate modeling of RF transmission communications signal attenuation within an LTF Communications layer?	(RQ1EH1) Completeness and accuracy of source and generated atmospheric conditions are correlated with the accuracy of predicted communications attenuation within the LTF communications layer.	Not tested.

Research Question	Specific Research Question	Hypotheses	Test Method or Not Tested.
(RQ1) As analogs to Planetary and Heliophysic effects, what factors must the LTF database represent and at what resolution must the LTF database model these factors in order to represent attenuation of various communications signals due to geospatial and atmospheric effect to the extent that they influence planning and execution of analog lunar surface operations ?	(RQ1F) For the Black Point lunar analog database as represented within an LTF communications layer and ignoring effects due to terrain elevation variability, signal reflection, signal refraction, and Fresnel effect, what LTF S and Ka signal based generation and attenuation models and representational techniques are significant to the accurate estimation of the actual signal strength attenuation that are related to the distance between the transmitting and receiving stations?	(RQ1FH1) The LTF communication layer signal generation and attenuation algorithm and related models account for all generation and attenuation sources including signal source power, frequency, free space path loss, reflection, diffraction, and refraction with respect to each earth-based RF communication signal that significantly influences astronaut communications during the Black Point analog exercises.	Not tested.
		(RQ1FH2) For the Black Point lunar analog database as represented within an LTF Communications layer and ignoring effects due to terrain elevation variability, signal reflection, signal refraction, and Fresnel effect , the LTF S band generation and attenuation models will predict signal strength reception for transmissions which are not blocked by the terrain.	Independent One SampleT Test μ_{LTFSS} = mean LTF signal strength prediction error Null hypothesis (H_0):$\mu_{LTFSS} = 0$ The alternative hypothesis (H_a): $\mu_{LTFSS} \neq 0$
		(RQ1FH3) For the Black Point lunar analog database as represented within an LTF Communications layer and ignoring effects due to terrain elevation variability, signal reflection, signal refraction, and Fresnel effect , the LTF Ka band generation and attenuation models will predict signal strength reception for transmissions which are not blocked by the terrain.	Not tested.

Research Question	Specific Research Question	Hypotheses	Test Method or Not Tested.
(RQ1) As analogs to Planetary and Heliophysic effects, what factors must the LTF database represent and at what resolution must the LTF database model these factors in order to represent attenuation of various communications signals due to geospatial and atmospheric effect to the extent that they influence planning and execution of analog lunar surface operations ?	(RQ1F) For the Black Point lunar analog database as represented within an LTF Communications layer and ignoring terrain elevation variability, what LTF S and Ka signal based generation and attenuation models and representational techniques are significant to the accurate estimation of the actual signal strength attenuation that are related to the distance between the transmitting and receiving stations?	(RQ1FH4) For S band signal types tested and without regard to terra firma material or atmospheric properties, databases generated from lower elevation accuracy and lower resolution (larger post spacing) source data will demonstrate lower accuracy for signal strength attenuation based on greater distance between the signal source and the receiving station for signals not blocked by terrain.	Independent T Test PE = Prediction error = Predicted signal strength - Actual Signal Strength μ_{DB1PE} = mean error for predictions from database 1 μ_{DB2PE} = mean error for predictions from database 2 Null hypothesis (H_0):$\mu_{DB1PE} <= \mu_{DB2PE}$ The alternative hypothesis (H_a): $\mu_{DB1PE} > \mu_{DB2PE}$
	(RQ1G) For the Black Point lunar analog database as represented within an LTF Communication layer, what LTF S band signal based generation and attenuation models and representational techniques are significant to the display of accurate signal strength prediction information to the user?	(RQ1GH1) Given combined Black Point LTF database and Friis transmission model, predicted Green/Red Coloration for either resolution terrain database are equivalent to observed signal reception.	Chi-Square Test of homogeneity Medium Effect size, $\beta = 0.02$, $\alpha = 0.05$. 188 independent LIDAR and 188 independent SRTM predicted signal receptions Null hypothesis (H_0): Treatments are equivalent The alternative hypothesis (H_a): Treatments are not equivalent
		(RQ1GH2) Given the 3 level RF signal strength depiction scheme requested by NASA, LTF signal attenuation models may not need to account for all attenuation sources (free space path loss, reflection, refraction, and diffraction) to accurately depict signal strength predictions to the user.	Analysis of Variance 3 Treatments - Free space model, Elgi model, and Free space + Fade depth values developed by Foore and Ida Null hypothesis (H_0):$\mu_{FS} \neq \mu_{Elgin} \neq \mu_{FS+FD}$ The alternative hypothesis (H_a): $\mu_{FS} = \mu_{Elgin} = \mu_{FS+FD}$

Research Question	Specific Research Question	Hypotheses	Test Method or Not Tested.
(RQ2) What are the human systems integration/interface components and what should their characteristics be so that astronauts receive spatial representations of various communications signal attenuations to affect timely and effective planning and execution of analog lunar surface operations?	(RQ2A) For the Black Point lunar analog database, what graphical characterization in LTF is significant to the successful usability of the communications attenuation model to an astronaut analog?	(RQ2AH1) The LTF communications predictions depicted as coverage maps will provide useful input for the user when antenna repositioning or relay antenna deployment is required to maintain LOS to the base antenna.	Not tested.
		(RQ2AH2) The LTF communication predictions depicted in a non-map format, such as metered scales, alpha-numeric reception power values, or colored alpha-numeric characters, will provide useful input for determining current EVA or own vehicle communication capability while minimizing data load on the operator.	Not tested.
	(RQ2B) For the Black Point lunar analog database, what algorithmic techniques are significant to the rapid and accurate transfers of the chosen LTF communications attenuation model to active formats and venues with the greatest number of end-user systems such as Google Earth(Moon)?	(RQ2BH1) LTF will need to support generation of KML coverage maps, for Google Earth end users, and will need to support extraction of query of location specific signal strength through the native API to accommodate all requirements of the NASA end users.	Not tested.

4 DATA COLLECTION AND ANALYSIS

Chapter 4 presents the communication coverage data collected during the two days of experiments executed at the Black Point Lava Flow site in Arizona. This field data was processed and filtered as required to provide specific data sets needed for evaluation with respect to LTF predicted communication coverage. The statistical tests and hypotheses used in the evaluation were those proposed in Chapter 3. Results of these statistical tests are discussed in detail including any anomalies noted during the experiment which may affect validity of the collected data or test results.

4.1 Raw Data

- The data collected in Black Point was recorded on NASA PC assets, therefore the raw data is provided in the format in which it was delivered by NASA to the UCF team. Black Point Lava Flow data collection trip occurred March 16-19, 2010.
- NASA provided Tropos Networks radios and data logging hardware, points of interest as defined in 2010 Desert RATS planning sessions, and Engineering support for execution of data collection and processing of collected data.
- Data collection consisted of deploying a fixed site antenna and then traversing a preplanned path with a mobile antenna (Figures 1 and 2).
- Data points recorded:
  - Fixed and Mobile antenna location (GPS)
  - Transmission Signal Strength (DB), noise and modulation rate
  - Transmit Power, Antenna Gains

Figure 1 Fixed Tropos Radio Deployment

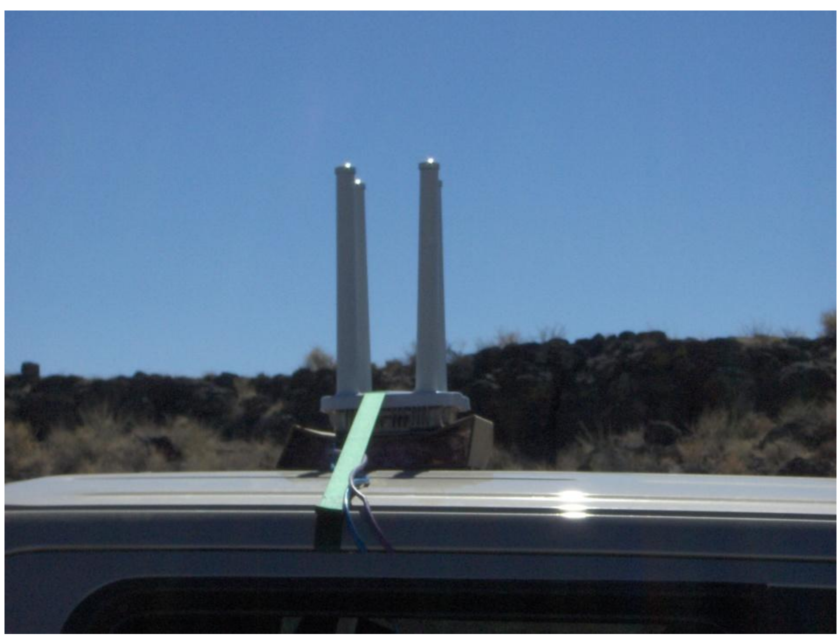

Figure 2 Mobile Tropos Radio Deployment

The delivered files were provided in Comma Separated Variable format to allow easy import to both Microsoft Excel and the LTF Viewer application. The files provided and their contents are summarized in Table 6. The numeric suffix on the file name is a timestamp that identifies related files. Appendix A provides the printed files.

Table 6 Tropos Output Data Files

Tropos.500 – 69Kb – Data for mobile radio on path1					
Data	Min	Max	Median	Average	Mode
Time (epoch)	1268847841	1268863304	1268852914	1268854730	1268849285
Latitude (degrees)	35.58922	35.63641	35.60538	35.60883	35.59746
Longitude (degrees)	-111.61611	-111.53287	-111.5924	-111.58697	-111.60172
Altitude (meters)	1680.196	1813.871	1754.57	1755.962	1796.204
Distance (meters)	0.783	6638.120	1614.764	2168.706	0.783
Signal Strength (dB)	-87	-22	-73	-70.34	-73
Noise (dB)	-100	-69	-91.5	-89.32	-95
Modulation (sym/sec)	2	108	36	47.6	108
Tropos.505 – 21Kb – Data for mobile radio on path 2					
Data	Min	Max	Median	Average	Mode
Time (epoch)	1268868583	1268871339	1268870019	1268870022	1268871339
Latitude (degrees)	35.65891	35.71626	35.66452	35.67821	35.65999
Longitude (degrees)	-111.53053	-111.46451	-111.50096	-111.49952	-111.53052
Altitude (meters)	1551.488	1629.644	1590.66	1590.545	1629.644
Distance (meters)	0.908	15601.066	4033.890	3793.869	6605.184
Signal Strength	-87	-20.5	-75.69	-70.84	-81
Noise (dB)	-99	-88	-95.62	-94.59	-96
Modulation (sym/sec)	2	108	33.62	37.87	48
Tropos.727 – 19Kb – Data for mobile radio on path 3					
Data	Min	Max	Median	Average	Mode
Time (epoch)	1268940836	1268945075	1268942993	1268942904	#N/A
Latitude (degrees)	35.55099	35.59464	35.56379	35.56665	35.55140
Longitude (degrees)	-111.65929	-111.62151	-111.63949	-111.63820	-111.63950
Altitude (meters)	1844.511	1976.33	1923.508	1919.046	1972.104
Distance (meters)	0	5124.993	1876.340	2047.113	0.941
Signal Strength (dB)	-89	-20	-74.88	-67.75	-85.89
Noise (dB)	-98	-84.8	-96	-94.81	-96
Modulation (sym/sec)	2	108	22.975	38.841	22

4.2 LTF Communication Coverage Predictions and Signal Strength Predictions

The LTF Viewer communication coverage prediction maps were generated using the target antenna locations provided in the target.xxx files (reference Table 6). The output maps are generated in a KML format allowing them to be imported/displayed in Google Earth (or equivalent GIS tool). For each antenna location two maps were generated as discussed further below, one using the LIDAR derived LTF database and the second using the SRTM derived LTF database. Figures 3 provides a Google Earth screenshot showing the coverage map generated with the LIDAR derived LTF database DB for the path 1 fixed antenna position. The green and yellow shading indicate the minimal signal strength levels of -71 db and -96 db respectively. 71db is the minimum signal strength which supports IEEE 801.11 G data rates, -96 db is the minimum signal strength which supports IEEE 801.11 A/B data rates. For coverage maps generated with the SRTM derived LTF database, the colors used are blue and orange. LTF is a proprietary product of Applied Research Associates (ARA). Details on LTF should be sought from ARA.

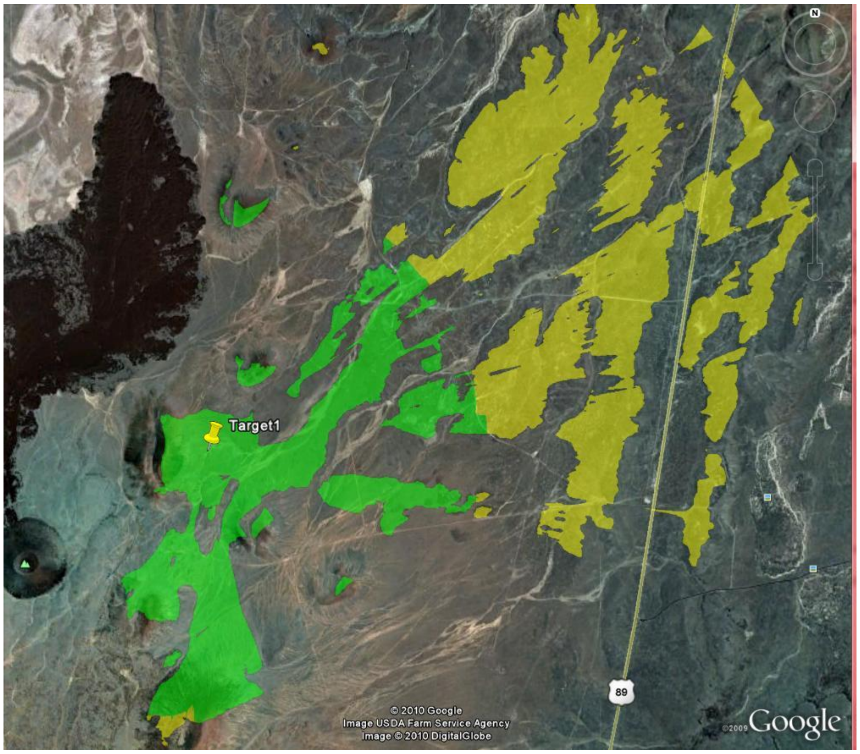

Figure 3 LIDAR Communications Coverage Prediction Map

Figures 4 through 6 show the superimposed SRTM and LIDAR coverage maps for fixed antenna locations for paths 1, 2, and 3. These over-laid graphical coverage maps provide a general indication of the difference in predicted coverage resulting from different resolution and accuracy levels of the LTF terrain database source.

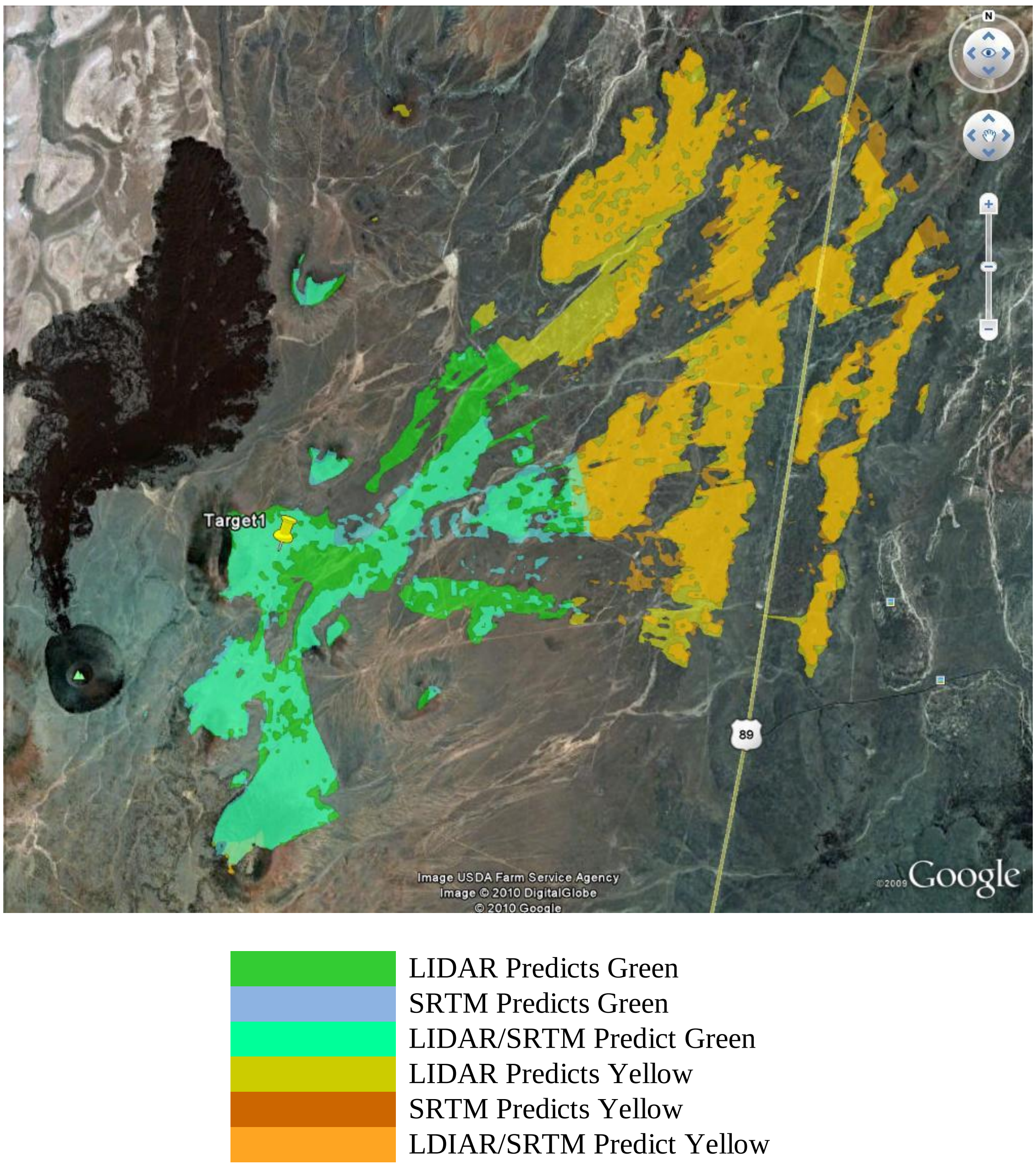

Figure 4 Overlaid SRTM and LIDAR Communications Coverage Prediction Maps for Path 1

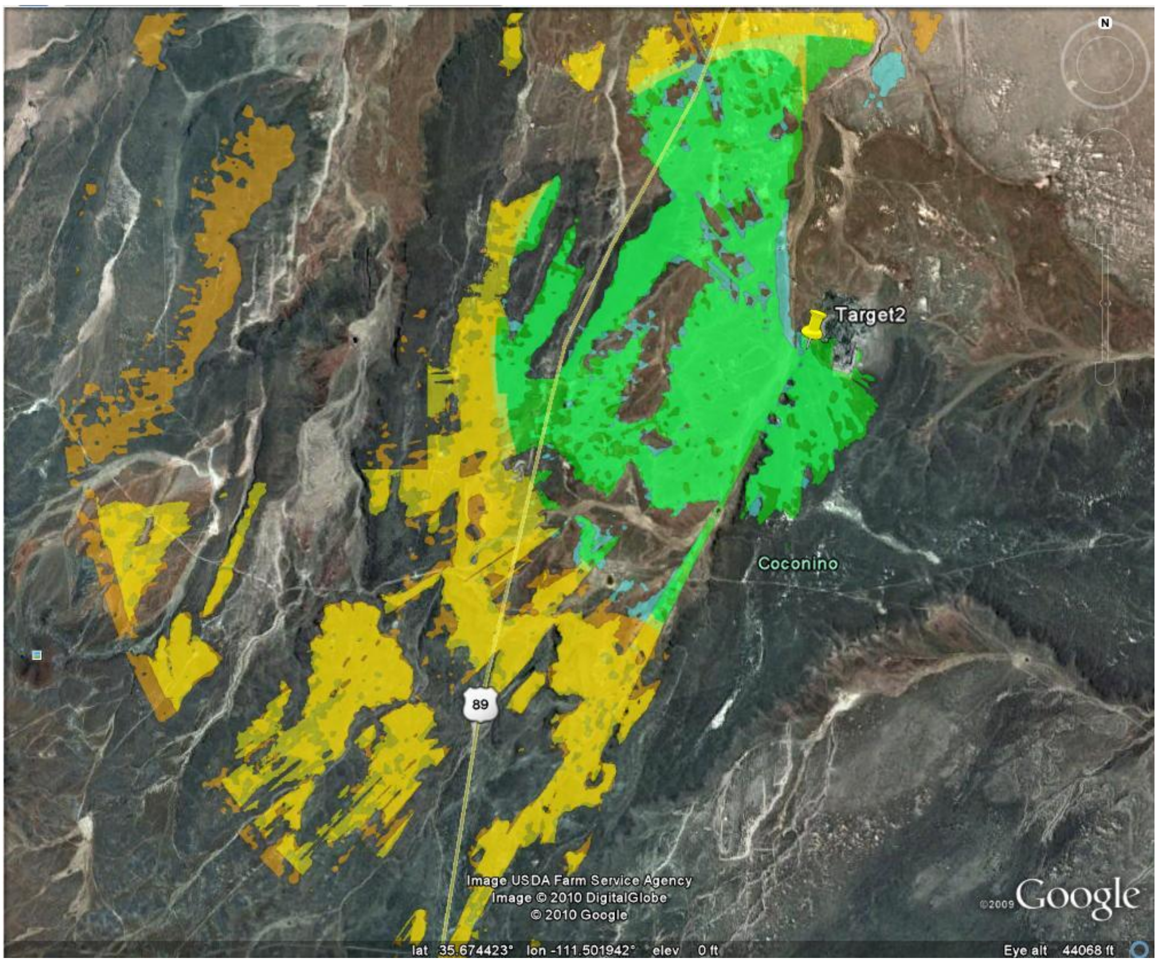

LIDAR Predicts Green
SRTM Predicts Green
LIDAR/SRTM Predict Green
LIDAR Predicts Yellow
SRTM Predicts Yellow
LDIAR/SRTM Predict Yellow

Figure 5 Overlaid SRTM and LIDAR Communications Coverage Prediction Maps for Path 2

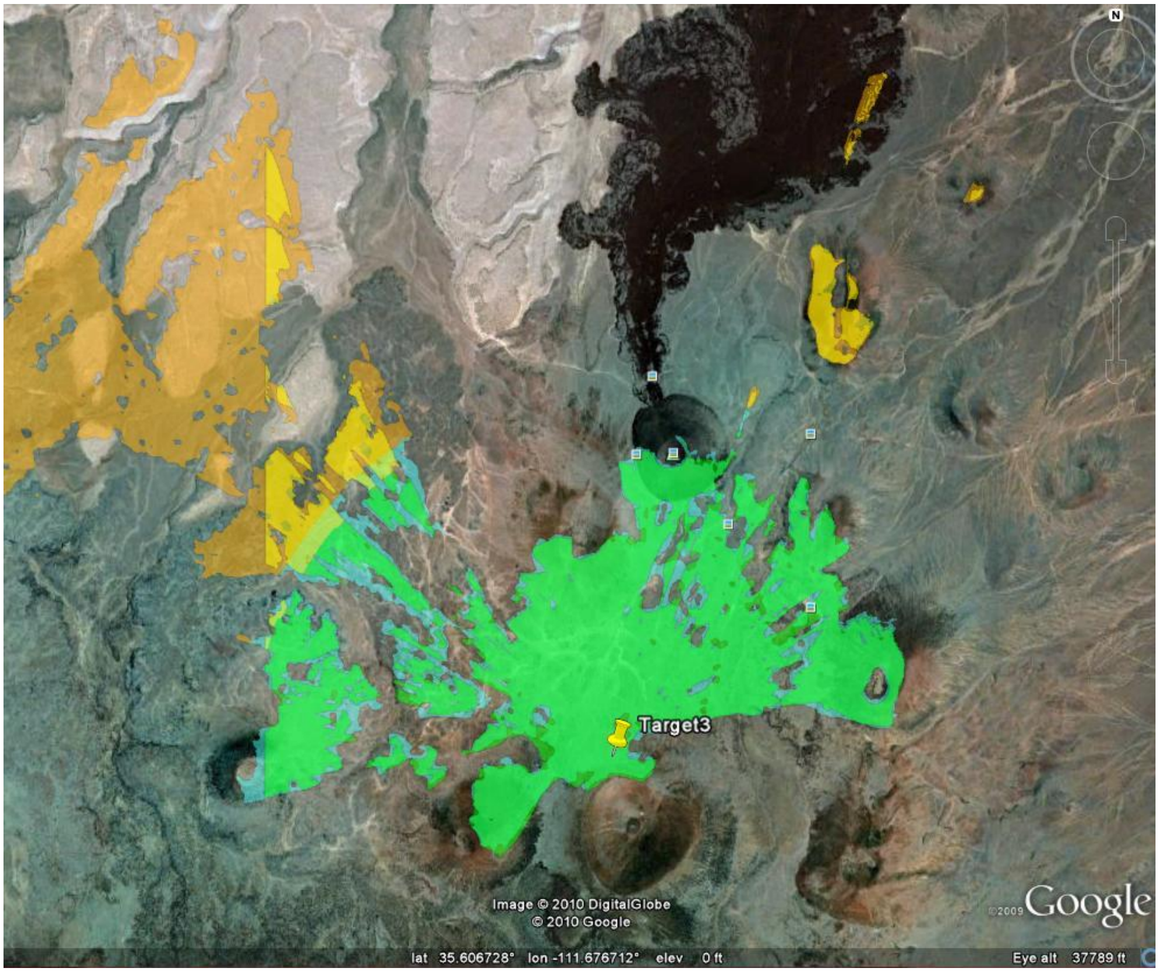

LIDAR Predicts Green
SRTM Predicts Green
LIDAR/SRTM Predict Green
LIDAR Predicts Yellow
SRTM Predicts Yellow
LDIAR/SRTM Predict Yellow

Figure 6 Overlaid SRTM and LIDAR Communications Coverage Prediction Maps for Path 3

In addition to generation of fixed antenna coverage maps, the LTF tool provides the capability to calculate signal strength between given antenna locations. Antennas locations may be manually entered in the viewer tool or positioned in the rendered view via mouse click. Antenna pairs can also be parsed in from a file. For the analysis of the Black Point data, the fixed antenna locations are entered into the tool manually via the user GUI, and the mobile antenna GPS locations provided in the tropos.xxx files are parsed in. LTF calculates the elevation and received signal strength for each location specified in the file. The results are output (along with the input data) to a user specified file.

The generation of communications coverage maps is a new capability in LTF that was funded through UCF and added by ARA to facilitate this research. To support the coverage map generation, UCF also funded ARA to implement the LTF Communications layer. The communications layer provides the capability to model antennas and provides an RF Signal attenuation algorithm which previously did not exist in LTF.

Additional modifications to the LTF Viewer (user interface) application funded by UCF and performed by ARA in support of the NASA defined case study include:

- GUI controls for coverage map generation capability. Coverage maps may be displayed as overlays within the LTF Viewer. LTF GUI also now supports export of coverage maps as saved images in a variety of formats with appropriate Google Earth KML to import into Google Earth
- GUI control for antenna deployment and antenna parameter setup. The relevant properties required and able to be supported when adding a radio model are: antenna height above surface, antenna gain (dBi), frequency, and transmit power (dBm). Radio specs for specific devices (LER / PCT / PUP) can be entered through the LTF

GUI. Antenna/Relay configuration can also be exported to Google Earth so users can show where the relays were that generated a coverage map.

- GUI control for dynamic antenna movement and RF relay placement with real time graphical signal-link updates.   Capability to switch between embedded signal models including Friis Transmission Equation and Geometric Line-Of-Site on the fly was also added.

The modifications funded by UCF and performed by ARA included no changes to Database Storage Architecture. Where possible, current capabilities were leveraged for the needs of NASA, such as the LTF high-performance ray tracer which is used to predict area radio coverage with millions of LOS queries.

The Google Earth export capabilities were added because the NASA Lunar Surface System team heavily uses Google Earth for mapping, coverage analysis, and manual route planning. With funding by UCF, ARA developed LTF / RAVEN support for export of coverage map to standard color image files with corresponding KML metadata for correct rendering in Google Earth.   UCF also funded ARA to produce multiple LTF terrain databases of region using GOTS software (RUGUD 1.4) from varying resolution and fidelity source data. SRTM and LIDAR databases were built successfully of roughly a 27km x 27km section of the Black Point area. SRTM DB used 30m (DTED2) +/- 16 meter source data. LIDAR DB used 1m +/- 10 Centimeters source data.

During testing of the LTF modifications, LTF radio prediction overlays matched well to the prediction overlays that were developed by a NASA LSS radio engineer, but were much higher resolution (10m grid vs. 100m radial sampling) and also took less time to generate. A coverage map based on sampled 10 meter post drawn from the one meter LIDAR database took overnight to generate. (27km x 27km). A coverage map for INTERPOLATED 10 meter post drawn from the 30 meter SRTM took a little over 2 hours to calculate. (27km x 27km). A LIDAR coverage map created using ONE meter posts WAS NOT attempted by ARA for the 27 Km by 27 Km area. The stated rationale was that it would take approximately “100x longer” (1200 hours) in a worst case scenario and thereby overrun the amount time available prior to the Arizona data collection trip and available funding. The databases were tested with approximately 36 million LOS queries, most of which are over a much longer distance than ever tested before, since typical Army LTF databases are 2Km x 2Km. The LTF software is capable of processing and producing the coverage maps needed for experiment. Radio specifications used for generating these coverage maps for each database were based on specifications from the Tropos Network radios: 36 dBm transmit power, 7.4 dBi antenna gain (Tropos 5320).

4.3 Statistical Analysis

For the proposal phase of the dissertation process, the size of the sample population for the statistical tests were designed using a traditionally accepted beta value of 0.2 and an alpha value of 0.05, as selected from the recommendations in Table 2 of Cohen (1992). These ESTIMATED parameters were used in conjunction with Table 2 of Cohen and the EXPECTED evaluable data to determine sample sizes required for each test, so that a data collection plan could be developed.   Since projected reception or non-reception of a data signal and signal reception measures are above or below threshold are dichotomous and ordinal, predictive and observed data can be categorized in a 2X2 matrix. The Chi-square test for homogeneity is more broadly used in inferential statistics to evaluate two independent samples whereas the McNemar test is used to evaluate two-related samples in such cases (Daniel, 1978, p 174 & 146). Cochran's Q test is used to test the homogeneity of three or more related samples (Daniel, 1978, p 241).   One or two sample t-tests are used when comparing means of interval data (Cohen, 1992).

During ACTUAL analysis, a statistical tool, G*Power (Faul, Erdfelder, Buchner, Lang, 2007) was used to calculate exact alpha, beta and power parameters for each test. G*Power allows the user to specify test type and multiple parameters to calculate a specific parameter such as required sample size.   In all cases, the sample size estimates indicated by Cohen’s tables were larger than the samples calculated by G*Power, given the same alpha, beta, and effect size values.   Rather than using fewer samples, the tests performed used the larger sample sizes initially estimated, thus providing better resulting values of beta, alpha and power. For each test discussed in chapter 4, the final test parameters as calculated by G*Power are provided.

4.4 RQ1BH1 Test and Analysis

(RQ1BH1) For S band signal type and without regard to terra firma material or atmospheric properties, databases generated from lower elevation accuracy and lower resolution (larger post spacing) source data will demonstrate lower accuracy for signal strength attenuation based on the first elevation post height along a line-of-sight azimuth between the signal source and the receiving station that is greater than both the elevation height of the signal source and the receiving station elevation post.

The simplified RQ1BH1 null hypothesis states: Higher (LIDAR) and lower (SRTM) resolution terrain databases will predict blockage using a go/no go standard of within range RF signal pairings with equal accuracy. Field data required to test hypothesis RQ1BH1, including the Tropos radio output data and the LTF signal strength predictions using both the LIDAR and SRTM databases. Both databases are combined in the data table provided in Appendix C. The LIDAR data was generated at the one meter post accuracy but sampled at 10 meter intervals in order to make the coverage map. Therefore the effective resolution of the LIDAR coverage map calculation was 10 meter posts. The SRTM database was generated at posts every meter but the values were based on post accuracy of every 30 meters. Furthermore, the SRTM coverage map was generated by sampling the interpolated posts every 10 meters. As this test is concerned with blockage of the radio signal by the terrain, Appendix C only contains the data for which the LIDAR and SRTM predictions indicated a blocked signal.

Data collected to test this hypothesis is ordinal and categorical and can be expressed in a 2X2 matrix. As explained above, the broadly accepted Chi-square test of homogeneity was implemented with the following estimated parameters.Using Cohen Table 2 designed for one degree of freedom (Colums-1)*(Rows - 1) = 1; a estimated medium effect size, β = 0.2, alpha of 0.05 yields a sample size of 87 for each sample. The medium effect size (0.3) is estimated based on the expectation that the difference in elevation accuracy of the two sample databases would provide significant differences in prediction accuracy, however these differences would be less apparent when looking at signal strength color assignments or terrain blockage than when looking at raw signal strength. In a worse case scenario where the actual effect size was small, 785 samples would be needed for each sample population. With our data collection limitations we were able to standardize on 188 data points in each sample population which would be more than enough to meet the expected parameter levels with medium effect size. The 188 independent LIDAR and 188 independent SRTM data points were selected randomly from all blocked predictions within each database group. The LTF predictions were then compared to actual Black Point signal measurements for each receiver location to determine if a blocked signal (<71 dBM) was recorded.

Figure 7 provides the statistical test parameters as calculated within the G*Power tool (Faul et al., 2009).

H_0: Observed = Expected.

H_a: Observed ≠ expected.

The critical value of X^2 is 3.8415.

The full test data are provided in Appendix C. The chi-square test matrix shown in Table 7 provides the results of the observations.

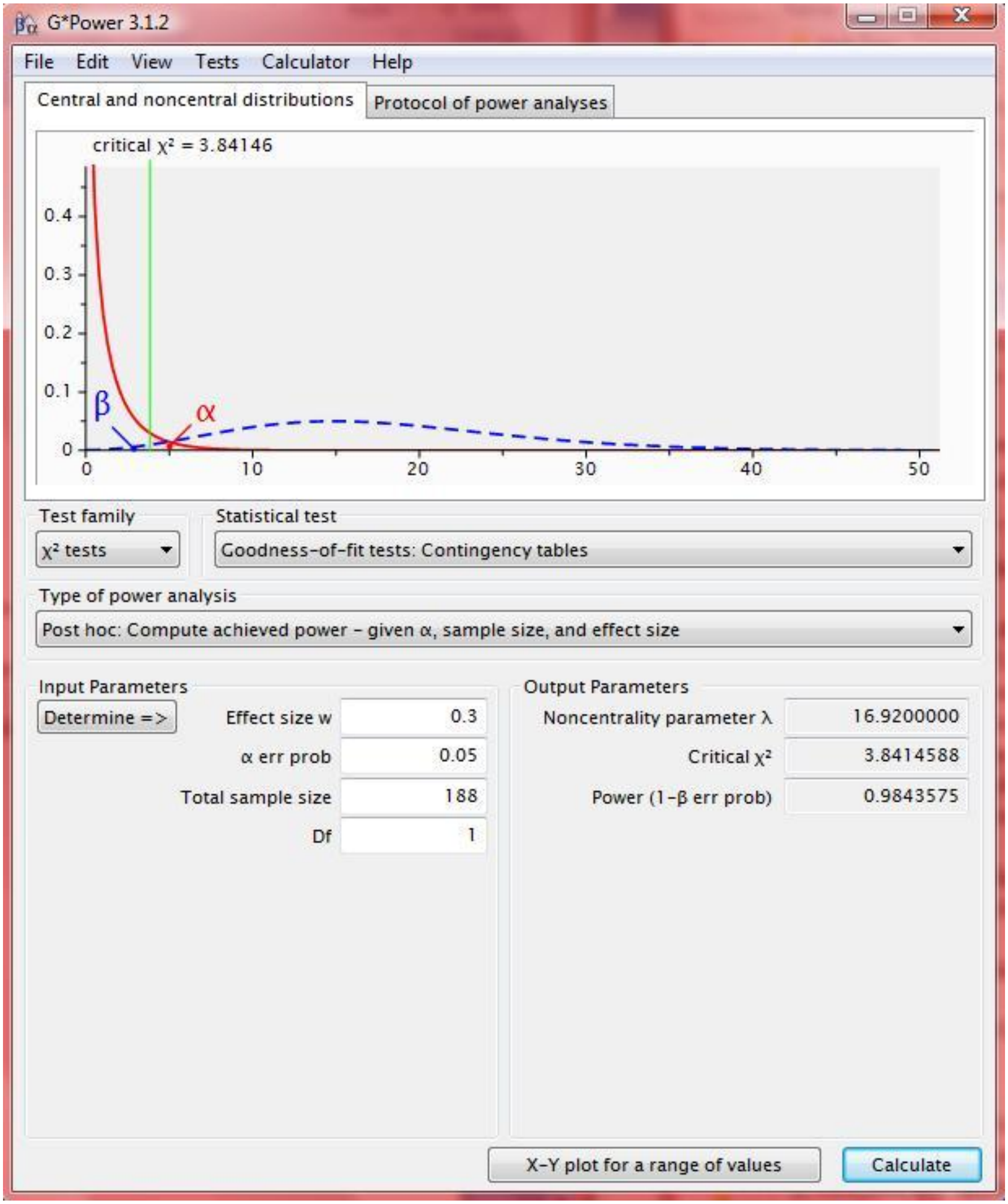

Figure 7 Statistical Test Parameters

Table 7 Chi Square Test Matrix for RQ1BH1

	Treatments		
	LIDAR predicts blockage	SRTM predicts blockage	*Row Totals*
Measured value matches prediction	149	140	289
Measured value does not match prediction	39	48	87
Column Totals	188	188	376

Expected frequencies are calculated as follows:

E_{11} = 188*289/376 = 144.5

E_{12} = 188*289/376 = 144.5

E_{21} = 188*87/376 = 43.5

E_{22} = 188*87/376 = 43.5

The formula for chi-square is

$$X^2 = \sum \frac{(O-E)^2}{E}$$

X^2 = (149-144.5)^2/144.5 + (140-144.5)^2/144.5 +

(39-43.5)^2/43.5 + (48-43.5)^2/43.5

X^2 = 0.14014 + 014014 + 0.46552+ 0.46552 = 1.21132 ,   p-value = 0.2711.

As shown by the test criteria calculations in Figure 7, the actual calculated Power is 0.983, yielding a beta value of 0.017.

The test to reject H_0 is if X^2 > 3.8415: We cannot reject H_0 because the calculated X^2 value is not greater than the Critical value.   The results of the Chi-square test performed on the collected RF signal measurements and generated LTF signal strength calculations do not show a statistical difference in the prediction of blocked signals between: (a) the 10 meter post LIDAR communication coverage map generated on the LTF LIDAR database that is extrapolated by sampling from one meter spaced elevation post source data, and (b) the 10 meter post SRTM communication coverage map generated on the LTF SRTM database that is interpolated from thirty meter spaced elevation source data. The formula for static reliability for a single component system is $R_s = 1 - q$ (Kapu & Lamberson, 1977, p 57). The static reliability of the communication coverage predictions were:

- *Reliability (LIDAR) = 0.793*
- *Reliability (SRTM) =0.745*

4.5 RQ1FH2 Test and Analysis

(RQ1FH2) For the Black Point lunar analog database as represented within an LTF Communications layer and ignoring effects due to terrain elevation variability, signal reflection, signal refraction, and Fresnel effect , the LTF S band generation and attenuation models will predict signal strength reception for transmissions which are not blocked by the terrain.

The simplified RQ1FH2 null hypothesis states: Using the LIDAR LTF database, the Friis S band generation and attenuation model will predict individual unblocked signal strength measurements that are statistically equal to values measured in the field test. Since both the Friis model and actual signal strength measured in the field are interval data, the statistical test is used to evaluate this hypothesis that a two tailed Independent One Sample T Test with the following estimated design parameters: Medium effect size, power = 0.8, $\beta = 0.2$, $\alpha = 0.05$ yields a sample size of 64. The large effect size (0.8) is likely based on the expectation that the large difference in elevation accuracy of the two test databases would provide significant differences in prediction accuracy. The test looks for the mean error for predicted signal strengths on an interval scale to be zero. Data required to test hypothesis RQ1BH2 included the Tropos radio signal strength measurements and LTF LIDAR database signal strength predictions (see Appendix D). A total of 64 sample measurements are provided.

μ_{LTFSS} = mean LTF signal strength prediction error

Null hypothesis (H_0):$\mu_{LTFSS} = 0$

The alternative hypothesis (H_a): $\mu_{LTFSS} \neq 0$.

Figure 8 provides the statistical test parameters as output by the G*Power software program. With a large effect size value, the resulting alpha and beta error probabilities are 0.0015. For a given transmitter location, 64 receiver locations where signal strength was unblocked were randomly selected. The resulting 64 antenna pairs were executed in the LIDAR LTF database. Resulting signal strength predictions are provided in Appendix D. The mean of the predictions is -2.4334, standard deviation is 11.36. The t value is calculated as:

$$t = \frac{-2.4334}{11.36/\sqrt{64}} = 1.7137$$

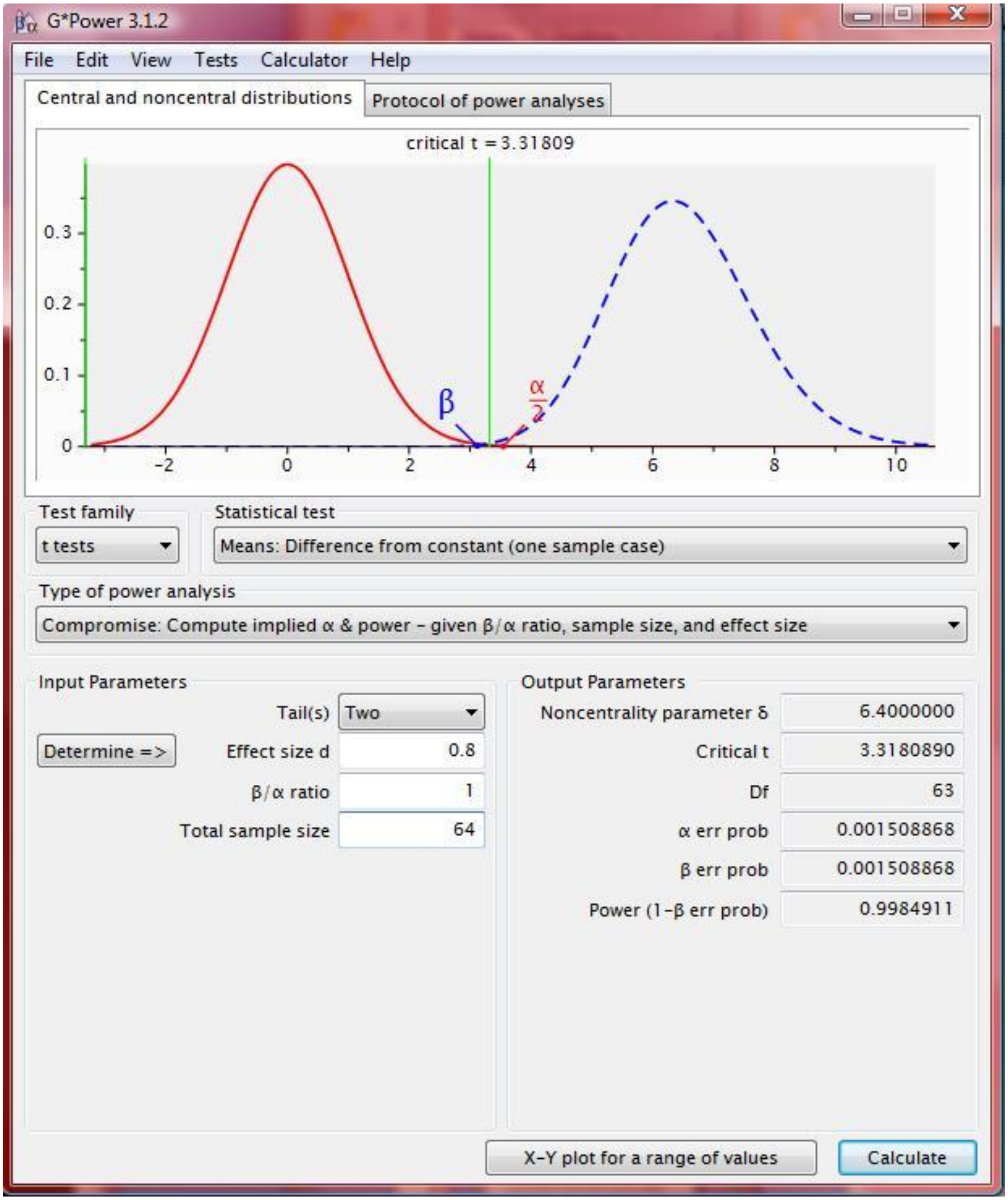

Figure 8 Statistical Test Parameters

Critical t = 3.32, but observed t = 1.714, p-value = 0.0915. Cannot reject H_0; since the calculated sample *t* is less than the critical t (3.32) the null hypothesis of equivalence could not be rejected. This finding infers that the attenuation model accurately attenuated the signal, which is good; however, our transmission distances were all below 10 KM which did not exceed the distance capabilities of Tropos transmission ranges meaning we were unable to test the attenuation model for accuracy beyond the theoretical range of the signal. A regression analysis that examines signal strength with distance will be performed to partially make up for this short coming.

4.6 RQ1FH4 Test and Analysis

(RQ1FH4) For S band signal types tested and without regard to terra firma material or atmospheric properties, databases generated from lower elevation accuracy and lower resolution (larger post spacing) source data will demonstrate lower accuracy for signal strength attenuation based on greater distance between the signal source and the receiving station for signals not blocked by terrain.

The simplified RQ1FH4 null hypothesis states that the higher resolution LIDAR database and the lower resolution SRTM database will predict unblocked signal strength with equal accuracy. The Two Sample T-Test was used to evaluate the hypotheses and based on Cohen used the following parameters: Medium effect size, Power= 0.80, $\beta = 0.2$, α= 0.05, and 64 samples per treatment. A large effect size (0.8) is likely based on the expectation that the large difference in elevation accuracy of the two test databases would provide significant differences in prediction accuracy. Data required to test hypothesis RQ1FH4, including the Tropos radio signal strength measurements, LTF LIDAR database signal strength predictions and LTF SRTM predictions are provided in Appendix E.

PE = Prediction error = Predicted signal strength - Actual Signal Strength

μ_{DB1PE} = mean error for predictions from database 1 (LIDAR database)

μ_{DB2PE} = mean error for predictions from database 2 (SRTM database)

Null hypothesis (H_0):$\mu_{DB1PE} = \mu_{DB2PE}$

The alternative hypothesis (H_a): $\mu_{DB1PE} \neq \mu_{DB2PE}$

64 samples are provided for each group providing 128 total samples and 126 degrees of freedom. Figure 9 provides the statistical parameters for this test.

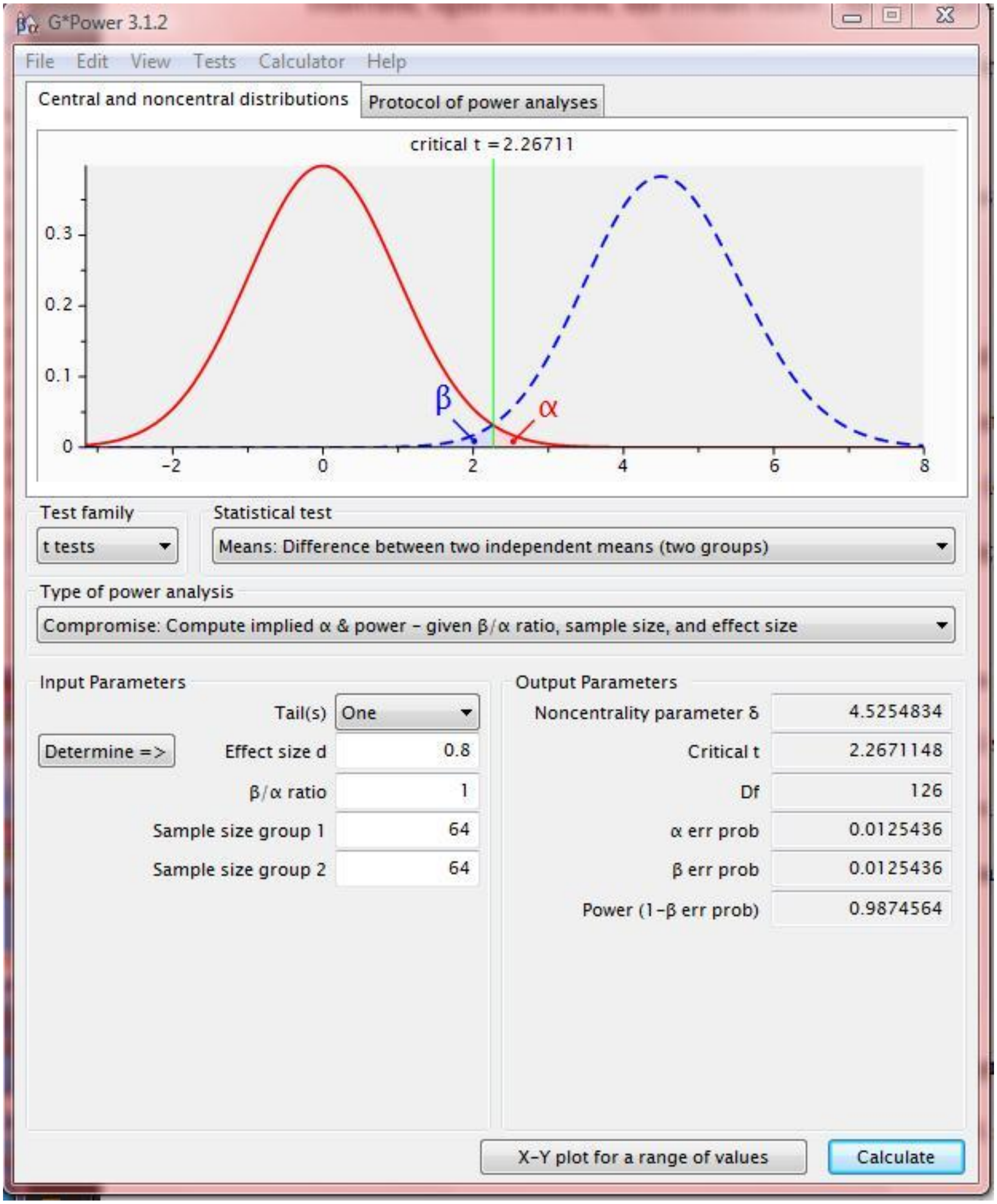

Figure 9 Statistical Test Parameters

The formula for the independent t-test is,

$$t = \frac{\bar{X}_1 - \bar{X}_2}{\sqrt{\left(\frac{SS_1 + SS_2}{n_1 + n_2 - 2}\right)\left(\frac{1}{n_1} + \frac{1}{n_2}\right)}}$$

$\bar{X}_1 = 9.9315$, is the mean error of the LIDAR prediction samples (μ_{DB1PE})

$\bar{X}_2 = 9.8436$, is the mean error of the SRTM prediction samples (μ_{DB2PE})

$n_1 = 64$, number of samples in LIDAR predictions

$n_2 = 64$, number of samples in LIDAR predictions

The Sum of Squares formula is,

$$SS_1 = \sum X_1^2 - \frac{(\sum X_1)}{n_1}$$

$SS_1 = 8871.193 - (404007.597 / 64) = 2558.575$, is the SS for LIDAR samples

$SS_2 = 8635.003 - (396890.172 / 64) = 2433.594$, is the SS for SRTM samples

The t-test value is calculated as

$$t = \frac{9.9315 - 9.8436}{\sqrt{\left(\frac{2558.575 + 2433.594}{64 + 64 - 2}\right)\left(\frac{1}{64} + \frac{1}{64}\right)}}$$

$$t = \frac{0.088}{2.476} = 0.0355$$

Cannot reject $H_{0,}$ Critical t = 2.267, t = 0.0355, p-value = 0.4858. The results indicated that there was NOT a significant difference in the predicted signal strength accuracy between: (a) the signal strength predictions generated on the LTF LIDAR database that is extrapolated from one meter spaced elevation post source data and (b) the signal strength predictions generated on the LTF SRTM database that is interpolated from thirty meter spaced elevation source data.

4.7 RQ1GH1 Test and Analysis

(RQ1BH1) Given combined Black Point LTF database and Friis transmission model, predicted Green/Red Coloration for either resolution terrain database are equivalent to observed signal reception.

The simplified RQ1GH1 null hypothesis states: Higher (LIDAR) and lower (SRTM) resolution terrain database will predict using a go/no go standard within range RF signal pairings equally accurately. Regardless to distance or blockage, each BP observed reception/no reception is compared to LTF predicted reception/no reception (excluding yellow areas) as assigned a colored depiction level with a corresponding signal strength level (1, 2, or 3) to represent the 3 levels of graphical depiction of signal strength desired by NASA**.**

Data collected to test this hypothesis is categorical and ordinal and can be expressed in a 2X2 matrix. As explained above, the Chi-square test of homogeneity may be used as inferential statistical test purposes. Again a Medium Effect size, $\beta = 0.2$, $\alpha = 0.05$ was estimated yielding a target data sample of a 87. The medium effect size (0.3) is expected based on the expectation that the difference in elevation accuracy of the two test databases would provide significant differences in prediction accuracy; however these differences would be less apparent when looking at signal strength color assignments or terrain blockage than when looking at raw signal strength. If a small effect size were to occur, then 785 samples would be required for each sample population. For our test, 188 independent LIDAR and 188 independent SRTM predicted signal receptions or no reception (NO Yellow) within range receiver locations were available and randomly selected as discussed previously.

Figure 10 shows the statistical test parameters as calculated in the G*Power tool. Predictions were compared to actual Black Point signal measurement to determine if a blocked signal (< -71 dBm) had occurred. The chi-square test matrix shown in Table 8 provides the results of the observations. The full data tables are provided in Appendix F.

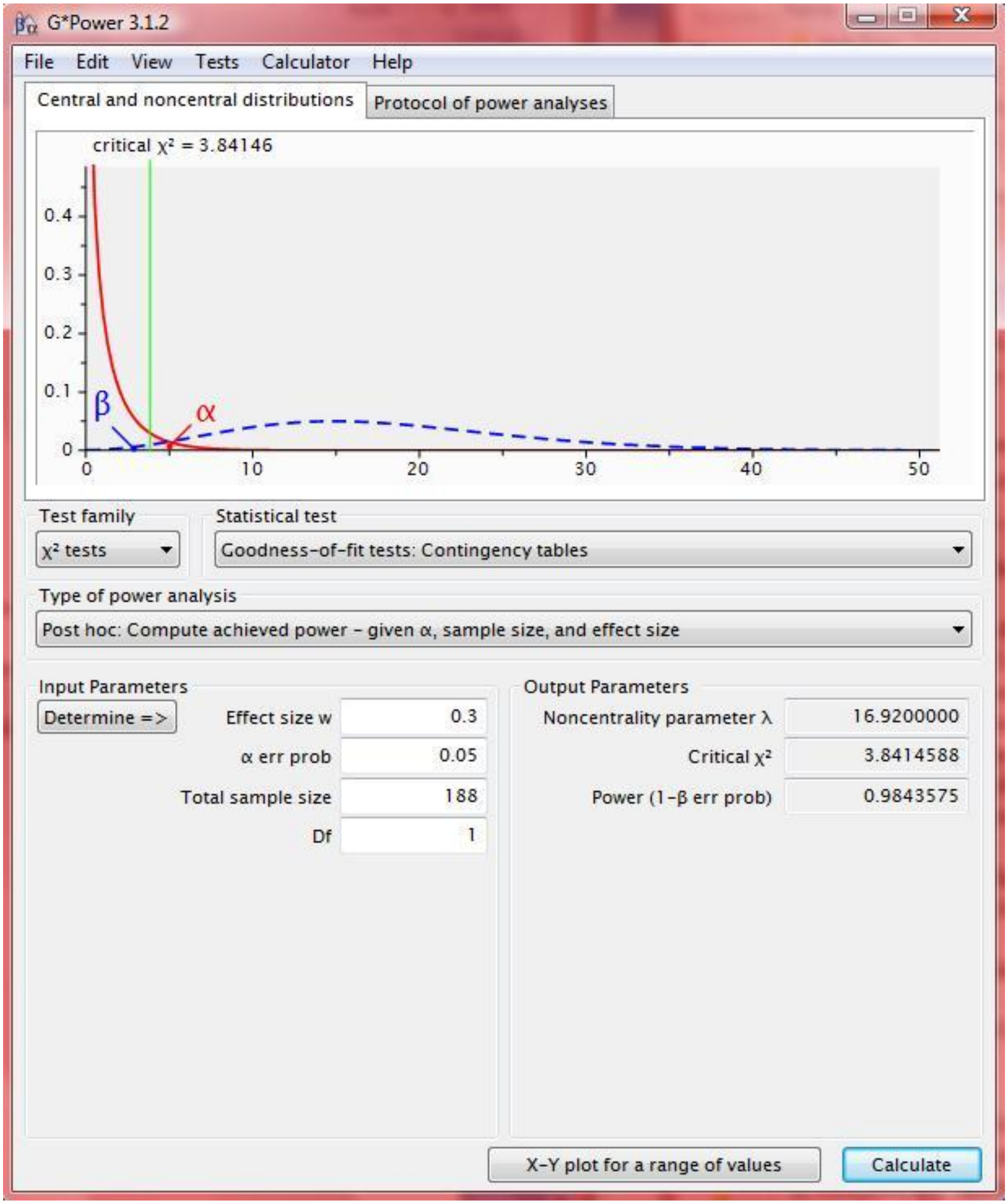

Figure 10 Statistical Test Parameters

Table 8 Chi Square Test Matrix

	Treatments		
	LIDAR Predicted Signal	SRTM Predicted Signal	*Row Totals*
Measured value matches predicted	136	150	286
Measured value does not match predicted	52	38	90
Column Totals	188	188	376

Expected frequencies are calculated as follows:

E_{11} = 188*286/376 = 143

E_{12} = 188*286/376 = 143

E_{21} = 188*90/376 = 45

E_{22} = 188*90/376 = 45

The chi-square value is

$$X^2 = (136-143)^2/143 + (150-143)^2/143 + (52-45)^2/45 + (38-45)^2/45$$

X^2 = 0.3427 + 03427 + 1.0889 + 1.0889 = 2.8632,   p-value = 0.09063.

Reject H_0 if $X^2 > 3.8416$: We cannot reject H_0 because the calculated X^2 value is not greater than the Critical value. The results of the Chi-square test performed on the collected RF signal measurements and generated LTF signal strength calculations do not show a statistical difference in the prediction signal strength color indication between the signal strength color predictions generated on the LTF LIDAR database that is extrapolated from one meter spaced elevation post source data, and the signal strength color predictions generated on the LTF SRTM database that is interpolated from thirty meter spaced elevation source data. No difference is statistically shown between the higher resolution (LIDAR) database and the lower resolution (SRTM) database predictions.

4.8 RQ1GH2 Test and Analysis

(RQ1GH2) Given the 3 level RF signal strength depiction scheme requested by NASA, LTF signal attenuation models may not need to account for all attenuation sources (free space path loss, reflection, refraction, and diffraction) to accurately depict signal strength predictions to the user.

The simplified RQ1GH2 null hypothesis states: The Egli, Foore & Ida, and Friis transmission models are equivalent for signal strength prediction. Data required to test hypothesis RQ1GH2, including the Tropos radio signal strength measurements, LTF LIDAR database signal strength predictions and modified LTF attenuation model signal strength calculated values are provided in Appendix G. The modified LTF attenuation model signal strengths are calculated using the alternative Elgi model and Foore and Ida fade depth approach discussed in Chapter 2. The Cochran Q Test is the appropriate statistical test to analyze three or more related samples with a binary success-failure outcomes . Again using Cohen and the following estimated parameters:

Medium effect size, Power= 0.80, $\beta = 0.2$, $\alpha = 0.05$. Degrees of freedom = 2.

Table 2 indicates 52 samples are used for each treatment.

Critical region will be $T > \chi^2_{.950} = 0.012587$ (Mendenhall, 1995).

For a given transmitter location, 52 receiver locations where signal strength was unblocked were randomly selected. The resulting 52 antenna pairs were executed in LTF database for the Friis model and then computed for Egli and Foore & Ida in an Excel spreadsheet. The test matrix provided in Table 9 details the test values as calculated within the spreadsheet in Table 21 (Appendix G).

Table 9 Cochrans Q Test Matrix

	Friis	Elgi	Foore and Ida
Agree with Measured Signal Color	36	24	23
Do not Agree with Measured Signal Color	16	28	29

This test revealed that there was a statistical difference between color indication between the three models with the Friis model matching observed more often than the other two. Cochran critical region T > $\chi^2_{.950}$ =0.012587, T = 24.15 p-value= 0.0006.

4.9 Additional Analysis Beyond What Was Proposed

4.9.1 Regression Analysis of LIDAR Predictions

To further investigate the influence of the selected Friis algorithm a regression analysis was performed. The 64 sample LIDAR signal strength predictions used in the test RQ1FH2 are charted (Figure 11) against the distance of the transmission range. Since the algorithm is implemented within LTF is a logarithmic calculation of signal strength (decibels) the resulting of curve is expected. Data tables for the test are provided in appendix H.

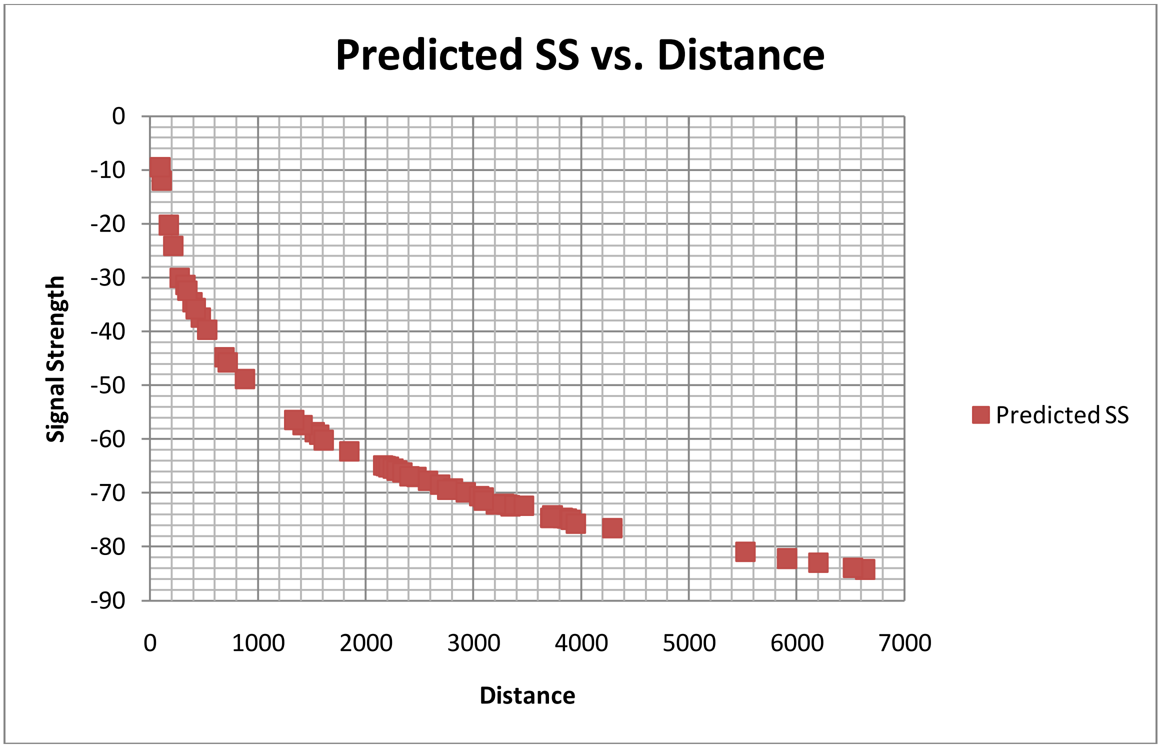

Figure 11 Signal Strength Prediction (dB) vs. Distance (meters)

Figure 12 provides a graph of the predicted signal strength error (predicted signal strength - measured signal strength) also plotted against distance of transmission. The distribution of points appears to be suitable for linear regression analysis. The calculation of Pearson's product moment coefficient of correlation (r) executed in excel provides a value r = 0.689, suggesting that a linear trend may exist between prediction error and distance of transmission. The equation for the least square line is $Y = -14.049 + 0.004399\ X$. The coefficient of determination ($r^2 = 0.476$) indicates that approximately 50% of the signal strength error could be attributable to this increasing distance. Therefore as distance increases, error increases. This would also indicate that at least 50% of the signal strength error is from other sources, such as signal reflection, refraction, and diffraction that are not accounted for by the Friis equation, or by errors in antenna gain or transmit power values which were are modeled in the Friis equation and were assumed constant throughout the experiments.

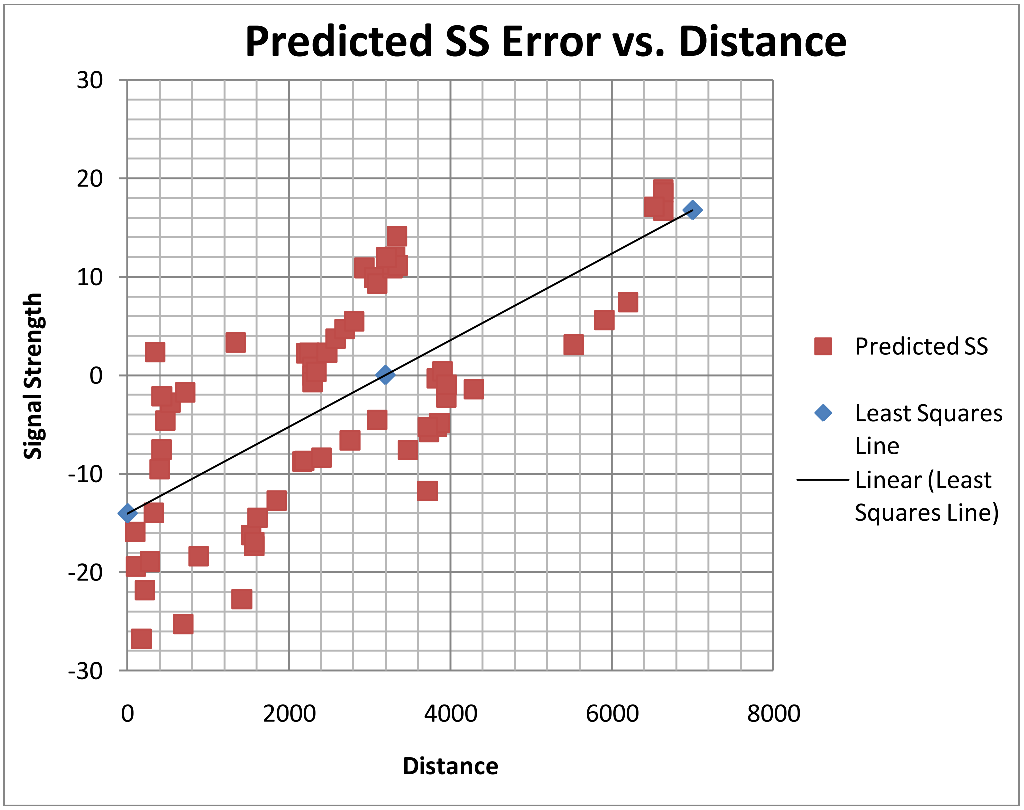

Figure 12 Predicted Signal Strength Error (dB) vs. Distance (meters)

4.9.2 Chi-Square Analysis of LIDAR Blocked and Unblocked predictions

An additional hypothesis was considered that impacted on those proposed above. Specifically, there is no difference between LIDAR prediction of blocked signals and actual measured signal strength. Data collected to test this hypothesis is categorical and ordinal and can be expressed in a 2X2 matrix. The Chi-square test of homogeneity may be used for two independent samples. The following test looks for a statistical difference in the capability of LTF to correctly predict blocked vs. unblocked transmissions. This test was performed using the LTF LIDAR database. Using the same parameters as other categorical evaluations, Medium Effect size, $\beta = 0.2$, $\alpha = 0.05$ yields a requirement for 87 samples. The medium effect size (0.3) was selected based on the expectation that the large difference in elevation accuracy of the two test databases would provide significant differences in prediction accuracy, however these differences would be less apparent when looking at signal strength color assignments or terrain blockage than when looking at raw signal strength. The statistical test criteria is the same as show in Figure 10. For this test and given the availability of additional data, 188 independent LIDAR Blocked predictions and 188 independent LIDAR Unblocked predictions were randomly selected. Predictions were compared to actual Black Point signal measurement to determine if a blocked signal (< -71 dBm) had occurred. The chi-square test matrix shown in Table 10 provides the results of the observations. The full data tables are provided in Appendix I.

Table 10 Chi Square Test Matrix

	Treatments		
	LIDAR Blocked	LIDAR Unblocked	*Row Totals*
Field measurement threshold Blocked	143	109	252
Field measurement threshold Unblocked	45	79	124
Column Totals	188	188	376

Expected frequencies are calculated as follows:

$E_{11} = 188*252/376 = 126$

$E_{12} = 188*252/376 = 126$

E_{21} = 188*124/376 = 62

E_{22} = 188*124/376 = 62

The chi-square value is

$X^2 = (143-126)^2/126 + (109-126)^2/126 + (45-62)^2/62 + (79-62)^2/62$

$X^2 = 2.2937 + 2.2937 + 4.6613 + 4.6613 = 13.91$, p-value = 0.000192.

Reject H_0 if $X^2 > 3.8416$: We reject H_0 because the calculated X^2 value is greater than the Critical value. The results of the Chi-square test performed on the collected RF signal measurements and generated LTF signal strength calculations show a statistical difference in the capability of LTF to prediction correct signal strength color indication and the capability to predict terrain blockage of signals. The results of this test indicate that for the tested LIDAR database, the LTF prediction of blocked terrain is more accurate than the LTF prediction of unblocked signal strength.

5 SUMMARY, CONCLUSIONS, RESEARCH LIMITATIONS, LESSONS LEARNED AND SUGGESTED FUTURE RESEARCH

5.1 Summary

The following paragraphs provide a brief review of the motivation for this research, the planned research tasks and the efforts performed in support of this research.

5.1.1 Motivation

The primary question posed in this dissertation questions the feasibility of applying the U.S. Army developed, uniquely architected LTF database to the general problem of celestial body representation. A number of more specific research questions were developed as the scope, limitations, and specific use case proposed for the research were defined.

- What levels of terrain source data are required for the database to accomplish the given communications prediction task?
- What communications attenuation algorithms are appropriate for this application?
- What user interfaces can be supported to display the LTF prediction data?

The level of research in this dissertation devoted to the above three questions was limited by resources. What was addressed is described in Chapter 3 and 4 above and summarized below. The motivation to do this research was largely driven by NASA's planned current and future space exploration missions defined in The Vision for Space Exploration. For any celestial body exploration endeavor, realistic validated terrain databases will be necessary to provide mission planning and rehearsal capability as well as to aid mission execution. The terrain fidelity level necessary for constituting models and simulations that are realistic enough to meet operational and safety concerns is at the heart of this dissertation. The technology embedded in LTF theoretically provides additional benefit in its small computational footprint - potentially allowing it to be embedded in robotic platforms and/or man wearable computers. Portable access theoretically provides REAL-TIME modeling and simulation support to REAL-TIME celestial operations. Past NASA history of celestial operations indicate a need for (a) accuracy and (b) real-time response from support models and simulation.

5.1.2 Research Design

This case study research design involved assessment through hypothesis testing and regression analysis of models and simulation based on high resolution LIDAR and lower resolution SRTM databases produced through LTF and compared with data collected at the NASA Black Point Lava Flow lunar analog 2010 Desert RATS exercise area. NASA commissioned a flyover of the Black Point area to collect the LIDAR data. This data was then processed by NASA to create a Digital Elevation Model which was provided for this research. SRTM data was available free, on-line in a format already usable by RUGUD, the LTF database generation tool. Each terrain source file was processed by RUGUD to produce a 27Km x 27Km LTF terrain database. The LTF databases have a one meter post spacing - in the case of the SRTM source which has 27 meter post spacing, all intermediate posts are interpolated based on known post heights and calculated slopes. The final size of each LTF database is: SRTM - 1.25 MB; LIDAR - 131 MB. The two databases were used in combination with the Friis transmission and attenuation algorithm to generate two sets of communication coverage maps - LIDAR and SRTM - for the 27x27 km section of the Black Point site.

Within to these generated databases, data layers were added to accommodate the specific data types required for communications simulation. The Army version of LTF already contained layers for representation of terrain and features. Three specific data layers were added for this research. The Radio Tower layer contains antenna data including height, gain and location, and also contains the transmit power value for transmitting antennas. The Link Grid layer stores the attenuated transmission links between antennas which have been specified. These links are visible as colored lines within the RAVEN viewer. The Map layer contains coverage map data including the attenuated signal color value assigned at each coverage map grid point. These colored points grids can be viewed as Communication Map overlays within RAVEN, or exported to KML format data for display in Google Earth. Figure 13 illustrates the communications specific layers added to LTF, identifying interaction with the embedded Friis algorithm.

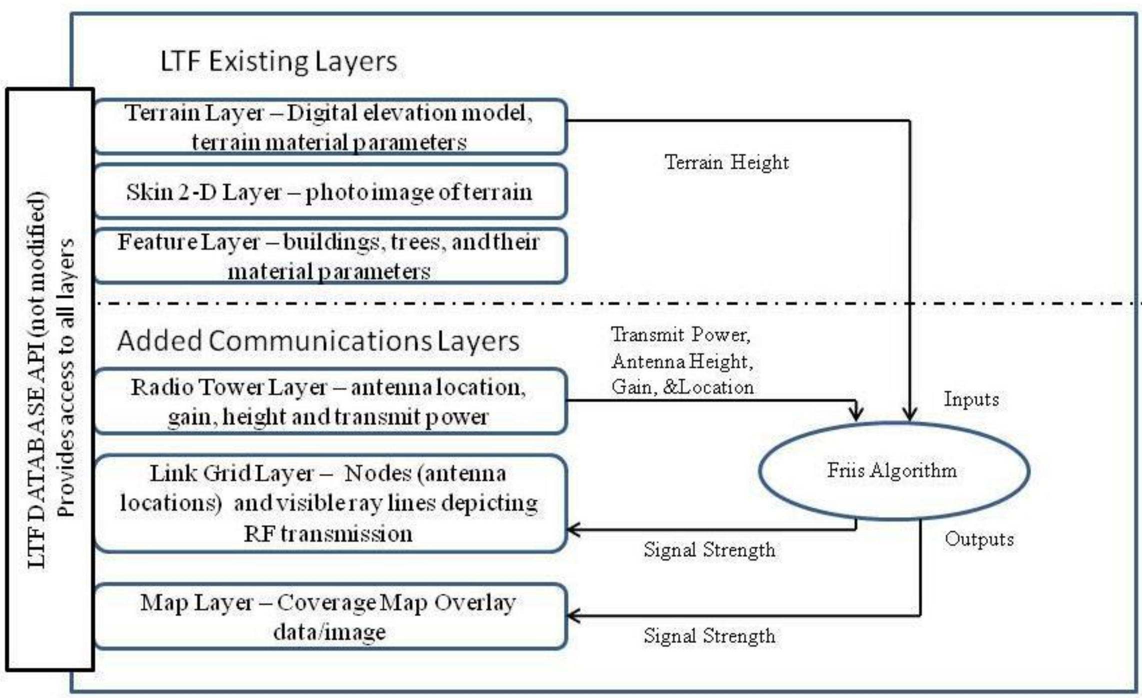

Figure 13 LTF Communication Layers Diagram

Figure 14 provides an Entity Relationship Diagram identifying the data and data type stored in each layer. Colored blocks provide an indication of references between layers.

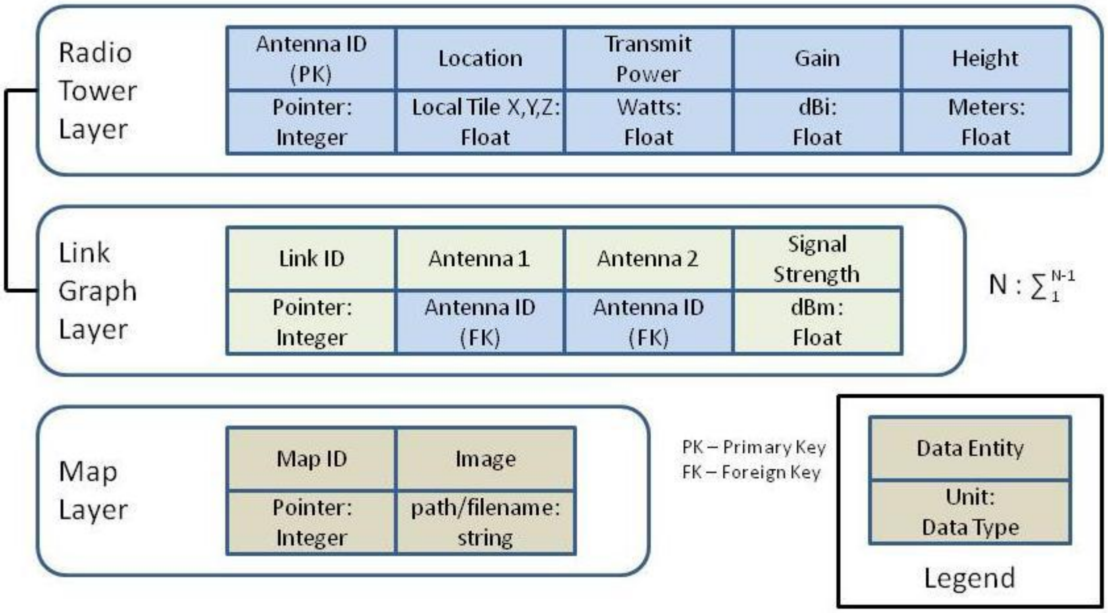

Figure 14 LTF Communication Layers Entity Relationship Diagram

The research required several changes to the RAVEN LTF Viewer application to allow access to the new LTF communication layers, specification of output characteristics for coverage map creation, and input of radio/antenna parameters. Figure 15 provides a flowchart showing the capabilities progression of the LTF Database and RAVEN (LTF Viewer) based on the identified NASA needs and the design efforts of both the researcher and ARA personnel. ARA implemented the code changes required for the RAVEN GUI interface modifications.

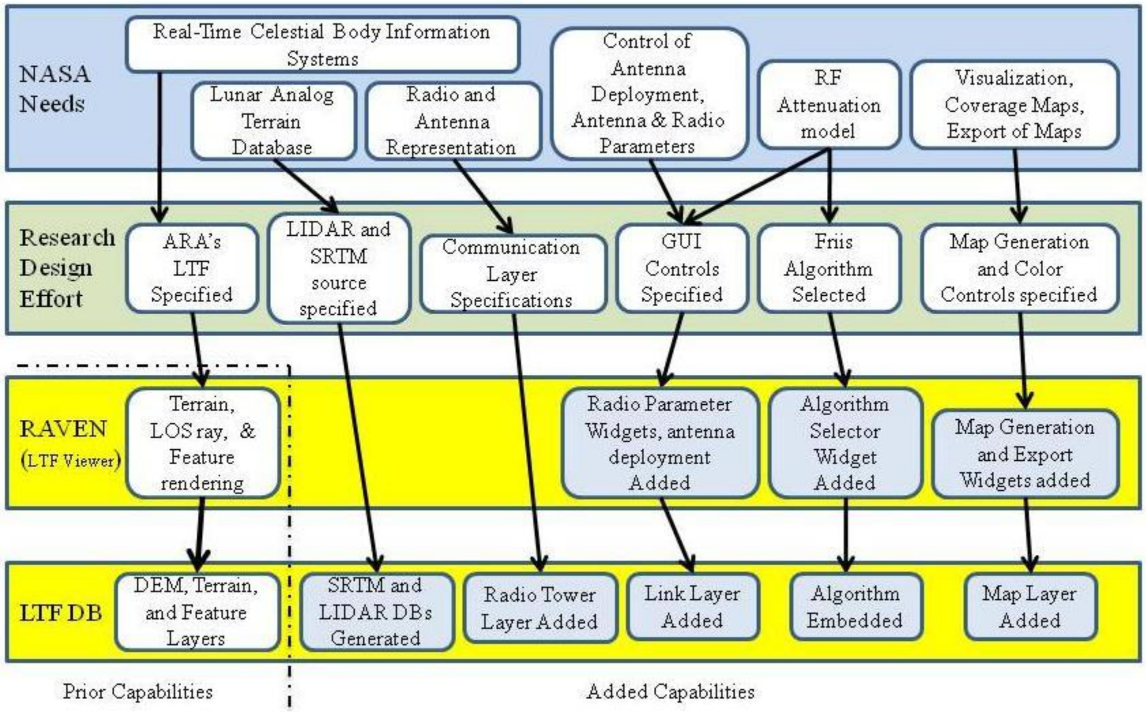

Figure 15 LTF Capability Modification Flowchart

The Friis transmission equation was used to model S-band signal strength attenuation within the LTF simulation. The selection of the Friis Transmission equation as the embedded LTF attenuation algorithm was made because it could be easily implemented in the code and would not be computationally expensive to execute.   The Friis algorithm is a free space path loss equation modified with factors to account for antenna gains and transmit power. The addition of a different RF attenuation algorithm would require modification and recompilation of the RAVEN Radio Services DLL, or creation of a new DLL and registration of that DLL with the LtfServices DLL.   Typically, no code changes to the database would be required.

The RAVEN viewer controls added for map generation and RF link visualization provide the capability to specify colors associated with attenuated signal levels. For coverage map generation, simulated transmissions are performed between a single transmitting antenna (positioned by the user) and a grid of points covering the entire database, each representing a receiving antenna. The distance between the nodes of the grid is user specified before the mapping function is started. A sample coverage map generated within LTF and rendered in RAVEN is shown in Figure 16.

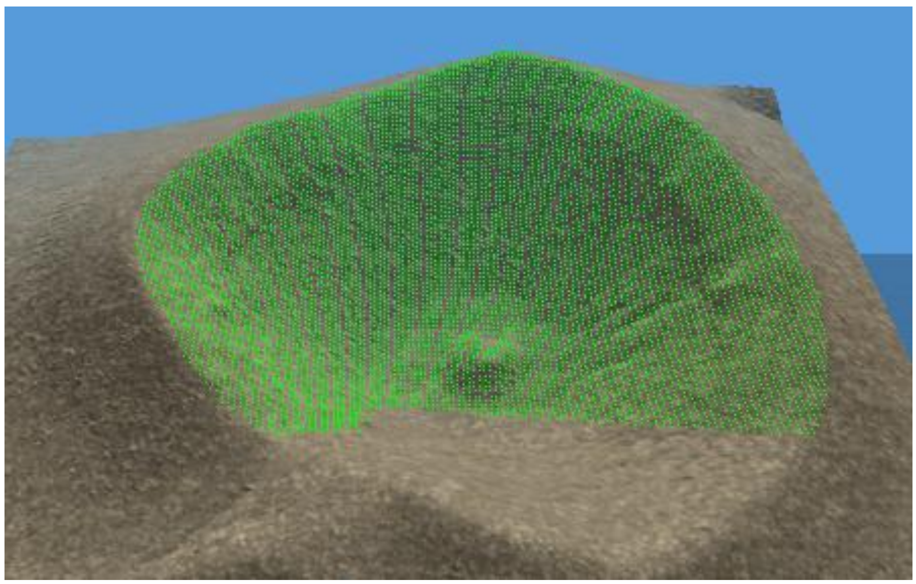

Figure 16 Coverage Map Overlay of BP Mountain as Shown in LTF Viewer

5.1.3 Data Collection

Actual communications signal power readings samples were collected in mid March 2010 from the site of NASA's planned 2010 Desert RATS analog tests, using the points of interest and antenna locations provided by NASA. The data collection team included two University of Central Florida graduate students and two NASA Communications Engineers. Communications signal parameters including signal strength, noise, and modulation were recorded between fixed antennas and mobile antennas following both preplanned and arbitrary routes. Fixed antenna locations and planned routes were selected based on points of interest defined by NASA in 2010 Desert Rats planning events. The communications data layer added to the LTF database provided the capability to generate S-Band communications coverage prediction maps for antenna locations of interest at the Black Point site. The RAVEN interactive interface, specified by this research, funded by UCF, and developed by ARA for the case study, proved useful in determining routes in real time. The raw data collected at black point, as well as data used for each statistical analysis are provided in the appendices. Table 11 below summarizes the content of each appendix.

Table 11 Test Data Provided in Appendices

Appendix A	Raw Data collected at Black Point Lava Flow
Appendix B	Test data for LTF LIDAR and SRTM elevation comparisons
Appendix C	Test data for LTF Prediction of signal blockage by terrain
Appendix D	Test data for LIDAR database error in signal strength prediction
Appendix E	Test data for comparison of accurate signal strength coloration matching of LIDAR and SRTM databases
Appendix F	Test data for
Appendix G	Test data for comparison of three attenuation models
Appendix H	Test data for linear regression analysis of LIDAR error
Appendix I	Test data for LIDAR Blocked vs LIDAR unblocked accuracy

5.1.4 Findings and Analysis

Chapter 4 and related appendices present the detailed data and analysis. Analysis involved inferential statistical analysis of hypotheses testing and regression on recorded and LTF predicted communications coverage maps, signal strength, and blockage of communications signals by terrain.

It was expected that for the case study of modeling 2.4 Ghz S-band communications that the higher fidelity database would provide better performance in terms of identifying signals that were blocked by the terrain. However the hypothesis test showed no significant statistical difference in the performance of the two databases. Further, both databases predicted equally accurate point reliability of predicted blockage of communications of within range S-band signal using a go/no go standard and the Black Point LIDAR and SRTM database.

Reliability (LIDAR) = 0.793

Reliability (SRTM) =0.745

Likewise, LIDAR and SRTM database predicted overall signal coverage of within range S-band signal using a go/no go standard equally accurately.

Reliability (LIDAR) = 0.723

Reliability (SRTM) = 0.798

Hence the interpolated 10 meter post versus the sampled 10 meter post proved to be equally accurate in predicting communications. However, from the real-time operational requirements point of view, the SRTM coverage map could be generated in approximately one sixth of the time (2 hours versus overnight) as the LIDAR coverage map. Additionally, creation of a coverage map at 1 meter resolution proved to be not possible from the perspective of the experiment or for real-time purposes as it theoretically would have taken 1200 hours to create using the same hardware and non-optimized algorithms. A further analysis of the height returned for 100 random points between the largely interpolated (SRTM) and the precise (LIDAR) database found that the mean height difference of actual elevation posts between the two databases to be 1.75 meters.

The statistical analysis of the LTF signal strength predictions for unblocked transmissions indicate that the Friis equation provides a good representation of actual signal strength attenuation seen a Black Point. The LTF technology used the LTF generated databases with the Friis algorithm and NASA specified antenna position and attribute data to create visual representations of communication coverage for the Black Point Lava Flow analog lunar test site. Limited hypothesis testing and regression analysis was conduct using the SRTM and LIDAR coverage maps to predict communications and the field data gathered from the Black Point Lava Flow site.

The fourth analyses performed investigated the capability of LTF predictions to match measured signal strength in terms of the 3 level (green, yellow, red) user indication desired by NASA. The results show no statistical difference in the performance of the SRTM and LIDAR source LTF databases.

In the final proposed analysis, the Friss algorithm was further evaluated against the Egli algorithm and the Foore and Ida model for determining signal strength color indication. This analysis was performed in Excel. Among these alternative attenuation models, results were shown to be not statistically equivalent. The Friis algorithm provided the most matches to actual signal strength measurements.

5.2 Conclusions

The results of the statistical tests as well as the experience gained at the data collection event, where the LTF generated coverage maps were used to derive routes and predict coverage in real time, suggest that the modeling of a celestial body, or in this specific case the analog of a celestial body, within the LTF layered database framework was successful and, for the specific case of communications predictions, is a feasible alternative to current tools in use by NASA.

The results indicate that for terrain surface, similar to the Lunar analog test site, an LTF generated communication coverage map that used interpolated SRTM data was faster to produce than either the LTF LIDAR coverage maps or coverage maps generated by NASA using the Mobile Radio (ITU model) product. The Mobile Radio tool using SRTM 100 meter source data takes overnight to generate a coverage map vs. 2 hours for the LTF database sourced from 30 meter SRTM data. Neither the Mobile Radio product nor NASA's LSOS simulation will provide real-time radio link updates allowing for dynamic antenna movement or relay deployment as was demonstrated with LTF. Collected Black Point RF transmission data was not loaded into the LTF database - the LTF database is a terrain database - the LIDAR and SRTM terrain source was used to create LIDAR and SRTM terrain databases. The location data recorded for a single Black Point transmission event (transmitting antenna location, receiving antenna location) can be used to position virtual radio/antennas within the added LTF communications layer. Additionally, the radio transmission power and antenna gains can be specified within the LTF communications layer. The LTF can then execute the Friis attenuation algorithms and line-of-sight algorithms against the communications layer data (and terrain layers) to predict the signal strength of the RF signal at the receiving antenna location, or blockage of the RF signal by terrain.

The accuracy of LTF predicted signal strength using the Friis transmission algorithm was not compared with Mobile Radio results, however when compared with actual measured signals no statistical difference was found. However, these results may not apply to terrain surfaces with greater variability in elevation than the Black Point Lava Point segment that was tested such as those surfaces more densely populated with canyons, ravines, or boulders of sizes under the 30 meter post spacing of the SRTM source data.

The RAVEN viewer, as modified for this research, provides the same visualization of coverage maps as can be viewed in Google Earth, but also provides user interaction not currently available through Google Earth, such as movement of an already positioned antenna or deployment of new antennas. These features allow real-time visibility of communications link impact when antennas are placed, moved, or parameters such as antenna height, gain or transmit power are changed.

LTF provides a unique set of capabilities that fulfill needs specified by NASA scientists involved in celestial body communications design. The capabilities provided by LTF can benefit space exploration mission planning and mission execution tasks as depicted in Figure 17. The following scenario provides an example of how LTF could be employed for a mission execution task.

Scenario: An astronaut is driving a rover towards a defined location of interest to collect mineral samples. The route he follows has been selected to keep him within LOS of the base radio tower based on LTF communications coverage maps generated when the tower was erected. As he traverses the route, he notices a surface feature which he would like to inspect. The feature is about 200 meters off route, this will take him outside of the communication coverage of the base station. Using his LTF visual interface, he places a 2 meter antenna icon at the location he wishes to explore. The base station antenna's position is already represented by a fixed icon. He places a relay antenna icon on a nearby ridge and moves its position around until visible linkage lines connect the three antennas, indicating a successful communications link can be achieved. He then radios his controllers at the base station, notifies them that he desires to go off route, but will maintain radio contact through a verified relay location.

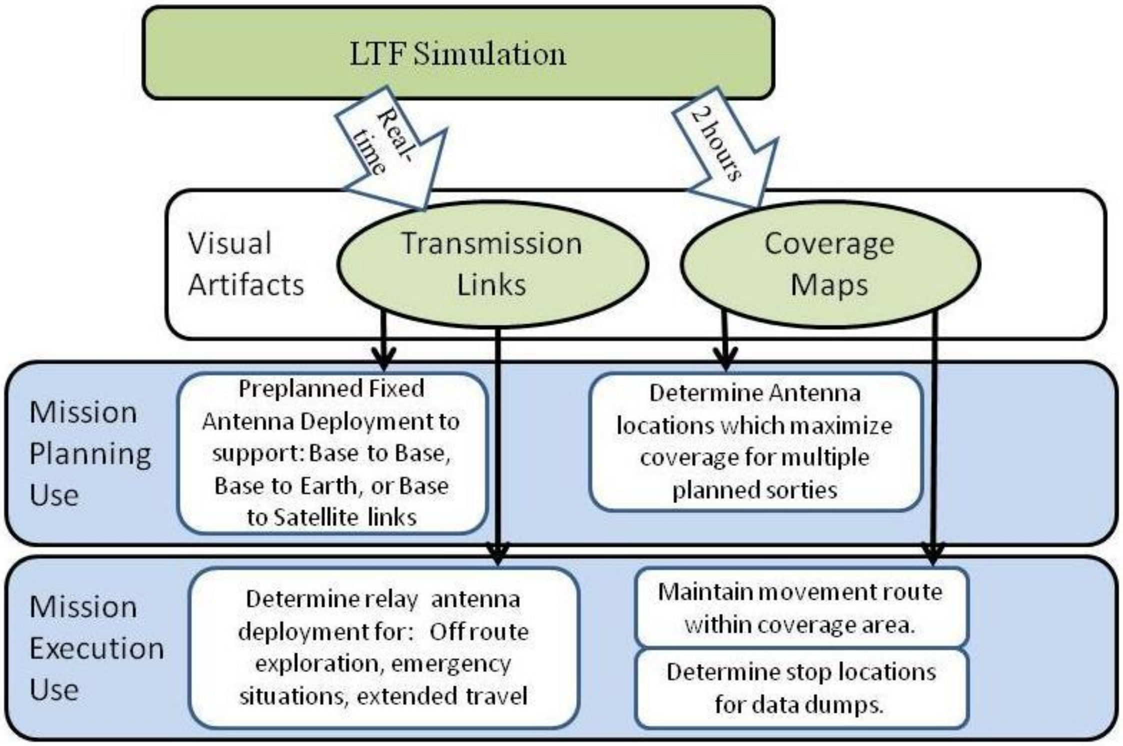

Figure 17 LTF Application in Mission Planning and Execution

Based on the statistical analyses performed, the SRTM source database provides the most logical choice given the current LTF capabilities. It provides accuracy, in terms of user output, statistically equivalent to the LIDAR source database, it has a lower cost, and generation of coverage maps can be accomplished much quicker. In the future, optimization of LTF line-of-sight algorithms, limiting the coverage map area, and increased hardware processing speeds may significantly decrease the computation time required to produce an LTF communication coverage map. These advances may also allow the greater resolution, that corresponds precisely to the LIDAR one meter elevation post source data, for the generated map. However, there is also increasing cost involved in the collection, processing, and storage of more detailed terrain data. The execution time required to generate cover maps on the SRTM database was demonstrated to take approximately 1/6 of the time required for the LIDAR database. Although ARA SME indicates advancements in LTF optimization and hardware capabilities will reduce both times, the SRTM generation will likely still be faster, and the benefit of having a higher resolution map will have to be weighed against the additional execution time. From the results experienced in this research, it is suggested that a careful review of the intended use case should be performed before determining what resolution of database source is elected for a specific application.

5.3 Potential Research Benefits and Inferences

Specific benefits of this research can be generalized beyond the communications use case posed by NASA. Discussions have been presented showing that the proprietary LTF architecture has the capability to represent celestial bodies of various sizes and shapes, including polar regions which are problematic for many simulation terrain database architectures. This research infers that celestial body terrain databases represented within LTF could be added to existing simulation systems, such as DSES, to allow those simulations to access geo-specific information not currently represented, or capable of being represented, in their native databases architectures.

Robotic exploration is another possible domain which has been mentioned throughout this text as potentially benefiting from LTF technology. Autonomous robots, including celestial or earth based explorers, would benefit from having an detailed yet compact embedded GIS. The LTF's high resolution (1-meter) terrain representation could be used to perform terrain referenced navigation in environments (celestial, underwater, under terrain) where GPS signals are not available. Geo-specific data such as soil type, hardness, and slope embedded in an LTF layer would permit trafficability calculations to aid in route planning decisions. An embedded mineralogy layer could allow mining robots to quickly locate elements of interest based on remote sensor readings from pre-mission satellite scans.

Robotic teams or flocks using LTF could include layers preloaded with satellite information that would be updated as discoveries and surface samples are explored. The ability to wirelessly stream these data updates between robotic platforms (a capability currently being developed for LTF under an RDECOM effort) provides a very unique architecture for a shared robotic information system. This approach would also minimize the loss of discovered data due to loss of a robot platform, reducing the risk to the exploration mission.

Finally, the LTF architecture was designed and optimized, by the US Army, to perform rapid LOS type simulations. Additionally, LTF allows users specification of attenuation parameters, if desired. Use cases which can be simulated using line of site models may benefit from the LTF capabilities. The modeling of solar radiation for instance could support simulations of both solar power collection arrays, as well as radiation exposure for equipment and personnel. These models could include radiation reflected off of surface elements as well as attenuation of radiation by atmospheric or shielding layers.

- Benefit to NASA in having a database and visualization tool for celestial body terrain and geo-specific data representation.
- Validated representation of celestial body within simulations is key to exploration planning and execution activities
    - Rehearsal & Assessment of Manned & Robotic Celestial Body Missions needs analogs (Black Point Lava Flow for the Moon) of the actual environment in order for learning transfer to occur accurately
    - In order for mission aspects to be rehearsed in a synthetic environment, the synthetic environment must have evidence that it correlates to known analogs (Black Point Lava Flow for the Moon) for the target mission environments
- Inquiry into the resolution required for the terrain database source data in order to provide useful output (prediction/planning) capabilities.
- Benefit to future robotic and manned space exploration missions through access to a terrain and geo-specific database which requires a small computational footprint and can be updated through wireless interaction.
- Benefit to future LTF researchers or adopters of LTF technology via ongoing Army development activities which will continue to enhance the current LTF capabilities.

5.4 Scope and Limitations

The scope of the research was defined both by the general research question - creating a celestial body representation within a layered terrain database, and by the specific case study - determine if the LTF celestial body representation could be used to fulfill a communications coverage prediction gap identified by NASA. While the initial plan was to create a database of a future planned lunar exploration site, the scope of the research was limited by a lack of lunar terrain data sources and lunar RF transmission data. At NASA's request, the LTF database was developed for Black Point Lava Flow, Arizona which is a site used by NASA for conducting lunar analogs. The communication coverage maps generated for the test were limited to 10 meter posts due the fact that the computational time required exceed the time available prior to the experiment.

The selection of an RF attenuation model to be embedded into LTF was limited to simplistic models due to a concern that more complex models such as ray tracing models would overwhelm the CPU and severely slow down generation of coverage maps, signal strength predictions, and LOS queries.

In addition to blockage by terrain or surface features that are modeled well within LTF there are a number of additional attenuation sources which could not be modeled due to lack of data, or could not be controlled for designed experiments such as atmospheric conditions and material properties of the terrain. The physical location of Black Point and availability of NASA and UCF personnel (students) limited the data collection to a single 2 day event. Addition data collection time may have permitted additional testing of LTF functions such as determination of LCT antenna deployments.

Time and budget constraints also limited the extent to which the LTF RAVEN Viewer could be modified to accommodate the requirements of the case study and the needs of

NASA. Modification were made to fulfill the use case functions desired by NASA, however little work was performed in optimizing the performance of these new capabilities.

5.5 Lessons Learned

There are two experiences from this research appropriate to define as lessons learned. For the Black Point data collection trip, the initial plan was to generate LTF coverage maps and determine routes to be followed for each day of the data gathering event. Although the team had two four wheel drive vehicles, the terrain on some of these preplanned routes was not drivable due to washouts, including washed out roads, and tire hazards such as volcanic rock. These hazards could not be seen on either the LTF View of the database or from Google Earth views of the Black Point location.

The SRTM source data turned out to be much more accurate than the advertised +/- 16 meters as advertised on the source website. A discussion with scientists at the Flagstaff AZ USGS office following the data collection event provided a likely reason. SRTM data was collected by the Space Shuttle using radar returns from ground - the quality of return data is highly dependent on terrain properties such as roughness and slope. The +/- 16 number is likely the worst case accuracy collected. The USGS personnel, who are very familiar with the Black Point Lava Flow area stated that they believed the SRTM data for this area was with +/- 2 meters - which was validated by the terrain height analysis performed.

5.6 Applicability of Current Research Findings and Suggested Future Research Opportunities

This research has demonstrated that it is feasible to represent planetary or celestial body terrain data within LTF in order to provide capabilities beneficial for space exploration mission planning and execution. As Lunar terrain data becomes available from NASA's ongoing LRO mission, it is now possible to create LTF Lunar databases and support communications related mission planning and analysis tasks beneficial to either manned or robotic exploration. The research has shown that the LTF layered architecture is suitable for representation of geo-specific data, such as radio and antenna position and related attributes, beyond the terrain representation for which it was originally intended. This capability allows LTF to be employed as a Geographic Information System housing user specified data of interest for the celestial body being explored.

This research and the specific case study provide the following contribution to Interactive Simulation Science. The research has identified the LTF architecture as an appropriate terrain architecture for the representation of celestial body terrain surface simulation. This capability makes possible follow on research for non-spheroid celestial body modeling, lunar and Martian mobility maps, solar radiation maps, other planetary and heliophysic effects modeling, etc. The research has implemented an interactive simulation model executing across multiple data type layers in a layered terrain database, taking advantage of algorithms optimized for specific data layers to improve performance and execution speed. The specific case study was focused on communications capabilities, but the technical approach has been generalized to other domains. The research has implemented of a real-time and portable celestial body geographic information system within the terrain database.   The specific data layers added to the LTF represented location specific non-terrain data of interest to the users, in addition to the terrain layers. The potential to employ LTF as a celestial body information system has been shown. Findings of this research will be disseminated through:

- Florida Space Grant Consortium Final Report
- Article Submitted to *Journal of Geographic Information Systems.*
- Publication of this dissertation document,
- Final NASA Presentation

Enhancement of LTFs current communications predictions capabilities would likely result from addition research including the investigation of more robust RF attenuation models which account for terrain material and environment properties and additional RF transmission bands which are being considered for use. As this project had very limited funding for NASA specific LTF enhancements, further development work related to the LTF Viewer GUI interface could provide additional use cases or streamline execution of current functions. Appendix J provides a section from the Final Report to NASA which details additional product improvements to the LTF Viewer as identified by Applied Research Associates, Inc. (Proctor, Guise, and Peele, 2010).

Follow-on research and improvement opportunities exist and are discussed below:

High-Fidelity Radio Physics: The LTF radio prototype uses a low-fidelity standardized radio physics model – the Friis Transmission Equation. Reliability predictions might improve by adapting LTF to use first-principles near-earth radio propagation model developed and validated by ARA Southeast Division to model…

- … atmospheric and humidity effects
- … terrain dielectric and conductivity properties
- … multipath effects
- … frequency-specific effects

Real-time Performance: The prototype LTF coverage mapping engine is completely un-optimized and purely relies on LTF LOS speed for performance. Modern ray tracing techniques might be employed to improve speed, as well as:

- Aggressive multithreading and SIMD optimizations
- Adaptive culling and problem partitioning
- Coherent ray tracing and other scene graph optimizations for analyzing large numbers of rays
- GPGPU processing via CUDA or OpenCL

Predict Optimal Relay Configurations: NASA and many other applications have very limited number of relays and must determine how to obtain optimal coverage with available resources. The development or integration of optimization algorithms that use LTF radio coverage prediction to suggest optimal relay placement could provide added functionality to:

- Maintain visibility to points or areas of interest
- Maintain direct or indirect uplink to "home" transmitter

- Maintain radio connection along a desired route plan
- Develop a route planner capability which takes into account radio coverage and suggests route plan to maximize coverage or bandwidth

Other Applications: LTF can be applied to terrestrial applications; analyzes of color camera placement, cell phone signals, or any other type of sensor coverage or wave propagation

- Signal processing model is very flexible - it supports adding new types of signals and algorithms without modifying current code
- Signal processing model does not assume direct line of sight and could be adapted to support multipath effects and other complex paths from emitter to receiver
- Low-level C++ SDK exposes all LTF ray tracing primitives used by signal models to third party developers
- Coverage mapping engine currently implements “point to point” relay configurations, but would be easy to extend to “infrastructure” configurations where connection to a “home” relay is important

APPENDIX A COLLECTED FIELD DATA

Table 12 Tropos.500 Raw Data

Time(epoch)	Lat(degrees)	Long(degrees)	Alt (meters)	Distance (meters)	Signal (dB)	Noise (dB)	Modul-ation
1268847841	35.59746758	-111.6017296	1796.786	1.311250696	-22.63	-88.26	18.74
1268847852	35.59746758	-111.6017296	1796.786	1.311250696	-22.63	-88.26	18.74
1268847874	35.59746758	-111.6017296	1796.786	1.311250696	-25	-89	108
1268847885	35.59746758	-111.6017296	1796.786	1.311250696	-25	-89	108
1268847895	35.59746758	-111.6017296	1796.786	1.311250696	-30	-89	108
1268847906	35.59746758	-111.6017296	1796.786	1.311250696	-27.33	-89	108
1268847917	35.59746758	-111.6017296	1796.786	1.311250696	-27.33	-89	108
1268847929	35.59746758	-111.6017296	1796.786	1.311250696	-28.75	-88.75	108
1268847939	35.59746758	-111.6017296	1796.786	1.311250696	-28.75	-88.75	108
1268847950	35.59746758	-111.6017296	1796.786	1.311250696	-27.4	-88.6	108
1268847960	35.59746758	-111.6017296	1796.786	1.311250696	-28.5	-88.67	108
1268847971	35.59746758	-111.6017296	1796.786	1.311250696	-28.5	-88.67	108
1268847982	35.59746758	-111.6017296	1796.786	1.311250696	-27.86	-88.71	108
1268847993	35.59746758	-111.6017296	1796.786	1.311250696	-27.86	-88.71	108
1268848004	35.59746026	-111.6017296	1796.204	0.78329967	-27.62	-88.75	108
1268848014	35.59746758	-111.6017296	1796.786	1.311250696	-27.11	-88.78	108
1268848025	35.59746026	-111.6017296	1796.204	0.78329967	-27.11	-88.78	108
1268848036	35.59746026	-111.6017296	1796.204	0.78329967	-26.5	-88.8	108
1268848047	35.59746026	-111.6017296	1796.204	0.78329967	-26.5	-88.8	108
1268848058	35.59746026	-111.6017296	1796.204	0.78329967	-27.09	-88.73	108
1268848068	35.59746026	-111.6017296	1796.204	0.78329967	-26.67	-88.67	108
1268848079	35.59746026	-111.6017296	1796.204	0.78329967	-26.67	-88.67	108
1268848090	35.59746026	-111.6017296	1796.204	0.78329967	-26.46	-88.69	108
1268848101	35.59746026	-111.6017296	1796.204	0.78329967	-26.46	-88.69	108
1268848113	35.59746026	-111.6017296	1796.204	0.78329967	-27	-88.71	108
1268848123	35.59746026	-111.6017296	1796.204	0.78329967	-26.6	-88.67	107.2
1268848134	35.59746026	-111.6017296	1796.204	0.78329967	-26.6	-88.67	107.2
1268848145	35.59746026	-111.6017296	1796.204	0.78329967	-26.19	-88.62	106.5
1268848155	35.59746026	-111.6017296	1796.204	0.78329967	-25.88	-88.59	105.88
1268848167	35.59746026	-111.6017296	1796.204	0.78329967	-25.88	-88.59	105.88
1268848178	35.59746026	-111.6017296	1796.204	0.78329967	-25.83	-88.61	106
1268848188	35.59746026	-111.6017296	1796.204	0.78329967	-25.83	-88.61	106
1268848199	35.59746026	-111.6017296	1796.204	0.78329967	-25.63	-88.63	106.11
1268848209	35.59746026	-111.6017296	1796.204	0.78329967	-22	-89	108
1268848221	35.59746026	-111.6017296	1796.204	0.78329967	-22	-89	108
1268848232	35.59746026	-111.6017296	1796.204	0.78329967	-27.5	-88.5	108
1268848243	35.59746026	-111.6017296	1796.204	0.78329967	-27.5	-88.5	108
1268848253	35.59746026	-111.6017296	1796.204	0.78329967	-30.22	-90	108

Time(epoch)	Lat(degrees)	Long(degrees)	Alt (meters)	Distance (meters)	Signal (dB)	Noise (dB)	Modul-ation
1268848505	35.59803547	-111.6025437	1799.796	98.35219885	-30.53	-90.21	108
1268848516	35.5980374	-111.6025334	1799.497	97.7932574	-30.53	-90.21	108
1268848527	35.5980374	-111.6025334	1799.497	97.7932574	-31.35	-90.4	108
1268848538	35.59810676	-111.6025783	1799.052	105.9861607	-31.35	-90.4	108
1268848548	35.59826837	-111.6026332	1799.767	122.2780152	-31.48	-90.62	108
1268848559	35.59842916	-111.6027824	1800.608	144.6147357	-32.05	-90.82	108
1268848570	35.59854602	-111.6029194	1801.39	162.5764458	-32.05	-90.82	108
1268848581	35.59863876	-111.6029478	1800.754	172.0576491	-47	-96	108
1268848592	35.59863876	-111.6029478	1800.754	172.0576491	-47	-96	108
1268848602	35.5987003	-111.6029743	1801.522	178.8578208	-49	-96	108
1268848613	35.5987899	-111.6031483	1803.093	196.6419067	-46	-95.67	108
1268848623	35.59882061	-111.6034105	1805.204	215.3778734	-46	-95.67	108
1268848634	35.59886067	-111.6037219	1807.582	239.108514	-48.5	-95.5	108
1268848646	35.59896502	-111.6039553	1810.302	262.7390977	-48.5	-95.5	108
1268848657	35.59917087	-111.6039219	1809.313	275.7458624	-49	-95.4	108
1268848667	35.59933847	-111.6037863	1807.381	280.6389064	-49	-94.67	108
1268848678	35.59956945	-111.6036074	1805.932	290.5096877	-49	-94.67	108
1268848688	35.59977519	-111.6035147	1804.958	304.7836641	-47	-94.14	108
1268848700	35.6000503	-111.6034668	1803.539	329.0048796	-45.38	-94	108
1268848711	35.60025228	-111.603454	1803.149	348.3715718	-45.38	-94	108
1268848721	35.60046555	-111.6034801	1802.728	370.7336068	-44.11	-93.78	108
1268848733	35.6007134	-111.6034693	1802.099	395.4338066	-44.11	-93.78	108
1268848743	35.60095738	-111.6034789	1802.069	420.7956072	-43.2	-93.6	108
1268848754	35.60121642	-111.6034475	1801.424	446.6228458	-42.09	-92.73	108
1268848766	35.60142959	-111.6034142	1801.018	467.9312617	-42.09	-92.73	108
1268848777	35.60160717	-111.6033933	1800.976	486.0593187	-42.17	-92	108
1268848787	35.60181108	-111.6033702	1800.287	507.061869	-42.17	-92	108
1268848798	35.60203361	-111.6033861	1800.149	531.1911884	-42.46	-92	108
1268848809	35.6022542	-111.6034122	1800.31	555.4290966	-43.07	-92	108
1268848820	35.60243371	-111.603381	1799.969	573.9196819	-43.07	-92	108
1268848832	35.60260517	-111.6035034	1799.158	595.269899	-44.27	-91.67	108
1268848842	35.60271012	-111.6035359	1798.35	607.3131739	-45.38	-91.62	108
1268848853	35.60271012	-111.6035359	1798.35	607.3131739	-45.38	-91.62	108
1268848864	35.60271745	-111.6035359	1798.932	608.0983566	-46.47	-91.59	108
1268848874	35.60271552	-111.6035462	1799.231	608.1428712	-47.61	-91.67	108
1268848886	35.60271552	-111.6035462	1799.231	608.1428712	-47.61	-91.67	108
1268848897	35.60271552	-111.6035462	1799.231	608.1428712	-48.74	-91.74	107.37
1268848907	35.60271552	-111.6035462	1799.231	608.1428712	-48.74	-91.74	107.37
1268848918	35.60271064	-111.6035421	1799.987	607.5205524	-49.7	-91.8	106.8
1268848929	35.60271552	-111.6035462	1799.231	608.1428712	-49.7	-91.8	106.8

Time(epoch)	Lat(degrees)	Long(degrees)	Alt (meters)	Distance (meters)	Signal (dB)	Noise (dB)	Modul-ation
1268848940	35.60271064	-111.6035421	1799.987	607.5205524	-66	-93	96
1268848952	35.60271552	-111.6035462	1799.231	608.1428712	-66	-93	96
1268848962	35.60272284	-111.6035462	1799.814	608.9277883	-66	-93	96
1268848973	35.60271552	-111.6035462	1799.231	608.1428712	-65	-92.67	96
1268848984	35.60272284	-111.6035462	1799.814	608.9277883	-64.5	-92.5	96
1268848994	35.60271797	-111.6035421	1800.569	608.3055447	-64.5	-92.5	96
1268849005	35.60271797	-111.6035421	1800.569	608.3055447	-64.4	-92.6	96
1268849016	35.60271552	-111.6035462	1799.231	608.1428712	-64.4	-92.6	96
1268849027	35.60271552	-111.6035462	1799.231	608.1428712	-64.83	-92.67	96
1268849037	35.60271064	-111.6035421	1799.987	607.5205524	-64.43	-92.71	96
1268849048	35.60271064	-111.6035421	1799.987	607.5205524	-64.43	-92.71	96
1268849059	35.60271797	-111.6035421	1800.569	608.3055447	-64.5	-92.75	96
1268849071	35.60271797	-111.6035421	1800.569	608.3055447	-64.5	-92.75	96
1268849081	35.60271064	-111.6035421	1799.987	607.5205524	-64.56	-92.78	96
1268849092	35.60271797	-111.6035421	1800.569	608.3055447	-64.7	-92.8	96
1268849102	35.60271797	-111.6035421	1800.569	608.3055447	-64.7	-92.8	96
1268849113	35.60271797	-111.6035421	1800.569	608.3055447	-64.55	-92.82	96
1268849124	35.60271064	-111.6035421	1799.987	607.5205524	-64.5	-92.83	96
1268849136	35.60271552	-111.6035462	1799.231	608.1428712	-64.5	-92.83	96
1268849147	35.60286725	-111.6035458	1798.042	624.4061588	-64.62	-92.85	96
1268849168	35.60322921	-111.6034977	1796.904	662.2815199	-65.07	-93.07	96
1268849178	35.60334178	-111.6037085	1796.633	679.244471	-65.87	-93.27	96
1268849189	35.6035224	-111.6037613	1796.12	699.8993894	-65.87	-93.27	96
1268849200	35.60371624	-111.6038427	1795.277	722.6591077	-65.75	-92.62	96
1268849210	35.60387265	-111.6040062	1795.081	743.4393336	-65.76	-92.06	96
1268849221	35.60409629	-111.6041061	1794.772	769.8676206	-65.76	-92.06	96
1268849231	35.60416168	-111.6041121	1794.942	777.0090457	-65.61	-91.33	96
1268849242	35.60415436	-111.6041121	1794.359	776.225811	-65.63	-90.68	96
1268849252	35.60417144	-111.6041202	1793.43	778.2569154	-65.63	-90.68	96
1268849264	35.6041929	-111.604114	1793.539	780.3954666	-65.9	-90.45	96
1268849274	35.60419778	-111.6041181	1792.783	781.0191019	-66.24	-90.1	96
1268849285	35.6041929	-111.604114	1793.539	780.3954666	-66.24	-83	96
1268849285	35.6041929	-111.604114	1793.539	780.3954666	-73	-83	96
1268849300	35.60418557	-111.604114	1792.957	779.611999	-73	-83	96
1268849311	35.60418557	-111.604114	1792.957	779.611999	-73	-83	96
1268849321	35.60418557	-111.604114	1792.957	779.611999	-73	-83	96
1268849333	35.60418557	-111.604114	1792.957	779.611999	-73	-83	96
1268849343	35.60418557	-111.604114	1792.957	779.611999	-73	-83	96
1268849354	35.60418557	-111.604114	1792.957	779.611999	-73	-83	96
1268849364	35.60418557	-111.604114	1792.957	779.611999	-73	-83	96

Time(epoch)	Lat(degrees)	Long(degrees)	Alt (meters)	Distance (meters)	Signal (dB)	Noise (dB)	Modul-ation
1268849375	35.60418557	-111.604114	1792.957	779.611999	-73	-83	96
1268849386	35.60418557	-111.604114	1792.957	779.611999	-73	-83	96
1268849396	35.60417825	-111.604114	1792.374	778.8285973	-73	-83	96
1268849407	35.60417825	-111.604114	1792.374	778.8285973	-73	-83	96
1268849418	35.60417825	-111.604114	1792.374	778.8285973	-73	-83	96
1268849429	35.60417825	-111.604114	1792.374	778.8285973	-73	-83	96
1268849439	35.60418557	-111.604114	1792.957	779.611999	-73	-83	96
1268849450	35.60418557	-111.604114	1792.957	779.611999	-73	-83	96
1268849461	35.60418557	-111.604114	1792.957	779.611999	-73	-83	96
1268849471	35.60418557	-111.604114	1792.957	779.611999	-73	-83	96
1268849482	35.60417825	-111.604114	1792.374	778.8285973	-73	-83	96
1268849492	35.60417825	-111.604114	1792.374	778.8285973	-73	-83	96
1268849504	35.60417825	-111.604114	1792.374	778.8285973	-73	-83	96
1268849514	35.60417825	-111.604114	1792.374	778.8285973	-73	-83	96
1268849525	35.60417825	-111.604114	1792.374	778.8285973	-73	-83	96
1268849536	35.60417825	-111.604114	1792.374	778.8285973	-73	-83	96
1268849546	35.60417825	-111.604114	1792.374	778.8285973	-73	-83	96
1268849557	35.60417825	-111.604114	1792.374	778.8285973	-73	-83	96
1268849568	35.60418557	-111.604114	1792.957	779.611999	-73	-83	96
1268849579	35.60417825	-111.604114	1792.374	778.8285973	-73	-83	96
1268849590	35.60417825	-111.604114	1792.374	778.8285973	-73	-83	96
1268849735	35.6047308	-111.6021989	1787.46	810.7794567	-81	-85	2
1268849746	35.60476407	-111.6019591	1787.456	813.6151737	-81	-85	2
1268849756	35.60477811	-111.6018935	1786.998	815.042057	-81	-85	2
1268849767	35.60477811	-111.6018935	1786.998	815.042057	-80.33	-87.33	2
1268849777	35.60478298	-111.6018976	1786.242	815.5919668	-81.5	-88.5	4.5
1268849788	35.60478298	-111.6018976	1786.242	815.5919668	-81.5	-88.5	4.5
1268849799	35.60478298	-111.6018976	1786.242	815.5919668	-82.4	-89.2	6
1268849810	35.60478298	-111.6018976	1786.242	815.5919668	-83	-89.83	7
1268849820	35.60478298	-111.6018976	1786.242	815.5919668	-83	-89.83	7
1268849831	35.60478298	-111.6018976	1786.242	815.5919668	-83.29	-90.29	7.71
1268849841	35.60477566	-111.6018976	1785.66	814.7765921	-82.75	-90.75	8.25
1268849852	35.60477566	-111.6018976	1785.66	814.7765921	-82.75	-90.75	8.25
1268849862	35.60477566	-111.6018976	1785.66	814.7765921	-82.67	-91.11	8.67
1268849873	35.60477566	-111.6018976	1785.66	814.7765921	-82.6	-91.3	9
1268849883	35.60477566	-111.6018976	1785.66	814.7765921	-82.6	-91.3	9
1268849894	35.60477566	-111.6018976	1785.66	814.7765921	-82.36	-91.45	9.27
1268849904	35.60477566	-111.6018976	1785.66	814.7765921	-82.36	-91.45	9.27
1268849915	35.60477566	-111.6018976	1785.66	814.7765921	-82	-91.58	9.5
1268849926	35.60477566	-111.6018976	1785.66	814.7765921	-81.85	-91.69	9.69

Time(epoch)	Lat(degrees)	Long(degrees)	Alt (meters)	Distance (meters)	Signal (dB)	Noise (dB)	Modul-ation
1268849936	35.60477566	-111.6018976	1785.66	814.7765921	-81.85	-91.69	9.69
1268849947	35.60477566	-111.6018976	1785.66	814.7765921	-81.57	-91.79	9.86
1268849957	35.60477566	-111.6018976	1785.66	814.7765921	-80	-93	12
1268849968	35.60477566	-111.6018976	1785.66	814.7765921	-80	-93	12
1268849978	35.60477566	-111.6018976	1785.66	814.7765921	-79.5	-93	12
1268849989	35.60477566	-111.6018976	1785.66	814.7765921	-79.33	-93.33	12
1268849999	35.60477566	-111.6018976	1785.66	814.7765921	-79.33	-93.33	12
1268850010	35.60477648	-111.6018033	1785.533	814.7454459	-79.75	-93.5	12
1268850021	35.60475197	-111.6017358	1785.896	811.9849248	-80.4	-93.8	12
1268850032	35.60484544	-111.6016105	1785.15	822.4501934	-80.4	-93.8	12
1268850042	35.60501111	-111.6014851	1783.519	841.1038073	-80.83	-94	12
1268850053	35.60519713	-111.6012695	1782.169	862.5104304	-81.71	-94.29	12
1268850064	35.60536657	-111.6010641	1779.955	882.4097279	-81.71	-94.29	12
1268850074	35.60538682	-111.6009145	1780.252	885.6723617	-82.38	-94.5	12
1268850085	35.60538204	-111.6006912	1779.274	887.0396521	-82.89	-94.67	12
1268850095	35.60532957	-111.6005356	1778.819	882.8322247	-82.89	-94.67	12
1268850106	35.60532917	-111.6002979	1778.88	885.6615588	-83.3	-94.8	12
1268850116	35.60534392	-111.6000786	1778.311	890.3852058	-83.64	-94.91	12
1268850127	35.6053487	-111.6000233	1777.571	891.759681	-83.64	-94.91	12
1268850137	35.6053487	-111.6000233	1777.571	891.759681	-83.64	-94.91	12
1268850148	35.60538145	-111.5997773	1775.93	899.4409427	-83.64	-94.91	12
1268850158	35.60541125	-111.599517	1774.746	907.5821523	-83.64	-94.91	12
1268850170	35.60548682	-111.5991992	1773.339	922.4853778	-83.64	-94.91	12
1268850180	35.60549516	-111.598945	1772.046	929.339199	-83.64	-94.91	12
1268850191	35.60548001	-111.598648	1770.959	935.3576501	-83.64	-94.91	12
1268850201	35.60545174	-111.5983817	1770.187	939.8270539	-83.64	-94.91	12
1268850212	35.60537263	-111.59805	1770.426	941.6639752	-83.64	-94.91	12
1268850222	35.60530591	-111.5978412	1770.46	941.6042978	-83.64	-94.91	12
1268850233	35.60531079	-111.5978452	1769.704	941.9710709	-83.5	-94.92	11.17
1268850243	35.60531079	-111.5978452	1769.704	941.9710709	-83.54	-95	10.46
1268850254	35.60531079	-111.5978452	1769.704	941.9710709	-83.54	-95	10.46
1268850265	35.60531079	-111.5978452	1769.704	941.9710709	-83.57	-95.07	9.86
1268850275	35.60531079	-111.5978452	1769.704	941.9710709	-83.57	-95.07	9.86
1268850286	35.60531079	-111.5978452	1769.704	941.9710709	-83.53	-95.13	10
1268850296	35.60531079	-111.5978452	1769.704	941.9710709	-83.62	-95.44	10.12
1268850307	35.60531079	-111.5978452	1769.704	941.9710709	-83.62	-95.44	10.12
1268850317	35.60531079	-111.5978452	1769.704	941.9710709	-86	-100	12
1268850328	35.60531079	-111.5978452	1769.704	941.9710709	-83.5	-98	12
1268850338	35.60531079	-111.5978452	1769.704	941.9710709	-83.5	-98	12
1268850349	35.60531079	-111.5978452	1769.704	941.9710709	-83.33	-97.33	12

Time(epoch)	Lat(degrees)	Long(degrees)	Alt (meters)	Distance (meters)	Signal (dB)	Noise (dB)	Modul-ation
1268850359	35.60529859	-111.5978412	1769.878	940.8476794	-83.75	-97.75	12
1268850370	35.60517309	-111.59778	1770.435	930.0102235	-83.75	-97.75	12
1268850380	35.60514308	-111.5976428	1769.932	931.7771817	-83.4	-98	12
1268850391	35.60515204	-111.5974543	1770.261	939.5766302	-82.67	-97.67	12
1268850402	35.60518733	-111.5972637	1769.944	950.3561923	-82.67	-97.67	12
1268850413	35.60524409	-111.5970668	1769.736	963.7343079	-82.14	-97.43	12
1268850423	35.60526809	-111.5968373	1769.451	975.377401	-81.5	-97.25	12
1268850434	35.60523981	-111.596571	1768.68	983.7633928	-81.5	-97.25	12
1268850444	35.6052208	-111.5962944	1768.192	994.028482	-81	-97.11	12
1268850455	35.60521489	-111.5959871	1767.389	1007.50228	-80.8	-97	12
1268850466	35.60517543	-111.5957413	1766.635	1015.421875	-80.8	-97	12
1268850476	35.60517543	-111.5957413	1766.635	1015.421875	-80.64	-96.91	12
1268850487	35.6051681	-111.5957413	1766.053	1014.731981	-80.64	-96.91	12
1268850497	35.60513525	-111.5956492	1765.991	1016.126177	-80.5	-96.92	12
1268850508	35.60505592	-111.5954895	1764.546	1016.65527	-80.38	-96.85	12
1268850518	35.60495848	-111.5952972	1764.189	1017.497972	-80.38	-96.85	12
1268850529	35.60484436	-111.5950557	1762.982	1019.877017	-80.21	-96.79	12
1268850539	35.60476829	-111.5947977	1762.75	1027.138718	-79.93	-96.73	12
1268850550	35.6048586	-111.5945393	1762.493	1049.446701	-79.93	-96.73	12
1268850560	35.60501634	-111.5943361	1762.092	1074.6332	-79.75	-96.69	12
1268850572	35.60525269	-111.5941675	1761.529	1104.736977	-79.35	-96.65	12
1268850583	35.60538449	-111.5939253	1759.995	1129.855196	-79.35	-96.65	12
1268850593	35.60538306	-111.5936631	1760.216	1144.70741	-79	-96.61	13.33
1268850605	35.60538479	-111.593534	1759.949	1152.33474	-78.74	-96.58	14.53
1268850615	35.60538479	-111.593534	1759.949	1152.33474	-78.74	-96.58	14.53
1268850626	35.60538479	-111.593534	1759.949	1152.33474	-78.55	-96.55	15.6
1268850637	35.60538479	-111.593534	1759.949	1152.33474	-78.29	-96.48	16.57
1268850648	35.60538479	-111.593534	1759.949	1152.33474	-78.29	-96.48	16.57
1268850659	35.60538479	-111.593534	1759.949	1152.33474	-78.14	-96.41	17.45
1268850670	35.60538286	-111.5935442	1760.248	1151.573107	-76	-96	36
1268850680	35.60538286	-111.5935442	1760.248	1151.573107	-76	-96	36
1268850692	35.60538286	-111.5935442	1760.248	1151.573107	-75.5	-96	36
1268850703	35.60538286	-111.5935442	1760.248	1151.573107	-75.67	-96	36
1268850713	35.60538286	-111.5935442	1760.248	1151.573107	-75.67	-96	36
1268850724	35.60538286	-111.5935442	1760.248	1151.573107	-75.5	-96	36
1268850735	35.60538286	-111.5935442	1760.248	1151.573107	-75.4	-96	36
1268850746	35.60538286	-111.5935442	1760.248	1151.573107	-75.4	-96	36
1268850757	35.60538286	-111.5935442	1760.248	1151.573107	-75.5	-96	36
1268850767	35.60538286	-111.5935442	1760.248	1151.573107	-75.57	-95.86	36
1268850779	35.60538286	-111.5935442	1760.248	1151.573107	-75.57	-95.86	36

Time(epoch)	Lat(degrees)	Long(degrees)	Alt (meters)	Distance (meters)	Signal (dB)	Noise (dB)	Modul-ation
1268850790	35.60538286	-111.5935442	1760.248	1151.573107	-75.62	-95.75	36
1268850800	35.60538286	-111.5935442	1760.248	1151.573107	-75.67	-95.67	36
1268850811	35.60538479	-111.593534	1759.949	1152.33474	-75.67	-95.67	36
1268850823	35.60538286	-111.5935442	1760.248	1151.573107	-75.6	-95.6	36
1268850833	35.60538479	-111.593534	1759.949	1152.33474	-75.55	-95.55	36
1268850844	35.60538479	-111.593534	1759.949	1152.33474	-75.55	-95.55	36
1268850855	35.6053735	-111.5934951	1759.981	1153.641903	-75.58	-95.5	36
1268850866	35.60535194	-111.5934419	1759.887	1154.929352	-76.08	-95.46	36
1268850877	35.6052843	-111.5932679	1760.064	1159.540918	-76.08	-95.46	36
1268850887	35.60526274	-111.5932147	1759.971	1160.927685	-76.14	-95.21	36
1268850899	35.60519226	-111.5930858	1760.589	1162.875971	-75.93	-95	35.2
1268850910	35.60509482	-111.5928935	1760.232	1166.722263	-75.93	-95	35.2
1268850920	35.60499057	-111.5927073	1760.93	1169.980762	-74.56	-94.06	33.69
1268850931	35.60487798	-111.5924966	1761.204	1174.513218	-73.88	-92.71	32.35
1268850942	35.60483394	-111.592425	1761.159	1175.700021	-73.88	-92.71	32.35
1268850953	35.60483394	-111.592425	1761.159	1175.700021	-71.94	-91.44	30.78
1268850964	35.60483394	-111.592425	1761.159	1175.700021	-71.37	-90.26	29.37
1268850974	35.60483394	-111.592425	1761.159	1175.700021	-71.37	-90.26	29.37
1268850985	35.60483882	-111.592429	1760.403	1175.816272	-69.85	-89.3	28.1
1268850996	35.60483882	-111.592429	1760.403	1175.816272	-69.19	-88.33	26.95
1268851007	35.60483394	-111.592425	1761.159	1175.700021	-69.19	-88.33	26.95
1268851018	35.60484127	-111.592425	1761.742	1176.269705	-68.77	-87.45	25.91
1268851039	35.60484127	-111.592425	1761.742	1176.269705	-58	-69	4
1268851049	35.60483394	-111.592425	1761.159	1175.700021	-54	-69	4
1268851061	35.60483394	-111.592425	1761.159	1175.700021	-54	-69	4
1268851072	35.60483394	-111.592425	1761.159	1175.700021	-56	-69	4
1268851082	35.60483394	-111.592425	1761.159	1175.700021	-58.75	-70.25	4
1268851094	35.60483394	-111.592425	1761.159	1175.700021	-58.75	-70.25	4
1268851104	35.60484127	-111.592425	1761.742	1176.269705	-59.4	-70	4
1268851115	35.60483394	-111.592425	1761.159	1175.700021	-59.83	-69.83	4
1268851126	35.604831	-111.5924107	1761.616	1176.398988	-59.83	-69.83	4
1268851137	35.60480923	-111.5922386	1761.555	1185.93108	-60.14	-69.71	4
1268851148	35.60480058	-111.5920358	1761.178	1198.627778	-60.62	-69.62	4
1268851159	35.60480504	-111.5918022	1760.486	1214.51273	-60.62	-69.62	4
1268851169	35.60480656	-111.5915543	1760.251	1231.30629	-61	-69.89	3.78
1268851180	35.60479882	-111.5913166	1759.732	1246.900731	-61	-69.89	3.78
1268851191	35.60479932	-111.5910441	1759.655	1265.668798	-61	-69.89	3.78
1268851202	35.60478954	-111.5907573	1759.452	1284.909623	-61.7	-70.1	3.6
1268851213	35.60479035	-111.5906631	1759.326	1291.56695	-62.36	-70.27	3.45
1268851223	35.60479035	-111.5906631	1759.326	1291.56695	-62.36	-70.27	3.45

Time(epoch)	Lat(degrees)	Long(degrees)	Alt (meters)	Distance (meters)	Signal (dB)	Noise (dB)	Modul-ation
1268851234	35.60479035	-111.5906631	1759.326	1291.56695	-63	-70.83	3.33
1268851245	35.60479035	-111.5906631	1759.326	1291.56695	-63.62	-71.31	4.46
1268851256	35.60478842	-111.5906733	1759.626	1290.711552	-63.62	-71.31	4.46
1268851267	35.60478842	-111.5906733	1759.626	1290.711552	-64.07	-71.71	6.71
1268851277	35.6047933	-111.5906774	1758.87	1290.770297	-64.53	-72.07	8.67
1268851289	35.6047933	-111.5906774	1758.87	1290.770297	-64.53	-72.07	8.67
1268851300	35.60478842	-111.5906733	1759.626	1290.711552	-64.94	-72.38	8.88
1268851310	35.60478842	-111.5906733	1759.626	1290.711552	-65	-72.65	9.06
1268851321	35.6047933	-111.5906774	1758.87	1290.770297	-65	-72.65	9.06
1268851332	35.6047933	-111.5906774	1758.87	1290.770297	-65.06	-72.89	9.22
1268851343	35.60479035	-111.5906631	1759.326	1291.56695	-65.16	-73.11	9.37
1268851354	35.60479014	-111.5905442	1759.359	1299.905589	-65.16	-73.11	9.37
1268851365	35.60478535	-111.5903209	1758.384	1315.368859	-65.15	-73.3	9.5
1268851376	35.60478493	-111.5900832	1758.448	1332.282935	-65.19	-73.48	9.57
1268851387	35.60478105	-111.589825	1757.332	1350.574905	-65.19	-73.48	9.57
1268851398	35.6047854	-111.589532	1756.657	1372.101659	-68	-77	11
1268851409	35.60478386	-111.5892104	1756.895	1395.519239	-69	-79	11
1268851420	35.60477601	-111.5889133	1756.394	1416.923468	-69	-79	11
1268851430	35.60477651	-111.5886408	1756.317	1437.204787	-69.67	-79.67	11.33
1268851442	35.60477395	-111.5882946	1756.714	1462.970732	-71.75	-81.5	14.5
1268851453	35.60477535	-111.5879872	1756.496	1486.245656	-71.75	-81.5	14.5
1268851463	35.60477391	-111.587725	1756.719	1506.068483	-73.4	-82.6	16.4
1268851475	35.60477532	-111.5874177	1756.501	1529.62522	-75	-84.5	17.67
1268851487	35.60476655	-111.5871554	1756.142	1549.254355	-75	-84.5	17.67
1268851498	35.60476266	-111.5868973	1755.027	1568.964626	-75.86	-85.86	30.57
1268851508	35.60476754	-111.5869013	1754.27	1568.93197	-75.86	-85.86	30.57
1268851520	35.60476754	-111.5869013	1754.27	1568.93197	-76.5	-86.38	40.25
1268851531	35.60476754	-111.5869013	1754.27	1568.93197	-76.33	-86.56	47.78
1268851541	35.60476754	-111.5869013	1754.27	1568.93197	-76.33	-86.56	47.78
1268851553	35.60476561	-111.5869116	1754.57	1568.026661	-76.1	-86.7	50.2
1268851563	35.60476561	-111.5869116	1754.57	1568.026661	-75.91	-86.82	52.18
1268851574	35.60476561	-111.5869116	1754.57	1568.026661	-75.91	-86.82	52.18
1268851585	35.60476561	-111.5869116	1754.57	1568.026661	-75.58	-86.92	53.83
1268851596	35.60476561	-111.5869116	1754.57	1568.026661	-75.46	-87	55.23
1268851607	35.60476561	-111.5869116	1754.57	1568.026661	-75.46	-87	55.23
1268851618	35.60476561	-111.5869116	1754.57	1568.026661	-75.43	-87.07	58.14
1268851629	35.60476561	-111.5869116	1754.57	1568.026661	-75.33	-87.13	60.67
1268851640	35.60476561	-111.5869116	1754.57	1568.026661	-75.33	-87.13	60.67
1268851651	35.60476561	-111.5869116	1754.57	1568.026661	-75.25	-87.19	59.88
1268851662	35.60476561	-111.5869116	1754.57	1568.026661	-75.18	-87.24	59.18

Time(epoch)	Lat(degrees)	Long(degrees)	Alt (meters)	Distance (meters)	Signal (dB)	Noise (dB)	Modul-ation
1268851673	35.60476561	-111.5869116	1754.57	1568.026661	-75.18	-87.24	59.18
1268851685	35.60476561	-111.5869116	1754.57	1568.026661	-75.11	-87.28	58.56
1268851696	35.60476561	-111.5869116	1754.57	1568.026661	-75	-87.32	58
1268851706	35.60476561	-111.5869116	1754.57	1568.026661	-75	-87.32	58
1268851717	35.60476561	-111.5869116	1754.57	1568.026661	-75	-87.4	57.5
1268851729	35.60476561	-111.5869116	1754.57	1568.026661	-74.95	-87.48	57.05
1268851750	35.60476561	-111.5869116	1754.57	1568.026661	-74.86	-87.5	56.09
1268851761	35.60475716	-111.5868276	1754.162	1574.045079	-74	-88	36
1268851782	35.60472255	-111.5865859	1752.654	1590.861776	-67.5	-86.5	36
1268851793	35.60474664	-111.5864157	1752.356	1605.494894	-64.67	-86	36
1268851805	35.60484203	-111.5862802	1751.313	1621.447083	-64.67	-86	36
1268851816	35.60495501	-111.586159	1750.978	1637.286415	-62.75	-84.75	54
1268851826	35.60506311	-111.5860338	1751.399	1653.179894	-61.4	-84	64.8
1268851838	35.60519847	-111.5858715	1751.032	1673.516417	-61.4	-84	64.8
1268851849	35.60532457	-111.5857196	1750.382	1692.542431	-60.5	-82.83	72
1268851859	35.6054468	-111.5855881	1750.33	1709.772868	-60.43	-82	75.43
1268851871	35.60558409	-111.5854156	1749.664	1731.062481	-60.88	-81.5	78
1268851882	35.60571944	-111.5852534	1749.298	1751.46278	-60.88	-81.5	78
1268851892	35.6058548	-111.5850912	1748.931	1771.878005	-61.22	-81.11	80
1268851904	35.60588449	-111.5850501	1749.481	1776.777497	-62.1	-80.9	81.6
1268851915	35.60588937	-111.5850542	1748.725	1776.752253	-62.1	-80.9	81.6
1268851925	35.60588937	-111.5850542	1748.725	1776.752253	-62.91	-80.73	82.91
1268851937	35.60588937	-111.5850542	1748.725	1776.752253	-63.58	-80.58	78
1268851948	35.60588256	-111.5850604	1749.78	1775.875425	-63.58	-80.58	78
1268851958	35.60588256	-111.5850604	1749.78	1775.875425	-64.23	-80.46	73.85
1268851970	35.60588256	-111.5850604	1749.78	1775.875425	-64.71	-80.36	70.29
1268851981	35.60588256	-111.5850604	1749.78	1775.875425	-64.71	-80.36	70.29
1268851991	35.60588256	-111.5850604	1749.78	1775.875425	-65.2	-80.27	67.2
1268852003	35.60588256	-111.5850604	1749.78	1775.875425	-65.44	-80.19	64.5
1268852014	35.60588256	-111.5850604	1749.78	1775.875425	-65.44	-80.19	64.5
1268852024	35.60588256	-111.5850604	1749.78	1775.875425	-65.82	-80.18	62.12
1268852036	35.60588256	-111.5850604	1749.78	1775.875425	-66.22	-80.17	60
1268852047	35.60588256	-111.5850604	1749.78	1775.875425	-66.22	-80.17	60
1268852057	35.60588256	-111.5850604	1749.78	1775.875425	-66.47	-80.11	58.11
1268852069	35.60588256	-111.5850604	1749.78	1775.875425	-66.6	-80.05	56.4
1268852080	35.60588256	-111.5850604	1749.78	1775.875425	-66.6	-80.05	56.4
1268852090	35.60588256	-111.5850604	1749.78	1775.875425	-66.76	-80	54.86
1268852102	35.60588256	-111.5850604	1749.78	1775.875425	-66.91	-79.95	53.45
1268852113	35.60588256	-111.5850604	1749.78	1775.875425	-66.91	-79.95	53.45
1268852123	35.60588256	-111.5850604	1749.78	1775.875425	-72	-79	24

Time(epoch)	Lat(degrees)	Long(degrees)	Alt (meters)	Distance (meters)	Signal (dB)	Noise (dB)	Modul-ation
1268852135	35.60588256	-111.5850604	1749.78	1775.875425	-71.5	-79	24
1268852146	35.60588256	-111.5850604	1749.78	1775.875425	-71.5	-79	24
1268852156	35.60587768	-111.5850563	1750.536	1775.900797	-71.33	-79.33	24
1268852168	35.60587768	-111.5850563	1750.536	1775.900797	-71	-79.5	24
1268852179	35.60587768	-111.5850563	1750.536	1775.900797	-70.8	-79.4	24
1268852189	35.60587768	-111.5850563	1750.536	1775.900797	-70.8	-79.4	24
1268852201	35.60587768	-111.5850563	1750.536	1775.900797	-70.67	-79.33	24
1268852212	35.6059926	-111.5849249	1749.902	1792.763506	-71	-79.29	24
1268852222	35.60611869	-111.5847729	1749.253	1811.872701	-71	-79.29	24
1268852234	35.60629788	-111.5845634	1748.963	1838.550857	-71	-79.25	24
1268852245	35.60631832	-111.5845326	1749.23	1842.121967	-71.22	-79.44	24
1268852255	35.6063232	-111.5845367	1748.474	1842.102512	-71.22	-79.44	24
1268852267	35.60631587	-111.5845367	1747.892	1841.665786	-71.6	-79.6	24
1268852279	35.6063232	-111.5845367	1748.474	1842.102512	-71.64	-79.73	24
1268852290	35.60631587	-111.5845367	1747.892	1841.665786	-71.64	-79.73	24
1268852300	35.60631587	-111.5845367	1747.892	1841.665786	-71.83	-79.83	24
1268852312	35.60631587	-111.5845367	1747.892	1841.665786	-71.85	-79.92	24
1268852323	35.60631587	-111.5845367	1747.892	1841.665786	-71.85	-79.92	24
1268852334	35.60631587	-111.5845367	1747.892	1841.665786	-71.93	-80	24
1268852345	35.60631587	-111.5845367	1747.892	1841.665786	-72.07	-80.07	24
1268852366	35.60631587	-111.5845367	1747.892	1841.665786	-72	-80.12	24
1268852378	35.60631099	-111.5845326	1748.648	1841.685486	-71.76	-80.18	23.88
1268852389	35.60631587	-111.5845367	1747.892	1841.665786	-71.76	-80.18	23.88
1268852399	35.60631587	-111.5845367	1747.892	1841.665786	-71.83	-80.28	23.78
1268852411	35.60631587	-111.5845367	1747.892	1841.665786	-71.84	-80.37	23.68
1268852422	35.60631587	-111.5845367	1747.892	1841.665786	-71.75	-80.4	23.6
1268852432	35.60631587	-111.5845367	1747.892	1841.665786	-71.75	-80.4	23.6
1268852444	35.60631587	-111.5845367	1747.892	1841.665786	-71.71	-80.43	23.52
1268852455	35.60631587	-111.5845367	1747.892	1841.665786	-71.64	-80.45	23.45
1268852466	35.60631587	-111.5845367	1747.892	1841.665786	-71.64	-80.45	23.45
1268852477	35.60640353	-111.5844422	1748.047	1854.116111	-71	-81	22
1268852488	35.60655007	-111.5842594	1747.664	1876.835966	-72.5	-81.5	22
1268852499	35.60672	-111.5840602	1747.092	1902.230869	-72.5	-81.5	22
1268852510	35.60691331	-111.5838445	1746.331	1930.313522	-73	-81.67	22
1268852521	35.60711049	-111.5836083	1744.971	1960.213259	-73.25	-81.75	22.5
1268852532	35.60730086	-111.5833783	1744.666	1989.249676	-73.25	-81.75	22.5
1268852543	35.60747271	-111.5831689	1743.795	2015.618477	-73.6	-81.8	22.8
1268852554	35.60763878	-111.5829902	1743.822	2039.327624	-73.83	-82.17	23
1268852565	35.60782375	-111.5827499	1742.637	2068.854507	-73.83	-82.17	23
1268852576	35.60799907	-111.5825609	1742.947	2093.945226	-74.29	-82.43	23.14

Time(epoch)	Lat(degrees)	Long(degrees)	Alt (meters)	Distance (meters)	Signal (dB)	Noise (dB)	Modul-ation
1268852588	35.60812516	-111.5824089	1742.298	2113.207265	-74.75	-82.75	24.75
1268852609	35.60812323	-111.5824192	1742.597	2112.318485	-74.89	-82.89	26
1268852620	35.60812323	-111.5824192	1742.597	2112.318485	-74.9	-83	27
1268852641	35.60812323	-111.5824192	1742.597	2112.318485	-75	-83.09	27.82
1268852652	35.60812323	-111.5824192	1742.597	2112.318485	-75.08	-83.17	28.5
1268852673	35.60812323	-111.5824192	1742.597	2112.318485	-75.15	-83.23	29.08
1268852684	35.60812323	-111.5824192	1742.597	2112.318485	-75.21	-83.29	29.57
1268852696	35.60812323	-111.5824192	1742.597	2112.318485	-75.07	-83.33	30
1268852707	35.60812079	-111.5824233	1741.259	2111.861476	-75.07	-83.33	30
1268852717	35.60812079	-111.5824233	1741.259	2111.861476	-74.94	-83.38	30.38
1268852729	35.60811591	-111.5824192	1742.015	2111.860272	-74.76	-83.35	30.71
1268852740	35.60811591	-111.5824192	1742.015	2111.860272	-74.76	-83.35	30.71
1268852751	35.60812323	-111.5824192	1742.597	2112.318485	-74.61	-83.33	31
1268852762	35.60813004	-111.582413	1741.542	2113.208633	-74.58	-83.37	31.26
1268852773	35.60802964	-111.5822063	1741.644	2122.487199	-74.58	-83.37	31.26
1268852784	35.60783687	-111.5819302	1740.602	2131.624591	-74.55	-83.4	31.5
1268852795	35.60764655	-111.5816501	1740.899	2141.685599	-74.33	-83.48	31.71
1268852806	35.60745185	-111.5813842	1740.156	2150.845687	-74.33	-83.48	31.71
1268852817	35.60723905	-111.5810857	1740.502	2161.991965	-74.05	-83.55	31.91
1268852828	35.60702818	-111.5807769	1740.548	2174.589876	-73.65	-83.52	32.09
1268852840	35.60680999	-111.5804681	1740.013	2187.336122	-73.65	-83.52	32.09
1268852852	35.60658203	-111.5801512	1740.99	2200.781744	-63	-83	96
1268852863	35.60637411	-111.5798567	1740.58	2213.990527	-63	-83.5	102
1268852874	35.60619406	-111.5795908	1741.003	2226.700295	-63	-83.5	102
1268852885	35.60599346	-111.5792964	1741.176	2241.151294	-63.67	-85	104
1268852896	35.60578553	-111.5790019	1740.767	2255.71054	-63.25	-85.75	105
1268852908	35.60555411	-111.5786645	1740.565	2273.254182	-63.25	-85.75	105
1268852919	35.60535645	-111.5783843	1740.281	2288.012483	-64.6	-87	105.6
1268852930	35.60523378	-111.5782781	1740.4	2291.697972	-65	-87.83	106
1268852941	35.60522158	-111.5782741	1740.573	2291.525447	-65	-87.83	106
1268852952	35.60522158	-111.5782741	1740.573	2291.525447	-65.86	-88.71	106.29
1268852975	35.60522453	-111.5782884	1740.116	2290.449104	-66.5	-89.38	106.5
1268852986	35.60522453	-111.5782884	1740.116	2290.449104	-66.44	-89.89	105.33
1268852996	35.60522453	-111.5782884	1740.116	2290.449104	-66.44	-89.89	105.33
1268853008	35.60522453	-111.5782884	1740.116	2290.449104	-66.4	-90.3	104.4
1268853019	35.60523185	-111.5782884	1740.699	2290.756982	-66.36	-90.64	103.64
1268853031	35.6053018	-111.5781202	1740.163	2307.795709	-66.36	-90.64	103.64
1268853042	35.60557992	-111.5778551	1739.998	2341.797922	-65.83	-90.75	104
1268853053	35.60594956	-111.577475	1739.39	2389.54285	-65.31	-90.85	104.31
1268853064	35.60628655	-111.5771216	1738.689	2433.851766	-65.31	-90.85	104.31

Time(epoch)	Lat(degrees)	Long(degrees)	Alt (meters)	Distance (meters)	Signal (dB)	Noise (dB)	Modul-ation
1268853075	35.60656558	-111.5768217	1738.383	2471.287926	-64.79	-91	104.57
1268853087	35.6068261	-111.5765423	1737.512	2506.297462	-64.47	-91.13	104.8
1268853098	35.60707056	-111.5762793	1737.412	2539.302491	-64.47	-91.13	104.8
1268853110	35.60735885	-111.5759692	1737.39	2578.341609	-64.06	-91.38	105
1268853121	35.60763594	-111.5756795	1737.385	2615.279741	-63.76	-91.59	105.18
1268853131	35.6078858	-111.5754268	1738.167	2647.982959	-63.76	-91.59	105.18
1268853143	35.6082116	-111.5750939	1737.484	2691.026631	-63.78	-91.94	105.33
1268853155	35.60852134	-111.5747775	1737.573	2732.069593	-63.84	-92.05	105.47
1268853166	35.60881989	-111.5744816	1737.678	2771.008746	-63.84	-92.05	105.47
1268853177	35.6091155	-111.5741714	1738.24	2811.054478	-63.75	-92.15	105.6
1268853188	35.60939259	-111.5738817	1738.236	2848.590046	-63.62	-92.19	105.71
1268853200	35.60970914	-111.5735591	1737.272	2890.903367	-59	-93	108
1268853212	35.61001643	-111.5732468	1736.024	2932.012861	-59	-93	108
1268853223	35.6103101	-111.5729468	1736.886	2971.502251	-61	-93	108
1268853245	35.61091684	-111.5723037	1735.605	3055.189199	-60.67	-93	108
1268853255	35.61118906	-111.57201	1736.359	3093.245452	-61.5	-93.5	108
1268853267	35.61150355	-111.5716382	1735.712	3139.826428	-61.5	-93.5	108
1268853278	35.61175805	-111.5712707	1735.777	3182.785008	-61.8	-93.8	108
1268853290	35.61198711	-111.5708705	1736.347	3226.902718	-61.5	-93.67	108
1268853301	35.61217825	-111.5705462	1735.925	3262.966135	-61.5	-93.67	108
1268853311	35.61230126	-111.5703204	1735.755	3287.510879	-61.14	-93.57	108
1268853323	35.61230319	-111.5703102	1735.456	3288.421671	-61	-93.75	108
1268853335	35.61230126	-111.5703204	1735.755	3287.510879	-61	-93.75	108
1268853346	35.61229638	-111.5703164	1736.511	3287.555473	-61.33	-93.89	108
1268853357	35.61229638	-111.5703164	1736.511	3287.555473	-60.8	-93	108
1268853368	35.61230126	-111.5703204	1735.755	3287.510879	-60.8	-93	108
1268853379	35.61229638	-111.5703164	1736.511	3287.555473	-60.73	-92.36	108
1268853391	35.61230126	-111.5703204	1735.755	3287.510879	-61.08	-91.83	105
1268853401	35.61229638	-111.5703164	1736.511	3287.555473	-61.08	-91.83	105
1268853413	35.61230126	-111.5703204	1735.755	3287.510879	-60.31	-91.31	104.31
1268853424	35.61231245	-111.5702999	1735.739	3289.742253	-60.14	-90.86	103.71
1268853435	35.61237029	-111.570187	1735.363	3301.809983	-60.14	-90.86	103.71
1268853446	35.61241888	-111.5700844	1734.703	3312.557149	-60.13	-90.53	103.2
1268853458	35.61248161	-111.5699756	1733.571	3324.580738	-60.62	-90.25	101.25
1268853469	35.61253997	-111.5698689	1734.832	3336.192221	-60.62	-90.25	101.25
1268853479	35.61261002	-111.5697601	1734.281	3348.626939	-61.29	-90	99.53
1268853491	35.61267467	-111.569641	1732.85	3361.562093	-62	-89.78	98
1268853502	35.61273546	-111.5695425	1732.017	3372.676815	-62	-89.78	98
1268853513	35.61273739	-111.5695322	1731.718	3373.587146	-62.95	-89.79	96.63
1268853524	35.61275345	-111.5695157	1730.946	3375.775591	-64.05	-89.85	93.6

Time(epoch)	Lat(degrees)	Long(degrees)	Alt (meters)	Distance (meters)	Signal (dB)	Noise (dB)	Modul-ation
1268853536	35.61284587	-111.5693659	1730.365	3392.676138	-64.05	-89.85	93.6
1268853547	35.61293198	-111.5692406	1729.044	3407.303848	-65.05	-89.9	90.86
1268853558	35.61303751	-111.5690599	1728.149	3427.34875	-85	-91	36
1268853569	35.61313866	-111.5688936	1726.214	3446.03072	-85	-91	36
1268853581	35.61313866	-111.5688936	1726.214	3446.03072	-85	-91	36
1268853592	35.61313866	-111.5688936	1726.214	3446.03072	-85	-91	36
1268853603	35.61313185	-111.5688998	1727.269	3445.162729	-85	-91	36
1268853614	35.61313866	-111.5688936	1726.214	3446.03072	-85	-91	36
1268853625	35.61313866	-111.5688936	1726.214	3446.03072	-85	-91	36
1268853636	35.61340216	-111.5684091	1723.167	3498.691384	-85	-91	36
1268853647	35.6137726	-111.5677154	1720.722	3573.717544	-85	-91	36
1268853659	35.61416196	-111.5669479	1720.5	3655.563568	-85.33	-91.5	30.33
1268853670	35.61449794	-111.5663506	1718.244	3721.133333	-85.33	-91.5	30.33
1268853680	35.61483739	-111.5657737	1717.168	3785.309338	-85	-91.86	26.29
1268853692	35.615302	-111.5650797	1715.589	3865.745125	-85.25	-92.38	23.25
1268853700	35.61557152	-111.5646711	1715.046	3912.887146	-65.25	-94.75	2
1268857268	35.61803107	-111.5328819	1684.278	6637.963943	-65.25	-94.75	2
1268857280	35.61803107	-111.5328819	1684.278	6637.963943	-65.31	-94.77	2
1268857303	35.61803107	-111.5328819	1684.278	6637.963943	-65.36	-94.71	9.57
1268857313	35.61803107	-111.5328819	1684.278	6637.963943	-65.27	-94.67	16.13
1268857325	35.61803107	-111.5328819	1684.278	6637.963943	-65.44	-94.69	21.88
1268857337	35.61803107	-111.5328819	1684.278	6637.963943	-65.44	-94.69	21.88
1268857348	35.61803107	-111.5328819	1684.278	6637.963943	-65.59	-94.71	26.94
1268857359	35.61803107	-111.5328819	1684.278	6637.963943	-65.67	-94.72	31.44
1268857370	35.61803107	-111.5328819	1684.278	6637.963943	-65.67	-94.72	31.44
1268857382	35.61803107	-111.5328819	1684.278	6637.963943	-65.63	-94.74	35.47
1268857393	35.61802618	-111.5328779	1685.034	6638.120811	-65.7	-94.8	39.1
1268857405	35.61802618	-111.5328779	1685.034	6638.120811	-65.7	-94.8	39.1
1268857415	35.61803107	-111.5328819	1684.278	6637.963943	-65.86	-94.86	42.38
1268857427	35.61803107	-111.5328819	1684.278	6637.963943	-65.86	-94.86	45.36
1268857438	35.61803107	-111.5328819	1684.278	6637.963943	-65.86	-94.86	45.36
1268857449	35.61803107	-111.5328819	1684.278	6637.963943	-66	-96	108
1268857460	35.61803107	-111.5328819	1684.278	6637.963943	-67.5	-96	108
1268857472	35.61803107	-111.5328819	1684.278	6637.963943	-67.5	-96	108
1268857483	35.61803107	-111.5328819	1684.278	6637.963943	-67.67	-95.67	108
1268857494	35.61803107	-111.5328819	1684.278	6637.963943	-67.25	-95.5	108
1268857505	35.61803159	-111.5331196	1684.196	6617.796266	-67.25	-95.5	108
1268857517	35.61812443	-111.534269	1685.269	6523.936681	-66.8	-95.4	108
1268857528	35.618235	-111.5357235	1685.312	6405.346768	-67.83	-95.33	102
1268857540	35.61830585	-111.5373358	1681.206	6272.402049	-67.83	-95.33	102

Time(epoch)	Lat(degrees)	Long(degrees)	Alt (meters)	Distance (meters)	Signal (dB)	Noise (dB)	Modul-ation
1268857550	35.61832256	-111.5376165	1680.335	6249.501974	-70.14	-95.29	94.29
1268857562	35.61831961	-111.5376022	1680.793	6250.582776	-71.38	-95.25	88.5
1268857573	35.61831961	-111.5376022	1680.793	6250.582776	-71.38	-95.25	88.5
1268857585	35.61832153	-111.5375919	1680.494	6251.524907	-72.67	-95.56	84
1268857595	35.61832153	-111.5375919	1680.494	6251.524907	-73.8	-95.8	78
1268857607	35.61832153	-111.5375919	1680.494	6251.524907	-73.8	-95.8	78
1268857618	35.61832346	-111.5375816	1680.196	6252.466999	-74.82	-96	73.09
1268857630	35.61834326	-111.5381554	1680.563	6205.112804	-75.58	-96.17	69
1268857651	35.61839906	-111.5404668	1682.223	6014.073822	-76.15	-96.38	65.54
1268857662	35.61842321	-111.5417085	1681.917	5911.698274	-76.57	-96.5	64.29
1268857673	35.61844929	-111.5427084	1683.03	5829.818526	-76.57	-96.5	64.29
1268857684	35.61847202	-111.5435158	1684.66	5763.973803	-77.07	-96.6	63.2
1268857696	35.61849577	-111.5443478	1686.133	5696.325092	-77.44	-96.56	62.25
1268857706	35.61851862	-111.5449952	1686.028	5644.014196	-77.94	-96.53	61.41
1268857718	35.61854879	-111.545862	1688.224	5574.16069	-77.94	-96.53	61.41
1268857729	35.61855187	-111.5459358	1687.747	5568.252673	-78.5	-96.56	60.67
1268857740	35.61854891	-111.5459215	1688.204	5569.289056	-78.5	-96.56	60.67
1268857751	35.61854403	-111.5459174	1688.96	5569.392799	-79	-96.58	60
1268857763	35.61854596	-111.5459072	1688.662	5570.325615	-79.35	-96.55	59.4
1268857774	35.61854108	-111.5459031	1689.418	5570.429374	-79.71	-96.52	58.86
1268857785	35.61856137	-111.5462637	1689.71	5541.80433	-79.71	-96.52	58.86
1268857796	35.61858858	-111.5468969	1690.646	5491.254073	-79.91	-96.5	58.36
1268857808	35.61858522	-111.5471551	1691.166	5469.984517	-78	-96	48
1268857819	35.61859203	-111.5471489	1690.111	5470.817764	-78	-96	48
1268857830	35.61859203	-111.5471489	1690.111	5470.817764	-78	-96	42
1268857841	35.61858778	-111.547442	1690.77	5446.678336	-78.33	-96.33	40
1268857853	35.61844255	-111.5482191	1690.947	5376.287584	-78.33	-96.33	40
1268857864	35.61821597	-111.5490661	1691.706	5296.296743	-79.5	-96.5	39
1268857875	35.61800712	-111.5499869	1693.153	5211.19464	-80.6	-97	38.4
1268857886	35.61794165	-111.5508826	1692.994	5135.242037	-80.6	-97	38.4
1268857898	35.61790532	-111.5519504	1693.471	5047.012287	-82.17	-97.33	38
1268857909	35.61789	-111.5523234	1694.128	5016.129806	-83	-97.29	37.71
1268857920	35.61789244	-111.5523193	1695.466	5016.580133	-83.75	-97.25	37.5
1268857931	35.61788368	-111.5525673	1695.107	4996.144603	-83.75	-97.25	37.5
1268857943	35.61784852	-111.5534876	1697.121	4920.320536	-84.22	-97.22	37.33
1268857954	35.61784123	-111.5544365	1699.968	4843.906432	-84.6	-97.2	37.2
1268857965	35.61775735	-111.5553999	1702.661	4762.605344	-84.6	-97.2	37.2
1268857976	35.61753714	-111.5562818	1704.15	4680.749634	-84.82	-97.45	37.09
1268857987	35.61739819	-111.5568028	1706.789	4631.943923	-85.08	-97.67	37
1268857998	35.61729407	-111.5571864	1707.466	4595.929417	-85.08	-97.67	37

Time(epoch)	Lat(degrees)	Long(degrees)	Alt (meters)	Distance (meters)	Signal (dB)	Noise (dB)	Modul-ation
1268858009	35.6171353	-111.5578159	1708.022	4537.482704	-85.46	-97.77	36.92
1268858021	35.61685737	-111.5588701	1709.87	4439.037736	-85.71	-97.86	36.86
1268858032	35.61662274	-111.5598587	1713.594	4348.217846	-85.87	-97.8	36.8
1268858043	35.6165333	-111.5607524	1715.431	4272.96207	-85.87	-97.8	36.8
1268858054	35.61653165	-111.5613918	1715.687	4222.754172	-85.38	-97.75	36.75
1268858066	35.61653846	-111.5613855	1714.632	4223.620719	-84.47	-97.41	38.82
1268858077	35.61653551	-111.5613712	1715.089	4224.575756	-84.47	-97.41	38.82
1268858089	35.61654626	-111.5616232	1715.141	4205.478488	-83.72	-97.11	40.67
1268858099	35.61657748	-111.5623547	1715.456	4150.264712	-83.21	-96.89	42.32
1268858111	35.61662114	-111.5632091	1715.562	4086.608491	-83.21	-96.89	42.32
1268858122	35.61662126	-111.5632685	1715.543	4082.028944	-82.85	-96.7	43.8
1268858134	35.61666216	-111.5637172	1716.075	4049.865427	-82.62	-96.57	43.43
1268858145	35.61669105	-111.5644999	1718.469	3991.593399	-82.62	-96.57	43.43
1268858156	35.6167464	-111.56534	1720.198	3930.999046	-82.59	-96.55	43.09
1268858167	35.61680933	-111.5660795	1720.752	3878.988479	-75	-96	36
1268858179	35.61688152	-111.5668089	1721.589	3828.80248	-75	-96	36
1268858190	35.61696323	-111.5674274	1720.951	3787.936758	-75	-94.5	36
1268858201	35.61702404	-111.5678391	1720.116	3761.38264	-76.33	-94	36
1268858213	35.61702404	-111.5678391	1720.116	3761.38264	-77.25	-92.75	36
1268858224	35.61702404	-111.5678391	1720.116	3761.38264	-77.25	-92.75	36
1268858235	35.61702404	-111.5678391	1720.116	3761.38264	-77.4	-92	36
1268858246	35.61702597	-111.5678288	1719.818	3762.264183	-77.5	-91.5	36
1268858258	35.61702597	-111.5678288	1719.818	3762.264183	-77.5	-91.5	36
1268858269	35.61703136	-111.5678391	1720.699	3761.85477	-77.43	-91.14	36
1268858280	35.61715734	-111.5681379	1720.071	3748.029623	-77.5	-90.75	36
1268858291	35.61734457	-111.5685758	1718.54	3728.295004	-77.5	-90.75	36
1268858303	35.61754701	-111.5688006	1718.086	3725.42479	-77.44	-90.44	36
1268858314	35.61754213	-111.5687966	1718.842	3725.392413	-77.9	-90.7	37.2
1268858326	35.61754406	-111.5687863	1718.543	3726.264264	-77.9	-90.7	37.2
1268858337	35.61753673	-111.5687863	1717.961	3725.775127	-78.36	-90.91	35.45
1268858348	35.61753185	-111.5687822	1718.717	3725.743047	-79	-91.17	33.42
1268858359	35.61753185	-111.5687822	1718.717	3725.743047	-79.38	-91.38	31.69
1268858370	35.61753185	-111.5687822	1718.717	3725.743047	-79.38	-91.38	31.69
1268858382	35.61753185	-111.5687822	1718.717	3725.743047	-79.79	-91.57	30.21
1268858393	35.61753185	-111.5687822	1718.717	3725.743047	-80.13	-91.73	28.47
1268858405	35.61753185	-111.5687822	1718.717	3725.743047	-80.13	-91.73	28.47
1268858416	35.61753185	-111.5687822	1718.717	3725.743047	-80.25	-91.88	26.94
1268858428	35.61774638	-111.5689517	1718.108	3727.900626	-80.29	-92	25.59
1268858439	35.61806832	-111.5691495	1718.03	3735.570559	-80	-92.11	24.39
1268858450	35.61852542	-111.5693571	1715.902	3752.344272	-80	-92.11	24.39

Time(epoch)	Lat(degrees)	Long(degrees)	Alt (meters)	Distance (meters)	Signal (dB)	Noise (dB)	Modul-ation
1268858462	35.61906348	-111.5695359	1714.971	3777.572357	-79.95	-92.26	25
1268858473	35.61954976	-111.5696841	1715.191	3802.021458	-79.9	-92.4	25.55
1268858484	35.62003593	-111.5697728	1715.43	3831.176317	-79.9	-92.4	25.55
1268858495	35.62061628	-111.5698614	1716.533	3867.881431	-79.62	-92.48	26.05
1268858507	35.62123989	-111.5701158	1717.804	3897.555816	-79.23	-92.55	26.5
1268858518	35.62169416	-111.5703563	1719.552	3916.264309	-79.23	-92.55	26.5
1268858529	35.62190251	-111.5705976	1721.619	3916.540789	-82	-95	22
1268858540	35.621954	-111.5707287	1722.228	3912.013525	-78.5	-95	22
1268858552	35.62195695	-111.570743	1721.771	3911.313389	-78.5	-95	22
1268858563	35.62198789	-111.5708454	1722.129	3907.08264	-76.67	-95	22
1268858575	35.62205352	-111.5709702	1722.266	3904.130025	-75.75	-95	22
1268858585	35.62205352	-111.5709702	1722.266	3904.130025	-75.2	-95	22
1268858597	35.62205352	-111.5709702	1722.266	3904.130025	-75.2	-95	22
1268858609	35.62205352	-111.5709702	1722.266	3904.130025	-74.83	-95	22
1268858620	35.62205352	-111.5709702	1722.266	3904.130025	-74.57	-95	22
1268858631	35.62204619	-111.5709702	1721.684	3903.558378	-74.57	-95	22
1268858642	35.62204619	-111.5709702	1721.684	3903.558378	-74.57	-95	22
1268858654	35.62204619	-111.5709702	1721.684	3903.558378	-74.57	-95	22
1268858665	35.62204812	-111.5709599	1721.385	3904.371122	-74.57	-95	22
1268858676	35.62204812	-111.5709599	1721.385	3904.371122	-74.57	-95	22
1268858687	35.62204619	-111.5709702	1721.684	3903.558378	-74.57	-95	22
1268858699	35.62204812	-111.5709599	1721.385	3904.371122	-74.57	-95	22
1268858710	35.62204812	-111.5709599	1721.385	3904.371122	-74.57	-95	22
1268858722	35.62204812	-111.5709599	1721.385	3904.371122	-74.57	-95	22
1268858732	35.62204812	-111.5709599	1721.385	3904.371122	-74.57	-95	22
1268858744	35.62204812	-111.5709599	1721.385	3904.371122	-74.57	-95	22
1268858755	35.622053	-111.570964	1720.629	3904.490173	-74.57	-95	22
1268858767	35.62204812	-111.5709599	1721.385	3904.371122	-74.57	-95	22
1268858777	35.62204812	-111.5709599	1721.385	3904.371122	-74.57	-95	22
1268858789	35.62204812	-111.5709599	1721.385	3904.371122	-74.57	-95	22
1268858801	35.62204812	-111.5709599	1721.385	3904.371122	-74.57	-95	22
1268858812	35.62204812	-111.5709599	1721.385	3904.371122	-74.57	-95	22
1268858823	35.62212146	-111.5710437	1720.326	3904.704284	-74.57	-95	22
1268858834	35.62234087	-111.5712172	1718.963	3910.812798	-74.57	-95	22
1268858846	35.62258968	-111.5714623	1716.48	3914.92683	-74.57	-95	22
1268858867	35.62303372	-111.5719917	1712.946	3917.336416	-74.57	-95	22
1268858922	35.62469129	-111.5735546	1708.597	3960.934316	-80	-86	2
1268858933	35.62488231	-111.5736811	1708.198	3969.903258	-80	-86	2
1268858945	35.62488424	-111.5736708	1707.899	3970.662236	-78	-88	2
1268858956	35.62488424	-111.5736708	1707.899	3970.662236	-80.67	-89	13.33

Time(epoch)	Lat(degrees)	Long(degrees)	Alt (meters)	Distance (meters)	Signal (dB)	Noise (dB)	Modul-ation
1268858968	35.62487936	-111.5736667	1708.655	3970.479347	-80.67	-89	13.33
1268858979	35.62487936	-111.5736667	1708.655	3970.479347	-81.75	-89.5	19
1268858990	35.62487936	-111.5736667	1708.655	3970.479347	-82	-89.8	22.4
1268859002	35.62492625	-111.5736932	1708.26	3972.961958	-82	-89.8	22.4
1268859013	35.62510751	-111.5738116	1709.373	3981.705501	-82.33	-90	24.67
1268859025	35.62531806	-111.5739422	1709.382	3992.398545	-82.29	-90.29	24.57
1268859035	35.6256111	-111.5740868	1708.636	4009.610431	-82.29	-90.29	24.57
1268859047	35.62603981	-111.5742475	1707.478	4038.049966	-82.38	-90.5	24.5
1268859059	35.62649345	-111.5744224	1707.611	4068.318694	-82.56	-90.78	24.44
1268859070	35.62693874	-111.5745728	1707.32	4099.636436	-82.8	-91	23.1
1268859081	35.62744301	-111.5746943	1706.479	4138.196405	-82.8	-91	23.1
1268859092	35.62798611	-111.5747051	1706.491	4186.542146	-83.27	-91.36	23.18
1268859104	35.62841347	-111.5746629	1705.545	4227.45967	-83.67	-91.67	23.25
1268859116	35.62841347	-111.5746629	1705.545	4227.45967	-83.67	-91.67	23.25
1268859127	35.62840615	-111.5746629	1704.963	4226.795259	-84	-91.92	23.31
1268859138	35.62840615	-111.5746629	1704.963	4226.795259	-84.29	-92.14	23.36
1268859149	35.62840615	-111.5746629	1704.963	4226.795259	-84.53	-92.33	23.4
1268859161	35.62839882	-111.5746629	1704.38	4226.130811	-84.53	-92.33	23.4
1268859172	35.62840615	-111.5746629	1704.963	4226.795259	-84.53	-92.33	23.4
1268859183	35.62839394	-111.5746588	1705.136	4225.900858	-84.53	-92.33	23.4
1268859195	35.62840615	-111.5746629	1704.963	4226.795259	-84.53	-92.33	23.4
1268859206	35.62867251	-111.5746314	1704.915	4252.638173	-84.53	-92.33	23.4
1268859217	35.62907454	-111.5746159	1704.457	4290.083016	-84.53	-92.33	23.4
1268859229	35.62958705	-111.5747025	1704.06	4332.575453	-84.53	-92.33	23.4
1268859240	35.62995576	-111.5748675	1703.614	4358.174999	-84.53	-92.33	23.4
1268859661	35.63232164	-111.583168	1716.642	4228.670651	-86	-96	2
1268859671	35.63232164	-111.583168	1716.642	4228.670651	-86	-96	2
1268859683	35.63232164	-111.583168	1716.642	4228.670651	-86	-96	2
1268859694	35.63232164	-111.583168	1716.642	4228.670651	-86	-96	2
1268859704	35.63232164	-111.583168	1716.642	4228.670651	-86	-96	2
1268859716	35.6323729	-111.5831802	1717.288	4233.471409	-86	-96	2
1268859727	35.63272134	-111.5832039	1718.265	4268.267757	-86	-96	6.4
1268859737	35.63330707	-111.5833028	1720.265	4324.851248	-86	-96	9.33
1268859749	35.63404111	-111.5836595	1721.618	4388.234851	-86	-96	9.33
1268859760	35.63457705	-111.5842874	1724.463	4423.071537	-86.14	-96.14	11.43
1268859770	35.63488861	-111.5846904	1726.003	4442.70619	-86.38	-96.25	13
1268859782	35.63522316	-111.585118	1729.133	4464.481763	-86.38	-96.25	13
1268859793	35.63561151	-111.5856131	1734.232	4490.468257	-86.22	-96.22	11.78
1268859803	35.63595531	-111.5860304	1737.647	4514.662942	-86.1	-96.2	10.8
1268859815	35.63618183	-111.5863639	1738.622	4529.253908	-86.1	-96.2	10.8

Time(epoch)	Lat(degrees)	Long(degrees)	Alt (meters)	Distance (meters)	Signal (dB)	Noise (dB)	Modul-ation
1268859826	35.63617695	-111.5863599	1739.378	4528.849471	-86	-96.18	10
1268859836	35.63617695	-111.5863599	1739.378	4528.849471	-85.92	-96.17	11.17
1268859848	35.63616962	-111.5863599	1738.795	4528.073656	-85.92	-96.17	11.17
1268859859	35.63616962	-111.5863599	1738.795	4528.073656	-85.85	-96.15	12.15
1268859869	35.63617156	-111.5863496	1738.496	4528.563571	-85.79	-96.14	13
1268859881	35.63617156	-111.5863496	1738.496	4528.563571	-85.79	-96.14	13
1268859892	35.63616423	-111.5863496	1737.913	4527.787709	-85.79	-96.14	13
1268859902	35.63616423	-111.5863496	1737.913	4527.787709	-85.79	-96.14	13
1268859914	35.63616423	-111.5863496	1737.913	4527.787709	-85.79	-96.14	13
1268859925	35.63616423	-111.5863496	1737.913	4527.787709	-85.79	-96.14	13
1268859935	35.63616423	-111.5863496	1737.913	4527.787709	-85.79	-96.14	13
1268859947	35.63618773	-111.5863926	1737.709	4529.084277	-85.79	-96.14	13
1268859958	35.63641803	-111.5869371	1736.383	4538.725344	-85.79	-96.14	13
1268860842	35.62767042	-111.6006262	1745.102	3364.726282	-87	-98	2
1268860853	35.62760197	-111.6005464	1745.401	3357.33137	-87	-98	2
1268860864	35.62759668	-111.6005956	1744.504	3356.604418	-87	-98	2
1268860875	35.62750463	-111.6007044	1743.309	3346.076894	-86.67	-97.33	2
1268860886	35.62743302	-111.6007824	1742.381	3337.921485	-86.67	-97.33	2
1268860898	35.62724641	-111.6006416	1743.814	3317.505116	-86	-97	2
1268860909	35.62716455	-111.6004143	1744.474	3309.067754	-86	-96.8	2
1268860919	35.62711991	-111.6002649	1746.237	3304.613708	-86	-96.8	2
1268860931	35.62712723	-111.6002649	1746.819	3305.428367	-85.67	-96.67	2
1268860942	35.62713404	-111.6002587	1745.764	3306.208488	-85.71	-96.86	3.43
1268860953	35.62713404	-111.6002587	1745.764	3306.208488	-85.71	-96.86	3.43
1268860964	35.62713404	-111.6002587	1745.764	3306.208488	-86	-97.25	4.5
1268860975	35.62713404	-111.6002587	1745.764	3306.208488	-86.22	-97.56	5.33
1268860996	35.62712672	-111.6002587	1745.182	3305.393835	-85	-97	12
1268861008	35.62713892	-111.6002627	1745.008	3306.736594	-85.5	-97	12
1268861029	35.6271316	-111.6002627	1744.426	3305.921936	-85	-97	12
1268861039	35.6271316	-111.6002627	1744.426	3305.921936	-85	-97	12
1268861061	35.6271316	-111.6002627	1744.426	3305.921936	-85.4	-97.6	12
1268861072	35.6271316	-111.6002627	1744.426	3305.921936	-86.17	-98	12
1268861084	35.6271316	-111.6002627	1744.426	3305.921936	-86.17	-98	12
1268861095	35.6271316	-111.6002627	1744.426	3305.921936	-86	-97.86	12
1268861106	35.6271316	-111.6002627	1744.426	3305.921936	-85.88	-97.75	12
1268861117	35.62713648	-111.6002668	1743.67	3306.450087	-85.56	-97.56	12
1268861128	35.62710811	-111.6002198	1744.63	3303.466719	-85.56	-97.56	12
1268861139	35.62696074	-111.600218	1743.419	3287.081664	-85.4	-97.4	12
1268861150	35.62687784	-111.6002571	1742.523	3277.7169	-85.18	-97.36	12
1268861161	35.62687591	-111.6002674	1742.822	3277.464588	-85.18	-97.36	12

Time(epoch)	Lat(degrees)	Long(degrees)	Alt (meters)	Distance (meters)	Signal (dB)	Noise (dB)	Modul-ation
1268861172	35.62673901	-111.6003989	1741.706	3261.778714	-85	-97.33	12
1268861183	35.62654474	-111.6006616	1739.175	3239.375677	-84.92	-97.31	12
1268861194	35.6263286	-111.6009716	1738.313	3214.611237	-84.92	-97.31	12
1268861205	35.62607157	-111.6013431	1736.917	3185.466419	-85.07	-97.29	12
1268861216	35.62575993	-111.6017292	1737.113	3150.590416	-85.2	-97.27	12
1268861237	35.62501717	-111.6019585	1737.123	3067.981131	-85.31	-97.25	12
1268861249	35.6239746	-111.6017705	1737.213	2951.851345	-85.41	-97.24	12
1268861260	35.62305501	-111.6015761	1738.861	2849.508721	-85.5	-97.22	12
1268861271	35.62220365	-111.6013426	1740.243	2754.919128	-85.5	-97.22	12
1268861282	35.62160646	-111.6010736	1741.747	2688.865644	-85.58	-97.21	12
1268861293	35.62122803	-111.6009005	1743.705	2647.142807	-85.58	-97.21	12
1268861304	35.62080139	-111.6007888	1744.546	2599.976312	-85.58	-97.21	12
1268861315	35.62047289	-111.6007159	1745.639	2563.653142	-85.58	-97.21	12
1268861326	35.6201566	-111.6006471	1746.558	2528.69765	-85.58	-97.21	12
1268861337	35.62014439	-111.600643	1746.731	2527.354278	-85.58	-97.21	12
1268861380	35.61822098	-111.6003693	1751.071	2314.59272	-86	-96	2
1268861391	35.61780664	-111.6003211	1751.726	2268.773364	-85.5	-95.5	2
1268861402	35.61780664	-111.6003211	1751.726	2268.773364	-85.5	-95.5	2
1268861413	35.61780858	-111.6003109	1751.427	2269.040157	-85.67	-94.67	2
1268861424	35.61780858	-111.6003109	1751.427	2269.040157	-85.5	-94.75	2
1268861435	35.61781346	-111.6003149	1750.671	2269.561776	-85.5	-94.75	2
1268861446	35.61781346	-111.6003149	1750.671	2269.561776	-85.4	-94.8	2
1268861457	35.61782078	-111.6003149	1751.254	2270.375912	-85.5	-94.83	2
1268861468	35.61782078	-111.6003149	1751.254	2270.375912	-85.5	-94.83	2
1268861479	35.61754211	-111.6002829	1751.497	2239.571004	-85.57	-94.86	2
1268861490	35.61705557	-111.6002349	1753.036	2185.765116	-85.5	-94.88	2
1268861501	35.61635625	-111.6001793	1753.197	2108.39749	-85.5	-94.88	2
1268861513	35.61528888	-111.6000243	1755.431	1990.887226	-85.33	-94.89	2
1268861524	35.61440497	-111.599877	1756.717	1893.928598	-85.3	-94.9	2
1268861545	35.61375447	-111.6001163	1757.905	1819.950017	-85.27	-94.91	2
1268861556	35.61375254	-111.6001266	1758.205	1819.661731	-85.25	-94.92	2
1268861567	35.61372914	-111.600143	1758.394	1816.948341	-85.23	-94.92	2
1268861578	35.61338443	-111.6011664	1760.287	1773.661145	-85.23	-94.92	2
1268861589	35.61290819	-111.6026102	1763.671	1721.813945	-85.21	-94.93	2
1268861600	35.61233368	-111.6039559	1766.824	1668.28335	-85.21	-94.93	2
1268861611	35.61166054	-111.6049658	1769.805	1608.082195	-85.21	-94.93	2
1268861622	35.61106774	-111.6058811	1772.359	1561.132758	-85.21	-94.93	2
1268861633	35.61005495	-111.6074675	1776.454	1495.645108	-85.21	-94.93	2
1268861644	35.60908707	-111.6090907	1780.459	1456.290427	-85.21	-94.93	2
1268861656	35.60823026	-111.6106029	1784.43	1443.692785	-85.21	-94.93	2

Time(epoch)	Lat(degrees)	Long(degrees)	Alt (meters)	Distance (meters)	Signal (dB)	Noise (dB)	Modul-ation
1268861666	35.60751746	-111.611877	1786.693	1448.775127	-85.21	-94.93	2
1268861678	35.60666448	-111.6133686	1790.073	1470.284734	-85.21	-94.93	2
1268861689	35.60587862	-111.6147371	1793.357	1505.519937	-85.21	-94.93	2
1268861700	35.60507616	-111.6161159	1795.779	1554.578954	-85.21	-94.93	2
1268862271	35.58964535	-111.6048365	1813.871	914.257051	-67	-82	2
1268862283	35.58964535	-111.6048365	1813.871	914.257051	-69	-82	25
1268862295	35.58963609	-111.6048468	1813.588	915.5239263	-69	-82	25
1268862306	35.58964096	-111.6048509	1812.832	915.1214338	-69.67	-82	32.67
1268862318	35.58964096	-111.6048509	1812.832	915.1214338	-69.5	-82	36.5
1268862329	35.58964096	-111.6048509	1812.832	915.1214338	-69.5	-82	36.5
1268862341	35.58964096	-111.6048509	1812.832	915.1214338	-69.6	-82	38.8
1268862353	35.58964096	-111.6048509	1812.832	915.1214338	-69.17	-81.83	40.33
1268862365	35.58964096	-111.6048509	1812.832	915.1214338	-68.71	-81.71	41.43
1268862377	35.58963364	-111.6048509	1812.25	915.897159	-68.71	-81.71	41.43
1268862389	35.58963364	-111.6048509	1812.25	915.897159	-68.5	-81.75	42.25
1268862400	35.58963364	-111.6048509	1812.25	915.897159	-68.44	-81.78	42.89
1268862412	35.58963364	-111.6048509	1812.25	915.897159	-68.44	-81.78	42.89
1268862424	35.58963364	-111.6048509	1812.25	915.897159	-68.2	-81.8	43.4
1268862436	35.58963364	-111.6048509	1812.25	915.897159	-68	-82	48
1268862448	35.58963364	-111.6048509	1812.25	915.897159	-68.5	-82	48
1268862460	35.58963364	-111.6048509	1812.25	915.897159	-68.5	-82	48
1268862471	35.58963364	-111.6048509	1812.25	915.897159	-67.67	-82	48
1268862483	35.58963364	-111.6048509	1812.25	915.897159	-67.75	-82	48
1268862495	35.58963364	-111.6048509	1812.25	915.897159	-67.75	-82	48
1268862506	35.58962631	-111.6048509	1811.668	916.6728478	-67.6	-82	48
1268862518	35.58963364	-111.6048509	1812.25	915.897159	-67.67	-82	48
1268862531	35.58963364	-111.6048509	1812.25	915.897159	-67.57	-81.86	48
1268862542	35.58963364	-111.6048509	1812.25	915.897159	-67.57	-81.86	48
1268862554	35.58963364	-111.6048509	1812.25	915.897159	-67.62	-81.75	48
1268862566	35.58962631	-111.6048509	1811.668	916.6728478	-67.67	-81.89	48
1268862578	35.58963364	-111.6048509	1812.25	915.897159	-67.67	-81.89	48
1268862590	35.58963648	-111.6048058	1811.809	914.3412381	-67.7	-82	48
1268862602	35.58963841	-111.6047955	1811.509	913.8534276	-67.55	-82	48
1268862614	35.58963841	-111.6047955	1811.509	913.8534276	-67.58	-82	48
1268862625	35.58963841	-111.6047955	1811.509	913.8534276	-67.58	-82	48
1268862637	35.58964849	-111.604691	1811.665	909.9460125	-67.69	-82.08	48
1268862649	35.58966031	-111.6044575	1811.55	902.6614508	-67.71	-82.14	48
1268862661	35.58967589	-111.604144	1810.853	893.610687	-67.71	-82.14	48
1268862673	35.58966899	-111.6038122	1810.204	887.4675536	-67.6	-82.2	48
1268862685	35.58967125	-111.6034107	1809.852	880.1853612	-67.25	-82.25	48

Time(epoch)	Lat(degrees)	Long(degrees)	Alt (meters)	Distance (meters)	Signal (dB)	Noise (dB)	Modul-ation
1268862697	35.58967341	-111.6029497	1809.517	873.6650114	-66.82	-82.41	48
1268862709	35.58966337	-111.6024848	1809.355	870.4258938	-66.82	-82.41	48
1268862721	35.58943211	-111.6022068	1809.135	894.5024959	-66.72	-82.56	50.67
1268862732	35.58922536	-111.6019963	1808.551	916.7769511	-66.74	-82.58	53.05
1268862744	35.5892743	-111.6015025	1807.834	911.2072459	-66.74	-82.58	53.05
1268862756	35.58931682	-111.6009738	1806.393	908.7811823	-66.45	-82.45	55.2
1268862768	35.58930229	-111.6004638	1805.21	914.9858944	-66.14	-82.33	56
1268862779	35.58931632	-111.6001195	1803.033	917.8408607	-62	-79	72
1268862791	35.58934459	-111.5998285	1800.368	919.2787383	-62	-79	72
1268862803	35.58935047	-111.5995785	1797.737	923.124129	-65	-79	72
1268862815	35.58935047	-111.5995785	1797.737	923.124129	-66	-79	72
1268862827	35.58935597	-111.5996482	1798.603	921.2205468	-66	-79	72
1268862838	35.58936147	-111.5997178	1799.469	919.3567718	-66.5	-79	72
1268862850	35.58936157	-111.5997772	1799.453	918.3001108	-66.8	-79	72
1268862862	35.58946989	-111.5997708	1799.838	906.5813556	-67	-79	72
1268862874	35.58952135	-111.5999018	1800.449	898.7142997	-67	-79	72
1268862885	35.58952135	-111.5999018	1800.449	898.7142997	-67.57	-78.57	72
1268862898	35.58952135	-111.5999018	1800.449	898.7142997	-68	-78.25	72
1268862909	35.58952135	-111.5999018	1800.449	898.7142997	-69.44	-78.89	68
1268862921	35.58952135	-111.5999018	1800.449	898.7142997	-69.44	-78.89	68
1268862932	35.58948098	-111.5999695	1801.555	902.0343814	-70.6	-79.4	64.8
1268862944	35.58934753	-111.5998428	1799.911	918.7157557	-70.82	-79.82	62.18
1268862956	35.58935139	-111.5995437	1797.595	923.6922087	-71.58	-80.17	60
1268862968	35.5893646	-111.5992937	1795.545	927.3564064	-71.58	-80.17	60
1268862980	35.58966555	-111.5992253	1795.269	896.3848129	-72.23	-80.46	58.15
1268862992	35.58984303	-111.5997022	1798.674	867.1631065	-72.79	-80.71	56.57
1268863003	35.58986643	-111.6002431	1801.92	855.6066494	-72.79	-80.71	56.57
1268863015	35.58979188	-111.600864	1804.89	856.8972534	-71.73	-80	55.2
1268863027	35.58945279	-111.6014467	1807.646	891.4688774	-70.94	-79.56	54
1268863039	35.58925333	-111.6020843	1809.368	913.9161458	-70.41	-79.18	52.94
1268863051	35.58967315	-111.6022021	1809.556	867.6817155	-70.41	-79.18	52.94
1268863063	35.59020893	-111.602213	1808.947	808.1740315	-70.56	-79.44	51.33
1268863074	35.59069782	-111.6021975	1808.735	753.7574611	-70.47	-79.68	49.89
1268863086	35.59125596	-111.6021674	1808.094	691.5708425	-70.05	-79.8	48.6
1268863098	35.59183171	-111.6021516	1808.16	627.5087887	-70.05	-79.8	48.6
1268863110	35.59200275	-111.6026059	1807.411	612.5148842	-69.24	-79.9	47.43
1268863123	35.59213766	-111.6033451	1807.11	610.2048447	-68.82	-79.55	49.64
1268863134	35.59252575	-111.6037334	1808.786	578.4560171	-68.82	-79.55	49.64
1268863146	35.5930837	-111.6035845	1808.176	515.3044371	-67.74	-79.22	51.65
1268863159	35.59384129	-111.6032077	1804.102	424.474485	-38	-73	96

Time(epoch)	Lat(degrees)	Long(degrees)	Alt (meters)	Distance (meters)	Signal (dB)	Noise (dB)	Modul-ation
1268863171	35.59459878	-111.6027714	1800.045	332.1548154	-38	-73	96
1268863183	35.59529018	-111.6024705	1799.364	250.6480767	-39	-73	102
1268863195	35.59596417	-111.6022742	1797.946	173.638234	-38.67	-74.33	104
1268863207	35.59654876	-111.6020228	1794.928	104.807217	-39.75	-76	105
1268863219	35.59703003	-111.601829	1794.186	48.60608369	-39.75	-76	105
1268863232	35.59743766	-111.601664	1792.836	5.666999926	-38.2	-77	105.6
1268863244	35.59747132	-111.6016619	1792.77	5.601393129	-37.33	-78.67	106
1268863256	35.597464	-111.6016619	1792.188	5.439757195	-37.33	-78.67	106
1268863268	35.59745667	-111.6016619	1791.606	5.397825546	-36.86	-79.86	106.29
1268863280	35.59745179	-111.6016578	1792.362	5.80292779	-36.38	-80.75	106.5
1268863292	35.59745179	-111.6016578	1792.362	5.80292779	-36.38	-80.75	106.5
1268863304	35.59744986	-111.6016681	1792.662	4.916114305	-36.11	-81.44	106.67

Table 13 Tropos.505 Raw Data

Time	Lat	Long	Alt	Dist	Signal	Noise	Modu-lation
1268868583	35.69075255	-111.4680497	1583.217	1.144608457	-20.7	-93.2	2
1268868596	35.69075255	-111.4680497	1583.217	1.144608457	-20.73	-93.27	8.36
1268868618	35.69075255	-111.4680497	1583.217	1.144608457	-20.83	-93.25	16.67
1268868630	35.69074766	-111.4680456	1583.973	0.908880616	-21.62	-93.23	23.69
1268868641	35.69071977	-111.468017	1583.14	4.195681845	-21.57	-93.29	29.71
1268868654	35.69088429	-111.4676943	1583.432	36.11116548	-21.57	-93.29	29.71
1268868666	35.69097335	-111.4669064	1585.099	106.8587554	-22.87	-93.27	34.93
1268868678	35.691646	-111.4662923	1584.019	188.3348799	-24	-93.25	39.5
1268868690	35.69278322	-111.4660455	1583.155	290.7895856	-24	-93.25	39.5
1268868702	35.69377462	-111.4660002	1580.826	385.1976737	-25.12	-93.29	43.53
1268868714	35.69473839	-111.4656655	1574.198	494.4239933	-27.22	-93.33	47.11
1268868726	35.69601135	-111.4656188	1567.799	626.445413	-30.26	-93.42	45.58
1268868737	35.69641243	-111.4650858	1565.829	685.8128696	-30.26	-93.42	45.58
1268868749	35.69628448	-111.4645243	1566.741	694.5356682	-32.9	-93.5	43.85
1268868761	35.69627524	-111.4645346	1566.454	693.1950616	-35.48	-93.57	42.29
1268868773	35.69627524	-111.4645346	1566.454	693.1950616	-35.48	-93.57	42.29
1268868784	35.69626792	-111.4645346	1565.871	692.4714017	-37.82	-93.64	40.86
1268868796	35.69619955	-111.4645144	1566.149	686.56992	-87	-95	11
1268868808	35.69634477	-111.4649712	1565.997	683.0483848	-87	-95	11
1268868819	35.69659968	-111.465565	1566.041	689.7185172	-87	-95	11
1268868832	35.69659775	-111.4655753	1566.338	689.213341	-85.67	-95.33	11
1268868843	35.69676271	-111.4659355	1564.851	696.9610679	-84.75	-95.5	11
1268868855	35.69740165	-111.4670567	1560.418	746.722308	-85.4	-95.4	13.6
1268868867	35.69749285	-111.4672143	1560.042	755.2372079	-85.4	-95.4	13.6
1268868879	35.69748745	-111.467204	1559.161	754.7339345	-85	-95.33	15.33
1268868891	35.69748256	-111.4671999	1559.917	754.2293964	-85	-95.43	14.71
1268868903	35.69748256	-111.4671999	1559.917	754.2293964	-85	-95.62	14.25
1268868915	35.69748256	-111.4671999	1559.917	754.2293964	-85	-95.62	14.25
1268868927	35.69747524	-111.4671999	1559.333	753.4190387	-85.11	-95.78	13.89
1268868939	35.69747035	-111.4671959	1560.089	752.9147711	-85	-95.8	13.6
1268868952	35.69747767	-111.4671959	1560.673	753.7250822	-84.91	-95.82	13.36
1268868963	35.69747767	-111.4671959	1560.673	753.7250822	-84.91	-95.82	13.36
1268868999	35.69747767	-111.4671959	1560.673	753.7250822	-84.86	-95.93	12.86
1268868975	35.69747767	-111.4671959	1560.673	753.7250822	-84.92	-95.83	13.17
1268868987	35.69747767	-111.4671959	1560.673	753.7250822	-84.85	-95.85	13
1268869011	35.69747767	-111.4671959	1560.673	753.7250822	-84.86	-95.93	12.86
1268869023	35.69747767	-111.4671959	1560.673	753.7250822	-84.87	-96	12.73
1268869035	35.69748064	-111.4672102	1560.214	753.9216568	-84.81	-96	12.62

Time	Lat	Long	Alt	Dist	Signal	Noise	Modu-lation
1268869047	35.6977204	-111.4676256	1559.17	777.7094909	-84.81	-96	12.62
1268869059	35.69813662	-111.4683274	1558.291	823.4510649	-84.47	-96	13.18
1268869070	35.69862434	-111.4691232	1556.651	882.6840907	-84.28	-96.06	13.78
1268869082	35.6991823	-111.4700891	1556.16	957.3351754	-83.89	-96.11	14.32
1268869094	35.69975245	-111.471059	1555.499	1039.104474	-83.89	-96.11	14.32
1268869106	35.70035677	-111.472033	1556.418	1129.07383	-82.75	-95.8	14.8
1268869118	35.7009004	-111.4729457	1556.427	1214.157688	-81.38	-95.52	17.52
1268869130	35.70151657	-111.473977	1555.515	1313.455813	-81.38	-95.52	17.52
1268869142	35.7021362	-111.4750289	1555.785	1416.427472	-80.18	-95.41	20
1268869154	35.70276611	-111.4760951	1556.181	1523.125773	-46	-93	72
1268869167	35.7034774	-111.4773109	1557.718	1646.212711	-48.5	-94	72
1268869179	35.70419278	-111.4782332	1558.625	1757.457424	-48.5	-94	72
1268869191	35.7051285	-111.4790745	1556.351	1886.050943	-46.33	-91.33	84
1268869203	35.70604222	-111.4799037	1555.762	2012.036183	-48	-90	90
1268869215	35.70690747	-111.4806756	1554.09	2130.734525	-48	-90	90
1268869227	35.70773802	-111.4814252	1552.64	2245.111595	-50.4	-90.6	93.6
1268869239	35.70856664	-111.482185	1551.488	2359.835273	-52.5	-91	94
1268869251	35.70934971	-111.4828897	1552.23	2467.621588	-52.5	-91	94
1268869263	35.71027122	-111.4837252	1553.873	2594.788224	-54	-91.57	96
1268869275	35.7112553	-111.4846118	1556.135	2730.333001	-55	-92	97.5
1268869287	35.71231473	-111.4855719	1557.047	2876.554542	-55	-92.11	98.67
1268869299	35.7133384	-111.4864851	1558.342	3017.130371	-55	-92.11	98.67
1268869346	35.71612492	-111.4877278	1559.898	3338.661733	-57.75	-92.25	101
1268869312	35.71446871	-111.487129	1560.308	3154.241528	-56.2	-92.4	99.6
1268869323	35.7154797	-111.4874799	1558.425	3266.00012	-57.18	-92.64	100.36
1268869359	35.71612789	-111.4877421	1559.44	3339.631317	-58.08	-91.92	98.77
1268869370	35.7161225	-111.4877318	1558.559	3338.628479	-58.14	-91.5	96.86
1268869382	35.7161176	-111.4877278	1559.314	3337.972557	-58.14	-91.5	96.86
1268869394	35.71621594	-111.4878259	1559.553	3351.960958	-58.27	-91.13	95.2
1268869406	35.71626405	-111.4879365	1558.979	3361.826219	-58.25	-90.88	93.75
1268869419	35.71514766	-111.4888949	1558.287	3306.079576	-58.25	-90.88	93.75
1268869430	35.71334888	-111.490139	1556.727	3212.281852	-58.12	-90.65	92.47
1268869442	35.71093686	-111.4918142	1555.621	3109.21486	-59.06	-90.5	91.33
1268869454	35.70880306	-111.4933426	1554.401	3044.415472	-60.21	-90.37	90.32
1268869466	35.70705638	-111.4945638	1553.384	3006.910836	-60.21	-90.37	90.32
1268869478	35.70525155	-111.4957668	1556.211	2980.842332	-61.25	-90.25	89.4
1268869490	35.70350857	-111.4969309	1564.917	2972.345967	-62.19	-90.14	88.57
1268869502	35.7017536	-111.4979902	1572.051	2971.049073	-81	-88	72
1268869513	35.70019304	-111.4989296	1574.872	2983.0362	-81	-88	72
1268869526	35.69837325	-111.5000135	1576.608	3011.670519	-81	-88	72

Time	Lat	Long	Alt	Dist	Signal	Noise	Modu-lation
1268869537	35.69684288	-111.5009301	1578.205	3048.879785	-81	-88	72
1268869549	35.69517413	-111.5019354	1580.614	3102.681858	-81	-88	72
1268869561	35.69349807	-111.5029407	1582.446	3169.012259	-81	-88	72
1268869573	35.69186876	-111.5039129	1583.916	3244.487352	-81	-88	72
1268869585	35.691725	-111.5039914	1583.843	3251.002198	-81.67	-89	48.67
1268869597	35.69189703	-111.5039004	1582.976	3243.484614	-81.67	-89	48.67
1268869609	35.69190435	-111.5039004	1583.56	3243.516839	-81.75	-89.5	37
1268869621	35.69191359	-111.5038902	1583.845	3242.629528	-81	-89.6	31.8
1268869633	35.69191359	-111.5038902	1583.845	3242.629528	-80.67	-89.67	28.33
1268869645	35.69192091	-111.5038902	1584.429	3242.662225	-80.67	-89.67	28.33
1268869657	35.69192091	-111.5038902	1584.429	3242.662225	-80.57	-89.71	25.86
1268869669	35.69192091	-111.5038902	1584.429	3242.662225	-80.5	-89.75	25.62
1268869681	35.69187607	-111.5039129	1584.5	3244.518776	-80.44	-89.78	25.44
1268869693	35.69108163	-111.504285	1583.828	3275.941987	-80.44	-89.78	25.44
1268869705	35.69002866	-111.5046951	1585.391	3313.777125	-80.5	-89.8	25.3
1268869717	35.68858729	-111.5051086	1585.259	3358.819787	-80.55	-89.82	25.18
1268869729	35.68691581	-111.505607	1586.403	3421.964066	-80.58	-90	25.08
1268869741	35.68670369	-111.5056653	1586.609	3430.206804	-80.58	-90	25.08
1268869777	35.68665397	-111.5056839	1587.436	3432.611868	-79.79	-90.86	26.5
1268869753	35.68671833	-111.5056653	1587.776	3429.993293	-80	-90.46	24.85
1268869765	35.68672322	-111.5056693	1587.02	3430.285089	-79.79	-90.86	26.5
1268869789	35.68502525	-111.5061105	1588.836	3499.269254	-79.33	-91.2	27.93
1268869802	35.68244286	-111.5068502	1590.189	3627.475908	-79.06	-91.5	29.19
1268869813	35.68022277	-111.507488	1592.136	3752.950652	-78.76	-91.76	30.29
1268869826	35.67750482	-111.5082712	1593.89	3923.681405	-78.76	-91.76	30.29
1268869837	35.67540089	-111.5089208	1595.05	4070.80069	-78.83	-92	30.61
1268869849	35.67447584	-111.5091682	1595.731	4135.186723	-78.89	-92.21	30.89
1268869862	35.67232395	-111.5097667	1597.457	4293.064109	-78	-96	36
1268869874	35.66992782	-111.5104564	1600.942	4479.969328	-78	-96	36
1268869886	35.66732396	-111.511202	1602.262	4692.494593	-78	-96	42
1268869898	35.66468256	-111.5119703	1604.252	4917.982916	-75.67	-95.67	44
1268869910	35.66168568	-111.5128341	1604.635	5182.719417	-74.75	-95.5	45
1268869922	35.65947028	-111.513404	1609.376	5379.34744	-74.75	-95.5	45
1268869934	35.65931028	-111.51322	1608.394	5378.248006	-75.8	-95.6	45.6
1268869946	35.65932441	-111.5132138	1607.923	5376.796857	-76.83	-95.67	44
1268869958	35.65934394	-111.5132179	1608.333	5375.660717	-77.86	-96	40.86
1268869970	35.65935319	-111.5132076	1608.618	5374.285568	-77.86	-96	40.86
1268869983	35.65935808	-111.5132116	1607.862	5374.209987	-78.62	-96.25	38.75
1268869995	35.65934159	-111.5130498	1608.697	5364.291621	-79.44	-96.56	37.11
1268870007	35.65924363	-111.5122874	1608.41	5319.372501	-79.6	-96.8	35.8

Time	Lat	Long	Alt	Dist	Signal	Noise	Modu-lation
1268870019	35.6591235	-111.511234	1608.122	5257.061999	-79.6	-96.8	35.8
1268870031	35.65903459	-111.5101825	1606.436	5193.546228	-79.73	-96.73	34.73
1268870043	35.65903548	-111.5101476	1606.298	5191.166546	-79.75	-96.67	33.83
1268870055	35.65904036	-111.5101516	1605.542	5191.065022	-79.77	-96.77	33.08
1268870067	35.65898672	-111.5093603	1603.547	5142.922717	-79.77	-96.77	33.08
1268870079	35.6589158	-111.5078904	1600.793	5052.740787	-80.29	-96.86	32.43
1268870115	35.66025937	-111.5046089	1595.383	4737.360377	-79.88	-96.88	31.25
1268870091	35.65934185	-111.5069211	1600.074	4957.059314	-79.73	-96.87	31.87
1268870103	35.66001509	-111.5058749	1597.145	4837.138256	-79.88	-96.88	31.25
1268870127	35.66060106	-111.5034758	1593.991	4638.847587	-80	-96.88	30.82
1268870139	35.66074046	-111.5030201	1593.014	4599.204055	-80.22	-96.89	30.44
1268870151	35.66127301	-111.5021139	1592.979	4499.848628	-80.22	-96.89	30.44
1268870163	35.66212443	-111.5015037	1591.654	4393.042772	-79.84	-96.89	30.11
1268870175	35.66301684	-111.5008914	1590.853	4282.955759	-79.65	-96.85	30.4
1268870187	35.66387172	-111.5003018	1590.711	4177.489559	-79.57	-96.81	31.24
1268870199	35.66461785	-111.4995403	1590.238	4069.949075	-79.57	-96.81	31.24
1268870211	35.66454384	-111.4988271	1591.391	4031.052613	-79.5	-96.91	32
1268870223	35.66454192	-111.4988374	1591.689	4031.849067	-76	-99	48
1268870235	35.66453267	-111.4988476	1591.403	4033.235187	-74.5	-97.5	48
1268870247	35.66453756	-111.4988517	1590.647	4033.094142	-74.5	-97.5	48
1268870259	35.66453563	-111.498862	1590.945	4033.890725	-74.33	-97	48
1268870271	35.66453563	-111.498862	1590.945	4033.890725	-73.75	-97	48
1268870284	35.66453563	-111.498862	1590.945	4033.890725	-73.6	-97	48
1268870297	35.66452831	-111.498862	1590.362	4034.480176	-73.6	-97	48
1268870309	35.66452831	-111.498862	1590.362	4034.480176	-73.83	-96.83	48
1268870321	35.66452831	-111.498862	1590.362	4034.480176	-73.71	-96.71	48
1268870333	35.66452831	-111.498862	1590.362	4034.480176	-73.71	-96.71	48
1268870345	35.66452831	-111.498862	1590.362	4034.480176	-73.38	-96.62	48
1268870358	35.66452639	-111.4988722	1590.66	4035.276772	-73.38	-96.62	48
1268870369	35.66452639	-111.4988722	1590.66	4035.276772	-73.44	-96.56	48
1268870382	35.66452639	-111.4988722	1590.66	4035.276772	-73.44	-96.56	48
1268870394	35.66452639	-111.4988722	1590.66	4035.276772	-73.5	-96.6	43.4
1268870406	35.6645215	-111.4988682	1591.416	4035.41774	-73.64	-96.64	39.64
1268870418	35.6645215	-111.4988682	1591.416	4035.41774	-73.64	-96.64	39.64
1268870430	35.66452639	-111.4988722	1590.66	4035.276772	-73.67	-96.58	40.33
1268870443	35.66452639	-111.4988722	1590.66	4035.276772	-73.67	-96.58	40.33
1268870455	35.66452639	-111.4988722	1590.66	4035.276772	-73.54	-96.62	40.92
1268870467	35.6645215	-111.4988682	1591.416	4035.41774	-73.5	-96.71	38.14
1268870480	35.6645215	-111.4988682	1591.416	4035.41774	-73.67	-96.93	35.73
1268870492	35.6645215	-111.4988682	1591.416	4035.41774	-73.67	-96.93	35.73

Time	Lat	Long	Alt	Dist	Signal	Noise	Modu-lation
1268870504	35.6645215	-111.4988682	1591.416	4035.41774	-73.88	-97.12	33.62
1268870516	35.66440423	-111.4986123	1590.684	4028.966035	-73.65	-97.06	31.76
1268870562	35.66388791	-111.4962685	1588.204	3930.209956	-73.15	-96.8	27.3
1268870538	35.66394195	-111.4975704	1590.138	4003.148025	-73.22	-97	30.11
1268870550	35.6639133	-111.4968528	1589.423	3962.58371	-73.16	-96.89	28.63
1268870574	35.66399918	-111.4962763	1588.147	3921.252563	-73.15	-96.8	27.3
1268870586	35.66398033	-111.4967295	1589.348	3949.634344	-71	-96	2
1268870598	35.66393003	-111.4972936	1590.266	3987.499162	-72.5	-96	2
1268870610	35.66412789	-111.4979654	1590.542	4011.741672	-76	-96.33	2
1268870622	35.66451403	-111.4988087	1590.856	4032.309093	-76	-96.33	2
1268870634	35.66450525	-111.4997806	1590.5	4094.116494	-74.75	-96.5	2
1268870647	35.66369549	-111.5004665	1590.522	4201.935495	-75	-96.6	2
1268870658	35.66298872	-111.5009633	1591.772	4289.721166	-75.33	-96.5	2
1268870671	35.6621279	-111.5015243	1592.833	4394.042168	-75.33	-96.5	2
1268870683	35.66109011	-111.5023442	1593.823	4528.95262	-75.14	-96.43	5.14
1268870695	35.66043546	-111.5039932	1595.59	4684.536784	-75.38	-96.38	10.5
1268870708	35.65998327	-111.5060268	1598.637	4849.362399	-75.78	-96.33	14.67
1268870720	35.65896316	-111.5077037	1600.328	5037.007968	-75.78	-96.33	14.67
1268870732	35.65900297	-111.5096228	1604.464	5158.944318	-75.6	-96.4	18
1268870744	35.65913585	-111.5112975	1607.927	5260.408899	-76.09	-96.45	20.73
1268870756	35.65934248	-111.5130149	1608.559	5361.835825	-76.33	-96.42	21
1268870768	35.65935394	-111.5131133	1608.502	5367.753659	-76.33	-96.42	21
1268870780	35.65938596	-111.5132403	1608.695	5374.160975	-76.62	-96.38	21.23
1268870792	35.65947456	-111.5135619	1608.714	5389.92813	-77.21	-96.43	21.43
1268870814	35.66003543	-111.5154913	1611.16	5485.157483	-77.53	-96.47	21.6
1268870827	35.66068258	-111.5165716	1612.269	5517.893128	-77.56	-96.62	21.75
1268870839	35.66147899	-111.5174238	1612.592	5526.626503	-77.88	-96.76	21.88
1268870851	35.662019	-111.5179836	1611.404	5532.629756	-77.88	-96.76	21.88
1268870863	35.66246018	-111.518427	1611.781	5537.316919	-77.61	-96.78	22
1268870876	35.66308708	-111.519206	1612.594	5556.426529	-77.32	-96.79	23.37
1268870912	35.66366226	-111.5214435	1623.123	5691.770345	-76.67	-96.9	25.71
1268870888	35.66335292	-111.5199987	1614.361	5600.060981	-77	-96.85	24.6
1268870900	35.66360334	-111.5208735	1618.513	5651.620962	-77	-96.85	24.6
1268870924	35.6636579	-111.5214578	1622.082	5693.12619	-76.14	-96.91	26.73
1268870937	35.66365494	-111.5214435	1622.54	5692.20222	-76.14	-96.91	26.73
1268870949	35.66365494	-111.5214435	1622.54	5692.20222	-75.78	-96.83	30.26
1268870961	35.66364762	-111.5214435	1621.957	5692.634179	-64	-95	108
1268870973	35.66364954	-111.5214332	1621.659	5691.732791	-64	-95	108
1268870985	35.66364954	-111.5214332	1621.659	5691.732791	-64.5	-95	108
1268870998	35.66364954	-111.5214332	1621.659	5691.732791	-68.33	-95	108

Time	Lat	Long	Alt	Dist	Signal	Noise	Modu-lation
1268871011	35.66364954	-111.5214332	1621.659	5691.732791	-68.33	-95	108
1268871023	35.66368108	-111.5217735	1621.928	5715.998524	-71	-95.5	108
1268871035	35.6637021	-111.5222121	1620.393	5748.519232	-69.8	-95.4	108
1268871047	35.66372284	-111.5225318	1618.9	5771.965675	-70.17	-95.33	108
1268871059	35.66378136	-111.5229356	1620.142	5799.784282	-70.17	-95.33	108
1268871071	35.66379861	-111.5232226	1620.904	5821.018527	-71.43	-95.43	102.86
1268871083	35.66379861	-111.5232226	1620.904	5821.018527	-72.25	-95.5	99
1268871096	35.66380054	-111.5232124	1620.606	5820.111889	-72.89	-95.44	93.33
1268871108	35.66380054	-111.5232124	1620.606	5820.111889	-72.89	-95.44	93.33
1268871120	35.66380786	-111.5232124	1621.189	5819.691763	-73.6	-95.4	88.8
1268871131	35.6637949	-111.5233026	1621.479	5827.432814	-74.18	-95.36	85.09
1268871144	35.66369245	-111.5239489	1621.886	5883.440972	-74.58	-95.33	82
1268871156	35.66355545	-111.5246321	1622.492	5944.359829	-74.58	-95.33	82
1268871168	35.66339327	-111.5254016	1623.562	6013.478325	-74.77	-95.23	81.23
1268871182	35.66320513	-111.5261322	1623.502	6081.077691	-75.14	-95.14	80.57
1268871193	35.66262474	-111.5271061	1624.073	6189.731669	-75.47	-95.13	80
1268871206	35.66192073	-111.5280086	1624.897	6299.848446	-75.47	-95.13	80
1268871218	35.66192265	-111.5279984	1624.599	6298.939783	-75.69	-95.12	79.5
1268871230	35.66192997	-111.5279984	1625.182	6298.524515	-76	-95.18	77.65
1268871242	35.6619319	-111.5279881	1624.884	6297.615889	-76.17	-95.22	76
1268871254	35.66161663	-111.5283952	1625.618	6347.187991	-76.17	-95.22	76
1268871266	35.6611287	-111.5290468	1627.329	6425.631837	-76.32	-95.21	74.53
1268871278	35.66051718	-111.5298588	1627.572	6523.6325	-76.1	-95.15	73.2
1268871301	35.6599844	-111.5305332	1629.359	6606.512354	-75.95	-95.1	73.14
1268871312	35.65998633	-111.5305229	1629.061	6605.606827	-76	-96	72
1268871325	35.65999365	-111.5305229	1629.644	6605.184225	-76	-96	72
1268871337	35.65999365	-111.5305229	1629.644	6605.184225	-76	-96	-93.54
1268871339	35.65999365	-111.5305229	1629.644	6605.184225	-71.46	-96	-93.54
1268871339	35.65999365	-111.5305229	1629.644	6605.184225	-71.36	-96	-93.54
1268871339	35.65999365	-111.5305229	1629.644	6605.184225	-71.36	-96	-93.54
1268871339	35.65999365	-111.5305229	1629.644	6605.184225	-71.47	-96	-93.54
1268871339	35.65999365	-111.5305229	1629.644	6605.184225	-71.5	-96	-93.54
1268871339	35.65999365	-111.5305229	1629.644	6605.184225	-71.5	-96	-93.54
1268871339	35.65999365	-111.5305229	1629.644	6605.184225	-71.53	-96	-93.54
1268871339	35.65999365	-111.5305229	1629.644	6605.184225	-71.61	-96	-93.54
1268871339	35.65999365	-111.5305229	1629.644	6605.184225	-71.53	-96	-93.54
1268871339	35.65999365	-111.5305229	1629.644	6605.184225	-71.53	-96	-93.54
1268871339	35.65999365	-111.5305229	1629.644	6605.184225	-71.45	-96	-93.54
1268871339	35.65999365	-111.5305229	1629.644	15601.06677	-20.5	-96	-93.54

Table 14 Tropos.727 Raw Data

Time	Lat	Long	Alt	Dist	Signal	Noise	Modu-lation
1268940836	35.55141312	-111.6395048	1971.048	0	-20.4	-84.8	2
1268940851	35.55141312	-111.6395048	1971.048	0	-20	-86	24
1268940864	35.55140632	-111.639511	1972.104	0.941631069	-20	-86	24
1268940877	35.55140632	-111.639511	1972.104	0.941631069	-22.5	-86	66
1268940890	35.55140632	-111.639511	1972.104	0.941631069	-22	-86	80
1268940904	35.55140632	-111.639511	1972.104	0.941631069	-22.75	-86	87
1268940918	35.55140579	-111.6395048	1970.466	0.816087154	-22.75	-86	87
1268940931	35.55140579	-111.6395048	1970.466	0.816087154	-23	-86	91.2
1268940944	35.55140579	-111.6395048	1970.466	0.816087154	-23.5	-86.17	94
1268940958	35.55140092	-111.6395008	1971.223	1.407145763	-23.86	-86.29	96
1268940971	35.55140092	-111.6395008	1971.223	1.407145763	-23.86	-86.29	96
1268940985	35.55143265	-111.6395089	1971.454	2.205142575	-23.25	-86.12	97.5
1268940998	35.55151898	-111.6395026	1970.087	11.78615561	-24.33	-86	97.33
1268941011	35.5515799	-111.6394635	1969.225	18.93965569	-24	-86.3	97.2
1268941025	35.5518554	-111.6393748	1965.997	50.62295222	-24	-86.3	97.2
1268941039	35.55225552	-111.6394415	1962.334	93.95172449	-25.45	-86.55	97.09
1268941052	35.5527981	-111.6395181	1957.187	154.1815735	-26.5	-86.58	98
1268941064	35.55339433	-111.6395434	1954.028	220.5768176	-27.77	-86.62	98.77
1268941079	35.55419154	-111.6395315	1950.618	309.3032239	-27.77	-86.62	98.77
1268941092	35.55450726	-111.6395943	1948.024	344.5358608	-30.07	-86.64	99.43
1268941106	35.55508251	-111.6396442	1942.967	408.6718063	-31.8	-87.2	100
1268941118	35.55559784	-111.6397577	1938.615	466.4058737	-34.5	-87.69	100.5
1268941132	35.55617007	-111.6397339	1934.028	529.9500081	-34.5	-87.69	100.5
1268941145	35.55682722	-111.6397202	1930.012	603.0138262	-36.82	-88.18	100.94
1268941159	35.55759902	-111.6396756	1927.112	688.7888238	-37.89	-88.61	101.33
1268941172	35.55766148	-111.6396673	1927.733	695.7235045	-38.74	-89	101.68
1268941186	35.55765415	-111.6396673	1927.151	694.9076001	-38.74	-89	101.68
1268941199	35.55766148	-111.6396673	1927.733	695.7235045	-39.2	-89.35	102
1268941213	35.55786934	-111.6396832	1926.413	718.8881137	-47	-96	108
1268941226	35.55786447	-111.6396791	1927.169	718.3379361	-47.5	-96	108
1268941267	35.55800145	-111.6399573	1926.536	734.5574472	-47	-96	108
1268941241	35.55786447	-111.6396791	1927.169	718.3379361	-47.5	-96	108
1268941254	35.55786447	-111.6396791	1927.169	718.3379361	-47.33	-96	108
1268941280	35.55838204	-111.6406957	1925.912	783.2420508	-50.6	-96	108
1268941294	35.55889281	-111.6417185	1925.713	856.4344941	-50.6	-96	108

Time	Lat	Long	Alt	Dist	Signal	Noise	Modu-lation
1268941307	35.55939044	-111.642772	1925.834	936.0332425	-50	-96	98
1268941320	35.5599594	-111.6439196	1925.198	1031.971741	-51	-96	90.86
1268941334	35.56058364	-111.6451776	1924.579	1142.84858	-51.25	-96	85.5
1268941347	35.56104642	-111.64609	1924.954	1227.054954	-53.11	-96.33	80
1268941361	35.56163883	-111.6472806	1924.119	1338.537182	-53.11	-96.33	80
1268941400	35.56307456	-111.6501098	1926.487	1614.8069	-54	-96.5	72
1268941373	35.56216327	-111.6483382	1925.24	1439.471563	-54	-96.6	76.8
1268941387	35.56268569	-111.6493468	1926.673	1539.196512	-53.73	-96.55	74.18
1268941414	35.56337388	-111.650699	1924.727	1673.484075	-54.62	-96.46	70.15
1268941426	35.56357021	-111.6512453	1923.481	1721.042904	-54.62	-96.46	70.15
1268941439	35.56364185	-111.6515769	1922.677	1745.964638	-56.57	-96.5	68.57
1268941451	35.56364185	-111.6515769	1922.677	1745.964638	-58.27	-96.53	67.2
1268941463	35.56365312	-111.6516158	1922.647	1749.149026	-59.75	-96.5	66
1268941475	35.56375957	-111.6520886	1921.598	1785.416508	-59.75	-96.5	66
1268941487	35.56379181	-111.6525124	1921.751	1812.883352	-60.82	-96.47	64.94
1268941499	35.56379375	-111.6525022	1921.451	1812.443985	-61.72	-96.5	64
1268941513	35.56374044	-111.6527787	1922.848	1824.342156	-62.58	-96.53	63.16
1268941526	35.56374237	-111.6527685	1922.548	1823.892599	-63.1	-96.5	62.4
1268941538	35.56374237	-111.6527685	1922.548	1823.892599	-63.1	-96.5	62.4
1268941552	35.56374237	-111.6527685	1922.548	1823.892599	-63.71	-96.48	60.48
1268941565	35.56363524	-111.6533154	1923.705	1848.091847	-75	-96	22
1268941577	35.56371724	-111.654118	1924.731	1904.589245	-73	-96	22
1268941589	35.5639007	-111.6549326	1923.763	1970.921546	-75.67	-97	22
1268941603	35.5642266	-111.6556856	1924.755	2044.971456	-75.67	-97	22
1268941615	35.56430327	-111.6557306	1924.891	2053.840903	-74.75	-97.5	22.5
1268941628	35.56467486	-111.6559694	1923.949	2098.267333	-72.8	-97.4	22.8
1268941641	35.56498936	-111.6566364	1921.552	2165.89043	-71.67	-97.33	23
1268941664	35.56534867	-111.6576186	1920.798	2257.764893	-71.86	-97.14	23.14
1268941775	35.56709657	-111.6578038	1914.265	2407.131271	-74.57	-96.79	23
1268941676	35.56536087	-111.6576227	1920.624	2258.965874	-73	-97	23.25
1268941690	35.56571501	-111.6579661	1918.954	2308.656169	-73.22	-97	23.33
1268941712	35.56591413	-111.6579985	1918.994	2326.1084	-73.6	-97	23.4
1268941725	35.56591413	-111.6579985	1918.994	2326.1084	-73.73	-96.91	23.27
1268941738	35.56616257	-111.6580533	1919.975	2348.934881	-73.83	-96.83	23.17
1268941750	35.56669594	-111.6581281	1917.994	2395.573433	-73.83	-96.83	23.17
1268941762	35.56697699	-111.6581685	1915.632	2420.444921	-74.31	-96.77	23.08
1268941787	35.56710237	-111.657773	1913.364	2405.683955	-74.87	-96.8	22.93
1268941799	35.56735591	-111.6572033	1913.555	2391.366909	-74.87	-96.8	22.93
1268941811	35.56766879	-111.6569017	1913.13	2399.304724	-75.44	-96.75	22.88
1268941823	35.56810282	-111.656735	1911.095	2426.212838	-75.76	-96.71	22.82

Time	Lat	Long	Alt	Dist	Signal	Noise	Modu-lation
1268941835	35.56833057	-111.6562451	1910.131	2417.61818	-75.83	-96.67	22.78
1268941874	35.56838969	-111.6559378	1907.833	2405.430171	-75.3	-96.65	22.7
1268941848	35.56839162	-111.6559275	1907.533	2405.025189	-75.47	-96.63	22.74
1268941862	35.56839162	-111.6559275	1907.533	2405.025189	-75.47	-96.63	22.74
1268941886	35.56838481	-111.6559337	1908.589	2404.776159	-75.14	-96.67	22.67
1268941900	35.56846346	-111.6556305	1906.698	2394.814776	-75.05	-96.68	22.64
1268941912	35.5686435	-111.6552799	1902.822	2391.63028	-75.05	-96.68	22.64
1268941925	35.56904417	-111.6549433	1902.528	2409.734351	-75.35	-96.7	22.61
1268941936	35.56923928	-111.6548774	1903.192	2424.025204	-85	-96	22
1268941949	35.56962007	-111.6550467	1902.546	2467.556226	-85.5	-96	22
1268941961	35.57020276	-111.6551439	1901.508	2526.029739	-86	-96.33	22
1268941973	35.57093764	-111.6551876	1900.922	2596.334042	-86	-96.33	22
1268941985	35.57178025	-111.6551594	1899.091	2673.989229	-85.75	-96.5	22
1268941999	35.57284589	-111.6551534	1898.749	2775.001526	-85.8	-96.6	22
1268942011	35.57384561	-111.6551351	1896.605	2870.429206	-85.83	-96.67	22
1268942023	35.57484866	-111.6550186	1895.667	2963.057586	-85.83	-96.67	22
1268942035	35.57596645	-111.6550021	1892.397	3072.496582	-85.86	-96.71	22
1268942048	35.57736576	-111.6549729	1888.422	3210.695386	-85.88	-96.75	22
1268942060	35.57868847	-111.6549581	1884.302	3343.240623	-85.89	-96.78	22
1268942083	35.58099758	-111.6555846	1878.407	3600.864013	-85.89	-96.78	22
1268942095	35.58214035	-111.6560515	1874.713	3734.326136	-85.89	-96.78	22
1268942108	35.58330711	-111.6565675	1872.457	3872.052503	-85.89	-96.78	22
1268942120	35.58412555	-111.6571068	1872.677	3975.084082	-85.89	-96.78	22
1268942132	35.58418075	-111.6571579	1872.707	3982.56904	-85.89	-96.78	22
1268942144	35.5846077	-111.6571571	1873.503	4026.118043	-85.89	-96.78	22
1268942156	35.58515728	-111.656853	1875.902	4071.636967	-85.89	-96.78	22
1268942168	35.58599396	-111.656411	1869.857	4142.760828	-85.89	-96.78	22
1268942182	35.58720684	-111.6571789	1863.895	4293.935023	-85.89	-96.78	22
1268942194	35.58854317	-111.6579588	1857.69	4458.305044	-85.89	-96.78	22
1268942206	35.58977144	-111.658104	1854.501	4590.159259	-85.89	-96.78	22
1268942218	35.59099916	-111.6581715	1853.119	4719.742418	-85.89	-96.78	22
1268942231	35.59220138	-111.6585564	1850.54	4857.199831	-85.89	-96.78	22
1268942243	35.59331688	-111.6590603	1847.665	4989.483178	-85.89	-96.78	22
1268942257	35.59454429	-111.6592998	1844.621	5124.993378	-85.89	-96.78	22
1268942269	35.59464472	-111.6588182	1844.511	5120.413048	-85.89	-96.78	22
1268942908	35.58442545	-111.6237097	1881.123	3943.449786	-80	-96	2
1268942920	35.58449462	-111.6236358	1880.704	3953.054071	-78	-95.5	2
1268942933	35.58450682	-111.6236398	1880.53	3954.185724	-77	-95.33	2
1268942946	35.58450682	-111.6236398	1880.53	3954.185724	-77	-95.33	2
1268942960	35.58450682	-111.6236398	1880.53	3954.185724	-76.75	-95.5	7

Time	Lat	Long	Alt	Dist	Signal	Noise	Modu-lation
1268942974	35.58450682	-111.6236398	1880.53	3954.185724	-76.2	-95.6	10
1268942987	35.58443506	-111.623937	1881.351	3937.028974	-76.17	-96	12
1268942999	35.58419468	-111.6240788	1879.111	3907.448283	-89	-98	22
1268943011	35.58377879	-111.624012	1874.879	3866.438362	-89	-98	22
1268943023	35.58338533	-111.623892	1874.045	3829.654784	-89	-97	22
1268943037	35.58301704	-111.6236143	1876.178	3801.032029	-89	-96.67	22
1268943049	35.58282233	-111.6235555	1880.603	3783.01082	-89	-96.5	22
1268943061	35.5825391	-111.6236853	1885.011	3749.383908	-86.4	-96.4	22
1268943074	35.58228958	-111.6238845	1885.908	3716.827396	-86.4	-96.4	22
1268943088	35.58226273	-111.6238804	1884.918	3714.202984	-83.67	-96.33	22
1268943101	35.58227005	-111.6238804	1885.5	3714.957224	-82.14	-96.14	22
1268943113	35.58227005	-111.6238804	1885.5	3714.957224	-81.12	-96	22
1268943137	35.58227738	-111.6238804	1886.082	3715.71149	-80.56	-96	22
1268943151	35.58232772	-111.6239275	1886.866	3719.276682	-79.9	-96	22
1268943163	35.58248652	-111.6237489	1886.293	3741.773871	-78.82	-96	22
1268943176	35.58281553	-111.6235617	1881.658	3782.096639	-78.5	-96	22
1268943188	35.58298289	-111.6235981	1878.039	3798.071624	-78.5	-96	22
1268943201	35.58303271	-111.6236389	1877.185	3801.804796	-79.23	-96	22
1268943213	35.58327937	-111.6238349	1875.013	3820.612912	-79.86	-96	22
1268943226	35.58389159	-111.6240507	1876.287	3876.874504	-80.4	-96	22
1268943238	35.58443878	-111.6241357	1882.492	3931.010311	-80.4	-96	22
1268943251	35.58489947	-111.6248087	1886.649	3958.110983	-80.81	-96	22
1268943263	35.58529256	-111.6250535	1882.388	3992.026693	-81.18	-96	22
1268943275	35.58552987	-111.6252004	1879.948	4012.680765	-81.5	-96	22
1268943313	35.58661848	-111.6259311	1874.356	4107.275519	-82.05	-96	22
1268943287	35.58587537	-111.6255601	1879.633	4038.798454	-81.79	-96	22
1268943300	35.58619862	-111.6257417	1877.613	4067.927542	-81.79	-96	22
1268943325	35.58683603	-111.6262338	1873.264	4122.318377	-82.29	-96	22
1268943337	35.58705327	-111.6266368	1873.939	4135.024487	-82.29	-96	22
1268943350	35.58749225	-111.6272216	1871.155	4167.489512	-82.29	-96	22
1268943362	35.58776375	-111.6277228	1868.571	4184.824551	-82.29	-96	22
1268943912	35.57855114	-111.6217981	1905.579	3420.149418	-69	-94	2
1268943926	35.57853701	-111.6218043	1906.053	3418.496975	-69	-94	2
1268943938	35.57855114	-111.6217981	1905.579	3420.149418	-63.5	-92	2
1268943953	35.57855307	-111.6217878	1905.279	3420.774727	-62	-91.33	17.33
1268943966	35.57809048	-111.6220797	1906.581	3362.898798	-61.25	-90.75	25
1268943980	35.57754138	-111.6226094	1907.553	3286.445684	-60	-90.4	29.6
1268943993	35.57679793	-111.6227012	1909.46	3209.484026	-60.17	-90.17	32.67
1268944006	35.57579255	-111.6225315	1910.757	3118.947621	-60.17	-90.17	32.67
1268944019	35.57539688	-111.6222435	1910.27	3093.790385	-62.71	-90	31.14

Time	Lat	Long	Alt	Dist	Signal	Noise	Modu-lation
1268944032	35.57540421	-111.6222435	1910.852	3094.49445	-64.38	-90.75	30
1268944046	35.57540228	-111.6222538	1911.151	3093.839928	-76	-96	22
1268944059	35.57516181	-111.621986	1910.648	3083.170974	-76.5	-96	22
1268944097	35.57351349	-111.621617	1910.296	2945.612187	-76.25	-95.5	22
1268944072	35.57474836	-111.621565	1909.482	3063.844044	-76.67	-96	22
1268944085	35.57415546	-111.6215131	1910.379	3010.631502	-76.25	-95.5	22
1268944111	35.57272856	-111.6216925	1913.488	2869.186572	-77.6	-95.2	22
1268944123	35.57214378	-111.621825	1916.566	2808.736086	-77.5	-94.83	22
1268944137	35.57160911	-111.6218979	1917.024	2756.222169	-76	-94.57	22
1268944150	35.57101498	-111.6223313	1918.115	2679.576447	-75.12	-93.88	22
1268944164	35.57020105	-111.622923	1920.656	2574.714233	-74.89	-93.33	22
1268944176	35.5695826	-111.6230576	1923.805	2511.867959	-74.89	-93.33	22
1268944190	35.56900708	-111.6231798	1927.168	2453.892918	-75.6	-93.3	22
1268944231	35.56638634	-111.6245309	1923.037	2148.762577	-75.69	-93.54	19.69
1268944202	35.56837999	-111.6234739	1924.783	2382.221279	-75.45	-93.27	21.09
1268944217	35.56739111	-111.6239348	1923.535	2269.768509	-75	-93.42	20.33
1268944244	35.56545127	-111.6250592	1923.758	2038.026052	-75.69	-93.54	19.69
1268944258	35.56453463	-111.6255077	1925.057	1934.02374	-75.14	-93.71	19.14
1268944271	35.56357397	-111.6258845	1926.315	1831.42752	-75	-93.8	19.33
1268944285	35.56280323	-111.6256753	1927.321	1782.218319	-74.75	-93.88	19.5
1268944297	35.56221142	-111.6257073	1928.062	1733.8778	-74.47	-94.06	19.65
1268944310	35.56146341	-111.6256947	1928.98	1678.08297	-74.47	-94.06	19.65
1268944323	35.56061165	-111.6257928	1930.532	1609.549675	-74.67	-94.22	19.89
1268944336	35.55970703	-111.6261265	1931.693	1523.294181	-74.26	-94.32	22.63
1268944349	35.55877416	-111.6264726	1933.804	1436.835527	-73.95	-94.4	22.7
1268944364	35.55776821	-111.6265752	1935.225	1368.097913	-73.62	-94.48	22.76
1268944377	35.55681704	-111.6264319	1936.74	1328.028933	-73.62	-94.48	22.76
1268944390	35.5559152	-111.6263111	1939.196	1295.762909	-62	-96	24
1268944403	35.55516233	-111.6262943	1940.88	1267.145875	-67.5	-96	24
1268944415	35.55448292	-111.62613	1943.193	1258.605925	-71	-96	24
1268944428	35.5536841	-111.626052	1945.135	1244.351711	-74.25	-95.75	24
1268944441	35.55302348	-111.6260453	1947.974	1232.120995	-74.25	-95.75	24
1268944453	35.55303081	-111.6260453	1948.555	1232.239923	-76.6	-95.6	24
1268944466	35.55303568	-111.6260494	1947.799	1231.955153	-78.33	-95.67	24
1268944478	35.55304494	-111.6260391	1948.08	1233.024846	-79.29	-95.71	24
1268944490	35.55304494	-111.6260391	1948.08	1233.024846	-79.29	-95.71	24
1268944503	35.55275325	-111.6260971	1948.662	1223.451056	-80.12	-95.75	24
1268944516	35.55225186	-111.6262088	1950.853	1207.821945	-81	-95.78	24
1268944529	35.55164435	-111.6261447	1954.045	1210.292109	-81.4	-95.7	24
1268944541	35.55099212	-111.6258841	1955.583	1234.515858	-81.73	-95.64	24

Time	Lat	Long	Alt	Dist	Signal	Noise	Modu-lation
1268944553	35.55107748	-111.626191	1956.086	1206.405086	-81.73	-95.64	24
1268944566	35.55154711	-111.6270376	1955.387	1129.247233	-82	-95.58	24
1268944579	35.55204184	-111.6280173	1955.951	1042.770734	-82.23	-95.54	24
1268944591	35.55252678	-111.629001	1954.598	959.3649537	-82.43	-95.5	24
1268944629	35.55396006	-111.6319584	1950.441	739.938717	-82.44	-95.5	22.62
1268944604	35.55304698	-111.6300727	1954.646	873.4001374	-82.53	-95.53	24
1268944616	35.55353576	-111.631036	1952.696	802.5819555	-82.53	-95.53	24
1268944643	35.55394979	-111.6319441	1950.315	740.6998029	-81.94	-95.71	21.41
1268944657	35.55393952	-111.6319298	1950.19	741.464137	-81.72	-95.89	22.22
1268944672	35.55410109	-111.6323348	1949.178	714.9973369	-81.16	-95.89	22.95
1268944685	35.5543686	-111.6327969	1947.193	690.8864164	-81.16	-95.89	22.95
1268944699	35.55468122	-111.6334146	1945.083	660.7540952	-80.5	-95.9	23.6
1268944713	35.55489066	-111.6338707	1943.516	640.4993704	-79.71	-95.9	24.19
1268944727	35.55527664	-111.6346315	1940.334	616.264146	-79.05	-95.91	25.27
1268944740	35.55557217	-111.635241	1939.157	602.8936126	-78.35	-96	26.26
1268944754	35.55559271	-111.6352696	1939.408	602.9984463	-64	-98	48
1268944768	35.55553843	-111.6351837	1939.238	603.3642661	-64	-98	48
1268944781	35.5554802	-111.6350589	1939.681	605.8953375	-67.5	-98	36
1268944796	35.55538529	-111.6348626	1940.661	610.1554668	-67	-98	32
1268944809	35.55532763	-111.6351535	1941.015	587.5351681	-65	-97.5	30
1268944823	35.55569866	-111.6356646	1940.153	590.3893063	-64.2	-97.2	28.8
1268944837	35.5560897	-111.6361981	1937.904	600.5919985	-63.67	-97	32
1268944850	35.55650507	-111.6370183	1937.038	609.9327293	-63.67	-97	32
1268944865	35.55691217	-111.6378733	1935.736	629.7366129	-63.43	-96.86	34.29
1268944878	35.55710831	-111.6382414	1934.516	644.2324376	-63.38	-96.75	36
1268944892	35.55760923	-111.6392088	1932.406	690.2722455	-63.56	-96.67	37.33
1268944907	35.55773518	-111.6396263	1931.766	703.8581739	-62.8	-96.6	40.8
1268944920	35.55773711	-111.639616	1931.466	704.0593314	-61.09	-96.55	43.64
1268944934	35.55772491	-111.639612	1931.641	702.696186	-61.09	-96.55	43.64
1268944948	35.55710391	-111.6396911	1933.482	633.7237042	-59.67	-96.5	46
1268944962	35.55600913	-111.6397323	1938.381	512.0428075	-58.69	-96.46	50.77
1268944976	35.55538077	-111.6397398	1943.086	442.1915983	-58.93	-96.64	54.86
1268944989	35.55451219	-111.6395861	1950.699	345.0670156	-58.33	-96.8	58.4
1268945004	35.55365004	-111.6395389	1955.595	249.0329465	-58.33	-96.8	58.4
1268945018	35.55255664	-111.6394921	1962.008	127.3020447	-58.06	-96.75	61.5
1268945032	35.5516482	-111.6394123	1972.376	27.48002477	-57.29	-96.71	64.24
1268945046	35.55145662	-111.6394865	1976.33	5.121403694	-55.67	-96.39	66.67
1268945060	35.55146882	-111.6394905	1976.155	6.335493289	-54.05	-96.11	68.84
1268945075	35.55147369	-111.6394946	1975.399	6.807020963	-54.05	-96.11	68.84

Table 15 Fixed Antenna Locations

Tropos File	Latitude	Longitude	Altitude
Tropos.500	35.597457831	-111.601721503	1798.298
Tropos.505	35.69074281	-111.468053706	1581.295
Tropos.727	35.551413116	-111.639504849	1971.048

APPENDIX B LTF LIDAR DATABASE AND SRTM DATABASE ELEVATION COMPARISONS

Table 16 Height Error Comparison

Sample Number	LAT LONG Coordinates		LIDAR DB Height		SRTM DB Height		Delta height	ABS ()
0	35.59747884	-111.6016945	1798.484983		1798.13739		-0.347593	0.347593
1	35.59843253	-111.6027714	1803.892442		1798.164445		-5.727997	5.727997
2	35.59879324	-111.6031372	1806.407946		1800.580776		-5.82717	5.82717
3	35.59896836	-111.6039441	1813.6942		1811.931287		-1.762913	1.762913
4	35.60005348	-111.6034557	1807.807646		1806.057307		-1.750339	1.750339
5	35.60071649	-111.6034582	1807.087037		1807.51369		0.426653	0.426653
6	35.60203653	-111.6033751	1804.735883		1803.617436		-1.118447	1.118447
7	35.60271834	-111.6035351	1802.984821		1803.365345		0.380524	0.380524
8	35.60272079	-111.603531	1802.970964		1803.322416		0.351452	0.351452
9	35.60287005	-111.6035347	1802.390788		1803.04003		0.649242	0.649242
10	35.60371892	-111.6038317	1799.550844		1798.650324		-0.90052	0.90052
11	35.60416431	-111.6041011	1798.609813		1795.657614		-2.952199	2.952199
12	35.60418819	-111.6041029	1798.512894		1795.535282		-2.977612	2.977612
13	35.60477819	-111.6018868	1792.572304		1788.572678		-3.999626	3.999626
14	35.6050136	-111.6014745	1789.894781		1789.09164		-0.803141	0.803141
15	35.60549755	-111.5989348	1778.022671		1777.54884		-0.473831	0.473831
16	35.6053132	-111.5978352	1775.81106		1773.472503		-2.338557	2.338557
17	35.60522322	-111.5962846	1773.949731		1771.168477		-2.781254	2.781254
18	35.60496092	-111.5952876	1770.020067		1768.058379		-1.961688	1.961688
19	35.60538543	-111.5936537	1765.853794		1766.043273		0.189479	0.189479
20	35.60538523	-111.5935348	1765.668787		1766.337742		0.668955	0.668955
21	35.60537587	-111.5934857	1765.67438		1766.488327		0.813947	0.813947
22	35.60483637	-111.5924158	1766.571698		1765.229302		-1.342396	1.342396
23	35.60483344	-111.5924015	1766.574202		1765.188819		-1.385383	1.385383
24	35.60479198	-111.5907483	1764.755413		1765.358358		0.602945	0.602945
25	35.60479574	-111.5906684	1764.604712		1765.820091		1.215379	1.215379
26	35.60478779	-111.5903119	1763.942791		1765.428375		1.485584	1.485584
27	35.60477635	-111.5877164	1762.10716		1760.09711		-2.01005	2.01005
28	35.60476996	-111.5868928	1760.981436		1759.954932		-1.026504	1.026504
29	35.60476805	-111.5869031	1761.001022		1759.964376		-1.036646	1.036646
30	35.60588484	-111.5850521	1754.465269		1749.195547		-5.269722	5.269722
31	35.60599486	-111.5849167	1753.994384		1750.371878		-3.622506	3.622506
32	35.60632542	-111.5845286	1752.670334		1753.296068		0.625734	0.625734
33	35.60655225	-111.5842513	1752.011438		1750.816316		-1.195122	1.195122
34	35.60800107	-111.5825531	1747.07693		1746.322312		-0.754618	0.754618
35	35.6081179	-111.5824114	1746.717454		1746.28808		-0.429374	0.429374
36	35.60724114	-111.581078	1745.812562		1747.260556		1.447994	1.447994
37	35.60522686	-111.5782811	1746.721772		1744.155458		-2.566314	2.566314

Sample Number	LAT LONG Coordinates		LIDAR DB Height		SRTM DB Height		Delta height	ABS ()
38	35.6078878	-111.5754198	1742.885226		1741.819391		-1.065835	1.065835
39	35.61119068	-111.5720035	1740.050138		1737.930524		-2.119614	2.119614
40	35.61248307	-111.5699693	1737.654152		1737.866046		0.211894	0.211894
41	35.61275487	-111.5695095	1735.151508		1733.975521		-1.175987	1.175987
42	35.61314003	-111.5688875	1731.037307		1730.485093		-0.552214	0.552214
43	35.61377389	-111.5677095	1725.967738		1724.676209		-1.291529	1.291529
44	35.61803183	-111.53288	1686.032492		1685.026713		-1.005779	1.005779
45	35.61823573	-111.5357213	1686.489415		1684.135929		-2.353486	2.353486
46	35.61842392	-111.5417057	1684.696569		1684.179851		-0.516718	0.516718
47	35.61844326	-111.5482156	1690.26474		1688.444803		-1.819937	1.819937
48	35.61788446	-111.5525633	1694.76699		1692.959646		-1.807344	1.807344
49	35.61713618	-111.5578112	1707.64014		1704.557406		-3.082734	3.082734
50	35.61666311	-111.5637118	1716.898376		1717.301384		0.403008	0.403008
51	35.6175449	-111.5687803	1718.019903		1715.720674		-2.299229	2.299229
52	35.61906415	-111.5695299	1714.403818		1712.833832		-1.569986	1.569986
53	35.62061678	-111.5698554	1714.735142		1711.449866		-3.285276	3.285276
54	35.62195435	-111.5707225	1721.18589		1719.077608		-2.108282	2.108282
55	35.62469133	-111.5735482	1708.929006		1708.72019		-0.208816	0.208816
56	35.6284131	-111.5746564	1704.323131		1702.907417		-1.415714	1.415714
57	35.63330614	-111.5832952	1721.597418		1720.558894		-1.038524	1.038524
58	35.63616294	-111.5863414	1741.399253		1739.887259		-1.511994	1.511994
59	35.62713867	-111.6002528	1750.321708		1753.942674		3.620966	3.620966
60	35.69739523	-111.467061	1564.448509		1565.137593		0.689084	0.689084
61	35.69747421	-111.4672145	1564.107413		1564.46274		0.355327	0.355327
62	35.70150984	-111.4739807	1559.452653		1560.854819		1.402166	1.402166
63	35.70855932	-111.4821879	1557.214799		1559.343274		2.128475	2.128475
64	35.70524446	-111.4957685	1562.353719		1561.070807		-1.282912	1.282912
65	35.69190741	-111.5038913	1587.776874		1582.555065		-5.221809	5.221809
66	35.69002266	-111.5046961	1587.233712		1587.267223		0.033511	0.033511
67	35.67749992	-111.5082719	1594.441301		1594.09274		-0.348561	0.348561
68	35.66731997	-111.5112024	1601.561932		1599.588003		-1.973929	1.973929
69	35.65912024	-111.5112344	1607.710808		1605.436946		-2.273862	2.273862
70	35.66001181	-111.5058758	1597.254349		1597.176496		-0.077853	0.077853
71	35.66454017	-111.4988287	1590.926064		1594.193948		3.267884	3.267884
72	35.66451783	-111.4988697	1590.838198		1594.414747		3.576549	3.576549
73	35.6639097	-111.4968545	1589.562219		1587.706548		-1.855671	1.855671
74	35.66298519	-111.5009646	1590.566908		1587.848623		-2.718285	2.718285
75	35.66003207	-111.5154913	1611.306947		1607.567832		-3.739115	3.739115
76	35.66245658	-111.5184267	1611.486014		1611.525928		0.039914	0.039914
77	35.66377758	-111.5229349	1620.867082		1619.095302		-1.77178	1.77178

Sample Number	LAT LONG Coordinates		LIDAR DB Height		SRTM DB Height		Delta height	ABS ()
78	35.66338952	-111.5254006	1623.312468		1620.286227		-3.026241	3.026241
79	35.65999019	-111.5305214	1628.688741		1625.734618		-2.954123	2.954123
80	35.55142459	-111.6394856	1990.628951		1993.665458		3.036507	3.036507
81	35.55159133	-111.6394444	1988.124035		1990.274881		2.150846	2.150846
82	35.55280918	-111.6394992	1975.427447		1975.163158		-0.264289	0.264289
83	35.55340528	-111.6395245	1971.195419		1972.458341		1.262922	1.262922
84	35.55509309	-111.6396256	1960.066843		1958.708038		-1.358805	1.358805
85	35.55618038	-111.6397155	1951.272537		1949.412635		-1.859902	1.859902
86	35.55760905	-111.6396573	1944.25728		1942.676633		-1.580647	1.580647
87	35.55890263	-111.6416998	1943.341372		1940.952706		-2.388666	2.388666
88	35.56164823	-111.6472612	1942.114148		1941.067305		-1.046843	1.046843
89	35.56365094	-111.6515569	1940.136575		1939.782145		-0.35443	0.35443
90	35.56710507	-111.6577831	1931.581623		1931.352174		-0.229449	0.229449
91	35.56698553	-111.6581477	1933.654584		1931.890696		-1.763888	1.763888
92	35.56811115	-111.6567145	1929.171815		1929.540867		0.369052	0.369052
93	35.56865167	-111.6552598	1919.515829		1920.008862		0.493033	0.493033
94	35.57285342	-111.6551334	1915.51828		1912.127965		-3.390315	3.390315
95	35.58413128	-111.6570871	1888.77251		1890.391985		1.619475	1.619475
96	35.58599941	-111.6563914	1885.78256		1882.783319		-2.999241	2.999241
97	35.59454842	-111.6592804	1859.981323		1857.182743		-2.79858	2.79858
98	35.58451251	-111.6236247	1891.39433		1885.012339		-6.381991	6.381991
99	35.58684135	-111.6262185	1883.885419		1882.299401		-1.586018	1.586018
							sum	175.3562
							mean delta	1.753562

APPENDIX C LTF PREDICTION OF TERRAIN BLOCKAGE

Table 17 Chi Square Test Data RQ1BH1

Black Point Measured Data					LTF LIDAR Predictions		Actual SS	Chi Square Matrix Values	
lat	Long	Elevation	SS	Color	Dist	SS Pred	is red	Cell A	Cell C
35.60260517	-111.6035034	1799.158	-44.27	G	0	Blocked	0	0	1
35.60271012	-111.6035359	1798.35	-45.38	G	0	Blocked	0	0	1
35.60271012	-111.6035359	1798.35	-45.38	G	0	Blocked	0	0	1
35.60271552	-111.6035462	1799.231	-47.61	G	0	Blocked	0	0	1
35.60271552	-111.6035462	1799.231	-64.83	G	0	Blocked	0	0	1
35.60271797	-111.6035421	1800.569	-64.5	G	0	Blocked	0	0	1
35.60322921	-111.6034977	1796.904	-65.07	G	0	Blocked	0	0	1
35.60387265	-111.6040062	1795.081	-65.76	G	0	Blocked	0	0	1
35.6041929	-111.604114	1793.539	-65.9	G	0	Blocked	0	0	1
35.60418557	-111.604114	1792.957	-73	R	0	Blocked	1	1	0
35.60418557	-111.604114	1792.957	-73	R	0	Blocked	1	1	0
35.60417825	-111.604114	1792.374	-73	R	0	Blocked	1	1	0
35.60418557	-111.604114	1792.957	-73	R	0	Blocked	1	1	0
35.60418557	-111.604114	1792.957	-73	R	0	Blocked	1	1	0
35.60417825	-111.604114	1792.374	-73	R	0	Blocked	1	1	0
35.60477811	-111.6018935	1786.998	-81	R	0	Blocked	1	1	0
35.60478298	-111.6018976	1786.242	-81.5	R	0	Blocked	1	1	0
35.60478298	-111.6018976	1786.242	-82.4	R	0	Blocked	1	1	0
35.60478298	-111.6018976	1786.242	-83	R	0	Blocked	1	1	0
35.60477566	-111.6018976	1785.66	-82.75	R	0	Blocked	1	1	0
35.60477566	-111.6018976	1785.66	-82.36	R	0	Blocked	1	1	0
35.60477566	-111.6018976	1785.66	-81.85	R	0	Blocked	1	1	0

Black Point Measured Data					LTF LIDAR Predictions		Actual SS	Chi Square Matrix Values	
lat	Long	Elevation	SS	Color	Dist	SS Pred	is red	Cell A	Cell C
35.60538145	-111.5997773	1775.93	-83.64	R	0	Blocked	1	1	0
35.60541125	-111.599517	1774.746	-83.64	R	0	Blocked	1	1	0
35.60548682	-111.5991992	1773.339	-83.64	R	0	Blocked	1	1	0
35.60531079	-111.5978452	1769.704	-83.5	R	0	Blocked	1	1	0
35.60531079	-111.5978452	1769.704	-83.57	R	0	Blocked	1	1	0
35.60531079	-111.5978452	1769.704	-83.62	R	0	Blocked	1	1	0
35.60531079	-111.5978452	1769.704	-83.62	R	0	Blocked	1	1	0
35.60514308	-111.5976428	1769.932	-83.4	R	0	Blocked	1	1	0
35.60517543	-111.5957413	1766.635	-80.64	R	0	Blocked	1	1	0
35.60513525	-111.5956492	1765.991	-80.5	R	0	Blocked	1	1	0
35.60525269	-111.5941675	1761.529	-79.35	R	0	Blocked	1	1	0
35.60538479	-111.593534	1759.949	-78.74	R	0	Blocked	1	1	0
35.60538479	-111.593534	1759.949	-78.29	R	0	Blocked	1	1	0
35.60538479	-111.593534	1759.949	-78.14	R	0	Blocked	1	1	0
35.60538286	-111.5935442	1760.248	-76	R	0	Blocked	1	1	0
35.60538286	-111.5935442	1760.248	-75.5	R	0	Blocked	1	1	0
35.60538286	-111.5935442	1760.248	-75.5	R	0	Blocked	1	1	0
35.60538286	-111.5935442	1760.248	-75.4	R	0	Blocked	1	1	0
35.60538286	-111.5935442	1760.248	-75.5	R	0	Blocked	1	1	0
35.60538286	-111.5935442	1760.248	-75.57	R	0	Blocked	1	1	0
35.60538286	-111.5935442	1760.248	-75.67	R	0	Blocked	1	1	0
35.60526274	-111.5932147	1759.971	-76.14	R	0	Blocked	1	1	0
35.60483394	-111.592425	1761.159	-73.88	R	0	Blocked	1	1	0
35.60483882	-111.592429	1760.403	-69.19	G	0	Blocked	0	0	1
35.60484127	-111.592425	1761.742	-58	G	0	Blocked	0	0	1

Black Point Measured Data					LTF LIDAR Predictions		Actual SS	Chi Square Matrix Values	
lat	Long	Elevation	SS	Color	Dist	SS Pred	is red	Cell A	Cell C
35.60483394	-111.592425	1761.159	-54	G	0	Blocked	0	0	1
35.60483394	-111.592425	1761.159	-58.75	G	0	Blocked	0	0	1
35.60480504	-111.5918022	1760.486	-60.62	G	0	Blocked	0	0	1
35.60479035	-111.5906631	1759.326	-62.36	G	0	Blocked	0	0	1
35.60478535	-111.5903209	1758.384	-65.15	G	0	Blocked	0	0	1
35.60588449	-111.5850501	1749.481	-62.1	G	0	Blocked	0	0	1
35.60588937	-111.5850542	1748.725	-62.1	G	0	Blocked	0	0	1
35.60588937	-111.5850542	1748.725	-62.91	G	0	Blocked	0	0	1
35.60588256	-111.5850604	1749.78	-66.91	G	0	Blocked	0	0	1
35.60588256	-111.5850604	1749.78	-66.91	G	0	Blocked	0	0	1
35.60588256	-111.5850604	1749.78	-71.5	R	0	Blocked	1	1	0
35.60587768	-111.5850563	1750.536	-71	R	0	Blocked	1	1	0
35.60587768	-111.5850563	1750.536	-70.67	G	0	Blocked	0	0	1
35.60631587	-111.5845367	1747.892	-71.64	R	0	Blocked	1	1	0
35.60631587	-111.5845367	1747.892	-71.83	R	0	Blocked	1	1	0
35.60631587	-111.5845367	1747.892	-72	R	0	Blocked	1	1	0
35.60631587	-111.5845367	1747.892	-71.76	R	0	Blocked	1	1	0
35.60631587	-111.5845367	1747.892	-71.84	R	0	Blocked	1	1	0
35.60631587	-111.5845367	1747.892	-71.75	R	0	Blocked	1	1	0
35.60631587	-111.5845367	1747.892	-71.75	R	0	Blocked	1	1	0
35.60631587	-111.5845367	1747.892	-71.64	R	0	Blocked	1	1	0
35.60640353	-111.5844422	1748.047	-71	R	0	Blocked	1	1	0
35.60711049	-111.5836083	1744.971	-73.25	R	0	Blocked	1	1	0
35.60812323	-111.5824192	1742.597	-74.61	R	0	Blocked	1	1	0
35.60802964	-111.5822063	1741.644	-74.58	R	0	Blocked	1	1	0

Black Point Measured Data					LTF LIDAR Predictions		Actual SS	Chi Square Matrix Values	
lat	Long	Elevation	SS	Color	Dist	SS Pred	is red	Cell A	Cell C
35.61273546	-111.5695425	1732.017	-62	G	0	Blocked	0	0	1
35.6137726	-111.5677154	1720.722	-85	R	0	Blocked	1	1	0
35.61858858	-111.5468969	1690.646	-79.91	R	0	Blocked	1	1	0
35.61859203	-111.5471489	1690.111	-78	R	0	Blocked	1	1	0
35.61794165	-111.5508826	1692.994	-80.6	R	0	Blocked	1	1	0
35.61775735	-111.5553999	1702.661	-84.6	R	0	Blocked	1	1	0
35.61739819	-111.5568028	1706.789	-85.08	R	0	Blocked	1	1	0
35.6171353	-111.5578159	1708.022	-85.46	R	0	Blocked	1	1	0
35.61685737	-111.5588701	1709.87	-85.71	R	0	Blocked	1	1	0
35.61662274	-111.5598587	1713.594	-85.87	R	0	Blocked	1	1	0
35.61654626	-111.5616232	1715.141	-83.72	R	0	Blocked	1	1	0
35.61662126	-111.5632685	1715.543	-82.85	R	0	Blocked	1	1	0
35.61702404	-111.5678391	1720.116	-76.33	R	0	Blocked	1	1	0
35.61702404	-111.5678391	1720.116	-77.25	R	0	Blocked	1	1	0
35.61702404	-111.5678391	1720.116	-77.4	R	0	Blocked	1	1	0
35.61703136	-111.5678391	1720.699	-77.43	R	0	Blocked	1	1	0
35.61753185	-111.5687822	1718.717	-79.38	R	0	Blocked	1	1	0
35.62204619	-111.5709702	1721.684	-74.57	R	0	Blocked	1	1	0
35.62204619	-111.5709702	1721.684	-74.57	R	0	Blocked	1	1	0
35.62234087	-111.5712172	1718.963	-74.57	R	0	Blocked	1	1	0
35.62488231	-111.5736811	1708.198	-80	R	0	Blocked	1	1	0
35.62487936	-111.5736667	1708.655	-81.75	R	0	Blocked	1	1	0
35.62510751	-111.5738116	1709.373	-82.33	R	0	Blocked	1	1	0
35.62798611	-111.5747051	1706.491	-83.27	R	0	Blocked	1	1	0
35.62841347	-111.5746629	1705.545	-83.67	R	0	Blocked	1	1	0

Black Point Measured Data					LTF LIDAR Predictions		Actual SS	Chi Square Matrix Values	
lat	Long	Elevation	SS	Color	Dist	SS Pred	is red	Cell A	Cell C
35.62840615	-111.5746629	1704.963	-84	R	0	Blocked	1	1	0
35.62839394	-111.5746588	1705.136	-84.53	R	0	Blocked	1	1	0
35.62995576	-111.5748675	1703.614	-84.53	R	0	Blocked	1	1	0
35.6323729	-111.5831802	1717.288	-86	R	0	Blocked	1	1	0
35.63330707	-111.5833028	1720.265	-86	R	0	Blocked	1	1	0
35.63617695	-111.5863599	1739.378	-86	R	0	Blocked	1	1	0
35.63617695	-111.5863599	1739.378	-85.92	R	0	Blocked	1	1	0
35.63616423	-111.5863496	1737.913	-85.79	R	0	Blocked	1	1	0
35.62750463	-111.6007044	1743.309	-86.67	R	0	Blocked	1	1	0
35.62716455	-111.6004143	1744.474	-86	R	0	Blocked	1	1	0
35.62712723	-111.6002649	1746.819	-85.67	R	0	Blocked	1	1	0
35.62713404	-111.6002587	1745.764	-85.71	R	0	Blocked	1	1	0
35.6271316	-111.6002627	1744.426	-85	R	0	Blocked	1	1	0
35.62696074	-111.600218	1743.419	-85.4	R	0	Blocked	1	1	0
35.62575993	-111.6017292	1737.113	-85.2	R	0	Blocked	1	1	0
35.62501717	-111.6019585	1737.123	-85.31	R	0	Blocked	1	1	0
35.6201566	-111.6006471	1746.558	-85.58	R	0	Blocked	1	1	0
35.61822098	-111.6003693	1751.071	-86	R	0	Blocked	1	1	0
35.61780664	-111.6003211	1751.726	-85.5	R	0	Blocked	1	1	0
35.61781346	-111.6003149	1750.671	-85.5	R	0	Blocked	1	1	0
35.61635625	-111.6001793	1753.197	-85.5	R	0	Blocked	1	1	0
35.61290819	-111.6026102	1763.671	-85.21	R	0	Blocked	1	1	0
35.61166054	-111.6049658	1769.805	-85.21	R	0	Blocked	1	1	0
35.60908707	-111.6090907	1780.459	-85.21	R	0	Blocked	1	1	0
35.60666448	-111.6133686	1790.073	-85.21	R	0	Blocked	1	1	0

Black Point Measured Data					LTF LIDAR Predictions		Actual SS	Chi Square Matrix Values	
lat	Long	Elevation	SS	Color	Dist	SS Pred	is red	Cell A	Cell C
35.58963364	-111.6048509	1812.25	-68.5	G	0	Blocked	0	0	1
35.58963364	-111.6048509	1812.25	-68	G	0	Blocked	0	0	1
35.58963364	-111.6048509	1812.25	-68.5	G	0	Blocked	0	0	1
35.58963364	-111.6048509	1812.25	-68.5	G	0	Blocked	0	0	1
35.58963364	-111.6048509	1812.25	-67.57	G	0	Blocked	0	0	1
35.58963364	-111.6048509	1812.25	-67.62	G	0	Blocked	0	0	1
35.58963841	-111.6047955	1811.509	-67.58	G	0	Blocked	0	0	1
35.58966337	-111.6024848	1809.355	-66.82	G	0	Blocked	0	0	1
35.58922536	-111.6019963	1808.551	-66.74	G	0	Blocked	0	0	1
35.58936147	-111.5997178	1799.469	-66.5	G	0	Blocked	0	0	1
35.58935139	-111.5995437	1797.595	-71.58	R	0	Blocked	1	1	0
35.58966555	-111.5992253	1795.269	-72.23	R	0	Blocked	1	1	0
35.59020893	-111.602213	1808.947	-70.56	G	0	Blocked	0	0	1
35.69641243	-111.4650858	1565.829	-30.26	G	0	Blocked	0	0	1
35.69676271	-111.4659355	1564.851	-84.75	R	0	Blocked	1	1	0
35.69740165	-111.4670567	1560.418	-85.4	R	0	Blocked	1	1	0
35.69749285	-111.4672143	1560.042	-85.4	R	0	Blocked	1	1	0
35.69747767	-111.4671959	1560.673	-84.92	R	0	Blocked	1	1	0
35.70035677	-111.472033	1556.418	-82.75	R	0	Blocked	1	1	0
35.71093686	-111.4918142	1555.621	-59.06	G	0	Blocked	0	0	1
35.7017536	-111.4979902	1572.051	-81	R	0	Blocked	1	1	0
35.69186876	-111.5039129	1583.916	-81	R	0	Blocked	1	1	0
35.69189703	-111.5039004	1582.976	-81.67	R	0	Blocked	1	1	0
35.69190435	-111.5039004	1583.56	-81.75	R	0	Blocked	1	1	0
35.66168568	-111.5128341	1604.635	-74.75	R	0	Blocked	1	1	0

Black Point Measured Data					LTF LIDAR Predictions		Actual SS	Chi Square Matrix Values	
lat	Long	Elevation	SS	Color	Dist	SS Pred	is red	Cell A	Cell C
35.65935319	-111.5132076	1608.618	-77.86	R	0	Blocked	1	1	0
35.65934159	-111.5130498	1608.697	-79.44	R	0	Blocked	1	1	0
35.65903548	-111.5101476	1606.298	-79.75	R	0	Blocked	1	1	0
35.66127301	-111.5021139	1592.979	-80.22	R	0	Blocked	1	1	0
35.66454384	-111.4988271	1591.391	-79.5	R	0	Blocked	1	1	0
35.66452831	-111.498862	1590.362	-73.71	R	0	Blocked	1	1	0
35.66452831	-111.498862	1590.362	-73.38	R	0	Blocked	1	1	0
35.66452639	-111.4988722	1590.66	-73.44	R	0	Blocked	1	1	0
35.66452639	-111.4988722	1590.66	-73.5	R	0	Blocked	1	1	0
35.66452639	-111.4988722	1590.66	-73.54	R	0	Blocked	1	1	0
35.6645215	-111.4988682	1591.416	-73.5	R	0	Blocked	1	1	0
35.66398033	-111.4967295	1589.348	-71	R	0	Blocked	1	1	0
35.66451403	-111.4988087	1590.856	-76	R	0	Blocked	1	1	0
35.6621279	-111.5015243	1592.833	-75.33	R	0	Blocked	1	1	0
35.65913585	-111.5112975	1607.927	-76.09	R	0	Blocked	1	1	0
35.66369245	-111.5239489	1621.886	-74.58	R	0	Blocked	1	1	0
35.66192265	-111.5279984	1624.599	-75.69	R	0	Blocked	1	1	0
35.56357021	-111.6512453	1923.481	-54.62	G	0	Blocked	0	0	1
35.56365312	-111.6516158	1922.647	-59.75	G	0	Blocked	0	0	1
35.56374237	-111.6527685	1922.548	-63.71	G	0	Blocked	0	0	1
35.56571501	-111.6579661	1918.954	-73.22	R	0	Blocked	1	1	0
35.56591413	-111.6579985	1918.994	-73.6	R	0	Blocked	1	1	0
35.56616257	-111.6580533	1919.975	-73.83	R	0	Blocked	1	1	0
35.5686435	-111.6552799	1902.822	-75.05	R	0	Blocked	1	1	0
35.56923928	-111.6548774	1903.192	-85	R	0	Blocked	1	1	0

Black Point Measured Data					LTF LIDAR Predictions		Actual SS	Chi Square Matrix Values	
lat	Long	Elevation	SS	Color	Dist	SS Pred	is red	Cell A	Cell C
35.56962007	-111.6550467	1902.546	-85.5	R	0	Blocked	1	1	0
35.57093764	-111.6551876	1900.922	-86	R	0	Blocked	1	1	0
35.57484866	-111.6550186	1895.667	-85.83	R	0	Blocked	1	1	0
35.58099758	-111.6555846	1878.407	-85.89	R	0	Blocked	1	1	0
35.58214035	-111.6560515	1874.713	-85.89	R	0	Blocked	1	1	0
35.59220138	-111.6585564	1850.54	-85.89	R	0	Blocked	1	1	0
35.59454429	-111.6592998	1844.621	-85.89	R	0	Blocked	1	1	0
35.58377879	-111.624012	1874.879	-89	R	0	Blocked	1	1	0
35.58389159	-111.6240507	1876.287	-80.4	R	0	Blocked	1	1	0
35.58529256	-111.6250535	1882.388	-81.18	R	0	Blocked	1	1	0
35.57415546	-111.6215131	1910.379	-76.25	R	0	Blocked	1	1	0
35.57272856	-111.6216925	1913.488	-77.6	R	0	Blocked	1	1	0
35.57020105	-111.622923	1920.656	-74.89	R	0	Blocked	1	1	0
35.55303568	-111.6260494	1947.799	-78.33	R	0	Blocked	1	1	0
35.55099212	-111.6258841	1955.583	-81.73	R	0	Blocked	1	1	0
35.55204184	-111.6280173	1955.951	-82.23	R	0	Blocked	1	1	0
							153	149	39
								Cell A	Cell C

Black Point Measured Data					LTF SRTM Predictions		Actual SS	Chi Square Matrix Values	
lat	Long	Elevation	SS	Color	Dist	SS Pred	is red	Cell B	Cell D
35.6022542	-111.6034122	1800.31	-43.07	G	0	Blocked	0	0	1
35.60271012	-111.6035359	1798.35	-45.38	G	0	Blocked	0	0	1
35.60271552	-111.6035462	1799.231	-47.61	G	0	Blocked	0	0	1
35.60271552	-111.6035462	1799.231	-49.7	G	0	Blocked	0	0	1
35.60272284	-111.6035462	1799.814	-66	G	0	Blocked	0	0	1
35.60271552	-111.6035462	1799.231	-65	G	0	Blocked	0	0	1
35.60271797	-111.6035421	1800.569	-64.5	G	0	Blocked	0	0	1
35.60286725	-111.6035458	1798.042	-64.62	G	0	Blocked	0	0	1
35.6041929	-111.604114	1793.539	-65.9	G	0	Blocked	0	0	1
35.6041929	-111.604114	1793.539	-66.24	G	0	Blocked	0	0	1
35.60418557	-111.604114	1792.957	-73	R	0	Blocked	1	1	0
35.60418557	-111.604114	1792.957	-73	R	0	Blocked	1	1	0
35.60417825	-111.604114	1792.374	-73	R	0	Blocked	1	1	0
35.60417825	-111.604114	1792.374	-73	R	0	Blocked	1	1	0
35.60417825	-111.604114	1792.374	-73	R	0	Blocked	1	1	0
35.60477811	-111.6018935	1786.998	-80.33	R	0	Blocked	1	1	0
35.60478298	-111.6018976	1786.242	-81.5	R	0	Blocked	1	1	0
35.60477566	-111.6018976	1785.66	-82.6	R	0	Blocked	1	1	0
35.60477566	-111.6018976	1785.66	-82.6	R	0	Blocked	1	1	0
35.60477566	-111.6018976	1785.66	-82.36	R	0	Blocked	1	1	0
35.60477566	-111.6018976	1785.66	-82.36	R	0	Blocked	1	1	0
35.60477566	-111.6018976	1785.66	-79.33	R	0	Blocked	1	1	0
35.60536657	-111.6010641	1779.955	-81.71	R	0	Blocked	1	1	0

Black Point Measured Data					LTF SRTM Predictions		Actual SS	Chi Square Matrix Values	
lat	Long	Elevation	SS	Color	Dist	SS Pred	is red	Cell B	Cell D
35.60532917	-111.6002979	1778.88	-83.3	R	0	Blocked	1	1	0
35.6053487	-111.6000233	1777.571	-83.64	R	0	Blocked	1	1	0
35.60531079	-111.5978452	1769.704	-83.62	R	0	Blocked	1	1	0
35.6052208	-111.5962944	1768.192	-81	R	0	Blocked	1	1	0
35.60517543	-111.5957413	1766.635	-80.8	R	0	Blocked	1	1	0
35.60495848	-111.5952972	1764.189	-80.38	R	0	Blocked	1	1	0
35.60476829	-111.5947977	1762.75	-79.93	R	0	Blocked	1	1	0
35.60525269	-111.5941675	1761.529	-79.35	R	0	Blocked	1	1	0
35.60538479	-111.593534	1759.949	-78.74	R	0	Blocked	1	1	0
35.60538286	-111.5935442	1760.248	-75.5	R	0	Blocked	1	1	0
35.60538286	-111.5935442	1760.248	-75.67	R	0	Blocked	1	1	0
35.60538479	-111.593534	1759.949	-75.55	R	0	Blocked	1	1	0
35.60538479	-111.593534	1759.949	-75.55	R	0	Blocked	1	1	0
35.6052843	-111.5932679	1760.064	-76.08	R	0	Blocked	1	1	0
35.60487798	-111.5924966	1761.204	-73.88	R	0	Blocked	1	1	0
35.60483882	-111.592429	1760.403	-69.19	G	0	Blocked	0	0	1
35.60478954	-111.5907573	1759.452	-61.7	G	0	Blocked	0	0	1
35.60478842	-111.5906733	1759.626	-65	G	0	Blocked	0	0	1
35.60479014	-111.5905442	1759.359	-65.16	G	0	Blocked	0	0	1
35.60478535	-111.5903209	1758.384	-65.15	G	0	Blocked	0	0	1
35.60477651	-111.5886408	1756.317	-69.67	G	0	Blocked	0	0	1
35.60477532	-111.5874177	1756.501	-75	R	0	Blocked	1	1	0
35.60476754	-111.5869013	1754.27	-76.33	R	0	Blocked	1	1	0
35.60476561	-111.5869116	1754.57	-75.91	R	0	Blocked	1	1	0
35.60476561	-111.5869116	1754.57	-75.25	R	0	Blocked	1	1	0

Black Point Measured Data					LTF SRTM Predictions		Actual SS	Chi Square Matrix Values	
lat	Long	Elevation	SS	Color	Dist	SS Pred	is red	Cell B	Cell D
35.60476561	-111.5869116	1754.57	-75	R	0	Blocked	1	1	0
35.60476561	-111.5869116	1754.57	-74.86	R	0	Blocked	1	1	0
35.60519847	-111.5858715	1751.032	-61.4	G	0	Blocked	0	0	1
35.60532457	-111.5857196	1750.382	-60.5	G	0	Blocked	0	0	1
35.60558409	-111.5854156	1749.664	-60.88	G	0	Blocked	0	0	1
35.6058548	-111.5850912	1748.931	-61.22	G	0	Blocked	0	0	1
35.60588937	-111.5850542	1748.725	-62.91	G	0	Blocked	0	0	1
35.60588256	-111.5850604	1749.78	-64.71	G	0	Blocked	0	0	1
35.60588256	-111.5850604	1749.78	-65.2	G	0	Blocked	0	0	1
35.60588256	-111.5850604	1749.78	-65.44	G	0	Blocked	0	0	1
35.60588256	-111.5850604	1749.78	-66.22	G	0	Blocked	0	0	1
35.60588256	-111.5850604	1749.78	-66.22	G	0	Blocked	0	0	1
35.60588256	-111.5850604	1749.78	-66.47	G	0	Blocked	0	0	1
35.60588256	-111.5850604	1749.78	-66.6	G	0	Blocked	0	0	1
35.60588256	-111.5850604	1749.78	-66.76	G	0	Blocked	0	0	1
35.60587768	-111.5850563	1750.536	-71	R	0	Blocked	1	1	0
35.60631587	-111.5845367	1747.892	-71.6	R	0	Blocked	1	1	0
35.60631587	-111.5845367	1747.892	-71.64	R	0	Blocked	1	1	0
35.60631587	-111.5845367	1747.892	-71.76	R	0	Blocked	1	1	0
35.60631587	-111.5845367	1747.892	-71.75	R	0	Blocked	1	1	0
35.60631587	-111.5845367	1747.892	-71.64	R	0	Blocked	1	1	0
35.60640353	-111.5844422	1748.047	-71	R	0	Blocked	1	1	0
35.60711049	-111.5836083	1744.971	-73.25	R	0	Blocked	1	1	0
35.60812323	-111.5824192	1742.597	-75.21	R	0	Blocked	1	1	0
35.60802964	-111.5822063	1741.644	-74.58	R	0	Blocked	1	1	0

Black Point Measured Data					LTF SRTM Predictions		Actual SS	Chi Square Matrix Values	
lat	Long	Elevation	SS	Color	Dist	SS Pred	is red	Cell B	Cell D
35.60783687	-111.5819302	1740.602	-74.55	R	0	Blocked	1	1	0
35.60764655	-111.5816501	1740.899	-74.33	R	0	Blocked	1	1	0
35.60535645	-111.5783843	1740.281	-64.6	G	0	Blocked	0	0	1
35.60557992	-111.5778551	1739.998	-65.83	G	0	Blocked	0	0	1
35.61303751	-111.5690599	1728.149	-85	R	0	Blocked	1	1	0
35.61313866	-111.5688936	1726.214	-85	R	0	Blocked	1	1	0
35.61313866	-111.5688936	1726.214	-85	R	0	Blocked	1	1	0
35.61340216	-111.5684091	1723.167	-85	R	0	Blocked	1	1	0
35.61831961	-111.5376022	1680.793	-71.38	R	0	Blocked	1	1	0
35.61832153	-111.5375919	1680.494	-72.67	R	0	Blocked	1	1	0
35.61849577	-111.5443478	1686.133	-77.44	R	0	Blocked	1	1	0
35.61855187	-111.5459358	1687.747	-78.5	R	0	Blocked	1	1	0
35.61854891	-111.5459215	1688.204	-78.5	R	0	Blocked	1	1	0
35.61858858	-111.5468969	1690.646	-79.91	R	0	Blocked	1	1	0
35.61859203	-111.5471489	1690.111	-78	R	0	Blocked	1	1	0
35.61844255	-111.5482191	1690.947	-78.33	R	0	Blocked	1	1	0
35.61775735	-111.5553999	1702.661	-84.6	R	0	Blocked	1	1	0
35.61729407	-111.5571864	1707.466	-85.08	R	0	Blocked	1	1	0
35.61669105	-111.5644999	1718.469	-82.62	R	0	Blocked	1	1	0
35.61702404	-111.5678391	1720.116	-76.33	R	0	Blocked	1	1	0
35.61754406	-111.5687863	1718.543	-77.9	R	0	Blocked	1	1	0
35.61753185	-111.5687822	1718.717	-79.38	R	0	Blocked	1	1	0
35.62123989	-111.5701158	1717.804	-79.23	R	0	Blocked	1	1	0
35.62190251	-111.5705976	1721.619	-82	R	0	Blocked	1	1	0
35.62205352	-111.5709702	1722.266	-75.75	R	0	Blocked	1	1	0

Black Point Measured Data					LTF SRTM Predictions		Actual SS	Chi Square Matrix Values	
lat	Long	Elevation	SS	Color	Dist	SS Pred	is red	Cell B	Cell D
35.62204619	-111.5709702	1721.684	-74.57	R	0	Blocked	1	1	0
35.62204812	-111.5709599	1721.385	-74.57	R	0	Blocked	1	1	0
35.62204812	-111.5709599	1721.385	-74.57	R	0	Blocked	1	1	0
35.62258968	-111.5714623	1716.48	-74.57	R	0	Blocked	1	1	0
35.62303372	-111.5719917	1712.946	-74.57	R	0	Blocked	1	1	0
35.62488231	-111.5736811	1708.198	-80	R	0	Blocked	1	1	0
35.6256111	-111.5740868	1708.636	-82.29	R	0	Blocked	1	1	0
35.62840615	-111.5746629	1704.963	-84.53	R	0	Blocked	1	1	0
35.63232164	-111.583168	1716.642	-86	R	0	Blocked	1	1	0
35.63522316	-111.585118	1729.133	-86.38	R	0	Blocked	1	1	0
35.63617695	-111.5863599	1739.378	-85.92	R	0	Blocked	1	1	0
35.63616962	-111.5863599	1738.795	-85.85	R	0	Blocked	1	1	0
35.63616423	-111.5863496	1737.913	-85.79	R	0	Blocked	1	1	0
35.63616423	-111.5863496	1737.913	-85.79	R	0	Blocked	1	1	0
35.62760197	-111.6005464	1745.401	-87	R	0	Blocked	1	1	0
35.62743302	-111.6007824	1742.381	-86.67	R	0	Blocked	1	1	0
35.62712723	-111.6002649	1746.819	-85.67	R	0	Blocked	1	1	0
35.6271316	-111.6002627	1744.426	-85.88	R	0	Blocked	1	1	0
35.62673901	-111.6003989	1741.706	-85	R	0	Blocked	1	1	0
35.62305501	-111.6015761	1738.861	-85.5	R	0	Blocked	1	1	0
35.62122803	-111.6009005	1743.705	-85.58	R	0	Blocked	1	1	0
35.61822098	-111.6003693	1751.071	-86	R	0	Blocked	1	1	0
35.61780858	-111.6003109	1751.427	-85.5	R	0	Blocked	1	1	0
35.61781346	-111.6003149	1750.671	-85.5	R	0	Blocked	1	1	0
35.61705557	-111.6002349	1753.036	-85.5	R	0	Blocked	1	1	0

Black Point Measured Data					LTF SRTM Predictions		Actual SS	Chi Square Matrix Values	
lat	Long	Elevation	SS	Color	Dist	SS Pred	is red	Cell B	Cell D
35.61635625	-111.6001793	1753.197	-85.5	R	0	Blocked	1	1	0
35.61375254	-111.6001266	1758.205	-85.25	R	0	Blocked	1	1	0
35.61338443	-111.6011664	1760.287	-85.23	R	0	Blocked	1	1	0
35.61290819	-111.6026102	1763.671	-85.21	R	0	Blocked	1	1	0
35.61166054	-111.6049658	1769.805	-85.21	R	0	Blocked	1	1	0
35.60908707	-111.6090907	1780.459	-85.21	R	0	Blocked	1	1	0
35.58964535	-111.6048365	1813.871	-67	G	0	Blocked	0	0	1
35.58963364	-111.6048509	1812.25	-68.44	G	0	Blocked	0	0	1
35.58963364	-111.6048509	1812.25	-68.5	G	0	Blocked	0	0	1
35.58963364	-111.6048509	1812.25	-67.67	G	0	Blocked	0	0	1
35.58963364	-111.6048509	1812.25	-67.75	G	0	Blocked	0	0	1
35.58963364	-111.6048509	1812.25	-67.57	G	0	Blocked	0	0	1
35.58963364	-111.6048509	1812.25	-67.62	G	0	Blocked	0	0	1
35.58963841	-111.6047955	1811.509	-67.58	G	0	Blocked	0	0	1
35.58964849	-111.604691	1811.665	-67.69	G	0	Blocked	0	0	1
35.58967589	-111.604144	1810.853	-67.71	G	0	Blocked	0	0	1
35.58934459	-111.5998285	1800.368	-62	G	0	Blocked	0	0	1
35.58948098	-111.5999695	1801.555	-70.6	G	0	Blocked	0	0	1
35.58934753	-111.5998428	1799.911	-70.82	G	0	Blocked	0	0	1
35.58935139	-111.5995437	1797.595	-71.58	R	0	Blocked	1	1	0
35.69641243	-111.4650858	1565.829	-30.26	G	0	Blocked	0	0	1
35.69619955	-111.4645144	1566.149	-87	R	0	Blocked	1	1	0
35.69634477	-111.4649712	1565.997	-87	R	0	Blocked	1	1	0
35.69659968	-111.465565	1566.041	-87	R	0	Blocked	1	1	0
35.69748256	-111.4671999	1559.917	-85	R	0	Blocked	1	1	0

Black Point Measured Data					LTF SRTM Predictions		Actual SS	Chi Square Matrix Values	
lat	Long	Elevation	SS	Color	Dist	SS Pred	is red	Cell B	Cell D
35.69748256	-111.4671999	1559.917	-85	R	0	Blocked	1	1	0
35.69747035	-111.4671959	1560.089	-85	R	0	Blocked	1	1	0
35.69747767	-111.4671959	1560.673	-84.92	R	0	Blocked	1	1	0
35.69747767	-111.4671959	1560.673	-84.87	R	0	Blocked	1	1	0
35.69813662	-111.4683274	1558.291	-84.47	R	0	Blocked	1	1	0
35.6991823	-111.4700891	1556.16	-83.89	R	0	Blocked	1	1	0
35.70690747	-111.4806756	1554.09	-48	G	0	Blocked	0	0	1
35.69684288	-111.5009301	1578.205	-81	R	0	Blocked	1	1	0
35.69189703	-111.5039004	1582.976	-81.67	R	0	Blocked	1	1	0
35.69191359	-111.5038902	1583.845	-81	R	0	Blocked	1	1	0
35.69187607	-111.5039129	1584.5	-80.44	R	0	Blocked	1	1	0
35.68671833	-111.5056653	1587.776	-80	R	0	Blocked	1	1	0
35.67540089	-111.5089208	1595.05	-78.83	R	0	Blocked	1	1	0
35.6591235	-111.511234	1608.122	-79.6	R	0	Blocked	1	1	0
35.66060106	-111.5034758	1593.991	-80	R	0	Blocked	1	1	0
35.66301684	-111.5008914	1590.853	-79.65	R	0	Blocked	1	1	0
35.65896316	-111.5077037	1600.328	-75.78	R	0	Blocked	1	1	0
35.65913585	-111.5112975	1607.927	-76.09	R	0	Blocked	1	1	0
35.66003543	-111.5154913	1611.16	-77.53	R	0	Blocked	1	1	0
35.65998633	-111.5305229	1629.061	-76	R	0	Blocked	1	1	0
35.65999365	-111.5305229	1629.644	-71.46	R	0	Blocked	1	1	0
35.65999365	-111.5305229	1629.644	-71.36	R	0	Blocked	1	1	0
35.65999365	-111.5305229	1629.644	-71.47	R	0	Blocked	1	1	0
35.65999365	-111.5305229	1629.644	-71.53	R	0	Blocked	1	1	0
35.65999365	-111.5305229	1629.644	-71.53	R	0	Blocked	1	1	0

Black Point Measured Data					LTF SRTM Predictions		Actual SS	Chi Square Matrix Values	
lat	Long	Elevation	SS	Color	Dist	SS Pred	is red	Cell B	Cell D
35.65999365	-111.5305229	1629.644	-71.45	R	0	Blocked	1	1	0
35.65999365	-111.5305229	1629.644	-20.5	G	0	Blocked	0	0	1
35.56375957	-111.6520886	1921.598	-59.75	G	0	Blocked	0	0	1
35.56697699	-111.6581685	1915.632	-74.31	R	0	Blocked	1	1	0
35.56710237	-111.657773	1913.364	-74.87	R	0	Blocked	1	1	0
35.57093764	-111.6551876	1900.922	-86	R	0	Blocked	1	1	0
35.57596645	-111.6550021	1892.397	-85.86	R	0	Blocked	1	1	0
35.58330711	-111.6565675	1872.457	-85.89	R	0	Blocked	1	1	0
35.59331688	-111.6590603	1847.665	-85.89	R	0	Blocked	1	1	0
35.58450682	-111.6236398	1880.53	-76.75	R	0	Blocked	1	1	0
35.58705327	-111.6266368	1873.939	-82.29	R	0	Blocked	1	1	0
35.57351349	-111.621617	1910.296	-76.25	R	0	Blocked	1	1	0
35.57020105	-111.622923	1920.656	-74.89	R	0	Blocked	1	1	0
35.55302348	-111.6260453	1947.974	-74.25	R	0	Blocked	1	1	0
35.55304494	-111.6260391	1948.08	-79.29	R	0	Blocked	1	1	0
							144	140	48
								Total	Total
								Cell B	Cell D

APPENDIX D TEST 2 - LIDAR CALCULATED SIGNAL STRENGTH ERROR

Table 18 LTF Predicted Signal Strength Error

Measured Data					LTF SS Prediction	SS Delta	ABS (SS Delta)
Time	Lat	Long	Distance	SS			
1268848538	35.59810676	-111.6025783	1799.052	-31.35	-11.9492	-19.4008	19.4008
1268848581	35.59863876	-111.6029478	1800.754	-47	-20.2334	-26.7666	26.7666
1268848623	35.59882061	-111.6034105	1805.204	-46	-24.1469	-21.8531	21.8531
1268848657	35.59917087	-111.6039219	1809.313	-49	-30.0653	-18.9347	18.9347
1268848700	35.6000503	-111.6034668	1803.539	-45.38	-31.3926	-13.9874	13.9874
1268848733	35.6007134	-111.6034693	1802.099	-44.11	-34.5633	-9.5467	9.5467
1268848766	35.60142959	-111.6034142	1801.018	-42.09	-37.4714	-4.6186	4.6186
1268848798	35.60203361	-111.6033861	1800.149	-42.46	-39.6666	-2.7934	2.7934
1268851475	35.60477532	-111.5874177	1756.501	-75	-58.7491	-16.2509	16.2509
1268851520	35.60476754	-111.5869013	1754.27	-76.5	-59.1833	-17.3167	17.3167
1268851553	35.60476561	-111.5869116	1754.57	-76.1	-59.1735	-16.9265	16.9265
1268851596	35.60476561	-111.5869116	1754.57	-75.46	-59.1735	-16.2865	16.2865
1268851685	35.60476561	-111.5869116	1754.57	-75.11	-59.1735	-15.9365	15.9365
1268851750	35.60476561	-111.5869116	1754.57	-74.86	-59.1735	-15.6865	15.6865
1268852828	35.60702818	-111.5807769	1740.548	-73.65	-64.8713	-8.7787	8.7787
1268852863	35.60637411	-111.5798567	1740.58	-63	-65.1948	2.1948	2.1948
1268852896	35.60578553	-111.5790019	1740.767	-63.25	-65.5329	2.2829	2.2829
1268852930	35.60523378	-111.5782781	1740.4	-65	-65.8258	0.8258	0.8258
1268852975	35.60522453	-111.5782884	1740.116	-66.5	-65.817	-0.683	0.683
1268853008	35.60522453	-111.5782884	1740.116	-66.4	-65.817	-0.583	0.583
1268853042	35.60557992	-111.5778551	1739.998	-65.83	-66.1793	0.3493	0.3493
1268853075	35.60656558	-111.5768217	1738.383	-64.79	-67.0606	2.2706	2.2706
1268853110	35.60735885	-111.5759692	1737.39	-64.06	-67.7603	3.7003	3.7003
1268853143	35.6082116	-111.5750939	1737.484	-63.78	-68.469	4.689	4.689
1268853177	35.6091155	-111.5741714	1738.24	-63.75	-69.1951	5.4451	5.4451
1268853212	35.61001643	-111.5732468	1736.024	-59	-69.899	10.899	10.899
1268853255	35.61118906	-111.57201	1736.359	-61.5	-70.7968	9.2968	9.2968
1268853311	35.61230126	-111.5703204	1735.755	-61.14	-72.0295	10.8895	10.8895
1268853357	35.61229638	-111.5703164	1736.511	-60.8	-72.0298	11.2298	11.2298
1268853391	35.61230126	-111.5703204	1735.755	-61.08	-72.0295	10.9495	10.9495
1268853446	35.61241888	-111.5700844	1734.703	-60.13	-72.1566	12.0266	12.0266
1268853479	35.61261002	-111.5697601	1734.281	-61.29	-72.4527	11.1627	11.1627
1268857303	35.61803107	-111.5328819	1684.278	-65.36	-84.2274	18.8674	18.8674
1268857405	35.61802618	-111.5328779	1685.034	-65.7	-84.2278	18.5278	18.5278
1268857460	35.61803107	-111.5328819	1684.278	-67.5	-84.2274	16.7274	16.7274
1268857517	35.61812443	-111.534269	1685.269	-66.8	-83.9312	17.1312	17.1312
1268857630	35.61834326	-111.5381554	1680.563	-75.58	-83.0156	7.4356	7.4356

Measured Data					LTF SS Prediction	SS Delta	ABS (SS Delta)
Time	Lat	Long	Distance	SS			
1268857662	35.61842321	-111.5417085	1681.917	-76.57	-82.1916	5.6216	5.6216
1268858179	35.61688152	-111.5668089	1721.589	-75	-74.6613	-0.3387	0.3387
1268858439	35.61806832	-111.5691495	1718.03	-80	-74.234	-5.766	5.766
1268858484	35.62003593	-111.5697728	1715.43	-79.9	-74.6505	-5.2495	5.2495
1268858495	35.62061628	-111.5698614	1716.533	-79.62	-74.7819	-4.8381	4.8381
1268858744	35.62204812	-111.5709599	1721.385	-74.57	-74.9684	0.3984	0.3984
1268862685	35.58967125	-111.6034107	1809.852	-67.25	-48.8728	-18.3772	18.3772
1268863086	35.59125596	-111.6021674	1808.094	-70.05	-44.7819	-25.2681	25.2681
1268863159	35.59384129	-111.6032077	1804.102	-38	-35.8632	-2.1368	2.1368
1268869142	35.7021362	-111.4750289	1555.785	-80.18	-57.4221	-22.7579	22.7579
1268869382	35.7161176	-111.4877278	1559.314	-58.14	-72.2466	14.1066	14.1066
1268869753	35.68671833	-111.5056653	1587.776	-80	-72.423	-7.577	7.577
1268869862	35.67232395	-111.5097667	1597.457	-78	-76.5951	-1.4049	1.4049
1268941039	35.55225552	-111.6394415	1962.334	-25.45	-9.51738	-15.9326	15.93262
1268941092	35.55450726	-111.6395943	1948.024	-30.07	-32.4478	2.3778	2.3778
1268941226	35.55786447	-111.6396791	1927.169	-47.5	-45.7511	-1.7489	1.7489
1268941361	35.56163883	-111.6472806	1924.119	-53.11	-56.4453	3.3353	3.3353
1268941565	35.56363524	-111.6533154	1923.705	-75	-62.2884	-12.7116	12.7116
1268941874	35.56838969	-111.6559378	1907.833	-75.3	-66.9235	-8.3765	8.3765
1268942920	35.58449462	-111.6236358	1880.704	-78	-75.7605	-2.2395	2.2395
1268942960	35.58450682	-111.6236398	1880.53	-76.75	-75.7654	-0.9846	0.9846
1268943074	35.58228958	-111.6238845	1885.908	-86.4	-74.6262	-11.7738	11.7738
1268943151	35.58232772	-111.6239275	1886.866	-79.9	-74.6384	-5.2616	5.2616
1268943993	35.57679793	-111.6227012	1909.46	-60.17	-72.1076	11.9376	11.9376
1268944046	35.57540228	-111.6222538	1911.151	-76	-71.4806	-4.5194	4.5194
1268944137	35.57160911	-111.6218979	1917.024	-76	-69.3889	-6.6111	6.6111
1268944323	35.56061165	-111.6257928	1930.532	-74.67	-60.1925	-14.4775	14.4775
					Total	-155.736	
				Average	Error	-2.43337	

APPENDIX E SIGNAL STRENGTH ERROR FOR SRTM AND LIDAR PREDICTIONS

Table 19 LIDAR and SRTM Prediction Errors

TROPOS DATA			LIDAR PREDICTIONS				SRTM PREDICTIONS			
Time	Altitude	SS	Distance	SS	SS Err	ABS (SS Error)	Distance	Predicted SS	SS Err	ABS (SS Error)
1268848766	1801.018	-42.09	466.674	-37.4714	-4.6186	4.6186	466.527	-37.3249	-4.7651	4.7651
1268848570	1801.39	-32.05	163.557	-19.2671	-12.7829	12.7829	163.239	-19.0803	-12.9697	12.9697
1268848602	1801.522	-49	179.661	-20.8974	-28.1026	28.1026	179.359	-20.7163	-28.2837	28.2837
1268848678	1805.932	-49	290.961	-29.2719	-19.7281	19.7281	290.689	-29.1072	-19.8928	19.8928
1268869346	1559.898	-57.75	3333.94	-72.2501	14.5001	14.5001	3333.71	-71.74	13.99	13.99
1268869430	1556.727	-58.12	3209.13	-71.5898	13.4698	13.4698	3208.86	-71.0919	12.9719	12.9719
1268853290	1736.347	-61.5	3225.46	-71.7191	10.2191	10.2191	3225.88	-71.2498	9.7498	9.7498
1268852828	1740.548	-73.65	2173.13	-64.8713	-8.7787	8.7787	2173.55	-64.2348	-9.4152	9.4152
1268852863	1740.58	-63	2212.89	-65.1948	2.1948	2.1948	2213.33	-64.5424	1.5424	1.5424
1268852896	1740.767	-63.25	2254.92	-65.5329	2.2829	2.2829	2255.37	-64.8632	1.6132	1.6132
1268852930	1740.4	-65	2291.19	-65.8258	0.8258	0.8258	2291.64	-65.1351	0.1351	0.1351
1268852975	1740.116	-66.5	2289.95	-65.817	-0.683	0.683	2290.4	-65.1257	-1.3743	1.3743
1268853008	1740.116	-66.4	2289.95	-65.817	-0.583	0.583	2290.4	-65.1257	-1.2743	1.2743
1268869191	1556.351	-46.33	1884.03	-62.3568	16.0268	16.0268	1883.79	-61.9167	15.5867	15.5867
1268853075	1738.383	-64.79	2470.64	-67.0606	2.2706	2.2706	2471.08	-66.4347	1.6447	1.6447
1268853110	1737.39	-64.06	2577.59	-67.7603	3.7003	3.7003	2578.03	-67.1662	3.1062	3.1062
1268853143	1737.484	-63.78	2690.14	-68.469	4.689	4.689	2690.57	-67.9036	4.1236	4.1236
1268853177	1738.24	-63.75	2810	-69.1951	5.4451	5.4451	2810.43	-68.6561	4.9061	4.9061
1268853212	1736.024	-59	2930.85	-69.899	10.899	10.899	2931.28	-69.3833	10.3833	10.3833
1268853255	1736.359	-61.5	3091.88	-70.7968	9.2968	9.2968	3092.31	-70.307	8.807	8.807
1268853311	1735.755	-61.14	3286.06	-72.0295	10.8895	10.8895	3286.49	-71.5664	10.4264	10.4264
1268853391	1735.755	-61.08	3286.06	-72.0295	10.9495	10.9495	3286.49	-71.5664	10.4864	10.4864
1268853446	1734.703	-60.13	3311.13	-72.1566	12.0266	12.0266	3311.55	-71.6959	11.5659	11.5659

TROPOS DATA			LIDAR PREDICTIONS				SRTM PREDICTIONS			
Time	Altitude	SS	Distance	SS	SS Err	ABS (SS Error)	Distance	Predicted SS	SS Err	ABS (SS Error)
1268869251	1552.23	-52.5	2464.7	-67.0915	14.5915	14.5915	2464.46	-66.5359	14.0359	14.0359
1268857303	1684.278	-65.36	6641.73	-84.2274	18.8674	18.8674	6642.18	-83.7217	18.3617	18.3617
1268857405	1685.034	-65.7	6641.87	-84.2278	18.5278	18.5278	6642.33	-83.7221	18.0221	18.0221
1268857460	1684.278	-67.5	6641.73	-84.2274	16.7274	16.7274	6642.18	-83.7217	16.2217	16.2217
1268857517	1685.269	-66.8	6527.45	-83.9312	17.1312	17.1312	6527.9	-83.4217	16.6217	16.6217
1268857630	1680.563	-75.58	6208.05	-83.0156	7.4356	7.4356	6208.5	-82.5554	6.9754	6.9754
1268857662	1681.917	-76.57	5914.04	-82.1916	5.6216	5.6216	5914.48	-81.7191	5.1491	5.1491
1268869898	1604.252	-75.67	4915.95	-78.9486	3.2786	3.2786	4915.6	-78.5697	2.8997	2.8997
1268870827	1612.269	-77.56	5515.29	-80.9451	3.3851	3.3851	5514.95	-80.5443	2.9843	2.9843
1268870888	1614.361	-77	5599.3	-81.2119	4.2119	4.2119	5598.94	-80.8118	3.8118	3.8118
1268870985	1621.659	-64.5	5691.43	-81.4895	16.9895	16.9895	5691.07	-81.0946	16.5946	16.5946
1268862685	1809.852	-67.25	879.259	-48.8728	-18.3772	18.3772	879.16	-48.3323	-18.9177	18.9177
1268863159	1804.102	-38	425.344	-35.8632	-2.1368	2.1368	425.174	-35.7112	-2.2888	2.2888
1268869142	1555.785	-80.18	1414.96	-57.4221	-22.7579	22.7579	1414.75	-56.9982	-23.1818	23.1818
1268869382	1559.314	-58.14	3333.26	-72.2466	14.1066	14.1066	3333.02	-71.7365	13.5965	13.5965
1268871047	1618.9	-70.17	5771.91	-81.7274	11.5574	11.5574	5771.54	-81.3374	11.1674	11.1674
1268943938	1905.579	-63.5	3409.88	-73.1678	9.6678	9.6678	3410.22	-72.1439	8.6439	8.6439
1268941039	1962.334	-25.45	95.7906	-9.51738	-15.9326	15.93262	96.8245	-8.9829	-16.4671	16.4671
1268941092	1948.024	-30.07	343.811	-32.4478	2.3778	2.3778	344.215	-31.8745	1.8045	1.8045
1268941226	1927.169	-47.5	716.541	-45.7511	-1.7489	1.7489	716.825	-45.1665	-2.3335	2.3335
1268941361	1924.119	-53.11	1337.82	-56.4453	3.3353	3.3353	1337.71	-55.8521	2.7421	2.7421
1268941565	1923.705	-75	1848.44	-62.2884	-12.7116	12.7116	1848.21	-61.4237	-13.5763	13.5763
1268941874	1907.833	-75.3	2404.26	-66.9235	-8.3765	8.3765	2404.05	-65.9222	-9.3778	9.3778
1268942920	1880.704	-78	3940.94	-75.7605	-2.2395	2.2395	3941.24	-74.74	-3.26	3.26
1268944019	1910.27	-62.71	3084.56	-71.4802	8.7702	8.7702	3084.92	-70.4229	7.7129	7.7129

TROPOS DATA			LIDAR PREDICTIONS				SRTM PREDICTIONS			
Time	Altitude	SS	Distance	SS	SS Err	ABS (SS Error)	Distance	Predicted SS	SS Err	ABS (SS Error)
1268944231	1923.037	-75.69	2142.41	-65.2383	-10.4517	10.4517	2142.86	-64.2028	-11.4872	11.4872
1268944258	1925.057	-75.14	1928.22	-63.2705	-11.8695	11.8695	1928.69	-62.4188	-12.7212	12.7212
1268943993	1909.46	-60.17	3199.67	-72.1076	11.9376	11.9376	3200.01	-71.0583	10.8883	10.8883
1268944046	1911.151	-76	3084.58	-71.4806	-4.5194	4.5194	3084.95	-70.4232	-5.5768	5.5768
1268944390	1939.196	-62	1292.9	-55.9858	-6.0142	6.0142	1293.53	-55.2591	-6.7409	6.7409
1268871278	1627.572	-76.1	6523.92	-83.839	7.739	7.739	6523.56	-83.4447	7.3447	7.3447
1268941641	1921.552	-71.67	2166.62	-64.9717	-6.6983	6.6983	0	-91	19.33	19.33
1268941664	1920.798	-71.86	0	-91	19.14	19.14	2258.34	-64.8758	-6.9842	6.9842
1268941775	1914.265	-74.57	2407.18	-66.9511	-7.6189	7.6189	0	-91	16.43	16.43
1268941712	1918.994	-73.6	0	-91	17.4	17.4	2326.52	-65.3837	-8.2163	8.2163
1268941725	1918.994	-73.73	0	-91	17.27	17.27	2326.52	-65.3837	-8.3463	8.3463
1268941738	1919.975	-73.83	0	-91	17.17	17.17	2349.18	-65.5489	-8.2811	8.2811
1268941787	1913.364	-74.87	2405.74	-66.9408	-7.9292	7.9292	0	-91	16.13	16.13
1268942946	1880.53	-77	3942.07	-75.7654	-1.2346	1.2346	0	-91	14	14
1268871266	1627.329	-76.32	6425.99	-83.5872	7.2672	7.2672	0	-91	14.68	14.68
1268871193	1624.073	-75.47	0	-91	15.53	15.53	6189.86	-82.5431	7.0731	7.0731
					AVG err	9.93149875			AVG err	9.84362813

APPENDIX F CHI-SQUARE TEST DATA RQ1GH1A

Table 20 Chi Square Test Data RQ1GH1A

Measured Black Point Data					LTF SRTM Predictions			SRTM	Chi Square Matrix Values			
lat	Long	Elevation	SS	Color	Dist	SS Pred	Color	Matches	Cell A	Cell B	Cell C	Cell D
35.60160717	-111.6033933	1800.976	-42.17	G	0	Blocked	R	0			0	1
35.60271552	-111.6035462	1799.231	-48.74	G	0	Blocked	R	0			0	1
35.6035224	-111.6037613	1796.12	-65.87	G	0	Blocked	R	0			0	1
35.60387265	-111.6040062	1795.081	-65.76	G	0	Blocked	R	0			0	1
35.60418557	-111.604114	1792.957	-73	R	0	Blocked	R	1			1	0
35.60418557	-111.604114	1792.957	-73	R	0	Blocked	R	1			1	0
35.60418557	-111.604114	1792.957	-73	R	0	Blocked	R	1			1	0
35.60418557	-111.604114	1792.957	-73	R	0	Blocked	R	1			1	0
35.60418557	-111.604114	1792.957	-73	R	0	Blocked	R	1			1	0
35.60417825	-111.604114	1792.374	-73	R	0	Blocked	R	1			1	0
35.60477566	-111.6018976	1785.66	-82.67	R	0	Blocked	R	1			1	0
35.60477566	-111.6018976	1785.66	-82.6	R	0	Blocked	R	1			1	0
35.60477566	-111.6018976	1785.66	-82.36	R	0	Blocked	R	1			1	0
35.60477566	-111.6018976	1785.66	-82.36	R	0	Blocked	R	1			1	0
35.60477566	-111.6018976	1785.66	-81.85	R	0	Blocked	R	1			1	0
35.60477566	-111.6018976	1785.66	-81.57	R	0	Blocked	R	1			1	0
35.60484544	-111.6016105	1785.15	-80.4	R	0	Blocked	R	1			1	0
35.60531079	-111.5978452	1769.704	-83.54	R	0	Blocked	R	1			1	0
35.60531079	-111.5978452	1769.704	-83.53	R	0	Blocked	R	1			1	0
35.60515204	-111.5974543	1770.261	-82.67	R	0	Blocked	R	1			1	0
35.60505592	-111.5954895	1764.546	-80.38	R	0	Blocked	R	1			1	0
35.60538479	-111.593534	1759.949	-78.55	R	0	Blocked	R	1			1	0
35.60538479	-111.593534	1759.949	-78.29	R	0	Blocked	R	1			1	0

Measured Black Point Data					LTF SRTM Predictions			SRTM	Chi Square Matrix Values			
lat	Long	Elevation	SS	Color	Dist	SS Pred	Color	Matches	Cell A	Cell B	Cell C	Cell D
35.60538479	-111.593534	1759.949	-78.29	R	0	Blocked	R	1			1	0
35.60538286	-111.5935442	1760.248	-76	R	0	Blocked	R	1			1	0
35.60538286	-111.5935442	1760.248	-76	R	0	Blocked	R	1			1	0
35.60538286	-111.5935442	1760.248	-75.67	R	0	Blocked	R	1			1	0
35.60538286	-111.5935442	1760.248	-75.5	R	0	Blocked	R	1			1	0
35.60538286	-111.5935442	1760.248	-75.57	R	0	Blocked	R	1			1	0
35.60487798	-111.5924966	1761.204	-73.88	R	0	Blocked	R	1			1	0
35.60483394	-111.592425	1761.159	-71.37	R	0	Blocked	R	1			1	1
35.60484127	-111.592425	1761.742	-68.77	G	0	Blocked	R	0			0	1
35.60483394	-111.592425	1761.159	-58.75	G	0	Blocked	R	0			0	1
35.60483394	-111.592425	1761.159	-59.83	G	0	Blocked	R	0			0	1
35.60480058	-111.5920358	1761.178	-60.62	G	0	Blocked	R	0			0	1
35.60479882	-111.5913166	1759.732	-61	G	0	Blocked	R	0			0	1
35.60479932	-111.5910441	1759.655	-61	G	0	Blocked	R	0			0	1
35.60479035	-111.5906631	1759.326	-62.36	G	0	Blocked	R	0			0	1
35.60478842	-111.5906733	1759.626	-64.07	G	0	Blocked	R	0			0	1
35.60477395	-111.5882946	1756.714	-71.75	R	0	Blocked	R	1			1	0
35.60476655	-111.5871554	1756.142	-75	R	0	Blocked	R	1			1	0
35.60476266	-111.5868973	1755.027	-75.86	R	0	Blocked	R	1			1	0
35.60476561	-111.5869116	1754.57	-75.91	R	0	Blocked	R	1			1	0
35.60476561	-111.5869116	1754.57	-75.46	R	0	Blocked	R	1			1	0
35.60476561	-111.5869116	1754.57	-75.33	R	0	Blocked	R	1			1	0
35.60476561	-111.5869116	1754.57	-75.18	R	0	Blocked	R	1			1	0
35.60476561	-111.5869116	1754.57	-74.95	R	0	Blocked	R	1			1	0

Measured Black Point Data					LTF SRTM Predictions			SRTM	Chi Square Matrix Values			
lat	Long	Elevation	SS	Color	Dist	SS Pred	Color	Matches	Cell A	Cell B	Cell C	Cell D
35.60588449	-111.5850501	1749.481	-62.1	G	0	Blocked	R	0			0	1
35.60588256	-111.5850604	1749.78	-64.71	G	0	Blocked	R	0			0	1
35.60588256	-111.5850604	1749.78	-65.44	G	0	Blocked	R	0			0	1
35.60588256	-111.5850604	1749.78	-66.47	G	0	Blocked	R	0			0	1
35.60588256	-111.5850604	1749.78	-66.76	G	0	Blocked	R	0			0	1
35.60588256	-111.5850604	1749.78	-72	R	0	Blocked	R	1			1	0
35.60588256	-111.5850604	1749.78	-71.5	R	0	Blocked	R	1			1	0
35.6059926	-111.5849249	1749.902	-71	R	0	Blocked	R	1			1	0
35.60629788	-111.5845634	1748.963	-71	R	0	Blocked	R	1			1	0
35.60631832	-111.5845326	1749.23	-71.22	R	0	Blocked	R	1			1	0
35.6063232	-111.5845367	1748.474	-71.22	R	0	Blocked	R	1			1	0
35.60631587	-111.5845367	1747.892	-71.64	R	0	Blocked	R	1			1	0
35.60631587	-111.5845367	1747.892	-71.83	R	0	Blocked	R	1			1	0
35.60631587	-111.5845367	1747.892	-71.85	R	0	Blocked	R	1			1	0
35.60631099	-111.5845326	1748.648	-71.76	R	0	Blocked	R	1			1	0
35.60631587	-111.5845367	1747.892	-71.75	R	0	Blocked	R	1			1	0
35.60631587	-111.5845367	1747.892	-71.64	R	0	Blocked	R	1			1	0
35.60812323	-111.5824192	1742.597	-74.89	R	0	Blocked	R	1			1	0
35.60812323	-111.5824192	1742.597	-75.15	R	0	Blocked	R	1			1	0
35.60802964	-111.5822063	1741.644	-74.58	R	0	Blocked	R	1			1	0
35.60764655	-111.5816501	1740.899	-74.33	R	0	Blocked	R	1			1	0
35.60557992	-111.5778551	1739.998	-65.83	G	0	Blocked	R	0			0	1
35.61303751	-111.5690599	1728.149	-85	R	0	Blocked	R	1			1	0
35.61313866	-111.5688936	1726.214	-85	R	0	Blocked	R	1			1	0

Measured Black Point Data					LTF SRTM Predictions			SRTM	Chi Square Matrix Values			
lat	Long	Elevation	SS	Color	Dist	SS Pred	Color	Matches	Cell A	Cell B	Cell C	Cell D
35.61313185	-111.5688998	1727.269	-85	R	0	Blocked	R	1			1	0
35.61557152	-111.5646711	1715.046	-65.25	G	0	Blocked	R	0			0	1
35.61858858	-111.5468969	1690.646	-79.91	R	0	Blocked	R	1			1	0
35.61858522	-111.5471551	1691.166	-78	R	0	Blocked	R	1			1	0
35.61859203	-111.5471489	1690.111	-78	R	0	Blocked	R	1			1	0
35.61859203	-111.5471489	1690.111	-78	R	0	Blocked	R	1			1	0
35.61858778	-111.547442	1690.77	-78.33	R	0	Blocked	R	1			1	0
35.61794165	-111.5508826	1692.994	-80.6	R	0	Blocked	R	1			1	0
35.61790532	-111.5519504	1693.471	-82.17	R	0	Blocked	R	1			1	0
35.61788368	-111.5525673	1695.107	-83.75	R	0	Blocked	R	1			1	0
35.61784852	-111.5534876	1697.121	-84.22	R	0	Blocked	R	1			1	0
35.61753714	-111.5562818	1704.15	-84.82	R	0	Blocked	R	1			1	0
35.61729407	-111.5571864	1707.466	-85.08	R	0	Blocked	R	1			1	0
35.61653846	-111.5613855	1714.632	-84.47	R	0	Blocked	R	1			1	0
35.61669105	-111.5644999	1718.469	-82.62	R	0	Blocked	R	1			1	0
35.61680933	-111.5660795	1720.752	-75	R	0	Blocked	R	1			1	0
35.61702404	-111.5678391	1720.116	-77.25	R	0	Blocked	R	1			1	0
35.61702404	-111.5678391	1720.116	-77.25	R	0	Blocked	R	1			1	0
35.61702404	-111.5678391	1720.116	-77.4	R	0	Blocked	R	1			1	0
35.61753185	-111.5687822	1718.717	-80.25	R	0	Blocked	R	1			1	0
35.62061628	-111.5698614	1716.533	-79.62	R	0	Blocked	R	1			1	0
35.62123989	-111.5701158	1717.804	-79.23	R	0	Blocked	R	1			1	0
35.62198789	-111.5708454	1722.129	-76.67	R	0	Blocked	R	1			1	0
35.62205352	-111.5709702	1722.266	-75.75	R	0	Blocked	R	1			1	0

Measured Black Point Data					LTF SRTM Predictions			SRTM	Chi Square Matrix Values			
lat	Long	Elevation	SS	Color	Dist	SS Pred	Color	Matches	Cell A	Cell B	Cell C	Cell D
35.62205352	-111.5709702	1722.266	-75.2	R	0	Blocked	R	1			1	0
35.62204619	-111.5709702	1721.684	-74.57	R	0	Blocked	R	1			1	0
35.62204812	-111.5709599	1721.385	-74.57	R	0	Blocked	R	1			1	0
35.622053	-111.570964	1720.629	-74.57	R	0	Blocked	R	1			1	0
35.62204812	-111.5709599	1721.385	-74.57	R	0	Blocked	R	1			1	0
35.62488231	-111.5736811	1708.198	-80	R	0	Blocked	R	1			1	0
35.62840615	-111.5746629	1704.963	-84	R	0	Blocked	R	1			1	0
35.62839882	-111.5746629	1704.38	-84.53	R	0	Blocked	R	1			1	0
35.62840615	-111.5746629	1704.963	-84.53	R	0	Blocked	R	1			1	0
35.63232164	-111.583168	1716.642	-86	R	0	Blocked	R	1			1	0
35.63232164	-111.583168	1716.642	-86	R	0	Blocked	R	1			1	0
35.63330707	-111.5833028	1720.265	-86	R	0	Blocked	R	1			1	0
35.63616962	-111.5863599	1738.795	-85.85	R	0	Blocked	R	1			1	0
35.63617156	-111.5863496	1738.496	-85.79	R	0	Blocked	R	1			1	0
35.63617156	-111.5863496	1738.496	-85.79	R	0	Blocked	R	1			1	0
35.63616423	-111.5863496	1737.913	-85.79	R	0	Blocked	R	1			1	0
35.62750463	-111.6007044	1743.309	-86.67	R	0	Blocked	R	1			1	0
35.62743302	-111.6007824	1742.381	-86.67	R	0	Blocked	R	1			1	0
35.62712723	-111.6002649	1746.819	-85.67	R	0	Blocked	R	1			1	0
35.6271316	-111.6002627	1744.426	-86.17	R	0	Blocked	R	1			1	0
35.62696074	-111.600218	1743.419	-85.4	R	0	Blocked	R	1			1	0
35.62607157	-111.6013431	1736.917	-85.07	R	0	Blocked	R	1			1	0
35.62220365	-111.6013426	1740.243	-85.5	R	0	Blocked	R	1			1	0
35.62080139	-111.6007888	1744.546	-85.58	R	0	Blocked	R	1			1	0

Measured Black Point Data					LTF SRTM Predictions			SRTM	Chi Square Matrix Values			
lat	Long	Elevation	SS	Color	Dist	SS Pred	Color	Matches	Cell A	Cell B	Cell C	Cell D
35.62047289	-111.6007159	1745.639	-85.58	R	0	Blocked	R	1			1	0
35.61780664	-111.6003211	1751.726	-85.5	R	0	Blocked	R	1			1	0
35.61780858	-111.6003109	1751.427	-85.5	R	0	Blocked	R	1			1	0
35.61754211	-111.6002829	1751.497	-85.57	R	0	Blocked	R	1			1	0
35.61440497	-111.599877	1756.717	-85.3	R	0	Blocked	R	1			1	0
35.61233368	-111.6039559	1766.824	-85.21	R	0	Blocked	R	1			1	0
35.60666448	-111.6133686	1790.073	-85.21	R	0	Blocked	R	1			1	0
35.58964096	-111.6048509	1812.832	-69.67	G	0	Blocked	R	0			0	1
35.58964096	-111.6048509	1812.832	-69.5	G	0	Blocked	R	0			0	1
35.58963364	-111.6048509	1812.25	-68.71	G	0	Blocked	R	0			0	1
35.58963364	-111.6048509	1812.25	-68.44	G	0	Blocked	R	0			0	1
35.58963648	-111.6048058	1811.809	-67.7	G	0	Blocked	R	0			0	1
35.58963841	-111.6047955	1811.509	-67.55	G	0	Blocked	R	0			0	1
35.58967589	-111.604144	1810.853	-67.71	G	0	Blocked	R	0			0	1
35.5892743	-111.6015025	1807.834	-66.74	G	0	Blocked	R	0			0	1
35.58934459	-111.5998285	1800.368	-62	G	0	Blocked	R	0			0	1
35.58935047	-111.5995785	1797.737	-65	G	0	Blocked	R	0			0	1
35.58952135	-111.5999018	1800.449	-67	G	0	Blocked	R	0			0	1
35.58934753	-111.5998428	1799.911	-70.82	G	0	Blocked	R	0			0	1
35.5893646	-111.5992937	1795.545	-71.58	R	0	Blocked	R	1			1	0
35.58979188	-111.600864	1804.89	-71.73	R	0	Blocked	R	1			1	0
35.58925333	-111.6020843	1809.368	-70.41	G	912.353	-48.9772	G	1			1	0
35.59020893	-111.602213	1808.947	-70.56	G	806.983	-46.8447	G	1			1	0
35.59596417	-111.6022742	1797.946	-38.67	G	0	Blocked	R	0			0	1

Measured Black Point Data					LTF SRTM Predictions			SRTM	Chi Square Matrix Values			
lat	Long	Elevation	SS	Color	Dist	SS Pred	Color	Matches	Cell A	Cell B	Cell C	Cell D
35.69377462	-111.4660002	1580.826	-25.12	G	0	Blocked	R	0			0	1
35.69626792	-111.4645346	1565.871	-37.82	G	0	Blocked	R	0			0	1
35.69748256	-111.4671999	1559.917	-85	R	0	Blocked	R	1			1	0
35.69747524	-111.4671999	1559.333	-85.11	R	0	Blocked	R	1			1	0
35.69747767	-111.4671959	1560.673	-84.91	R	0	Blocked	R	1			1	0
35.69748064	-111.4672102	1560.214	-84.81	R	0	Blocked	R	1			1	0
35.70690747	-111.4806756	1554.09	-48	G	0	Blocked	R	0			0	1
35.70350857	-111.4969309	1564.917	-62.19	G	0	Blocked	R	0			0	1
35.7017536	-111.4979902	1572.051	-81	R	0	Blocked	R	1			1	0
35.69684288	-111.5009301	1578.205	-81	R	0	Blocked	R	1			1	0
35.69517413	-111.5019354	1580.614	-81	R	0	Blocked	R	1			1	0
35.691725	-111.5039914	1583.843	-81.67	R	0	Blocked	R	1			1	0
35.69187607	-111.5039129	1584.5	-80.44	R	0	Blocked	R	1			1	0
35.68502525	-111.5061105	1588.836	-79.33	R	0	Blocked	R	1			1	0
35.66468256	-111.5119703	1604.252	-75.67	R	4915.6	-78.5697	R	1			1	0
35.65934394	-111.5132179	1608.333	-77.86	R	5371.38	-80.0875	R	1			1	0
35.65903459	-111.5101825	1606.436	-79.73	R	5188.43	-79.4906	R	1			1	0
35.66461785	-111.4995403	1590.238	-79.57	R	0	Blocked	R	1			1	0
35.66453756	-111.4988517	1590.647	-74.5	R	4027.57	-75.0212	R	1			1	0
35.66453563	-111.498862	1590.945	-74.33	R	4028.37	-75.0247	R	1			1	0
35.6645215	-111.4988682	1591.416	-73.5	R	4029.89	-75.0312	R	1			1	0
35.65998327	-111.5060268	1598.637	-75.78	R	0	Blocked	R	1			1	0
35.65896316	-111.5077037	1600.328	-75.78	R	0	Blocked	R	1			1	0
35.65935394	-111.5131133	1608.502	-76.33	R	5363.46	-80.0621	R	1			1	0

Measured Black Point Data					LTF SRTM Predictions			SRTM	Chi Square Matrix Values			
lat	Long	Elevation	SS	Color	Dist	SS Pred	Color	Matches	Cell A	Cell B	Cell C	Cell D
35.6637949	-111.5233026	1621.479	-74.18	R	5827.21	-81.5035	R	1			1	0
35.66355545	-111.5246321	1622.492	-74.58	R	5944.33	-81.8465	R	1			1	0
35.65998633	-111.5305229	1629.061	-76	R	0	Blocked	R	1			1	0
35.56709657	-111.6578038	1914.265	-74.57	R	0	Blocked	R	1			1	0
35.56591413	-111.6579985	1918.994	-73.6	R	2326.52	-65.3837	G	0			0	1
35.56710237	-111.657773	1913.364	-74.87	R	0	Blocked	R	1			1	0
35.56846346	-111.6556305	1906.698	-75.05	R	2393.32	-65.8438	G	0			0	1
35.57284589	-111.6551534	1898.749	-85.8	R	0	Blocked	R	1			1	0
35.58854317	-111.6579588	1857.69	-85.89	R	0	Blocked	R	1			1	0
35.59220138	-111.6585564	1850.54	-85.89	R	0	Blocked	R	1			1	0
35.58450682	-111.6236398	1880.53	-77	R	0	Blocked	R	1			1	0
35.58450682	-111.6236398	1880.53	-76.2	R	0	Blocked	R	1			1	0
35.58419468	-111.6240788	1879.111	-89	R	0	Blocked	R	1			1	0
35.58248652	-111.6237489	1886.293	-78.82	R	0	Blocked	R	1			1	0
35.58281553	-111.6235617	1881.658	-78.5	R	0	Blocked	R	1			1	0
35.58443878	-111.6241357	1882.492	-80.4	R	0	Blocked	R	1			1	0
35.58529256	-111.6250535	1882.388	-81.18	R	0	Blocked	R	1			1	0
35.56061165	-111.6257928	1930.532	-74.67	R	0	Blocked	R	1			1	0
35.55303568	-111.6260494	1947.799	-78.33	R	0	Blocked	R	1			1	0
35.55164435	-111.6261447	1954.045	-81.4	R	0	Blocked	R	1			1	0
35.55304698	-111.6300727	1954.646	-82.53	R	0	Blocked	R	1			1	0
								154			150	39

APPENDIX G COLOR ASSIGNMENT COMPARISONS FOR THREE ATTENUATION MODELS

Table 21 Friis, Egli, and Foore and Ida Model Results for Cochran's Q Test

Measured Data		LTF Friis Model			Elgi Model			Foore and Ida		
Signal Strength	Color	Signal Strength	Color	Match	Signal Strength	Color	Match	Signal Strength	Color	Match
-42.09	G	-11.9492	G	1	-17.4492	G	1	-17.9492	G	1
-32.05	G	-20.2334	G	1	-25.7334	G	1	-26.2334	G	1
-49	G	-24.1469	G	1	-29.6469	G	1	-30.1469	G	1
-49	G	-30.0653	G	1	-35.5653	G	1	-36.0653	G	1
-57.75	G	-31.3926	G	1	-36.8926	G	1	-37.3926	G	1
-58.12	G	-34.5633	G	1	-40.0633	G	1	-40.5633	G	1
-61.5	G	-37.4714	G	1	-42.9714	G	1	-43.4714	G	1
-73.65	R	-39.6666	G	0	-45.1666	G	0	-45.6666	G	0
-63	G	-58.7491	G	1	-64.2491	G	1	-64.7491	G	1
-63.25	G	-59.1833	G	1	-64.6833	G	1	-65.1833	G	1
-65	G	-59.1735	G	1	-64.6735	G	1	-65.1735	G	1
-43.2	G	-35.6376	G	1	-41.1376	G	1	-41.6376	G	1
-73.65	R	-64.9762	G	0	-70.4762	G	0	-70.9762	G	0
-65.86	G	-65.8251	G	1	-71.3251	R	0	-71.8251	R	0
-64.79	G	-64.8713	G	1	-70.3713	G	1	-70.8713	G	1
-64.06	G	-65.1948	G	1	-70.6948	G	1	-71.1948	R	0
-63.78	G	-65.5329	G	1	-71.0329	R	0	-71.5329	R	0
-63.75	G	-65.8258	G	1	-71.3258	R	0	-71.8258	R	0
-59	G	-65.817	G	1	-71.317	R	0	-71.817	R	0
-60.67	G	-70.5889	G	1	-76.0889	R	0	-76.5889	R	0
-61.14	G	-66.1793	G	1	-71.6793	R	0	-72.1793	R	0
-61.08	G	-67.0606	G	1	-72.5606	R	0	-73.0606	R	0

Measured Data		LTF Friis Model			Elgi Model			Foore and Ida		
Signal Strength	Color	Signal Strength	Color	Match	Signal Strength	Color	Match	Signal Strength	Color	Match
-60.13	G	-67.7603	G	1	-73.2603	R	0	-73.7603	R	0
-52.5	G	-68.469	G	1	-73.969	R	0	-74.469	R	0
-65.36	G	-69.1951	G	1	-74.6951	R	0	-75.1951	R	0
-65.7	G	-69.899	G	1	-75.399	R	0	-75.899	R	0
-67.5	G	-70.7968	G	1	-76.2968	R	0	-76.7968	R	0
-66.8	G	-72.0295	R	0	-77.5295	R	0	-78.0295	R	0
-75.58	R	-72.0298	R	1	-77.5298	R	1	-78.0298	R	1
-76.57	R	-72.0295	R	1	-77.5295	R	1	-78.0295	R	1
-75.67	R	-72.1566	R	1	-77.6566	R	1	-78.1566	R	1
-77.56	R	-72.4527	R	1	-77.9527	R	1	-78.4527	R	1
-77	R	-84.2274	R	1	-89.7274	R	1	-90.2274	R	1
-64.5	G	-84.2278	R	0	-89.7278	R	0	-90.2278	R	0
-77.88	R	-80.9758	R	1	-86.4758	R	1	-86.9758	R	1
-38	G	-83.9312	R	0	-89.4312	R	0	-89.9312	R	0
-80.18	R	-83.0156	R	1	-88.5156	R	1	-89.0156	R	1
-58.14	G	-82.1916	R	0	-87.6916	R	0	-88.1916	R	0
-70.17	G	-74.6613	R	0	-80.1613	R	0	-80.6613	R	0
-63.5	G	-74.234	R	0	-79.734	R	0	-80.234	R	0
-25.45	G	-74.6505	R	0	-80.1505	R	0	-80.6505	R	0
-30.07	G	-74.7819	R	0	-80.2819	R	0	-80.7819	R	0
-47.5	G	-74.9684	R	0	-80.4684	R	0	-80.9684	R	0
-53.11	G	-48.8728	G	1	-54.3728	G	1	-54.8728	G	1
-75	R	-44.7819	G	0	-50.2819	G	0	-50.7819	G	0
-75.3	R	-35.8632	G	0	-41.3632	G	0	-41.8632	G	0
-78	R	-57.4221	G	0	-62.9221	G	0	-63.4221	G	0

Measured Data		LTF Friis Model			Elgi Model			Foore and Ida		
Signal Strength	Color	Signal Strength	Color	Match	Signal Strength	Color	Match	Signal Strength	Color	Match
-62.71	G	-72.2466	R	0	-77.7466	R	0	-78.2466	R	0
-75.69	R	-72.423	R	1	-77.923	R	1	-78.423	R	1
-75.14	R	-76.5951	R	1	-82.0951	R	1	-82.5951	R	1
-60.17	G	-9.51738	G	1	-15.01738	G	1	-15.51738	G	1
-76	R	-32.4478	G	0	-37.9478	G	0	-38.4478	G	0
-62	G	-45.7511	G	1	-51.2511	G	1	-51.7511	G	1
-76.1	R	-56.4453	G	0	-61.9453	G	0	-62.4453	G	0
-71.67	R	-62.2884	G	0	-67.7884	G	0	-68.2884	G	0
-71.86	R	-66.9235	G	0	-72.4235	R	1	-72.9235	R	1
-74.57	R	-75.7605	R	1	-81.2605	R	1	-81.7605	R	1
-73.6	R	-75.7654	R	1	-81.2654	R	1	-81.7654	R	1
-73.73	R	-74.6262	R	1	-80.1262	R	1	-80.6262	R	1
-73.83	R	-74.6384	R	1	-80.1384	R	1	-80.6384	R	1
-74.87	R	-72.1076	R	1	-77.6076	R	1	-78.1076	R	1
-77	R	-71.4806	R	1	-76.9806	R	1	-77.4806	R	1
-76.32	R	-69.3889	G	0	-74.8889	R	1	-75.3889	R	1
-75.47	R	-60.1925	G	0	-65.6925	G	0	-66.1925	G	0
			Matches	43		Matches	33		Matches	32

APPENDIX H LINEAR REGRESSION ANALYSIS

Table 22 Linear Regression Analysis

Measured Data			LIDAR Data				
Lat	Long	SS	Predicted SS	Error (Y)	Distance meters(X)	(x)*(y)	(x*x)
35.59810676	-111.6025783	-31.35	-11.9492	-19.4008	106	-2056.4848	11236
35.59863876	-111.6029478	-47	-20.2334	-26.7666	172.1	-4606.53186	29618.41
35.59882061	-111.6034105	-46	-24.1469	-21.8531	215.4	-4707.15774	46397.16
35.59917087	-111.6039219	-49	-30.0653	-18.9347	275.7	-5220.29679	76010.49
35.6000503	-111.6034668	-45.38	-31.3926	-13.9874	329	-4601.8546	108241
35.6007134	-111.6034693	-44.11	-34.5633	-9.5467	395.4	-3774.76518	156341.16
35.60095738	-111.6034789	-43.2	-35.6376	-7.5624	420.8	-3182.25792	177072.64
35.60142959	-111.6034142	-42.09	-37.4714	-4.6186	467.9	-2161.04294	218930.41
35.60203361	-111.6033861	-42.46	-39.6666	-2.7934	532	-1486.0888	283024
35.60477532	-111.5874177	-75	-58.7491	-16.2509	1529	-24847.6261	2337841
35.60476754	-111.5869013	-76.5	-59.1833	-17.3167	1569	-27169.9023	2461761
35.60476561	-111.5869116	-76.1	-59.1735	-16.9265	1568	-26540.752	2458624
35.60702818	-111.5807769	-73.65	-64.8713	-8.7787	2163	-18988.3281	4678569
35.60680999	-111.5804681	-73.65	-64.9762	-8.6738	2187	-18969.6006	4782969
35.60637411	-111.5798567	-63	-65.1948	2.1948	2214	4859.2872	4901796
35.60578553	-111.5790019	-63.25	-65.5329	2.2829	2256	5150.2224	5089536
35.60523378	-111.5782781	-65	-65.8258	0.8258	2292	1892.7336	5253264
35.60522158	-111.5782741	-65.86	-65.8251	-0.0349	2291	-79.9559	5248681
35.60522453	-111.5782884	-66.5	-65.817	-0.683	2290	-1564.07	5244100
35.60557992	-111.5778551	-65.83	-66.1793	0.3493	2342	818.0606	5484964
35.60656558	-111.5768217	-64.79	-67.0606	2.2706	2471	5610.6526	6105841
35.60735885	-111.5759692	-64.06	-67.7603	3.7003	2578	9539.3734	6646084
35.6082116	-111.5750939	-63.78	-68.469	4.689	2691	12618.099	7241481

Measured Data			LIDAR Data				
Lat	Long	SS	Predicted SS	Error (Y)	Distance meters(X)	(x)*(y)	(x*x)
35.6091155	-111.5741714	-63.75	-69.1951	5.4451	2811	15306.1761	7901721
35.61001643	-111.5732468	-59	-69.899	10.899	2932	31955.868	8596624
35.61091684	-111.5723037	-60.67	-70.5889	9.9189	3055	30302.2395	9333025
35.61118906	-111.57201	-61.5	-70.7968	9.2968	3093	28755.0024	9566649
35.61230126	-111.5703204	-61.14	-72.0295	10.8895	3287	35793.7865	10804369
35.61229638	-111.5703164	-60.8	-72.0298	11.2298	3287	36912.3526	10804369
35.61241888	-111.5700844	-60.13	-72.1566	12.0266	3312	39832.0992	10969344
35.61261002	-111.5697601	-61.29	-72.4527	11.1627	3348	37372.7196	11209104
35.61803107	-111.5328819	-65.36	-84.2274	18.8674	6637	125222.9338	44049769
35.61802618	-111.5328779	-65.7	-84.2278	18.5278	6638	122987.5364	44063044
35.61803107	-111.5328819	-67.5	-84.2274	16.7274	6638	111036.4812	44063044
35.61812443	-111.534269	-66.8	-83.9312	17.1312	6524	111763.9488	42562576
35.61834326	-111.5381554	-75.58	-83.0156	7.4356	6204	46130.4624	38489616
35.61842321	-111.5417085	-76.57	-82.1916	5.6216	5911	33229.2776	34939921
35.61688152	-111.5668089	-75	-74.6613	-0.3387	3829	-1296.8823	14661241
35.61806832	-111.5691495	-80	-74.234	-5.766	3735	-21536.01	13950225
35.62003593	-111.5697728	-79.9	-74.6505	-5.2495	3831	-20110.8345	14676561
35.62061628	-111.5698614	-79.62	-74.7819	-4.8381	3867	-18708.9327	14953689
35.62204812	-111.5709599	-74.57	-74.9684	0.3984	3904	1555.3536	15241216
35.58967125	-111.6034107	-67.25	-48.8728	-18.3772	880	-16171.936	774400
35.59125596	-111.6021674	-70.05	-44.7819	-25.2681	692	-17485.5252	478864
35.59384129	-111.6032077	-38	-35.8632	-2.1368	425	-908.14	180625
35.7021362	-111.4750289	-80.18	-57.4221	-22.7579	1416	-32225.1864	2005056
35.7161176	-111.4877278	-58.14	-72.2466	14.1066	3338	47087.8308	11142244
35.68671833	-111.5056653	-80	-72.423	-7.577	3471	-26299.767	12047841

Measured Data			LIDAR Data				
Lat	Long	SS	Predicted SS	Error (Y)	Distance meters(X)	(x)*(y)	(x*x)
35.67232395	-111.5097667	-78	-76.5951	-1.4049	4293	-6031.2357	18429849
35.66147899	-111.5174238	-77.88	-80.9758	3.0958	5526	17107.3908	30536676
35.55225552	-111.6394415	-25.45	-9.51738	-15.9326	93	-1481.73366	8649
35.55450726	-111.6395943	-30.07	-32.4478	2.3778	344	817.9632	118336
35.55786447	-111.6396791	-47.5	-45.7511	-1.7489	718	-1255.7102	515524
35.56163883	-111.6472806	-53.11	-56.4453	3.3353	1338	4462.6314	1790244
35.56363524	-111.6533154	-75	-62.2884	-12.7116	1848	-23491.0368	3415104
35.56838969	-111.6559378	-75.3	-66.9235	-8.3765	2405	-20145.4825	5784025
35.58449462	-111.6236358	-78	-75.7605	-2.2395	3953	-8852.7435	15626209
35.58450682	-111.6236398	-76.75	-75.7654	-0.9846	3954	-3893.1084	15634116
35.58228958	-111.6238845	-86.4	-74.6262	-11.7738	3716	-43751.4408	13808656
35.58232772	-111.6239275	-79.9	-74.6384	-5.2616	3719	-19567.8904	13830961
35.57679793	-111.6227012	-60.17	-72.1076	11.9376	3209	38307.7584	10297681
35.57540228	-111.6222538	-76	-71.4806	-4.5194	3094	-13983.0236	9572836
35.57160911	-111.6218979	-76	-69.3889	-6.6111	2756	-18220.1916	7595536
35.56061165	-111.6257928	-74.67	-60.1925	-14.4775	1609	-23294.2975	2588881
				SumY	Sum x	Sum (x*Y)	Sum(x*X)
			Total	-155.736	168995.3	467760.4167	646060802
			AVGerr	-2.43337	2640.552		

APPENDIX I CHI SQUARE TEST OF LIDAR BLOCKED VS UNBLOCKED PREDICTIONS

Table 23 Chi Square Analysis of LTF Prediction of Blocked/Unblocked Signals

Measured Data					LTF LIDAR Predictions		LTF SRTM Predictions	LIDAR	Actual SS	Chi Square Matrix	
lat	Long	Elevation	SS	Color	Dist	SS Pred	Dist	Blocked	is red	Cell A	Cell C
35.60271	-111.60354	1798.35	-45.38	G	0	Blocked	0	1	0	0	1
35.60272	-111.60355	1799.231	-47.61	G	0	Blocked	0	1	0	0	1
35.60272	-111.60355	1799.231	-48.74	G	0	Blocked	0	1	0	0	1
35.60271	-111.60354	1799.987	-66	G	0	Blocked	0	1	0	0	1
35.60272	-111.60355	1799.814	-64.5	G	0	Blocked	0	1	0	0	1
35.60272	-111.60354	1800.569	-64.4	G	0	Blocked	0	1	0	0	1
35.60271	-111.60354	1799.987	-64.43	G	0	Blocked	0	1	0	0	1
35.60271	-111.60354	1799.987	-64.43	G	0	Blocked	0	1	0	0	1
35.60271	-111.60354	1799.987	-64.56	G	0	Blocked	0	1	0	0	1
35.60272	-111.60354	1800.569	-64.55	G	0	Blocked	0	1	0	0	1
35.60387	-111.60401	1795.081	-65.76	G	0	Blocked	0	1	0	0	1
35.60415	-111.60411	1794.359	-65.63	G	0	Blocked	0	1	0	0	1
35.6042	-111.60412	1792.783	-66.24	G	0	Blocked	0	1	0	0	1
35.60419	-111.60411	1792.957	-73	R	0	Blocked	0	1	1	1	0
35.60419	-111.60411	1792.957	-73	R	0	Blocked	0	1	1	1	0
35.60418	-111.60411	1792.374	-73	R	0	Blocked	0	1	1	1	0
35.60419	-111.60411	1792.957	-73	R	0	Blocked	0	1	1	1	0
35.60478	-111.6019	1785.66	-82.67	R	0	Blocked	0	1	1	1	0
35.60478	-111.6019	1785.66	-82.36	R	0	Blocked	0	1	1	1	0
35.60478	-111.6019	1785.66	-81.57	R	0	Blocked	0	1	1	1	0
35.60478	-111.6019	1785.66	-80	R	0	Blocked	0	1	1	1	0
35.60478	-111.6018	1785.533	-79.75	R	0	Blocked	0	1	1	1	0

Measured Data					LTF LIDAR Predictions		LTF SRTM Predictions	LIDAR	Actual SS	Chi Square Matrix	
lat	Long	Elevation	SS	Color	Dist	SS Pred	Dist	Blocked	is red	Cell A	Cell C
35.60475	-111.60174	1785.896	-80.4	R	0	Blocked	0	1	1	1	0
35.6052	-111.60127	1782.169	-81.71	R	0	Blocked	0	1	1	1	0
35.60539	-111.60091	1780.252	-82.38	R	0	Blocked	0	1	1	1	0
35.60538	-111.60069	1779.274	-82.89	R	0	Blocked	0	1	1	1	0
35.60535	-111.60002	1777.571	-83.64	R	0	Blocked	0	1	1	1	0
35.60541	-111.59952	1774.746	-83.64	R	0	Blocked	0	1	1	1	0
35.60531	-111.59785	1769.704	-83.53	R	0	Blocked	0	1	1	1	0
35.60531	-111.59785	1769.704	-83.62	R	0	Blocked	0	1	1	1	0
35.60531	-111.59785	1769.704	-83.5	R	0	Blocked	0	1	1	1	0
35.60531	-111.59785	1769.704	-83.33	R	0	Blocked	0	1	1	1	0
35.6053	-111.59784	1769.878	-83.75	R	0	Blocked	0	1	1	1	0
35.60517	-111.59778	1770.435	-83.75	R	0	Blocked	0	1	1	1	0
35.60524	-111.59707	1769.736	-82.14	R	0	Blocked	0	1	1	1	0
35.60525	-111.59417	1761.529	-79.35	R	0	Blocked	0	1	1	1	0
35.60538	-111.59366	1760.216	-79	R	0	Blocked	0	1	1	1	0
35.60538	-111.59353	1759.949	-78.14	R	0	Blocked	0	1	1	1	0
35.60538	-111.59354	1760.248	-75.5	R	0	Blocked	0	1	1	1	0
35.60538	-111.59354	1760.248	-75.67	R	0	Blocked	0	1	1	1	0
35.60538	-111.59354	1760.248	-75.5	R	0	Blocked	0	1	1	1	0
35.60538	-111.59354	1760.248	-75.57	R	0	Blocked	0	1	1	1	0
35.60538	-111.59354	1760.248	-75.67	R	0	Blocked	0	1	1	1	0
35.60538	-111.59353	1759.949	-75.67	R	0	Blocked	0	1	1	1	0
35.60499	-111.59271	1760.93	-74.56	R	0	Blocked	0	1	1	1	0
35.60483	-111.59242	1761.159	-73.88	R	0	Blocked	0	1	1	1	0

Measured Data					LTF LIDAR Predictions		LTF SRTM Predictions	LIDAR	Actual SS	Chi Square Matrix	
lat	Long	Elevation	SS	Color	Dist	SS Pred	Dist	Blocked	is red	Cell A	Cell C
35.60483	-111.59242	1761.159	-71.94	R	0	Blocked	0	1	1	1	0
35.60483	-111.59242	1761.159	-54	G	0	Blocked	0	1	0	0	1
35.60483	-111.59242	1761.159	-56	G	0	Blocked	0	1	0	0	1
35.60481	-111.59224	1761.555	-60.14	G	0	Blocked	0	1	0	0	1
35.60481	-111.59155	1760.251	-61	G	0	Blocked	0	1	0	0	1
35.60479	-111.59067	1759.626	-64.07	G	0	Blocked	0	1	0	0	1
35.60479	-111.59068	1758.87	-64.53	G	0	Blocked	0	1	0	0	1
35.60479	-111.59054	1759.359	-65.16	G	0	Blocked	0	1	0	0	1
35.60478	-111.58921	1756.895	-69	G	0	Blocked	0	1	0	0	1
35.60478	-111.58799	1756.496	-71.75	R	0	Blocked	0	1	1	1	0
35.60532	-111.58572	1750.382	-60.5	G	0	Blocked	0	1	0	0	1
35.60572	-111.58525	1749.298	-60.88	G	0	Blocked	0	1	0	0	1
35.60589	-111.58505	1748.725	-63.58	G	0	Blocked	0	1	0	0	1
35.60588	-111.58506	1749.78	-65.82	G	0	Blocked	0	1	0	0	1
35.60588	-111.58506	1749.78	-66.22	G	0	Blocked	0	1	0	0	1
35.60588	-111.58506	1749.78	-66.6	G	0	Blocked	0	1	0	0	1
35.60588	-111.58506	1749.78	-66.76	G	0	Blocked	0	1	0	0	1
35.60588	-111.58506	1750.536	-71	R	0	Blocked	0	1	1	1	0
35.60599	-111.58492	1749.902	-71	R	0	Blocked	0	1	1	1	0
35.60632	-111.58453	1749.23	-71.22	R	0	Blocked	0	1	1	1	0
35.60632	-111.58454	1747.892	-71.6	R	0	Blocked	0	1	1	1	0
35.60632	-111.58454	1747.892	-72	R	0	Blocked	0	1	1	1	0
35.60632	-111.58454	1747.892	-71.71	R	0	Blocked	0	1	1	1	0
35.60632	-111.58454	1747.892	-71.64	R	0	Blocked	0	1	1	1	0

Measured Data					LTF LIDAR Predictions		LTF SRTM Predictions	LIDAR	Actual SS	Chi Square Matrix	
lat	Long	Elevation	SS	Color	Dist	SS Pred	Dist	Blocked	is red	Cell A	Cell C
35.60747	-111.58317	1743.795	-73.6	R	0	Blocked	0	1	1	1	0
35.60782	-111.58275	1742.637	-73.83	R	0	Blocked	0	1	1	1	0
35.608	-111.58256	1742.947	-74.29	R	0	Blocked	0	1	1	1	0
35.60813	-111.58241	1742.298	-74.75	R	0	Blocked	0	1	1	1	0
35.60812	-111.58242	1742.597	-75.21	R	0	Blocked	0	1	1	1	0
35.60812	-111.58242	1741.259	-75.07	R	0	Blocked	0	1	1	1	0
35.60812	-111.58242	1742.015	-74.76	R	0	Blocked	0	1	1	1	0
35.61293	-111.56924	1729.044	-65.05	G	0	Blocked	0	1	0	0	1
35.61314	-111.56889	1726.214	-85	R	0	Blocked	0	1	1	1	0
35.61484	-111.56577	1717.168	-85	R	0	Blocked	0	1	1	1	0
35.6153	-111.56508	1715.589	-85.25	R	0	Blocked	0	1	1	1	0
35.61832	-111.53759	1680.494	-72.67	R	0	Blocked	0	1	1	1	0
35.61832	-111.53759	1680.494	-73.8	R	0	Blocked	0	1	1	1	0
35.61847	-111.54352	1684.66	-77.07	R	0	Blocked	0	1	1	1	0
35.61855	-111.54586	1688.224	-77.94	R	0	Blocked	0	1	1	1	0
35.61855	-111.54592	1688.204	-78.5	R	0	Blocked	0	1	1	1	0
35.61789	-111.55232	1694.128	-83	R	0	Blocked	0	1	1	1	0
35.61776	-111.5554	1702.661	-84.6	R	0	Blocked	0	1	1	1	0
35.61686	-111.55887	1709.87	-85.71	R	0	Blocked	0	1	1	1	0
35.61658	-111.56235	1715.456	-83.21	R	0	Blocked	0	1	1	1	0
35.61675	-111.56534	1720.198	-82.59	R	0	Blocked	0	1	1	1	0
35.61702	-111.56784	1720.116	-77.25	R	0	Blocked	0	1	1	1	0
35.61702	-111.56784	1720.116	-77.25	R	0	Blocked	0	1	1	1	0
35.61702	-111.56784	1720.116	-77.4	R	0	Blocked	0	1	1	1	0

Measured Data					LTF LIDAR Predictions		LTF SRTM Predictions	LIDAR	Actual SS	Chi Square Matrix	
lat	Long	Elevation	SS	Color	Dist	SS Pred	Dist	Blocked	is red	Cell A	Cell C
35.61753	-111.56878	1718.717	-79.38	R	0	Blocked	0	1	1	1	0
35.61753	-111.56878	1718.717	-80.13	R	0	Blocked	0	1	1	1	0
35.61753	-111.56878	1718.717	-80.13	R	0	Blocked	0	1	1	1	0
35.61753	-111.56878	1718.717	-80.25	R	0	Blocked	0	1	1	1	0
35.6219	-111.5706	1721.619	-82	R	0	Blocked	0	1	1	1	0
35.62212	-111.57104	1720.326	-74.57	R	0	Blocked	0	1	1	1	0
35.62303	-111.57199	1712.946	-74.57	R	0	Blocked	0	1	1	1	0
35.62488	-111.57367	1707.899	-80.67	R	0	Blocked	0	1	1	1	0
35.62488	-111.57367	1708.655	-80.67	R	0	Blocked	0	1	1	1	0
35.62694	-111.57457	1707.32	-82.8	R	0	Blocked	0	1	1	1	0
35.62744	-111.57469	1706.479	-82.8	R	0	Blocked	0	1	1	1	0
35.62841	-111.57466	1705.545	-83.67	R	0	Blocked	0	1	1	1	0
35.62841	-111.57466	1705.545	-83.67	R	0	Blocked	0	1	1	1	0
35.62841	-111.57466	1704.963	-84	R	0	Blocked	0	1	1	1	0
35.62841	-111.57466	1704.963	-84.53	R	0	Blocked	0	1	1	1	0
35.62841	-111.57466	1704.963	-84.53	R	0	Blocked	0	1	1	1	0
35.63404	-111.58366	1721.618	-86	R	0	Blocked	0	1	1	1	0
35.63618	-111.58636	1738.622	-86.1	R	0	Blocked	0	1	1	1	0
35.63617	-111.58635	1738.496	-85.79	R	0	Blocked	0	1	1	1	0
35.63616	-111.58635	1737.913	-85.79	R	0	Blocked	0	1	1	1	0
35.63619	-111.58639	1737.709	-85.79	R	0	Blocked	0	1	1	1	0
35.6276	-111.6006	1744.504	-87	R	0	Blocked	0	1	1	1	0
35.62713	-111.60026	1744.426	-86	R	0	Blocked	0	1	1	1	0
35.62696	-111.60022	1743.419	-85.4	R	0	Blocked	0	1	1	1	0

Measured Data					LTF LIDAR Predictions		LTF SRTM Predictions	LIDAR	Actual SS	Chi Square Matrix	
lat	Long	Elevation	SS	Color	Dist	SS Pred	Dist	Blocked	is red	Cell A	Cell C
35.62633	-111.60097	1738.313	-84.92	R	0	Blocked	0	1	1	1	0
35.6208	-111.60079	1744.546	-85.58	R	0	Blocked	0	1	1	1	0
35.61781	-111.60031	1751.427	-85.67	R	0	Blocked	0	1	1	1	0
35.61781	-111.60031	1751.427	-85.5	R	0	Blocked	0	1	1	1	0
35.61782	-111.60031	1751.254	-85.5	R	0	Blocked	0	1	1	1	0
35.61754	-111.60028	1751.497	-85.57	R	0	Blocked	0	1	1	1	0
35.61529	-111.60002	1755.431	-85.33	R	0	Blocked	0	1	1	1	0
35.61375	-111.60012	1757.905	-85.27	R	0	Blocked	0	1	1	1	0
35.61375	-111.60013	1758.205	-85.25	R	0	Blocked	0	1	1	1	0
35.61373	-111.60014	1758.394	-85.23	R	0	Blocked	0	1	1	1	0
35.60823	-111.6106	1784.43	-85.21	R	0	Blocked	0	1	1	1	0
35.60588	-111.61474	1793.357	-85.21	R	0	Blocked	0	1	1	1	0
35.58964	-111.60485	1812.832	-69.5	G	0	Blocked	0	1	0	0	1
35.58963	-111.60485	1812.25	-68.44	G	0	Blocked	0	1	0	0	1
35.58963	-111.60485	1812.25	-68	G	0	Blocked	0	1	0	0	1
35.58964	-111.6048	1811.509	-67.58	G	0	Blocked	0	1	0	0	1
35.58966	-111.60446	1811.55	-67.71	G	0	Blocked	0	1	0	0	1
35.58923	-111.602	1808.551	-66.74	G	0	Blocked	915.174	1	0	0	1
35.58932	-111.60012	1803.033	-62	G	0	Blocked	0	1	0	0	1
35.58952	-111.5999	1800.449	-67	G	0	Blocked	0	1	0	0	1
35.58979	-111.60086	1804.89	-71.73	R	0	Blocked	0	0	1	0	1
35.58925	-111.60208	1809.368	-70.41	G	0	Blocked	912.353	1	0	0	1
35.69628	-111.46452	1566.741	-32.9	G	0	Blocked	0	1	0	0	1
35.69628	-111.46453	1566.454	-35.48	G	0	Blocked	0	1	0	0	1

Measured Data					LTF LIDAR Predictions		LTF SRTM Predictions	LIDAR	Actual SS	Chi Square Matrix	
lat	Long	Elevation	SS	Color	Dist	SS Pred	Dist	Blocked	is red	Cell A	Cell C
35.6962	-111.46451	1566.149	-87	R	0	Blocked	0	1	1	1	0
35.69634	-111.46497	1565.997	-87	R	0	Blocked	0	1	1	1	0
35.69676	-111.46594	1564.851	-84.75	R	0	Blocked	0	1	1	1	0
35.69748	-111.4672	1559.917	-85	R	0	Blocked	0	1	1	1	0
35.69748	-111.4672	1559.333	-85.11	R	0	Blocked	0	1	1	1	0
35.69747	-111.4672	1560.089	-85	R	0	Blocked	0	1	1	1	0
35.69748	-111.46721	1560.214	-84.81	R	0	Blocked	0	1	1	1	0
35.69772	-111.46763	1559.17	-84.81	R	0	Blocked	0	1	1	1	0
35.69975	-111.47106	1555.499	-83.89	R	0	Blocked	1038.05	1	1	1	0
35.71094	-111.49181	1555.621	-59.06	G	0	Blocked	0	1	0	0	1
35.70525	-111.49577	1556.211	-61.25	G	0	Blocked	0	1	0	0	1
35.69837	-111.50001	1576.608	-81	R	0	Blocked	0	1	1	1	0
35.69187	-111.50391	1583.916	-81	R	0	Blocked	0	1	1	1	0
35.6919	-111.5039	1583.56	-81.75	R	0	Blocked	0	1	1	1	0
35.65935	-111.51321	1608.618	-77.86	R	0	Blocked	5370.01	1	1	1	0
35.65934	-111.51305	1608.697	-79.44	R	0	Blocked	5359.98	1	1	1	0
35.65903	-111.51018	1606.436	-79.73	R	0	Blocked	5188.43	1	1	1	0
35.66127	-111.50211	1592.979	-80.22	R	0	Blocked	4493.72	1	1	1	0
35.66453	-111.49885	1591.403	-74.5	R	0	Blocked	4027.71	1	1	1	0
35.66453	-111.49886	1590.362	-73.71	R	0	Blocked	4028.95	1	1	1	0
35.66391	-111.49685	1589.423	-73.16	R	0	Blocked	0	1	1	1	0
35.66213	-111.50152	1592.833	-75.33	R	0	Blocked	4388.14	1	1	1	0
35.65934	-111.51301	1608.559	-76.33	R	0	Blocked	5357.51	1	1	1	0
35.65947	-111.51356	1608.714	-77.21	R	0	Blocked	5385.79	1	1	1	0

Measured Data					LTF LIDAR Predictions		LTF SRTM Predictions	LIDAR	Actual SS	Chi Square Matrix	
lat	Long	Elevation	SS	Color	Dist	SS Pred	Dist	Blocked	is red	Cell A	Cell C
35.6638	-111.52322	1620.904	-72.25	R	0	Blocked	5820.78	1	1	1	0
35.66262	-111.52711	1624.073	-75.47	R	0	Blocked	6189.86	1	1	1	0
35.66192	-111.528	1624.599	-75.69	R	0	Blocked	0	1	1	1	0
35.66193	-111.52799	1624.884	-76.17	R	0	Blocked	0	1	1	1	0
35.66162	-111.5284	1625.618	-76.17	R	0	Blocked	0	1	1	1	0
35.56357	-111.65125	1923.481	-54.62	G	0	Blocked	0	1	0	0	1
35.56365	-111.65162	1922.647	-59.75	G	0	Blocked	0	1	0	0	1
35.5667	-111.65813	1917.994	-73.83	R	0	Blocked	0	1	1	1	0
35.56736	-111.6572	1913.555	-74.87	R	0	Blocked	2390.82	1	1	1	0
35.57094	-111.65519	1900.922	-86	R	0	Blocked	0	1	1	1	0
35.57385	-111.65514	1896.605	-85.83	R	0	Blocked	0	1	1	1	0
35.58721	-111.65718	1863.895	-85.89	R	0	Blocked	0	1	1	1	0
35.591	-111.65817	1853.119	-85.89	R	0	Blocked	0	1	1	1	0
35.59464	-111.65882	1844.511	-85.89	R	0	Blocked	0	1	1	1	0
35.58378	-111.62401	1874.879	-89	R	0	Blocked	0	1	1	1	0
35.58298	-111.6236	1878.039	-78.5	R	0	Blocked	0	1	1	1	0
35.58662	-111.62593	1874.356	-82.05	R	0	Blocked	0	1	1	1	0
35.57273	-111.62169	1913.488	-77.6	R	0	Blocked	2861.4	1	1	1	0
35.55304	-111.62604	1948.08	-79.29	R	0	Blocked	0	1	1	1	0
35.55155	-111.62704	1955.387	-82	R	0	Blocked	0	1	1	1	0
35.55204	-111.62802	1955.951	-82.23	R	0	Blocked	0	1	1	1	0
35.55396	-111.63196	1950.441	-82.44	R	0	Blocked	0	1	1	1	0
										143	45

Measured Signal Strength Data					LIDAR Prediction			LIDAR UnBlocked	Actual SS is green	Cell B	Cell D
35.5528	-111.64	1957.187	-26.5	G	155.235	-18.3497	G	1	1	1	0
35.55339	-111.64	1954.028	-27.77	G	220.723	-24.6453	G	1	1	1	0
35.55419	-111.64	1950.618	-27.77	G	308.589	-30.5537	G	1	1	1	0
35.55451	-111.64	1948.024	-30.07	G	343.811	-32.4478	G	1	1	1	0
35.5556	-111.64	1938.615	-34.5	G	465.655	-37.7509	G	1	1	1	0
35.55683	-111.64	1930.012	-36.82	G	601.888	-42.7993	G	1	1	1	0
35.5576	-111.64	1927.112	-37.89	G	687.219	-45.0419	G	1	1	1	0
35.55766	-111.64	1927.733	-38.74	G	694.037	-45.2104	G	1	1	1	0
35.55787	-111.64	1926.413	-47	G	717.159	-45.7641	G	1	1	1	0
35.55786	-111.64	1927.169	-47.33	G	716.541	-45.7511	G	1	1	1	0
35.55838	- 111.641	1925.912	-50.6	G	781.688	-47.2315	G	1	1	1	0
35.55889	- 111.642	1925.713	-50.6	G	855.032	-48.764	G	1	1	1	0
35.55939	- 111.643	1925.834	-50	G	934.777	-50.2916	G	1	1	1	0
35.55996	- 111.644	1925.198	-51	G	1030.89	-51.97	G	1	1	1	0
35.56105	- 111.646	1924.954	-53.11	G	1226.2	-54.9487	G	1	1	1	0
35.56164	- 111.647	1924.119	-53.11	G	1337.82	-56.4453	G	1	1	1	0
35.56307	-111.65	1926.487	-54	G	1614.17	-60.0254	G	1	1	1	0
35.56337	-	1924.727	-54.62	G	1672.96	-60.6223	G	1	1	1	0

Measured Signal Strength Data					LIDAR Prediction			LIDAR UnBlocked	Actual SS is green	Cell B	Cell D
	111.651										
35.56372	-111.654	1924.731	-73	R	1905.14	-62.7974	G	1	0	0	1
35.5639	-111.655	1923.763	-75.67	R	1971.68	-63.3769	G	1	0	0	1
35.5643	-111.656	1924.891	-74.75	R	2054.58	-64.0732	G	1	0	0	1
35.56499	-111.657	1921.552	-71.67	R	2166.62	-64.9717	G	1	0	0	1
35.5671	-111.658	1913.364	-74.87	R	2405.74	-66.9408	G	1	0	0	1
35.56839	-111.656	1907.833	-75.3	R	2404.26	-66.9235	G	1	0	0	1
35.56839	-111.656	1907.533	-75.47	R	2403.86	-66.9206	G	1	0	0	1
35.58449	-111.624	1880.704	-78	R	3940.94	-75.7605	R	1	0	0	1
35.58451	-111.624	1880.53	-77	R	3942.07	-75.7654	R	1	0	0	1
35.58451	-111.624	1880.53	-76.75	R	3942.07	-75.7654	R	1	0	0	1
35.58227	-111.624	1885.5	-82.14	R	3703.54	-74.6175	R	1	0	0	1
35.58227	-111.624	1885.5	-81.12	R	3703.54	-74.6175	R	1	0	0	1
35.58228	-111.624	1886.082	-80.56	R	3704.28	-74.621	R	1	0	0	1
35.58233	-	1886.866	-79.9	R	3707.8	-74.6384	R	1	0	0	1

Measured Signal Strength Data					LIDAR Prediction			LIDAR UnBlocked	Actual SS is green	Cell B	Cell D
	111.624										
35.57855	-111.622	1905.579	-69	G	3409.88	-73.1678	R	1	1	1	0
35.57855	-111.622	1905.279	-62	G	3410.51	-73.1708	R	1	1	1	0
35.5768	-111.623	1909.46	-60.17	G	3199.67	-72.1076	R	1	1	1	0
35.5754	-111.622	1911.151	-76	R	3084.58	-71.4806	R	1	0	0	1
35.57516	-111.622	1910.648	-76.5	R	3074.06	-71.4185	R	1	0	0	1
35.57475	-111.622	1909.482	-76.67	R	3054.99	-71.2614	R	1	0	0	1
35.57214	-111.622	1916.566	-77.5	R	2800.68	-69.7072	G	1	0	0	1
35.56639	-111.625	1923.037	-75.69	R	2142.41	-65.2383	G	1	0	0	1
35.56739	-111.624	1923.535	-75	R	2263.09	-66.1466	G	1	0	0	1
35.56545	-111.625	1923.758	-75.69	R	2031.95	-64.1497	G	1	0	0	1
35.56453	-111.626	1925.057	-75.14	R	1928.22	-63.2705	G	1	0	0	1
35.56357	-111.626	1926.315	-75	R	1825.92	-62.3559	G	1	0	0	1
35.5628	-111.626	1927.321	-74.75	R	1777.03	-61.8926	G	1	0	0	1
35.55528	-	1940.334	-79.05	R	613.107	-43.343	G	1	0	0	1

Measured Signal Strength Data					LIDAR Prediction			LIDAR UnBlocked	Actual SS is green	Cell B	Cell D
	111.635										
35.55557	-111.635	1939.157	-78.35	R	599.753	-43.0675	G	1	0	0	1
35.55559	-111.635	1939.408	-64	G	599.828	-43.0767	G	1	1	1	0
35.55554	-111.635	1939.238	-64	G	600.226	-43.0697	G	1	1	1	0
35.55548	-111.635	1939.681	-67.5	G	602.732	-43.119	G	1	1	1	0
35.55539	-111.635	1940.661	-67	G	606.934	-43.2063	G	1	1	1	0
35.55533	-111.635	1941.015	-65	G	584.356	-42.5992	G	1	1	1	0
35.5557	-111.636	1940.153	-64.2	G	587.166	-42.796	G	1	1	1	0
35.55691	-111.638	1935.736	-63.43	G	626.93	-43.5184	G	1	1	1	0
35.55711	-111.638	1934.516	-63.38	G	641.579	-43.9009	G	1	1	1	0
35.55774	-111.64	1931.766	-62.8	G	701.723	-45.406	G	1	1	1	0
35.55774	-111.64	1931.466	-61.09	G	701.943	-45.4109	G	1	1	1	0
35.55772	-111.64	1931.641	-61.09	G	700.572	-45.378	G	1	1	1	0
35.55601	-111.64	1938.381	-58.69	G	510.853	-39.3779	G	1	1	1	0
35.55538	-111.64	1943.086	-58.93	G	441.156	-36.8193	G	1	1	1	0
35.55451	-111.64	1950.699	-58.33	G	343.987	-32.4742	G	1	1	1	0
35.55256	-111.639	1962.008	-58.06	G	127.998	-14.9559	G	1	1	1	0

Measured Signal Strength Data					LIDAR Prediction			LIDAR UnBlocked	Actual SS is green	Cell B	Cell D
35.69278	- 111.466	1583.155	-24	G	291.973	-29.1996	G	1	1	1	0
35.70152	- 111.474	1555.515	-81.38	R	1312.11	-56.2189	G	1	0	0	1
35.70348	- 111.477	1557.718	-48.5	G	1644.52	-59.8766	G	1	1	1	0
35.70419	- 111.478	1558.625	-48.5	G	1755.62	-61.1869	G	1	1	1	0
35.70604	-111.48	1555.762	-48	G	2009.82	-63.7395	G	1	1	1	0
35.70935	- 111.483	1552.23	-52.5	G	2464.7	-67.0915	G	1	1	1	0
35.71027	- 111.484	1553.873	-54	G	2591.64	-67.9226	G	1	1	1	0
35.71126	- 111.485	1556.135	-55	G	2726.94	-68.7669	G	1	1	1	0
35.71334	- 111.486	1558.342	-55	G	3013.26	-70.5619	G	1	1	1	0
35.71447	- 111.487	1560.308	-56.2	G	3150.04	-71.3009	R	1	1	1	0
35.71548	- 111.487	1558.425	-57.18	G	3261.49	-71.8824	R	1	1	1	0
35.71613	- 111.488	1559.44	-58.08	G	3334.91	-72.2548	R	1	1	1	0
35.71612	- 111.488	1559.314	-58.14	G	3333.26	-72.2466	R	1	1	1	0
35.68672	- 111.506	1587.02	-79.79	R	3434.13	-72.4244	R	1	0	0	1
35.68503	-	1588.836	-79.33	R	3502.88	-73.2922	R	1	0	0	1

Measured Signal Strength Data					LIDAR Prediction			LIDAR UnBlocked	Actual SS is green	Cell B	Cell D
	111.506										
35.68244	- 111.507	1590.189	-79.06	R	3630.63	-73.7443	R	1	0	0	1
35.67448	- 111.509	1595.731	-78.89	R	4136.32	-75.9953	R	1	0	0	1
35.67232	-111.51	1597.457	-78	R	4293.54	-76.5951	R	1	0	0	1
35.66993	-111.51	1600.942	-78	R	4479.69	-77.2889	R	1	0	0	1
35.66732	- 111.511	1602.262	-78	R	4691.35	-78.0526	R	1	0	0	1
35.66026	- 111.505	1595.383	-79.88	R	4731.71	-78.3023	R	1	0	0	1
35.66004	- 111.515	1611.16	-77.53	R	5482.04	-80.8423	R	1	0	0	1
35.66068	- 111.517	1612.269	-77.56	R	5515.29	-80.9451	R	1	0	0	1
35.66246	- 111.518	1611.781	-77.61	R	5535.85	-81.0146	R	1	0	0	1
35.66335	-111.52	1614.361	-77	R	5599.3	-81.2119	R	1	0	0	1
35.6636	- 111.521	1618.513	-77	R	5651.17	-81.3692	R	1	0	0	1
35.66365	- 111.521	1622.54	-76.14	R	5691.91	-81.4909	R	1	0	0	1
35.66365	- 111.521	1621.659	-64.5	G	5691.43	-81.4895	R	1	1	1	0
35.66365	- 111.521	1621.659	-68.33	G	5691.43	-81.4895	R	1	1	1	0
35.66372	-	1618.9	-70.17	G	5771.91	-81.7274	R	1	1	1	0

Measured Signal Strength Data					LIDAR Prediction			LIDAR UnBlocked	Actual SS is green	Cell B	Cell D
	111.523										
35.66378	-111.523	1620.142	-70.17	G	5799.84	-81.8095	R	1	1	1	0
35.66113	-111.529	1627.329	-76.32	R	6425.99	-83.5872	R	1	0	0	1
35.66052	-111.53	1627.572	-76.1	R	6523.92	-83.839	R	1	0	0	1
35.65998	-111.531	1629.359	-75.95	R	6606.75	-84.0491	R	1	0	0	1
35.65999	-111.531	1629.061	-76	R	6605.84	-84.0468	R	1	0	0	1
35.65999	-111.531	1629.644	-71.36	R	6605.43	-84.0457	R	1	0	0	1
35.65999	-111.531	1629.644	-71.36	R	6605.43	-84.0457	R	1	0	0	1
35.65999	-111.531	1629.644	-71.5	R	6605.43	-84.0457	R	1	0	0	1
35.65999	-111.531	1629.644	-71.53	R	6605.43	-84.0457	R	1	0	0	1
35.65999	-111.531	1629.644	-71.61	R	6605.43	-84.0457	R	1	0	0	1
35.65999	-111.531	1629.644	-71.53	R	6605.43	-84.0457	R	1	0	0	1
35.65999	-111.531	1629.644	-71.45	R	6605.43	-84.0457	R	1	0	0	1
35.59804	-111.603	1799.796	-30.53	G	99.8322	-10.6901	G	1	1	1	0
35.59804	-111.603	1799.497	-31.35	G	99.2535	-10.588	G	1	1	1	0

Measured Signal Strength Data					LIDAR Prediction			LIDAR UnBlocked	Actual SS is green	Cell B	Cell D
35.59811	-111.603	1799.052	-31.35	G	107.352	-11.9492	G	1	1	1	0
35.59827	-111.603	1799.767	-31.48	G	123.351	-14.3642	G	1	1	1	0
35.59864	-111.603	1800.754	-47	G	172.922	-20.2334	G	1	1	1	0
35.5987	-111.603	1801.522	-49	G	179.661	-20.8974	G	1	1	1	0
35.59978	-111.604	1804.958	-47	G	304.914	-30.0836	G	1	1	1	0
35.60096	-111.603	1802.069	-43.2	G	419.896	-35.6376	G	1	1	1	0
35.60122	-111.603	1801.424	-42.09	G	445.525	-36.6663	G	1	1	1	0
35.60143	-111.603	1801.018	-42.09	G	466.674	-37.4714	G	1	1	1	0
35.60203	-111.603	1800.149	-42.46	G	529.567	-39.6666	G	1	1	1	0
35.60477	-111.587	1754.27	-76.33	R	1566.94	-59.1833	G	1	0	0	1
35.60477	-111.587	1754.27	-76.33	R	1566.94	-59.1833	G	1	0	0	1
35.60477	-111.587	1754.57	-76.1	R	1566.02	-59.1735	G	1	0	0	1
35.60477	-111.587	1754.57	-75.91	R	1566.02	-59.1735	G	1	0	0	1
35.60477	-111.587	1754.57	-75.58	R	1566.02	-59.1735	G	1	0	0	1

Measured Signal Strength Data					LIDAR Prediction			LIDAR UnBlocked	Actual SS is green	Cell B	Cell D
35.60477	- 111.587	1754.57	-75.46	R	1566.02	-59.1735	G	1	0	0	1
35.60477	- 111.587	1754.57	-75.43	R	1566.02	-59.1735	G	1	0	0	1
35.60477	- 111.587	1754.57	-75.25	R	1566.02	-59.1735	G	1	0	0	1
35.60477	- 111.587	1754.57	-75.18	R	1566.02	-59.1735	G	1	0	0	1
35.60477	- 111.587	1754.57	-75.18	R	1566.02	-59.1735	G	1	0	0	1
35.60477	- 111.587	1754.57	-75.11	R	1566.02	-59.1735	G	1	0	0	1
35.60477	- 111.587	1754.57	-75	R	1566.02	-59.1735	G	1	0	0	1
35.60477	- 111.587	1754.57	-74.95	R	1566.02	-59.1735	G	1	0	0	1
35.60477	- 111.587	1754.57	-74.86	R	1566.02	-59.1735	G	1	0	0	1
35.60703	- 111.581	1740.548	-73.65	R	2173.13	-64.8713	G	1	0	0	1
35.60637	-111.58	1740.58	-63	G	2212.89	-65.1948	G	1	1	1	0
35.60522	- 111.578	1740.573	-65	G	2291.02	-65.8251	G	1	1	1	0
35.60522	- 111.578	1740.116	-66.4	G	2289.95	-65.817	G	1	1	1	0
35.60523	- 111.578	1740.699	-66.36	G	2290.24	-65.8189	G	1	1	1	0
35.60629	-	1738.689	-65.31	G	2433.24	-66.8096	G	1	1	1	0

Measured Signal Strength Data					LIDAR Prediction			LIDAR UnBlocked	Actual SS is green	Cell B	Cell D
	111.577										
35.60707	-111.576	1737.412	-64.47	G	2538.6	-67.5082	G	1	1	1	0
35.60764	-111.576	1737.385	-63.76	G	2614.49	-67.9957	G	1	1	1	0
35.60821	-111.575	1737.484	-63.78	G	2690.14	-68.469	G	1	1	1	0
35.60852	-111.575	1737.573	-63.84	G	2731.13	-68.7206	G	1	1	1	0
35.60912	-111.574	1738.24	-63.75	G	2810	-69.1951	G	1	1	1	0
35.60971	-111.574	1737.272	-59	G	2889.77	-69.6629	G	1	1	1	0
35.6115	-111.572	1735.712	-61.5	G	3138.43	-71.0482	R	1	1	1	0
35.6123	-111.57	1735.755	-60.8	G	3286.06	-72.0295	R	1	1	1	0
35.6123	-111.57	1736.511	-61.08	G	3286.1	-72.0298	R	1	1	1	0
35.6123	-111.57	1735.755	-60.31	G	3286.06	-72.0295	R	1	1	1	0
35.61231	-111.57	1735.739	-60.14	G	3288.3	-72.0408	R	1	1	1	0
35.61237	-111.57	1735.363	-60.14	G	3300.37	-72.1021	R	1	1	1	0
35.61248	-111.57	1733.571	-60.62	G	3323.17	-72.2171	R	1	1	1	0
35.61261	-111.57	1734.281	-61.29	G	3347.2	-72.4527	R	1	1	1	0
35.61803	-111.533	1684.278	-65.25	G	6641.73	-84.2274	R	1	1	1	0
35.61803	-111.533	1684.278	-65.36	G	6641.73	-84.2274	R	1	1	1	0
35.61803	-	1684.278	-65.27	G	6641.73	-84.2274	R	1	1	1	0

Measured Signal Strength Data					LIDAR Prediction			LIDAR UnBlocked	Actual SS is green	Cell B	Cell D
	111.533										
35.61803	- 111.533	1684.278	-65.44	G	6641.73	-84.2274	R	1	1	1	0
35.61803	- 111.533	1684.278	-65.44	G	6641.73	-84.2274	R	1	1	1	0
35.61803	- 111.533	1684.278	-65.59	G	6641.73	-84.2274	R	1	1	1	0
35.61803	- 111.533	1685.034	-65.7	G	6641.87	-84.2278	R	1	1	1	0
35.61803	- 111.533	1684.278	-65.86	G	6641.73	-84.2274	R	1	1	1	0
35.61803	- 111.533	1684.278	-66	G	6641.73	-84.2274	R	1	1	1	0
35.61803	- 111.533	1684.278	-67.5	G	6641.73	-84.2274	R	1	1	1	0
35.61803	- 111.533	1684.278	-67.67	G	6641.73	-84.2274	R	1	1	1	0
35.61803	- 111.533	1684.196	-67.25	G	6621.53	-84.1755	R	1	1	1	0
35.61812	- 111.534	1685.269	-66.8	G	6527.45	-83.9312	R	1	1	1	0
35.61824	- 111.536	1685.312	-67.83	G	6408.6	-83.6176	R	1	1	1	0
35.61834	- 111.538	1680.563	-75.58	R	6208.05	-83.0156	R	1	0	0	1
35.61842	- 111.542	1681.917	-76.57	R	5914.04	-82.1916	R	1	0	0	1
35.61688	-	1721.589	-75	R	3826.61	-74.6613	R	1	0	0	1

Measured Signal Strength Data					LIDAR Prediction			LIDAR UnBlocked	Actual SS is green	Cell B	Cell D
	111.567										
35.61807	-111.569	1718.03	-80	R	3732.55	-74.234	R	1	0	0	1
35.61906	-111.57	1714.971	-79.95	R	3774.16	-74.417	R	1	0	0	1
35.61955	-111.57	1715.191	-79.9	R	3798.38	-74.5236	R	1	0	0	1
35.62205	-111.571	1721.385	-74.57	R	3899.35	-74.9684	R	1	0	0	1
35.62205	-111.571	1721.385	-74.57	R	3899.35	-74.9684	R	1	0	0	1
35.62205	-111.571	1721.385	-74.57	R	3899.35	-74.9684	R	1	0	0	1
35.62205	-111.571	1721.385	-74.57	R	3899.35	-74.9684	R	1	0	0	1
35.62205	-111.571	1721.385	-74.57	R	3899.35	-74.9684	R	1	0	0	1
35.62205	-111.571	1721.385	-74.57	R	3899.35	-74.9684	R	1	0	0	1
35.58967	-111.604	1810.204	-67.6	G	886.69	-50.1372	G	1	1	1	0
35.58967	-111.603	1809.852	-67.25	G	879.259	-48.8728	G	1	1	1	0
35.58967	-111.603	1809.517	-66.82	G	872.573	-48.7404	G	1	1	1	0
35.58932	-111.601	1806.393	-66.45	G	906.938	-49.3931	G	1	1	1	0
35.5893	-111.6	1805.21	-66.14	G	913.007	-49.5079	G	1	1	1	0
35.592	-	1807.411	-69.24	G	612.201	-42.7513	G	1	1	1	0

Measured Signal Strength Data					LIDAR Prediction			LIDAR UnBlocked	Actual SS is green	Cell B	Cell D
	111.603										
35.59214	-111.603	1807.11	-68.82	G	610.301	-42.7116	G	1	1	1	0
35.59253	-111.604	1808.786	-68.82	G	578.959	-41.8415	G	1	1	1	0
35.59703	-111.602	1794.186	-39.75	G	50.6377	1.27128	G	1	1	1	0
35.59744	-111.602	1792.836	-38.2	G	9.10808	44.9637	G	1	1	1	0
35.59747	-111.602	1792.77	-37.33	G	8.60838	52.9507	G	1	1	1	0
35.59746	-111.602	1791.606	-36.86	G	9.79292	51.3892	G	1	1	1	0
35.59745	-111.602	1792.362	-36.38	G	9.26675	48.1163	G	1	1	1	0
										Cell B	Cell D
										109	79

APPENDIX J NASA LTF VIEWER POTENTIAL IMPROVEMENTS

Modeling Multipath Effects and Fresnel Diffraction

The current LTF prototype only models the direct path from transmitter to receiver, taking into account blockage by solid objects (such as terrain) and free space path loss using the Friis Transmission Equation.

This assumption only truly applies to a specific range of frequencies when modeling paths longer than a frequency-dependent cutoff distance where Fresnel diffraction can be considered negligible - roughly 150m for 2.4 Ghz signals that were tested in this effort. It also ignores the effects of constructive and destructive interference due to reflected and diffracted radio waves, which might not be negligible in complex terrain such as craters and canyons.

This gap can be addressed by integrating a high-fidelity radio model that takes into account multipath effects. There are multiple government-purpose radio modeling packages (for example EMPIRE) that could potentially be adapted to use LTF as their terrain representation; these packages would benefit from the much higher fidelity of terrain that LTF provides, while providing a much more accurate radio prediction.

The existing direct path model would still be important for real time predictions as performance may be an issue with more complex models and in open terrain the direct path model may be sufficient.

Modeling Antenna Directionality

The current LTF prototype assumes optimal alignment and polarization between transmitter and receiver. For omnidirectional antennas this may be sufficient - though no antenna is perfectly omnidirectional - but for sector and directional antennas this assumption is problematic. This gap can be addressed by including properties characterizing antenna directionality on radio asset definitions, and by including antenna orientation as a property on individual antenna instances. The radio model would then take into account directionality of transmitter and receiver and predict correspondingly lower signals for misaligned antennas.

Electromagnetic Interference

The current LTF prototype does not take into account any sources of electromagnetic interference. This would be a nontrivial gap to fully address; a characterization of the severity of various effects would be needed to understand which effects are relevant and which are negligible. Solar / cosmic radiation and high-powered Earth-based transmitters would be the most likely candidates for interference in lunar environments; many more factors would be relevant on Earth itself, and likely only solar / cosmic radiation would be relevant on a Martian environment.

Traverse Planning Support

The current LTF prototype does not provide any support for traverse planning. Such a capability would be extremely useful for mission planning. rehearsal, and operation, especially if recommended traverse plans could take into account the communications layer to attempt to stay within radio coverage.

Traverse planning functionality is scheduled to be implemented under US Army RDECOM funding by April 2011; however there is currently some uncertainty as to when or whether the funding will be available. The scheduled functionality would take into account terrain mobility issues - e.g. steepness of terrain and surface material properties - as well as user-defined criteria. Ideally the interaction with the communications layer could be implemented via the user-defined criteria interface.

The RAVEN linear feature capability could be used to easily provide support for interactive traverse planning guided by the automated LTF traverse planning algorithm - the GUI would enable the user to interactively place waypoints via the same mechanism that radio relays are currently placed, and then use the scheduled LTF traverse planning functionality to suggest what LTF believes to be the optimal traverse plan through those waypoints.

Analyzing Traverse Plans for Radio Coverage

The LTF prototype as delivered does not support displaying traverse plans, nor analyzing them for radio coverage along the traversal, though this functionality was initially demonstrated as proof of concept in the legacy LTF viewer. The two software baselines are entirely separate so porting the capability from one to the other was not feasible in this initial study.

To address this gap, use the RAVEN linear feature toolkit to display and create route plans, and re-implement the traversal radio coverage analysis using similar functionality as coverage mapping. This could even take a corridor width to analyze small corridors around the traverse plan. It would also be helpful to be able to import traverse plans from Google Earth, flat text records, and ESRI Shape Files, and to be capable of exporting traverse plans to these formats.

Interaction Between Displayed and Saved Coverage Maps

The LTF prototype currently supports displaying coverage maps in the LTF/RAVEN viewer, and exporting them to standard image formats capable of being loaded in Google Earth. However, the two capabilities are entirely disjoint - maps generated for display cannot be saved, and maps saved to disk cannot be displayed within LTF/RAVEN. To accomplish both, the same map must be recalculated twice; a very expensive operation.

To address this usability issue, the two coverage map calculations must be reconciled into a common framework where they both accept the same input data. Additionally, an interface for loading saved coverage maps must be developed, as well as an interface to save coverage maps originally only generated for display.

Coverage Map Decal Display within LTF/RAVEN

The LTF prototype exports coverage maps to Google Earth as terrain surface decal textures, but is currently incapable of displaying such decals itself. Coverage maps are displayed within LTF/RAVEN as a cloud of sampled points, which when zoomed out obstruct the underlying terrain. This functionality was not available in the version of RAVEN used for the delivery, but recent development in RAVEN has made this functionality possible. Addressing this gap should be very straightforward.

Change Colors Without Recalculating Maps

The LTF prototype supports specifying which colors to use for each signal range to be displayed. However, changing the colors currently requires completely recalculating the coverage map; an expensive operation. If coverage maps were generated as palette images rather than RGB images, changing the colors would be an instantaneous operation as long of the number of different colors did not change.

Color Code Individual Relays

The LTF prototype applies the same signal color gradient to all relays. This is sufficient to show users what quality of signal is predicted, but not to which particular relay that signal originates from. Managing signal colors per relay would make it clear on the overall composite coverage map which particular relay provides the best coverage at each point.

To support this, a separate coverage map would be developed for each relay using its own color scheme. The final coverage map displayed to the user would be the composite view of all individual coverage maps. It would even be possible to show each relay coverage map as its own layer and enable/disable without recalculating any coverage maps.

Radio Relay Placement Missing Some Interactions in LTF/RAVEN

The LTF prototype supports placing radio relays by interactive mouse selection or by entering coordinates. However, some other useful operations are only partially supported. For example, moving an existing relay can be accomplished by mouse dragging but not by coordinate entry. It is also not possible to use the mouse to select coordinates by clicking on the map or 3D view - coordinates can only be entered by hand. New relays support choosing which radio asset to use, but existing relays cannot be reassigned to use a different radio asset type; RAVEN itself supports this, but it was not implemented for the LTF Radio Tool.

Switch Between Databases in LTF/RAVEN

The LTF prototype does not implement a way to close the current database and open a different one, requiring users to exit and restart the program to load a different database. This should not be difficult to implement but would require testing of the various LTF/RAVEN tools to make sure they do not attempt to hold onto database-specific resources.

Once this capability is in place, it would be helpful to add the capability to have multiple databases open at the same time so you can see the same locations side by side and compare correlation issues. However this would likely place severe strain on graphics resources and would require better terrain paging capability to be capable of unloading unseen terrain data from the graphics card, which may be nontrivial to implement.

LIST OF REFERENCES

Baer, W., Campbell, T. R., Campos, J., Powell, W. (2008). Modeling Terrain for Geo-pairing and Casualty Assessment in OneTESS. *Modelling and Simulation for Military Operations III, Proceedings of SPIE, 6965,* 11 April 2008. doi:10.1117/12.777165.

Beran, B., Piasecki, M. (2009). Engineering New Paths to Water Data. *Computers & Geosciences,35*(4). 753 - 760. doi:10.1016/j.cageo.2008.02.017.

Bhasin, K., Hayden, J. L. (2004). Evolutionary Space Communication Architecture for Human/Robotic Exploration and Science Missions. NASA Technical Manual – 2440-213074, April 2004. *AIP Conference Proceedings, 699*. 893. doi:10.163/1/1649654.

Borkman, S., Peele, G., Cambell, C. (2007). An Optimized Synthetic Environment Representation Developed for OneTESS Live Training. *Interservice/Industry Training, Simulation, and Education Conference,2007.*

Boulos, M. N. K., Scotch, M., Cheung, K.-H., Burden, D. (2008). Web GIS in Practice VI: A Demo Playlist of Geo-mashups for Public Health Neogrographers. *International Journal of Health Geographic, 7*(38). doi:10.1186/1476-072X-7-38

Campos, J., Borkman, S., Peele, G., Cambell, C. (2008). Toward Cross Domain Terrain Services. *Interservice/Industry Training, Simulation, and Education Conference,2008*.

Cavalcante, A. M., Jose de Sousa, M., Costa, J. C. W., Albuquerque, Frances, C. R. L., Cavalcante, G. P. (2007). A Parallel Approach for 3D Ray-Tracing Techniuqes in the Radio Propagation Prediction. *Journal of Microwaves and Optoelectronics, Vol. 6*(1).

Chen, A., Leptoukhm, G., Kempler, S., Di, L.. (2008). Visualization of NASA Earth Science Data in Google Earth. Conference Chairs Lin Liu, Xia LI, Kai Liu, Xinchang Zhang, Ajun Chen. *Geoinformatics 2008 and Joint Conference on GIS and Built Environment: GeoSimulation and Virtual GIS Environments, Proceedings of SPIE, (7143).* doi:10.1117/12.812610

Cohen, B. A., Nall, M. E., French, R. A., Muery, G., Lavoie, A. R. (2008). The Lunar Mapping and Modeling Project. *Proceedings of Lunar and Planetary Science XXXIX*, 2008. Retrieved January 16 from www.lpi.usra.edu/meetings/lpsc2008/pdf/1640.pdf.

Cohen, J. (1992). A Power Primer. *Psychological Bulletin, Vol. 112*(1), 155 - 159. doi:10.1016/0301-0511(92)90028-S

Connolly, J. F. (2006). Constellation Program Overview. NASA Presentation, 2006. http://www.nasa.gov/pdf/163092main_constellation_program_overview.pdf

Crues, E. Z. (2006). Distributed Simulation for Space Exploration. *SISO Spring Simulation Interoperability Workshop 2006*, Huntsville, AL, 2 - 7 April 2006. Retrieved December 13 2009 from http://hdl.handle.net/2060/20080031615.

Crues, E. Z., Chung, V. I., Blum, M. G., Bowman, J. D. (2007). The Distributed Space Exploration System (DSES). *2007 Spring Simulation Interoperability Workshop*, Norfolk, VA, 25-30 Mar. 2007**.** Retrieved December 13, 2009 from http://hdl.handle.net/2060/20070006475

Daniel, Wayne W. (1978). *Applied Nonparametric Statisitcs*. Boston, MA: Houghton Mifflin Company.

Faul, F., Erdfelder, E., Buchner, A., & Lang, A.-G. (2009). Statistical power analyses using G*Power 3.1: Tests for correlation and regression analyses. *Behavior Research Methods, 41*, 1149-1160.

Faul, F., Erdfelder, E., Lang, A.-G., & Buchner, A. (2007). G*Power 3: A flexible statistical power analysis program for the social, behavioral, and biomedical sciences. *Behavior Research Methods, 39*, 175-191.

Foore, Larry, Ida, Nathan. (July 2007). Path Loss Prediction Over the Lunar Surface Utilizing a Modified Longley-Rice Irregular Terrain Model, NASA/TM—2007-214825**.** Retrieved January 12 2009 from gltrs.grc.nasa.gov/reports/2007/TM-2007-214825.pdf

Hwu, S. U., Upanavage, M., Sham, C. C. (2008). Lunar Surface Propagation Modeling and Effects on Communications. *28th Internation Communications Satellite Systems Conference,* 10-12 June 2008, San Diego, CA.

Kamadjeu, R. (2009). Tracking the polio virus down the Congo River: a case study on the use of Google Earth in public health planning and mapping**.** *International Journal of Health Graphics, 8*(4). doi:10.1186/1476-072X-8-4

Kapur, K.C and Lamberson, L.R, (1977). *Reliability in Engineering Design.* New York, NY: John Wiley & Sons.

Lavergnat, J., Sylvain, M.. (2000). *Radio Wave Propagation Principles and Techniques*. West Sussex, England: John Wiley & Sons, Ltd.

Linmartz, J.-P. M. G. (1996). Wireless Communication, The Interactive Multimedia CD-ROM. Baltzer Science Publishers.

Lunar Communication Terminals for NASA Exploration Missions: Needs, Operations Concepts and Architectures. 28th Internation Communications Satellite Systems Conference, 10-12 June 2008, San Diego, CA.

McLarnon, B. (1997). VHF/UHF/Microwave Radio Propagation: A Primer for Digital Experimenters. Proceedings of the 16th AARL and TAPR Digital Communications Conference (Baltimore MD, October 10-12, 1997).

Mendenhall, W., Sincich, T. (1995). *Statistics for Engineering and the Sciences*, (Fourth Ed). Upper Saddle River, NJ: Prentice-Hall, Inc.

Monell, D. (2007). NASA Constellation Program Modeling and Simulation (NASA presentation). Retrieved January 12, 2010 from www.msco.mil/files/DMSC/2007/Monell_NASA.ppt

NASA Fact Sheet, ATHLETE (All-Terrain, Hex-Limbed, Extra-Terrestrial Explorer) Fact Sheet. (undated). Retrieved August 22, 2009 from http://www.nasa.gov/pdf/390539main_Athlete%20Fact%20Sheet.pdf

NASA Fact Sheet, LOLA Fact Sheet. (2009). Retrieved August 22, 2009 from http://lunar.gsfc.nasa.gov/lola/images/LOLA_Fact_Sheet.pdf.

NASA's Desert Research and Technology Studies (D-RATS), Retrieved December 8 2010 from http://science.ksc.nasa.gov/d-rats.

NASA/SP-2004-6113**,** Bioastronautics Roadmap, A Risk Reduction Strategy for Human Space Exploration. NASA Scientific and Information Program Office. (February 2005). Retrieved January 12 from http://bioastroroadmap.nasa.gov/%5CDocuments%5Cbaselinedocument.pdf

Nath, S., Liu, J., Zhao, F. (2007). SensorMap for Wide-Area Sensor Webs. *Computer*, *40*(7). 90–93.

National Aeronautics and Space Administration Small Business Innovation Research & Technology Transfer 2009 Program Solicitations, Topic: X6 Lunar Operations (2009), Retrieved January 12 2010 from http://sbir.nasa.gov/SBIR/sbirsttr2009/solicitation/SBIR/TOPIC_X6.html

National Aeronautics and Space Administration The Vision for Space Exploration, (February 2004). Retrieved October 29 from http://www.nasa.gov/pdf/55583main_vision_space_exploration2.pdf.

National Aeronautics and Space Administration PRESS Kit, Lunar Reconnaissance Orbiter (LRO): Leading NASA's Way Back to the Moon; Lunar Crater Observation and Sensing Satellite (LCROSS): NASA's Mission to Search for Water on the Moon. (June 2009). Retrieved February 2, 2010 from http://lunar.gsfc.nasa.gov/images/LRO_LCROSS_presskit.pdf

Simulation-based Engineering Science Final Report. (May 2006). National Science Foundation. Retrieved January 12 from http://www.nsf.gov/pubs/reports/sbes_final_report.pdf

Nayar, H., Jain, A., Balaram, J., Cameron, J., Lim, C., Mukherjee, R., Pomerantz, M., Reder, l., Myint, S. , Serrano, N., Wall, S. (2009). Recent Developments on a Simulator for Lunar Surface Operations, AIAA SPACE 2009 Conference & Exposition, September 2009.

PEO STRICOM, STRICOM Omnibus Contract Lot II (STOCII). Retrieved January 5 2010 from www.northropgrumman.com/contracts/pdf/STOC-II-Web-data.pdf.

Pomerantz, M. I., Jain, A., Myint, S.. (2009). Dspace: Real-time 3D Visualization System for Spacecraft Dynamics Simulation. Third IEEE International Conference on Space Mission Challenges for Information Technology, 2009. 237-245. doi:10.1109/SMC-IT.2009.36

Proctor, M., Guise, B., Peele, G. (2010). Feasibility of Rehearsal & Assessment of Manned & Robotic Celestial Body Missions. Final Report to Florida Space Grant Consortium.

Schier, J. (2008). NASA's Lunar Space Communication and Navigation Architecture. American Institute of Aeronautics and Astronautics 26th International Communications Satellite Systems Conference, September 24 2008.

Seybold, J. (2005). *Introduction to RF Propagation.* Hoboken, NJ: John Wiley & Sons.

The Propagation Model. (2008). Retrieved July 29, 2010 from http://www.itu.int/ITU-D/tech/digital-broadcasting/MoscowDec2008/Presentations/Moscow_Dec08_File11.pdf

Tomayko, J. E., (1988). Computers in Space Flight: The NASA Experience. NASA Contract Report 182505, March 1988, Chapter9-2. Retrieved November 23, 2009 from http://history.nasa.gov/computers/Ch9-2.html

Tropos 5320 Outdoor Mesh Router Specification Sheet. (2009). Retrieved February 26, 2010 at http://www.tropos.com/pdf/datasheets/tropos_datasheet_5320.pdf.

Wall, S. (2007). Lunar Surface Operations Simulator Overview (NASA presentation), October 2007.